Structure-function studies of the neuronal Src kinases

Sarah Keenan

PhD Thesis

University of York

Department of Biology

September 2012

Abstract

N1- and N2-Src are neuronal specific splice variants of the ubiquitously expressed tyrosine kinase C-Src. They differ only by short amino acid inserts within their SH3 domains, a region known to confer substrate specificity. Due to their highly identical sequence it has been difficult to attribute specific neuronal functions to each Src enzyme, however, many C-Src SH3 domain substrates do not bind to the N-Src SH3 domains. The limited functional N1-Src data indicate that it is involved in neuronal differentiation. Furthermore, high expression levels of the N-Srcs in childhood neuroblastoma correlate with cases in which the tumour spontaneously differentiates to a harmless neuronal phenotype. In this study, I sought to explain how the amino acid inserts in the N-Src SH3 domains affect substrate specificity and kinase activity and how they might act to drive neuronal differentiation.

I employed a multi-disciplinary approach to investigate the functions of the N-Srcs. Studies in heterologous cells revealed a specific role for the N-Srcs in cytoskeletal rearrangement. A sensitive *in vitro* kinase assay was developed and this showed that the N-Src SH3 domain ligand preferences differ from those of C-Src. A subsequent phage display screen was able to identify a novel consensus sequence for the N1-Src SH3 domain and peptides containing this consensus motif were shown to be highly specific N1-Src inhibitors both *in vitro* and in cells. Bioinformatic analyses revealed the consensus sequence to be present in many neuronal proteins and identified a number of putative N1-Src substrates. In cultured neurons I identified a specific role for N1-Src acting in the L1-CAM pathway to modulate neurite outgrowth.

The data presented here provide evidence that the inserts in the SH3 domains of the N-Srcs confer significant differences in their substrate preferences and that the functions mediated by the N-Srcs are different to those of C-Src. A role for N1-Src has been identified in the modulation of axon outgrowth in cultured neurons and the putative substrates identified now provide promising targets for the further study of N1-Src function. Future investigations will be able to utilise the data presented here to elucidate how N1-Src regulates the neuronal cytoskeleton, while tools I have developed; including a highly specific N1-Src inhibitor will greatly aid these investigations.

Table of Contents

List of figures

Chapter 1

Chapter 2

Chapter 3

Chapter 4

Chapter 5

List of tables

Chapter 2

Chapter 4

Chapter 6

Acknowledgements

I would like to thank my supervisor, Gareth Evans, for his help and support throughout the project and for giving me my first taste of lab life as an undergrad all those years ago. I would also like to thank all other members of the Evans lab, especially Chris for showing me how everything works and Phil for lots of entertaining conversations! Thank you to Jen Potts for being on my TAP committee and for the time I spent in the Potts lab.

Thank you to my parents for giving me somewhere quiet to write and keeping me fed for the last month. Thanks to my friends in York; Rich, Matt, Toby, Sarah and Sam for many tea breaks, lots of cake and Friday night pub trips, and particularly to Fiona for many fun times as housemates. To my friends back home, especially Hayley and Laura for always being there for a chat. And to David, for putting up with me for the last couple of months, hopefully I haven't put you off writing your own too much!

Declaration

The work presented in this thesis was performed by the author between October 2008 and October 2012 in the Department of Biology, University of York in the lab of Dr Gareth Evans. All experiments were performed by the author, with the exception of the preparation of hippocampal neurons, which was performed by Dr Sangeeta Chawla as described in the methods. Neither this thesis nor any part of it has previously been submitted for acceptance of a higher degree.

1 Introduction

1.1 Protein phosphorylation

The opposing actions of phosphorylation and dephosphorylation are able to regulate a protein in almost every conceivable way. They can increase or decrease activity, stabilise a protein or mark it for destruction, promote or prevent movement between subcellular compartments and initiate or disrupt protein-protein interactions. The addition of a phosphate group to a protein is simple, flexible and reversible. It is now thought to represent the most general regulatory mechanism within the eukaryotic cell, its prevalence possibly driven by the ready abundance of ATP within the cell. It has been estimated that as many as 30% of proteins within the human genome can be phosphorylated, many of them at multiple sites (Cohen, 2002b). However, the ability of the simple incorporation of a phosphate moiety to alter so many aspects of a protein's characteristics means that uncontrolled or abnormal phosphorylation is now recognised both as a major cause and consequence of a huge range of disease processes (Cohen, 2002a).

Addition of a phosphate group to an amino acid is mediated by kinase enzymes while phosphatases reverse the process, by removing the phosphate. The human genome contains two broad classes of protein kinase; serine/theonine kinases and tyrosine kinases. 518 (1.7%) genes in the human genome code for protein kinases, 90 of these are known tyrosine kinases and an extra 43 are predicted to have tyrosine kinase activity (Manning et al, 2002b). For the purposes of this study the majority of the discussion will be focussed on the tyrosine kinases and their functions.

There are two classes of tyrosine kinase. Receptor tyrosine kinases (RTKs) are type I transmembrane proteins with an N-terminal extracellular domain that can bind ligands, a single transmembrane domain, and a C-terminal cytoplasmic domain that includes the catalytic domain. RTKs comprise 58 of the 90 tyrosine kinases in the human genome (Manning et al, 2002b). Most RTKs are activated through binding of their extracellular domain to specific protein ligands, such as growth factors and cytokines. Ligand binding promotes RTK oligomerization and subsequent activation of the cytoplasmic catalytic domain by transphosphorylation of tyrosine residues in the juxtamembrane region. Transphosphorylation can also

result in the creation of binding sites for cellular adapters and signalling molecules, resulting in the transduction of extracellular signals across the plasma membrane (Hubbard & Till, 2000).

Nonreceptor tyrosine kinases lack a transmembrane domain and may either be soluble intracellular proteins or associate with membranes via membrane targeting lipid modifications. Nonreceptor tyrosine kinases are also activated by ligand binding, commonly resulting in either a conformational change or oligomerisation. They mediate a wide range of cellular processes including growth, differation, proliferation and migration (Hubbard & Till, 2000).

1.1.1 The study of protein phosphorylation

Tyrosine phosphorylation was first identified within immunoprecipitates of the polyomavirus middle T antigen (Eckhart et al, 1979). This discovery represented a new form of protein phosphorylation but it initially came to be associated with the ability of cytoplasmic retroviral oncoproteins (v-Src, v-Abl, v-Fps) to elicit cellular transformation (Rodrigues & Park, 1994). The normal cellular counterparts of these viral proteins were rapidly identified and shown to have intrinsic tyrosine kinase activity. Importantly, this kinase activity was shown to function within cells, acting to influence a wide range of signalling processes ranging from migration and differentiation to wound healing and immune cell function (Pawson, 2004). However, the unregulated signalling resulting from tyrosine kinases has continued to be associated with disease processes, in particular cancer. A notable example is the prevalence of the Bcr-Abl fusion protein in chronic myeloid leukaemia (CML) (Konopka et al, 1984). Therefore, as well as continuing to understand the normal signalling processes of the kinases, recent work has been focussed on targeting kinases for therapy.

Prior to the discovery of tyrosine phosphorylation a precedent for the importance of protein modification by phosphorylation had been set by seminal work elucidating the functions of serine/threonine kinases. The purification of the first kinase enzyme, cAMP dependent protein kinase (PKA) followed by the elucidation of its composition and structural requirements for activation began to allow analysis of the functional consequences of kinase signalling at a molecular level (Taylor et al, 1990). The first crystal structure of a kinase, phosphorylase a, (Barford & Johnson,

1989) facilitated further understanding of how kinases function and how they are regulated.

It was only when this knowledge of kinase structure was combined with the discoveries of cAMP, heterotrimeric G-proteins and G-protein coupled receptors that the outline of a canonical signal transduction pathway was put together, with serine/threonine phosphorylation established as a key mechanism for rapidly modulating protein function. These discoveries resulted in a new way of thinking about protein phosphorylation and established it as a major target of research to understand how cells respond to extracellular cues and the signalling pathways that elicit biological responses. The discovery of tyrosine phosphorylation provided an additional mechanism that the cell could utilise to regulate signal transduction.

Modern genomic and proteomic techniques mean that we now know most, if not all, of the kinases within the human genome, known as the 'kinome' (Manning et al, 2002b). Large numbers of phosphorylated sites within proteins have been established through high throughput techniques including mass spectrometry. The current challenge in the field is to match kinases with their substrates in order to separate functions performed by different kinases within the cell. In addition, we need to begin to understand the mechanisms of spatio-temporal regulation of kinase-substrate interactions and to elucidate the roles of multi-site and multi-PTM (post translational modification) of proteins. These complex modes of regulation may mean that protein modification by kinases will come to rival RNA splicing and gene regulation as a method of biological control (Pawson & Scott, 2005).

1.1.2 The evolution of tyrosine kinase signalling

Tyrosine phosphorylation appears to be a feature of eukaryotes and has been linked to the emergence of multicellularity. Phosphorylation in prokaryotes is dominated by histidine phosphorylation, a process that is very much in the minority in eurkaryotic cells. Prokaryotes have the more evolutionary ancient serine and threonine kinases but tyrosine kinases are nearly absent (Manning et al, 2002a). The prokaryotic tyrosine kinases that do exist do not share the same common ancestor as eukaryotic tyrosine kinases, which are all derived from the same initial tyrosine kinase. In fact, tyrosine kinases appear relatively recently in evolution, with eukaryotic-like tyrosine kinases absent in plants, yeast and fungi. Tyrosine kinase signalling is thought to be

specific to metazoans and tyrosine kinases seem to have evolved primarily to function as signalling enzymes allowing cell to cell communication (King et al, 2003).

It has been suggested that the emergence of the signalling components of tyrosine phosphorylation was the crucial step that allowed the rapid development of multicellular organisms. True tyrosine kinase signal transduction emerges about 600 million years ago, just prior to the development of multicellularity (King et al, 2003; Manning et al, 2008; Pincus et al, 2008). Tyrosine kinase signalling is now known to be crucial for the complex cell to cell communication that is a feature of metazoan biology and is involved in diverse processes ranging from the regulation of proliferation, differentiation, adhesion, hormone responses and immune functions (Hunter, 2009). This diverse and complex signalling is possible due to the tripartite system of kinases, phosphatases and phosphotyrosine binding SH2 domains. Recent work sequencing the genomes of many organisms has allowed speculation about how the evolution of these components occurred.

Surprisingly, it was not the tyrosine kinase domains themselves that were first observed during evolution. The genome of the single celled eukaryote *Sacchromyces cerevisiae* has no tyrosine kinases, one proto-SH2 domain and 3 phosphatase domains (Pincus et al, 2008). Most fungi have no tyrosine kinase or SH2 domains but ~5 phosphatase domains. The *S. cerevisiae* proto-SH2 domain shares overall sequence and structural similarity with modern SH2 domains but does not possess phosphotyrosine binding ability. Instead, it has been shown to bind phosphorylated serine and theonine residues (Dengl et al, 2009).

The appearance of protein tyrosine phosphatase (PTP) domains prior to the advent of tyrosine kinases may be due to the presence of dual specificity serine/threonine kinases that are able to phosphorylate tyrosine residues. Serine/threonine kinases are more ancient than tyrosine kinases, dating approximately from the emergence of eukaryotes. Organisms lacking tyrosine kinases, such as yeast, do have a small but detectable level of phosphotyrosine that must be present due to the action of dual specificity kinases (Schieven et al, 1986). It is known that some processes, such as the activation of mitogen-activated protein (MAP) kinases and the inhibiton of cyclin dependent kinase 1 (cdk1), require phosphorylation on tyrosine residues and that these phosphorylation events must have taken place before dedicated tyrosine kinases existed. Therefore, the evolution

of PTP domains that could remove these phosphotyrosine residues would provide a mechanism of negative regulation for these rare, but functionally important, phosphorylation events. In addition they would provide a way to buffer the occasional errant phosphorylation of a tyrosine residue. It is likely that these first dedicated PTPs arose from a common ancestor of the dual specificity phosphatases that are still found in most single celled eukaryotes (Alonso et al, 2004; Kennelly, 2001). The catalytic domains of PTPs and dual specificity phosphatases are distinct from each other but evolutionarily related.

The next portion of the tyrosine kinase signalling machinery to emerge was probably the SH2 domain. The slime mould *Dictyostelium discoideum* is a soil dwelling amoeba that is unicellular in the presence of abundant bacterial food but it is able to aggregate and form a pseudo-multicellular organism in the absence of a sufficient food source. It possesses the simplest SH2 domain genome complement of any sequenced genome and probably represents the closest living relative of the second stage of tyrosine kinase signalling evolution (Eichinger et al, 2005).

The ability of *Dictyostelium* to aggregate is reliant on the PTP and SH2 domains. Its genome contains 12 SH2 domains that fall into 5 classes of protein. Notably, the Shk proteins are kinases that contain a dual-specificity kinase domain followed by a SH2 domain. This domain arrangement is similar to that observed in Src Family Kinases (SFKs) (Moniakis et al, 2001). *Dictyostelium* has no dedicated tyrosine kinases, indicating that they probably evolved following the emergence of tyrosine specific SH2 domains, but there is a massive expansion of the putative dual-specificity kinase complement in the genome to approximately 70 (Manning et al, 2008). This shows the increased functionality of kinase signalling when it can be controlled and directed by SH2 domains.

True tyrosine kinase domains are only present in metazoans and choanoflagellates, the closest known single-celled relatives of metazoans (King et al, 2008). This indicates that tyrosine kinases arose very close to the separation of metazoans from choanoflagellates, probably as a branch of the pre-existing serine/threonine kinases. Choanoflagellates and metazoans both have a full complement of tyrosine kinases, PTPs and SH2 domains but the proteins that they are contained in and the functions that they perform vary widely. This reinforces the opinion that the tripartite system was acquired only shortly before their divergence. There are some tyrosine kinases present in the genomes of bacteria (known as BYs),

however these are not evolutionarily related to the eukaryotic tyrosine kinases and have emerged separately (Lee & Jia, 2009).

Interestingly, all choanoflagellates and metazoans sequenced have between 30 and 150 tyrosine kinases (Manning et al, 2008; Pincus et al, 2008). There is a notable absence of genomes with small numbers of tyrosine kinases. This implies that tyrosine kinase signalling was very important for the functions of multicellular organisms and resulted in their rapid expansion within the genome. The rapid increase in the number of tyrosine kinases also coincides with a dramatic increase in the numbers of SH2 and PTP domains in genomes (Pincus et al, 2008). Where *Dictyostelium* has ~10 SH2 domains and ~5 PTP domains in its genome, the genomes of all available metazoans and choanoflagellates have ~100 SH2 domains and 30-40 PTP domains per genome. As well as the increase in number, proteins containing SH2 and PTP domains also became more complex, with proteins containing SH2 or PTP domains commonly also containing 3-10 other domains (Jin et al, 2009). It seems that the advent of the true dedicated tyrosine kinase made the PTP and SH2 domains more useful in themselves, this is reflected in the large increase in their prevalence within the genome following the emergence of the tyrosine kinase domain. The tripartite system also allowed for a wider, more diverse range of regulatory roles mediated by tyrosine kinase signalling.

The emergence of tyrosine kinase signalling represented a novel mechanism for regulation of proteins. Therefore, it allowed for the rapid accumulation of new regulatory functions that, importantly, did not interfere with existing networks of regulation such as those mediated by the serine/threonine kinases.

1.2 The Src Family Kinases

Src Family Kinases (SFKs) are a group of structurally and functionally related non-receptor tyrosine kinases (Brown & Cooper, 1996; Thomas & Brugge, 1997). Src is the founding member of the family and it was first identified as the transforming protein of the oncogenic retrovirus, Rous sarcoma virus. This viral form of the protein (v-Src) was soon shown to have a normal cellular counterpart, C-Src, a ubiquitously expressed tyrosine kinase that is highly conserved through evolution. Following the identification of Src, 8 other tyrosine kinases with a high degree of both amino acid and structural similarity have been identified in verebrates. The SFK

family members are Src, Fyn, Yes, Yrk, Blk, Fgr, Hck, Lck and Lyn. The expression patterns of the SFKs are varied with some expressed ubiquitously and some showing restricted expression (Thomas & Brugge, 1997). It is likely that all cells will express at least one SFK member, with some expressing multiple isoforms of the same protein. The variety in the specificity of these related kinases along with their broad expression patterns mean that they regulate a wide variety of biological functions including proliferation, cytoskeletal rearrangement, differentiation, survival, adhesion and migration (Thomas & Brugge, 1997).

1.2.1 Structure of the SFKs

The SFKs range between 52 and 62 kDa and share a conserved modular domain organisation composed of 6 regions: i) SH4 domain, ii) unique domain, iii) SH3 domain, iv) SH2 domain, v) kinase domain, vi) negative regulatory C-terminal tail (Figure 1.2.1.1).

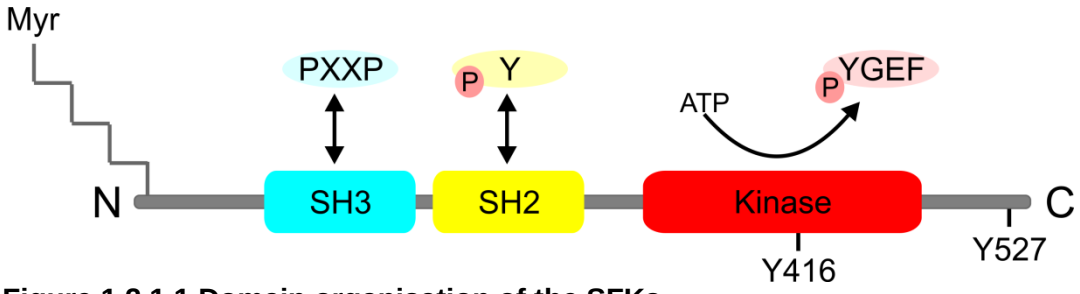

Figure 1.2.1.1 Domain organisation of the SFKs.

SFKs share a common, modular domain organisation They are N-terminally myristoylated and some family members are additionally palmitoylated. The SH3 domain interacts with ligands containing the consensus motif PxxP. SH2 domains interact with phosphotyrosine residues. The SH3 and SH2 domains function in substrate selection. The kinase domain is responsible for substrate phosphorylation. The approximate positions of two important phosphorylation sites are indicated. Phosphorylation at Y416 in the kinase domain promotes the active conformation of the kinase and phosphorylation of Y527 in the C-terminal tail promotes the inactive conformation of the kinases are discussed in section 1.2.2.

1.2.1.1 SH4 domain

SFKs are generally found associated with the plasma membrane and other intracellular membranes (Courtneidge et al, 1980; Garber et al, 1983). Their signalling is reliant on this membrane association (Spencer et al, 1995), indicating

that they predominantly phosphorylate substrates that are also membrane associated. The SH4 domain is a ~15 amino acid sequence at the extreme N-terminal tail of the kinase that contains the sequences required for lipid modification of the kinases, although the 7 residues located at the extreme N-terminus are sufficient for myristoylation to occur (Cross et al, 1984). Myristoylation is an irreversible modification that occurs during translation (Buss et al, 1984). A glycine residue at position 2 (all residue numbering refers to the amino acid sequence of the prototypical chicken Src) is required as the site of myristoylation and is essential for the addition to occur. The residues in positions 3-7 are also important and are relatively conserved between the family members. Myristoylation enhances membrane association of the kinase and non-myristoylated Src is not membrane associated (David-Pfeuty et al, 1993). A small amount of myristoylated Src is, however, found free in the cytoplasm (Buss et al, 1984).

Src and Blk contain a high proportion of basic residues within their SH4 domains (Resh, 1994). These are thought to contribute to membrane association, most likely by interacting with the polar headgroups of the phopholipid membrane.

All SFKs other than Src and Blk lack these basic residues but do have one or more cysteine residues within their SH4 domains. The cysteine at position 3, and potentially others, can be palmitoylated (Shenoy-Scaria et al, 1993). Palmitoylation occurs post translationally and can be dynamically regulated by a cycle of palmitoylation and depalmitoylation (Koegl et al, 1994; Paige et al, 1993). This cycle may be a mechanism to allow the re-localisation of the kinase upon stimulation. The addition of a palmitoyl group acts to stabilise the kinase at the membrane. Experiments using mutants of Hck that cannot be palmitoylated have shown that, while the palmitoylated protein is essentially all membrane bound, only about 30% of the non-palmitoylated protein is (Lock et al, 1991; Robbins et al, 1995).

The processes of palmitoylation and myristoylation allow membrane association but also facilitate membrane clustering within domains of the plasma membrane. The palmitoyl modification allows certain SFKs to enter lipid rafts and to associate with specific signalling complexes. Therefore, these lipid modifications are essential for the localisation and signalling of the kinases.

1.2.1.2 Unique domain

As the name suggests, the unique domain of the SFKs is the only domain that varies greatly between the members of the family. The SFK unique domains are between 50 and 80 amino acids in length. Their roles are not entirely clear but they would be predicted to mediate protein-protein interactions that are specific to each member of the family. The unique domain is dispensable for the regulation of the kinases *in vitro* (Carrera et al, 1995). Serine and threonine phosphorylation sites have been identified within the Src and Lck unique domains, although the cellular consequences of these phosphorylation events remain unclear.

Src, but not other SFKs, is phosphorylated in the unique domain by Cdc2 during M phase at Y34, Y46 and S72 (Chackalaparampil & Shalloway, 1988; Morgan et al, 1989; Shenoy et al, 1989). Src can also be phosphorylated within its unique domain in response to PKC activation in cells and is constitutively phosphorylated by PKA at S17 (Collett et al, 1979; Cross & Hanafusa, 1983).

S42 and S59 in the Lck unique domain are also phosphorylated in response to PKC activation in cells. S42 has been shown to be an *in vitro* PKC site, while S59 is an *in vitro* MAPK site (Winkler et al, 1993).

1.2.1.3 SH3 domain

SH3 domains are small, globular non-catalytic domains, approximately 60 amino acids in length that are important for both intra- and intermolecular interactions of the kinases. The SH3 domain acts to modulate the dual roles of kinase activity regulation and substrate specificity determination.

The structure of the Src SH3 domain was first solved by Yu et al (1992) and this revealed that it consists of two three stranded anti-parallel β-sheets. The two sheets pack against each other at approximately right angles, forming a hydrophobic core. The ligand binding site consists of a slightly curved, hydrophobic depression on the SH3 domain surface with an acidic cluster at one end.

SH3 domains bind to short, contiguous amino acid sequences that are rich in proline. The high proline content means that they adopt a left-handed helical conformation (a polyproline type II (PPII) helix) (Yu et al, 1994). Combinatorial peptide library and phage display studies have shown that the Src SH3 domain is

able to bind to two distinct classes of substrate, both with the core motif PxxP. The consensus sequences are RPLPPLP and φPPLPxR (where φ represents a hydrophobic amino acid) and are termed Class I and Class II respectively (Feng et al, 1994; Rickles et al, 1994). Class I sequences have an arginine residue before a PxxP motif and Class II sequences have an arginine residue after the PxxP. They bind to the SH3 domain in opposite orientations (Feng et al, 1994).

The binding affinity of these short peptides is low (K_ms are typically low micromolar) and their sequence specificity is poor (small changes in the amino acid sequence has little effect on binding affinity) (Yu et al, 1994). However, phage display experiments using a biased peptide library with the core residues of the interaction fixed have revealed that the flanking residues play an important role in establishing specificity (Feng et al, 1995; Rickles et al, 1995). Importantly, when the flanking residues are considered, the binding preferences of the individual SFK members are different. This would allow each SFK to be able to specifically select its own substrates *in vivo*.

The affinity of the SH3 domain for protein substrates is higher than that for the isolated peptide. This is partly because many Src substrates are multi-domain proteins, able to form contacts with both the SH2 domain and the SH3 domain. Additionally, some substrates, such as the p85 subunit of phosphoinosidide 3-kinase (PI3K), contain multiple SH3 domain binding motifs. This increases the local concentration of SH3 domain binding sites and results in a reduction in K_m.

The molecular basis for substrate binding to the Src SH3 domain was elucidated by Feng et al (1994). These solution structures showed the C-Src SH3 domain bound to both Class I and Class II ligands and confirmed the prediction that the two substrates would bind to the same surface but in opposite orientations. Previous structures of the PI3K, Abl and Fyn SH3 domains had shown that SH3 domain ligands adopt a PPII helix (Musacchio et al, 1994). Src SH3 domain ligands were also shown to bind as a PPII helix, confirming this as a general mechanism for interaction with SH3 domains (Yu et al, 1994). The ligand bound structure of the C-Src SH3 domain is essentially the same as the free structure, but ligand binding appears to slow the unfolding rate, stabilising the domain (Feng et al, 1994).

The PPII helix has three residues per turn, meaning that residues i and i + 3 within a substrate will be on the same face of the helix. Taking the Class I C-Src SH3 domain peptide R^1ALPPLPRY^9 as an example binding peptide, residues 1, 4

and 7 on one face and 3 and 6 on a second face all form contacts with the SH3 domain surface (Feng et al, 1994). The ligand binding site contains three binding pockets. The first is an arginine binding pocket that binds the arginine residues in both Class I and Class II substrates and is commonly known as the specificity pocket. R1 of the Class I peptide interacts with W118 of the Src SH3 domain via a hydrogen bond and D99 via a salt bridge. The importance of this interaction is demonstrated by the fact that SH3 domains with the mutation D99N bind the Class I ligand with a ~40 fold decrease in affinity compared to the wild type SH3 domain (Feng et al, 1995). The second and third pockets are responsible for docking the proline residues. They are commonly referred to as dipeptide binding pockets as they also bind the residue immediately prior to the proline. Residues Y92, W118, P133 and Y136 form the second binding pocket and it makes extensive hydrophobic contacts with L3 and P4. The methyl group of L3 also form additional contacts with the side chains of D117 and N135. L6 and P7 dock into a binding site formed by Y90 and Y136 (Yu et al, 1994). The residues that form the binding interactions are shown in Figure 1.2.1.

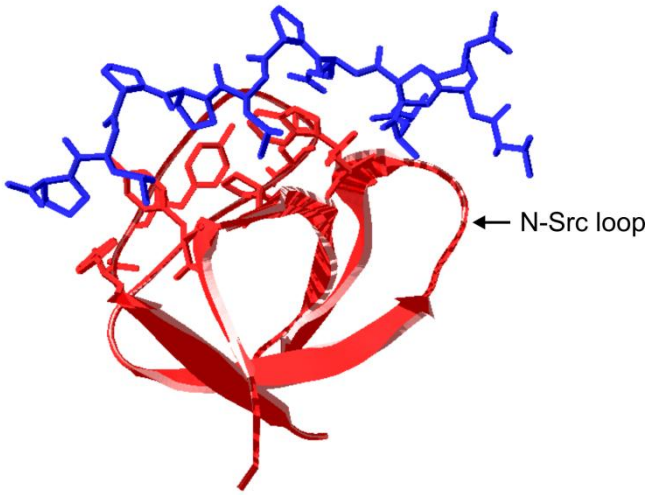

Figure 1.2.1 Structure of the C-Src SH3 domain.

The C-Src SH3 domain (red) bound to a Class I ligand (blue). The sidechains of the C-Src SH3 domain amino acids that form binding interactions with the ligand are shown. W118 and D99 form the first binding pocket for the arginine residue (R1). Y92, W118, P133, Y136, D117 and N135 form the first dipeptide binding pocket and contact L3 and P4. Y90 and Y136 form the second dipeptide binding pocket and contact L6 and P7. The n-Src loop is the location of the extra residues contained in N1- and N2-Src and can be seen to be adjacent to the substrate binding site.

An increasing number of SH3 domain binding peptides identified do not conform to the PxxP consensus motif originally identified. While some bind to surfaces entirely separate to the well characterised SH3 domain binding site, others bind to the same surface but utilise other contacts (Kami et al, 2002). It has become clear that it is not necessary for an SH3 domain binding peptide to adopt a PPII helix to form binding contacts. In general, atypical SH3 domain binding motifs form extensive contacts around the negatively charged area of the specificity pocket. This area consists of a shallow groove formed by the β3 and β4 strands, flanked at one end by parts of the β2 strand, n-Src loop and the RT loop. Many SH3 domains have one or more subpockets within this area that are able to contribute to the binding interactions. Ligands that bind in this area may or may not also utilise additional contacts in the dipeptide binding pockets (Saksela & Permi, 2012). Surprisingly, many atypical SH3 domain binding peptides bind with a higher affinity than substrates containing the canonical binding motifs.

Notably, interactions with the residues of the n-Src loop often contribute to the binding of atypical SH3 domain ligands. In both the interactions of the Csk SH3 domain with the PEP-3BP1 (Ghose et al, 2001) and the C-terminal SH3 domain of $p67^{phox}$ with $p47^{phox}$ (Kami et al, 2002) the ligands bind in the minus orientation via both canonical contracts with the dipeptide binding pockets but also additional interactions with an acid pocket adjacent to the specificity pocket. Both binding peptides adopt a helical conformation but the nature of their interaction with the SH3 domain differs slightly. The PEP-3BP1 peptide forms a 3_{10} helix that presents a hydrophobic isoleucine residue to K33 of the Csk SH3 domain, a residue contained within the n-Src loop. In the $p67^{phox}$-$p47^{phox}$ complex the 47^{phox} peptide forms a helix-turn-helix structure that is able to interact with residues in the β4 strand and n-Src loop of the $p67^{phox}$ SH3 domain.

Some SH3 domains are able to interact in both canonical and atypical modes. The Fyn SH3 domain is known to bind to classical PxxP motifs but has also been shown to bind to the atypical sequence RKxxYxxY in the immune cell adaptor SKAP55 (Kang et al, 2000). This interaction also constituted the first reported example of a SH3 domain interaction that was not reliant on at least one proline residue. Prior to this the atypical motif PxxDY (Mongioví et al, 1999) had been reported but it still required the proline residue in order to bind.

1.2.1.4 SH2 domain

SH2 domains bind phosphotyrosine residues within proteins (Moran et al, 1990). The specificity of this interaction is achieved by individual SH2 domain recognition of the residues flanking the phosphotyrosine. Songyang et al (1993a) used a random library of phosphopeptides to identify the binding preferences of a number of SH2 domains. SFK members Src, Fyn, Lck and Fgr all select the sequence pYEEI, while the SH2 domain of Abl selects pYENP and Crk selects pYDHP (Songyang & Cantley, 2004; Songyang et al, 1993b).

The molecular basis for this interaction is apparent from the structures of the Src and Lck SH2 domains (Eck et al, 1993; Waksman et al, 1992). Both have a deep hydrophobic pocket that is able to accept the isoleucine in position pY + 3. Other β-branched amino acids, such as valine, are also able to fit into the pocket, but methionine and leucine are too long. The acidic residues at positions pY + 1 and pY + 2 are positioned in a shallow groove on the SH2 domain surface, oriented towards basic residues on the otherwise neutral SH2 domain surface.

The residues in the binding sites of the individual SH2 domains directly modulate the sequences that are able to bind. Changing a residue adjacent to the Y + 2 binding site (Y215) to tryptophan in the Src SH2 domain, as it is in the Grb2 SH2 domain, alters the binding preferences of the SH2 domain to pYENP. The binding preference of the Grb2 SH2 domain is pYQNY/Q. Therefore the Src SH2 domain now favours asparagine in the Y + 2 position, as Grb2 does (Songyang et al, 1993a).

The ability of SH2 domains to select ligands from random peptide libraries indicated that they would be able to bind to similar short contiguous sequences in their substrates. Investigation of the sequences of their substrates has shown this to be partially true. Focal adhesion kinase (FAK) is known to be phosphorylatted at Y397 and to bind to the Src SH2 domain. The sequence that the SH2 domain is binding to in this instance is pYAEI, which closely matches the ideal sequence of pYEEI (Xing et al, 1994). Some substrates do not contain such apparently ideal sequences. The platelet derived growth factor receptor (PDGF-R) and colony stimulating factor-1 (CSF-1) are phosphorylated at pYIYV and pYTFI respectively (Alonso et al, 1995). Both of these sequences lack the acidic residues selected by the SH2 domain *in vitro*; they do, however, both retain the long, branched amino acid at

position pY + 3. It is likely that, as there are more contacts from the SH2 domain surface to the residue at pY + 3 than to the other two residues that binding of an appropriate amino acid in this position is able to compensate for the lack of acidic amino acids. In addition the tyrosine residue at position pY + 2 in the PDGF binding sequence is itself phosphorylated and this phosphorylation increases the acidity of the local peptide sequence and enhances the interaction. Therefore, there can be multiple layers of modulation that influence the affinity of the interaction.

It is also common that longer range interactions are also involved when the phosphorylation of a protein is considered as opposed to that of a peptide. In general, the binding affinity of SH2 domains to phosphoproteins is lower than that to the phosphopeptides derived from them. In the case of the SFKs, it is known that substrates are themselves commonly modular and able to interact with both the SH2 domain and the SH3 domain. Therefore, *in vivo* substrates may not require the ideal binding motif to be able to bind to the SH2 domain.

In addition to phosphotyrosine binding, certain SH2 domains also seem to be able to interact with phospholipids (Zhao et al, 1993). Association with phospholipids of the plasma membrane would be able to aid membrane association. However, it remains to be shown how the balance between substrate binding and phospholipid binding is achieved *in vivo* and how the balance between the two is regulated.

1.2.1.5 The kinase domain

The Src kinase domain is broadly conserved across all SFK members and other tyrosine kinases. It is both necessary and sufficient for kinase activity. It also plays a major role in the determination of substrate specificity. If the kinase domain of the v-ErbB kinase, a heterologous tyrosine kinase oncoprotein, is replaced with the kinase domain of Src then the substrate preferences of the resulting kinase become more similar to those of C-Src (Chang et al, 1995).

Studies using combinatorial peptide libraries have shown that the substrate preferences of the two kinases are indeed different with Src preferring EEEIYG/EEFD and EGF-R (the normal cellular counterpart of v-ErbB) preferring EEEEYFEφ (where φ represents a hydrophobic amino acid) (Songyang et al, 1995a). Importantly, this study also showed that the substrate preferences of the individual

members of the SFKs also differ, with the Lck kinase domain selecting XEXIYGVφφ (where φ represents a hydrophobic amino acid) (Songyang et al, 1995b). It has also been noted that the kinase domain substrate preferences resemble the SH2 domain preferences of the kinases. The Src SH2 domain binds to substrates containing pYEEI. This means that the SH2 domain is able to dock onto tyrosine residues phosphorylated by the kinase domain, allowing further phosphorylation of the substrate by the kinase domain. This is a process known as processive phosphorylation (Mayer et al, 1995).

The first structure of a tyrosine kinase elucidated was that of the insulin receptor kinase (InsR kinase) (Hubbard et al, 1994). This allowed for the comparison of a tyrosine kinase structure with the serine/threonine kinase PKA. The specificity of the InsR kinase for tyrosine over serine or threonine was shown to be caused by the proximity of a loop that is conserved between all tyrosine kinases to the substrate binding site. In Src this loop is FP^{425}IKWTA. The proline residue within this sequence binds to the phenyl ring of the substrate tyrosine, aiding its binding. This would not be beneficial for the binding of either serine or threonine.

A major site of autophosphorylation for Src occurs in the kinase domain at Y416 (Smart et al, 1981). There has been a large amount of debate about whether this phosphorylation occurs intra- or intermolecularly. Initial studies found that the phosphorylation occurred entirely or mostly intramolecularly (Feder & Bishop, 1990; Sugimoto et al, 1985). Subsequent experiments have shown that autophosphorylation of catalytically inactive kinases can occur and therefore phosphorylation must be able to proceed in trans (Cooper & MacAuley, 1988). It remains unclear whether other kinases are able to contribute to phosphorylation at this site. The phosphorylation event at Y416 is important for regulation of the kinase conformation and activity and will be discussed further in section 1.2.2.

1.2.1.6 The C-terminal tail

All vertebrate SFKs have a C-terminal extension of 15-17 residues following their kinase domains. This region contains a tyrosine residue (Y527 in chicken Src) contained within a conserved sequence at a constant position. This C-terminal phosphorylation site has been shown to be a major site of phosphorylation within the cell and in resting fibroblasts, both Src and Lck are quantitatively phosphorylated at

this site (Cooper et al, 1986; Kussick & Cooper, 1992; Marth et al, 1988). The cycle of phosphorylation and dephosphorylation of this C-terminal site is involved in the regulation of the activity and conformation of the SFKs, the mechanism by which this is achieved is discussed further in section 1.2.2.

1.2.2 Regulation of the Src Family Kinases

The first crystal structure of full length C-Src was obtained in 1997 by Xu et al (1997) and it revealed the nature of the intramolecular associations that regulate Src kinase activity. It was already known that a highly conserved tyrosine residue (Y527) in the C-terminal tail region interacts with the phosphotyrosine binding site in the SH2 domain and this was confirmed by the crystal structure. In addition, another unexpected association was observed. The linker between the SH2 domain and the kinase domain is able to adopt a polyproline type II (PPII) helix, despite containing only one proline residue, and bind to the SH3 domain.

The SH2:tail association is facilitated by a regulatory kinase known as Csk (C-terminal Src kinase) and the closely related kinase CSK-homologous kinase (Chk) that phosphorylate the highly conserved tail residue Y527 (Nada et al, 1991; Okada et al, 1991). Knockout studies suggest that Csk is a master regulator of SFK activity; the Csk knockout is embryonic lethal and biochemical analysis showed a substantial overall increase in SFK activity in the embryo (Imamoto & Soriano, 1993; Nada et al, 1993).

When the tail residue is phosphorylated it is able to interact with the phosphotyrosine binding SH2 domain, forcing the kinase into an inactive conformation. The importance of this interaction in the regulation of kinase activity becomes apparent when the product of the transforming retroviral oncogene v-src is considered. The primary structural difference between v-Src and C-Src protein is a deleted tail region in v-Src. As a result, v-Src is constitutively active, its kinase activity is unregulated and it has a transforming phenotype when transfected into cells. Mutation of the single residue Y527F in C-Src was subsequently shown to recreate the constitutive activity of v-Src (Briggs & Smithgall, 1999).

When the SH2:tail and SH3:linker intramolecular interactions are in place, the kinase activity of C-Src is downregulated. The crystal structure revealed that, in this conformation, the activation loop in the kinase domain adopts a partially helical

conformation which results in the autophosphorylation site (Y416) pointing inwards. In contrast, the crystal structure of the activated kinase shows that the activation loop is re-orientated to a position more compatible with ATP and substrate binding. In this conformation Y416 becomes surface exposed, allowing autophosphorylation which acts to stabilise the open (active) conformation (Xu et al, 1997).

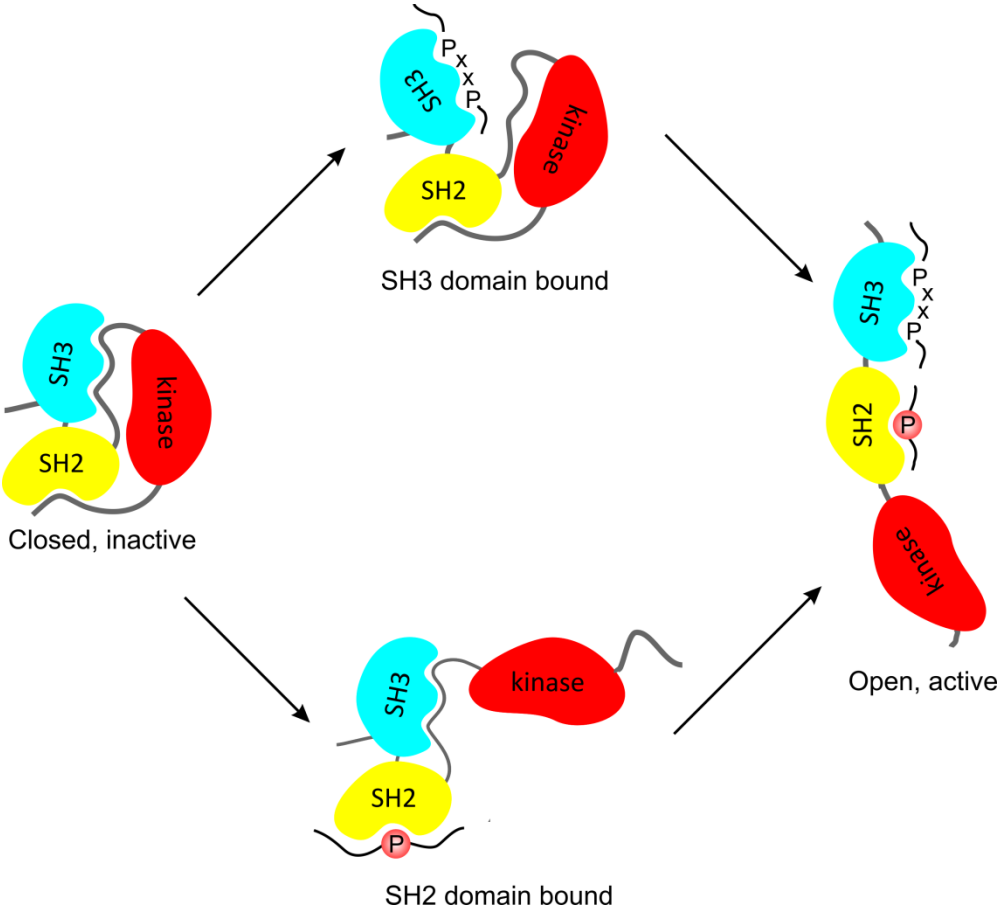

Figure 1.2.2.1 SFK activation scheme

SFKs can be activated by the displacement of the intramolecular interactions that serve to constrain the kinase activity in the absence of a substrate. Substrate binding can displace either the SH3:linker interaction or the SH2:tail interaction. It remains unclear whether displacement of one intramolecular interaction acts to destabilise the second interaction and produces a fully open and active kinase or if it can result in two distinct partially activated forms of the kinase that phosphorylate different subsets of substrates.

Mutation of the residues involved in the SH2:tail and SH3:linker interactions result in an increase in the kinase activity of the SFKs. This led to the hypothesis that interaction of the SH2 and SH3 domains with their high affinity substrates could have the same effect *in vivo*. Numerous studies have shown that disruption of either

SH2:tail or SH3:linker interactions, either by mutation, interaction with other proteins, or tail dephosphorylation, is sufficient to induce SFK activation *in vitro* but the minimal component for activation *in vivo* is still a matter of much debate. It has been suggested that disruption of the SH3 association alone may result in transient kinase activation, substrate phosphorylation and release, followed by a return of the kinase to its inactive state (Pellicena and Miller, 2002).

One of the best studied examples of kinase activation resulting from SH3 domain displacement is the association between the Hck SH3 domain and Nef, a HIV accessory factor that is involved in AIDS progression (Lee et al, 1995; Saksela et al, 1995). Nef binds to the Hck SH3 domain by the sequence PQVPXR (Saksela et al, 1995). This sequence is able to form a PPII helix that contacts the Hck SH3 domain surface (Grzesiek et al, 1996). Nef binding to full length Hck results in an increase in kinase activity that has been demonstrated *in vitro* (Moarefi et al, 1997; Trible et al, 2006) and in cell based assays (Briggs & Smithgall, 1999; Lerner & Smithgall, 2002). Mutagenesis of the PxxP motif in Nef prevents this association and in turn prevents the increase in kinase activity (Choi & Smithgall, 2004).

SH3 domain release is also shown to result in an increase in kinase activity when binding to p130Cas (Burnham et al, 2000; Pellicena & Miller, 2001), the progesterone receptor (Boonyaratanakornkit et al, 2001) and Stat3 (Schreiner et al, 2002), among others. This supports the theory that SH3 domain displacement primes the kinase for activation.

SFK activation by SH2 domain displacement has also been shown to occur *in vivo*. SFK activation by growth factor receptor tyrosine kinases involves the displacement of the SH2 domain from the SH2:tail interaction and onto the phosphorylated residues of the activated, autophosphorylated receptor. This is able to activate the kinase to phosphorylate the receptor, initiating a signalling cascade (Parsons & Parsons, 1997).

The presence of two distinct regulatory interactions within the kinase molecule means that there are a number of structural possibilities upon activation. If the displacement of either SH2:tail or SH3:linker interactions is sufficient to independently induce kinase activity, there would be more than one active conformation. This raises the possibility of the existence of distinct active states with distinct signalling properties. Alternatively, the disruption of one intramolecular

association may serve to destabilise the second leading to only one, fully open, active state.

Molecular dynamics experiments using Hck kinase support the second hypothesis, indicating that the movements of the SH2 and SH3 domains are highly correlated in the inactive state (Young et al, 2001). However, there is some compelling evidence that, *in vivo,* alternate mechanisms of activation are possible. Rat-2 fibroblasts transfected with either Hck Y527F (SH2 activated) or Hck bound to a SH3 ligand (SH3 activated) have been analysed for phosphotyrosine content by 2D electrophoresis followed by detection using an antiphosphotyrosine antibody (Engen et al, 2008). Multiple unique phosphotyrosine containing spots were observed in each case, supporting the idea that Hck substrate selection can be influenced by the mechanism of activation. If this can be demonstrated to be true for other SFK members and to occur under physiologically relevant signalling conditions, it would provide evidence that there are distinct mechanisms of activations and that the mode of activation can impact upon the substrates phosphorylated and the downstream signalling events that occur.

A more recent C-Src crystal structure (Cowan-Jacob et al, 2005) appears to support the idea that a similar mechanism of alternate activation could also be true of C-Src. The structure was obtained using unphosphorylated C-Src and, as a result, the tail is released from the SH2 domain. The activation loop of the kinase domain can be seen to adopt a conformation similar to that observed in active kinase domains. Despite this, the linker remains bound to the SH3 domain but the SH2:SH3:linker complex is rotated approximately 130^{o} compared to its position in the downregulated kinase structure. The biological relevance and kinase activity of this structure have not been determined and further investigation is needed.

There is mounting evidence that suggests the SFKs can adopt multiple active conformations *in vivo*. This conformational plasticity may go some way to explaining how the SFKs are able to function in such a diverse range of cellular processes.

1.3 Functions of SFKs

SFKs play diverse roles in many different cellular processes; including cytoskeletal rearrangement, differentiation, adhesion, migration, survival and immune function

(Thomas & Brugge, 1997) and function in all mammalian tissues. For the purposes of this study only the neuronal roles of SFKs are considered in detail.

1.3.1 SFKs in development

SFK signalling is crucial for a wide range of functions in neuronal development including neural tube formation, axonal growth and guidance, myelination and synapse stability. These functions are primarily mediated by Src, Fyn, Yes and Lyn; the major SFKs expressed in neurons. Src, Fyn and Yes are all broadly expressed throughout the central nervous system (CNS) (Maness, 1992) while Lyn expression is more restricted (Chen et al, 1996). The expression of Src and Fyn appears to be developmentally regulated, while the expression of Yes remains relatively unchanged throughout development (Inomata et al, 1994). Src and Fyn expression first occurs in neuroectodermal cells during neural fold formation at the onset of neuronal differentiation (Maness et al, 1986). Both Src and Fyn are enriched in the growth cone, or growing tip, of neurons and expression of both declines, although remains detectable, during neuronal maturation (Bixby & Jhabvala, 1993; Wiestler & Walter, 1988). However, there are differences in the expression patterns of Src and Fyn. Fyn expression is more highly enriched in axons than that of Src, and following sciatic nerve transection injury, Src expression is upregulated while Fyn expression remains constant (Zhao et al, 2003). This indicates that, despite being highly related, they mediate specific and individual roles within the neuron.

Surprisingly, the single knockout mice of Src and Yes have no detectable neurological deficits (Lowell & Soriano, 1996), although it is possible that reassessment using modern techniques for assessment of neuronal function may reveal more subtle phenotypes. In support of this, mice that are lacking Fyn will upregulate Src activity, presumably as a mechanism to compensate for the loss of Fyn activity (Grant et al, 1995; Stein et al, 1994).

The single knockout of Fyn does have some mild cognitive impairment, characterised by a reduction in long term potentiation (LTP), an activity dependent signalling cascade associated with the capacity to learn and form memories (Grant et al, 1992). $Fyn^{-/-}$ mice also show an associated defect in a test of the conversion of short term to long term memory. These phenotypes are thought to be due to mild morphological abnormalities observed in the hippocampus. The granule cell layer of

the dentate gyrus and the pyramidial cell layer of the CA3 region in the hippocampus have approximately 25% more neurons than wild type mice, indicating a role for Fyn in the regulation of neuronal differentiation and proliferation, possibly by influencing the extent of cell death. The brains of mice lacking Fyn have reduced global levels of tyrosine phosphorylation and phosphorylation of the SFK substrate FAK is reduced. FAK is also known to be a substrate of Src so it would be surprising if the effects of Fyn knockout were mediated through FAK as it would be thought that compensation through Src phosphorylation could occur.

$Fyn^{-/-}$ mice with a different strain background were shown to have a neurological defect in that the neonates fail to suckle (Yagi et al, 1993). This has been partially attributed to the 40-50% decrease in the amount of myelination observed in these mice (Sperber et al, 2001). Therefore, it seems that Fyn also plays a role in the myelination of neurons. Fyn is expressed in oligodendrocytes, the cells responsible for myelination, but the mechanistic requirement for Fyn in myelination remains to be elucidated. It is interesting that the two different $Fyn^{-/-}$ lines showed different phenotypes and therefore important that further investigation is carried out to rule out effects due to the strain background. It is possible that the production of a $Src^{-/-}$ mouse in a different strain background would reveal a phenotype.

Elucidation of SFK function from knockout studies is complicated by their high degree of functional redundancy and ability to compensate. A good indication that there is functional redundancy between the kinases is that the double knockout of Src and Fyn has a much more severe phenotype and the triple knockout of Src, Fyn and Yes is embryonic lethal (Stein et al, 1994).

Src, Yes and Fyn are all expressed in the growth cone, the growing tip of the developing neuron (Maness, 1992), but the functions of Src and its roles in mediating axon guidance are the most well studied. Src signalling is required downstream of axon guidance receptors and cell adhesion molecules including L1 and NCAM. Neurons taken from $Src^{-/-}$ mice are unable to extend on a substrate of L1-CAM but show wild type growth on laminin (Ignelzi et al, 1994). Conversely, neurons taken from $Fyn^{-/-}$ mice are unable to grow on a substrate of NCAM, while growth is normal on both L1-CAM and laminin (Beggs et al, 1994). These results indicate that both Src and Fyn play a role in the processes of neurite outgrowth, with Src signalling downstream of L1-CAM and Fyn signalling downstream of NCAM. These results indicate that, despite some amount of functional redundancy, the

individual isoforms of the SFKs are able to mediate individual functions within neurons. The subtle phenotypes were not observed in neuronal slices taken from single knockout mice as, in the intact brain, the neurons would be migrating through regions containing both L1-CAM and NCAM.

Inhibition of Src results in an increase of laminin mediated outgrowth in chick sensory neurons and application of tyrosine kinase inhibitors are able to promote neurite outgrowth in culture (Hoffman-Kim et al, 2002). In addition, application of the extracellular domains of L1-CAM or NCAM results in a decrease in tyrosine phosphorylation mediated by endogenous SFKs in the growth cone (Atashi et al, 1992). These data are in contrast with the previous neurite outgrowth studies that demonstrated a requirement for SFK signalling in neuronal outgrowth. This is probably because the SFKs play specialised roles in the processes of neuronal outgrowth and may be able to play opposing roles depending on the developmental stage. The differing effects could be achieved through the tight regulation of kinase activity and localisation.

In addition to roles in regulating neurite outgrowth as a response to L1-CAM signalling, Src is also involved in the internalisation and recycling of L1 between the plasma membrane and the endosomes (Schaefer et al, 2002). Therefore, Src signalling is able to influence neurite growth as a result of L1-CAM by at least two different mechanisms. The molecular basis for the role of Src in L1-CAM signalling will be discussed further in section 1.6.

Studies in *Drosophila melanogaster* have also provided evidence for a role of the SFKs in neuronal development. Overexpression of *Drosophila* Src in embryos is lethal and specific inhibition in the neuronal precursors of the developing eye results in a block of neuronal specification and differentiation (Kussick et al, 1993; Takahashi et al, 1996). This result would imply that Src kinase activity plays a positive role in the specification and differentiation of neurons.

SFK signalling has also been implicated in growth cone guidance signalling originating from a large number of pathways including responses to netrin, brain derived neurotrophic factor (BDNF), ephrin A and semaphorin 3A (Sema3A). The molecular basis for these responses will be discussed further in section 1.5.

1.3.2 SFKs in the mature brain

Synaptic transmission is the mechanism by which neurons in the CNS communicate. This communication occurs at specialised intercellular connections between the presynaptic nerve terminals and postsynaptic targets, called synapses. In the mammalian CNS, signalling at synapses is primarily chemically mediated and can be segregated broadly into two classes; excitatory and inhibitory. Transmission at excitatory synapses increases the likelihood that an action potential will be produced in the postsynaptic neuron and that the signal will be potentiated. This occurs through membrane depolarisation in the postsynaptic neuron. Conversely, transmission at an inhibitory synapse reduces the likelihood of an action potential being produced by eliciting membrane hyperpolarisation. Both excitatory and inhibitory synaptic transmissions are mediated by binding of neurotransmitters released from the presynaptic neuron to transmembrane receptors on the postsynaptic neuron. Normal CNS function is based on a balance between excitatory and inhibitory synaptic transmission and abnormality in this can result in neurological or psychiatric disease (Cline, 2005).

Signalling at excitatory synapses is predominantly mediated by glutamate released from the presynaptic cell by calcium dependent exocytosis of synaptic vesicles and binding to ionotrophic glutamate receptors in the postsynaptic cell membrane. There are three pharmacologically and molecularly defined classes of ionotrophic glutamate receptors, named according to their preferred agonists; the N-methyl-D-aspartate (NMDA), α-amino-3-hydroxy-5-methylisoxazole-3-proprionic acid (AMPA) and kainate receptors (Dingledine et al, 1999).

Glutamatergic synaptic transmission is dynamically controlled and highly plastic. This plasticity is essential for key physiological processes, but can also lead to disease states. Changes in the function, or number, of postsynaptic glutamate receptors is associated with the control of learning and memory (Bliss & Collingridge, 1993) but also chronic pain, epilepsy and neurodegeneration. Phosphorylation has emerged as a key regulatory process in the functions of glutamate receptors (Köles et al, 2001; Soderling & Derkach, 2000; Swope et al, 1999), with tyrosine phosphorylation, predominantly carried out by SFKs, crucial for the regulation of NMDA-R function and number (Ali & Salter, 2001; Salter & Kalia, 2004).

The neuronal functions of SFKs were originally thought to be limited to proliferation and differentiation. However, the discovery of SFKs in post-mitotic, differentiated neurons (Cooke & Perlmutter, 1989; Cotton & Brugge, 1983; Sudol & Hanafusa, 1986; Zhao et al, 1990) suggested a role beyond development, in the mature brain. In support of this, mice lacking Fyn or Lyn have behavioural abnormalities (Grant et al, 1992; Umemori et al, 2003). This suggests a role for the SFKs in the molecular processes of neuronal plasticity which often presents as a defect in learning and memory or behaviour in mouse models. The molecular mechanisms underlying these effects and the specific kinases and substrates involved are only recently beginning to be understood.

A major role of SFKs in the developed CNS is now thought to be the regulation of ion channels. The first ion channel identified as being regulated by SFKs was the NMDA-R (Wang & Salter, 1994). Subsequently potassium channels (Fadool et al, 1997), calcium channels (Cataldi et al, 1996), γ-aminobutyric acid type A ($GABA_A$) receptors (Moss et al, 1995) and nicotinic acetylcholine receptors (Wang et al, 2004) have all been shown to be regulated by SFK phosphorylation.

Native NMDA-Rs are multiprotein complexes, with the NMDA receptor subunits at their core and physical associations with numerous scaffold proteins, adaptor proteins and signalling enzymes (Husi et al, 2000). NMDA-R activation requires binding of both glutamate and the co-agonist glycine to sites in the extracellular domain. Once activated the channel becomes permeable to $K^{+,}$ Na^+ and Ca^{2+}. As an additional mechanism of regulation, the current passing through the channels can be mediated by a balance between phosphorylation and dephosphorylation.

Inhibition of endogenous tyrosine kinase activity or upregulation of phosphatase activity results in a reduction in NMDA-R mediated currents. Conversely, inhibition of phosphatase activity or increase of tyrosine kinase activity results in an enhancement of NMDA-R mediated current (Wang & Salter, 1994; Wang et al, 1996). Therefore, it was concluded that NMDA-Rs are regulated by the opposing actions of phosphorylation and dephosphorylation.

Both Src and Fyn are able to potentiate currents through recombinantly expressed NMDA-Rs in HEK cells (Köhr & Seeburg, 1996) or *Xenopus* oocytes (Chen & Leonard, 1996). Single channel recordings of NMDA-Rs showed that increasing tyrosine phosphorylation and inhibition of phosphatases results in an

increase in the gating properties of the channels with no change in the single channel conductance (Wang et al, 1996).

SFKs were first implicated in the regulation of NMDA-Rs because the SFK activating peptide (pYEEI), which works by binding to the SH2 domain of the SFKs, is able to increase the activity of NMDA-R mediated currents in both cultured neurons (Yu et al, 1997) and hippocampal slices (Lu et al, 1998). Src (Huang et al, 2001), Fyn (Suzuki & Okumura-Noji, 1995), Lck, Lyn and Yes (Kalia & Salter, 2003) are all found within the post-synaptic density (PSD) in the postsynaptic cell and Src (Yu et al, 1997), Fyn (Yaka et al, 2002), Lyn and Yes (Kalia & Salter, 2003) are all present within the NMDA-R complex. Therefore, there are multiple SFK family members located in the correct position to be able to regulate NMDA-R function. Src itself was implicated because application of both the inhibitory antibody (α-src1) (Roche et al, 1995) and the inhibitory peptide (Src40-58) (Yu et al, 1997), that are able to inhibit Src selectively over the other SFK family members, results in a reduction in NMDA-R mediated currents. This reduction occurs through a reduction in channel gating, the same effect observed when the SFKs were inhibited non-specifically. The peptide Src40-58 binds to the corresponding residues within the unique domain of Src. It has therefore been hypothesised that Src may be interacting directly with the NMDA-R via its unique domain and that application of the peptide prevents this interaction.

Direct SFK phosphorylation of neurotransmitter receptors is beginning to be established as the method by which SFKs may regulate synaptic transmission. NMDA-Rs are tetramers that consist of two NR1 subunits and two modulatory subunits (either NR2A-D or NR3A-D). Both Src and Fyn phosphorylate residues in the tails of NR2A and NR2B (Nakazawa et al, 2001; Yang & Leonard, 2001). Site directed mutagenesis studies have identified specific tyrosine residues that are phosphorylated by Src or Fyn when the NMDA-R subunits and the kinases are co-expressed in heterologous cells (Cheung & Gurd, 2001). The phosphorylation events have been demonstrated to have functional consequences and mutation of the residues required results in learning deficits (Nakazawa et al, 2006).

Src is also enriched in pre-synaptic vesicles (Linstedt et al, 1992) and has well characterised pre-synaptic targets including the synaptic vesicle proteins dynamin, synapsin (Foster-Barber & Bishop, 1998) and synaptophysin (reviewed by (Evans & Cousin, 2005)). The pre-synaptic association between Src and synapsin is

the best characterised and results in the regulation of synaptic vesicle trafficking (Messa et al, 2010).

1.4 Neuronal Src kinases

C-Src kinase has two splice variants expressed solely in neuronal tissue (Brugge et al, 1985; Pyper & Bolen, 1989; Pyper & Bolen, 1990). These have been termed N1- and N2-Src and contain short inserts within their SH3 domains, of 6 and 17 amino acids respectively (Martinez et al, 1987; Pyper & Bolen, 1990). The splicing event occurs between exons 3 and 4 of the C-Src mRNA. The N2-Src protein is a product of expression of both the N1 and N2 exons; expression of the N2 exon alone has never been observed. The reason for this remains unclear because expression of exon 3 and exon N2 would not result in an alteration of the reading frame (Black, 1992). Expression of the neuronal Src isoforms is suppressed in non-neuronal cells by binding of the polypyrimidine tract binding protein (PTB) to the intron sequence upstream of the N1 exon (Chan & Black, 1997; Chou et al, 2000). Neuronal Src expression is also under positive control in neuronal cells, with a sequence in the intron downstream of the N1 exon acting as a splice enhancer (Modafferi & Black, 1997).

The presence of alternative splicing of the C-Src gene product to produce neuron specific isoforms appears to be a feature of 'higher' animals, and is conserved in mammals, birds, reptiles and teleost fish (Raulf et al, 1989; Yang et al, 1989). It was later demonstrated that frogs have a neuron specific splice variant of C-Src but it has only a 5 amino acid insert in the SH3 domain rather than the 6 amino acids seen in other organisms. The charge of the amino acids contained within the insert is retained and it is therefore predicted to carry out similar functions to the kinases with a 6 amino acid insert (Collett & Steele, 1992; Collett & Steele, 1993). There is no N2-Src equivalent in frogs. In contrast to the comparatively late emergence of the N1-Src gene product, C-Src appears for the first time in the most primitive of multicellular organisms, the sponges (Barnekow & Schartl, 1984; Ottilie et al, 1992). This has led to the suggestion that the neuronal Src kinases may function in advanced brain functions including the molecular mechanisms underlying learning and memory. However, the *in vivo* substrates of the neuronal Srcs largely remain to be identified

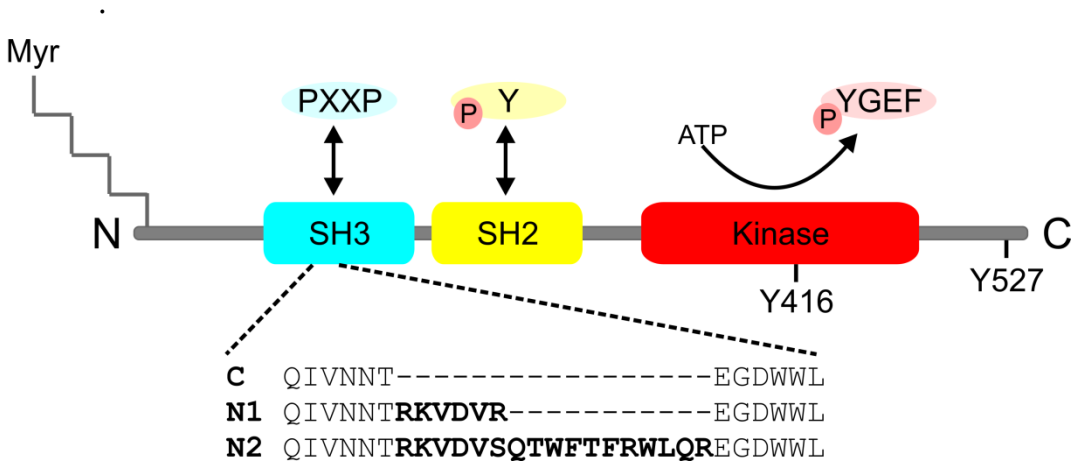

Figure 1.4.1 The N-Src kinases contain SH3 domain inserts.

The only structural difference between C-Src and the N-Src kinases is the presence of short SH3 domain inserts in the neuronal isoforms. The amino acid sequences of the insets are indicated. As previously indicated in Figure 1.2.1.1 the SH3 and SH2 domains are involved in substrate selection while the kinase domain is responsible for substrate phosphorylation. The important regulatory phosphorylation sites Y416 and Y527 are indicated and their significance discussed in section 1.2.2.

The SH3 domain inserts are within the n-Src loop, directly adjacent to the substrate binding site. Due to the critical role played by the SH3 domain in substrate recognition, it would be predicted that their binding to known C-Src ligands would be altered (Yu et al, 1992). Indeed, all studies that have looked specifically at N-Src binding have shown that it is either reduced or abolished, as compared to C-Src. The N1-Src SH3 domain does not interact with FAK or the neuron specific isoform FAK^{+} (Messina et al, 2003), dynamin or synapsin (Foster-Barber & Bishop, 1998), Tau (Reynolds et al, 2008) 3BP1 (Cicchetti et al, 1992) and shows reduced interaction with Sam68 (Finan Kellie, 1996). In fact, the N1-Src SH3 domain has been shown to interact with far fewer substrates than the C-Src SH3 domain in resting 3T3 cells (Weng et al, 1993).

Some putative N1-Src SH3 domain binding partners have been identified. The Ena/VASP-like protein (EVL), a PKA substrate shown to play a role in the regulation of actin dynamics, has been demonstrated to bind the N1-Src SH3 domain, while binding to the C-Src SH3 domain is minimal (Lambrechts et al, 2000). Currently, the functional implications of this interaction, and whether EVL is a substrate of the N1-Src kinase domain remains to be determined.

A yeast two-hybrid experiment performed in 1997 in the laboratory of Eric Kandel using the N1-Src SH3 domain as bait produced a single positively reacting fusion product (Santoro et al, 1997). The protein they isolated was shown to interact strongly with N1-Src but not C-Src, Fyn or Abl (a non-receptor tyrosine kinase belonging to a different family). Western blot analysis confirmed that the protein identified was expressed specifically in the brain, with no expression observed in any other tissue tested. Sequence analysis of the protein identified led Santoro et al to identify it as a novel cAMP and voltage-gated potassium channel.

It is now known that the protein identified by the Kandel lab is a hyperpolarization-activated and cyclic nucleotide gated (HCN) channel, HCN1. HCN channels are expressed both in the heart and the brain and are unique in that they are activated by membrane hyperpolarization rather than depolarization. A number of important neuronal functions are thought to be in part regulated by the currents produced by HCN channels. These are reviewed by Wahl-Schott and Biel (2009) and include maintenance of membrane potential, dendritic integration, constraint of LTP, motor learning and synaptic transmission.

The interaction of N1-Src with HCN1 has not been confirmed beyond the initial yeast two-hybrid interaction, although regulation of HCN channels by phosphorylation is not unprecedented. HCN2 has been shown to interact with the C-Src SH3 domain in yeast two-hybrid and GST pulldown experiments; the resulting phosphorylation both enhances the activation kinetics of the channel and regulates its trafficking (Zong et al, 2005). Regulation of HCN channel current by phosphorylation has been demonstrated under physiological conditions in the rat heart (Arinsburg et al, 2006) as well as neurons (Zong et al, 2005). This supports the idea that the HCN channels are indeed under phosphorylation control *in vivo* and that members of the SFKs are responsible. In addition, HCN channels contain extensive proline rich domains which are attractive potential SH3 domain ligands.

A second, biased, yeast two-hybrid experiment has identified another possible N1-Src substrate. Miyagi et al (2002) demonstrated that the SH3 domain of N1-Src can bind to Delphilin. Delphilin is a PDZ domain containing protein that interacts with the orphan glutamate receptor GluRδ2 (Miyagi et al, 2002). There is currently no biological role assigned to GluRδ2 and although its binding to Delphilin is under phosphorylation control, this phosphorylation is thought to be carried out by

PKA. Sequence analysis of Delphilin reveals that it does contain a proline rich region with a number of PxxP motifs that could potentially bind to an SH3 domain.

In addition to differing substrate specificities, the expression patterns and subcellular localisation of the neuronal Src kinases may differ from those of C-Src. C-Src and N1-Src are both enriched in axons and dendrites compared to the cell soma (Sugrue et al, 1990). N1-Src activity first occurs slightly later than that of C-Src but N1-Src activity increases sharply at E12 and remains substantially higher than C-Src into the adult mouse (Wiestler & Walter, 1988). It is generally agreed that both C- and N1-Src are present in the growth cones of developing neurons (Brugge et al, 1985; Maness et al, 1990), but it has been reported that N1-Src may be preferentially recruited to lipid rafts (Mukherjee et al, 2003). Lipid raft localisation of Src would not be expected because it is normally the dual lipid modified SFKs (not Src or Blk) that are found in lipid rafts.

The presence of the additional residues within the N-Src SH3 domain has also been shown to result in an increase in the tyrosine kinase activity of the proteins. This increased activity has been repeatedly reported in association with the neuronal kinases (Brugge et al, 1985; Levy & Brugge, 1989), but there do seem to be some instances in which the activities of C- and N-Src do not differ greatly (Yang & Walter, 1988); implying that the activity of the N-Srcs can be regulated. Highly active SFKs, such as v-Src, are known to illicit cellular transformation while their normal cellular counterparts are not transforming (Kmiecik & Shalloway, 1987). The transforming potential of N1-Src was found to be intermediate between the non-transforming C-Src and the highly transforming v-Src (Levy & Brugge, 1989).

Mutational analysis of the C-Src SH3 domain has revealed the importance of the n-Src loop in the regulation of the kinases. Mutation of a residue within the n-Src loop (D117N) results in an increase in kinase activity (Brábek et al, 2002). This increase in activity has been interpreted as a reduction in the ability of the SH3 domain to form the SH3:linker intramolecular association that normally constrains the activity of the kinase. The presence of an insert in the n-Src loop is thought to decrease the folding rate but not affect the overall structure of SH3 domains on a large scale (Grantcharova et al, 2000).

Existing studies into the functions of the N-Src kinases point to roles in neuronal development. Kotani et al (2007) showed that overexpression of a constitutively active form of N1-Src specifically in the Purkinje cells of mice

resulted in aberrant neurite outgrowth and cell body mislocalisation, while overexpression of constitutively active C-Src had little effect. The aberrant outgrowth was shown to be restricted to the dendrites, with axons appearing morphologically normal. Overexpression of C- and N1-Src in the developing *Xenopus* retina were also shown to differentially impair neurite outgrowth (Worley et al, 1997). In this case, it is the axons that are primarily affected, with the axons of C-Src overexpressing ventral forebrain neurons shorter than the control and N1-Src overexpressing neurons longer. Conversely, in the neurons of the optic pathway, overexpression of constitutively active N1-Src acted to inhibit axonogenesis. Work by Schmidt et al (1992) has also identified a role for N1-Src in the inhibition of neuronal differentiation. It is not yet clear why the overexpression has differing effects in the two neuronal types but it is possible that the kinase may be interacting with different substrates in the various neuronal cell types investigated.

There are currently no known potential N2-Src substrates. However, there is a known association between N2-Src expression levels and prognosis for the cancer neuroblastoma. Neuroblastoma is a childhood cancer of neural crest derivation and is the most common solid tumour diagnosed in children. The tumour cells of neuroblastoma are arrested at various stages during their differentiation and the grade of differentiation is related to the clinical course and prognosis (Rudolph et al, 1997). In general, a more differentiated tumour is considered to be less aggressive. Neuroblastomas are divided into stages 1 to 4 and 4s according to the International Neuroblastoma Staging System (Brodeur et al, 1988). An intriguing property of stage 4s tumours is their ability to spontaneously differentiate to mature non-proliferative cells resembling ganglion cells (Evans et al, 1980). The age of the patient is known to be an important factor in this phenomenon. Infants (under 1 year) are commonly diagnosed with stage 4s disease and an associated good prognosis, whereas older children frequently have a more aggressive form of the cancer. Interestingly, infant stage 4s tumours appear by histology to be poorly differentiated but the occurrence of spontaneous remission into histologically differentiated cells means that they do possess the ability to differentiate over time (Evans et al, 1980).

Neuronal Src has been shown to be expressed in neuroblastoma and retinoblastoma tumours but not in Askin tumours or esthesioneuroblastoma, which are also derived from neuronal tissue (Bjelfman et al, 1990a). The neuronal Srcs are not expressed in non-neuronal derived tumours. Importantly, low stage and stage 4s

infant neuroblastomas have high levels of N2-Src expression, indicating that N2-Src expression is an indicator of the capacity of a tumour to differentiate. In contrast neuroblastomas expressing only C-Src or C- and N1-Src are more often malignant; this type of tumour is typical in older children (Bjelfman et al, 1990a; Matsunaga et al, 1993). In general, tumours that are expressing more N2-Src than C-Src are less aggressive than the converse situation and have a good prognosis.

N2-Src has therefore been considered to be a potential marker both for the identification of neuroblastoma as opposed to other neuronal derived tumours and a prognostic marker of the severity of the disease and a predictor of a tumour's capacity to spontaneously differentiate.

1.5 Neuronal development mediated by guidance cues

The complex array of information processing carried out by the brain relies on an intricate network of connections forming between neurons. In the adult human approximately 1 trillion neurons make on average 1000 connections and the precise patterning of these interactions is essential for normal neuronal function. Connections between neurons form during neuronal development when each developing neuron produces an axon. At the growing tip of this axon is a structure called the growth cone that is responsible for the guidance of the axon to the correct location. The growth of a new axon *in vivo* appears to occur in a directed manner with few errors and it was therefore assumed that axon grow in direct response to guidance cues.

Over a century ago Ramon y Cajal proposed that axon guidance may be mediated by chemoattraction. This model was refined in the 1940s by Roger Sperry's chemoaffinity hypothesis (Sperry, 1963). Cell culture experiments have since confirmed that neurons will grow towards their target cells, indicating the presence of diffusible chemoattractive substances. The converse is also true, with axons shown to grow away from cells that they would not make contacts with *in vivo*. In addition to the long range actions of chemoattraction and chemorepulsion, axon growth has also been shown to be regulated by short range contact-mediated mechanisms involving non-diffusable cell surface or ECM molecules. It is known that axon growth in culture requires a substrate for growth that is both adhesive and allows growth, as not all neurons are able to grow on all adhesive substrates. Contact

repulsion is also observed in culture. These processes are reviewed by Tessier-Lavigne and Goodman (1996).

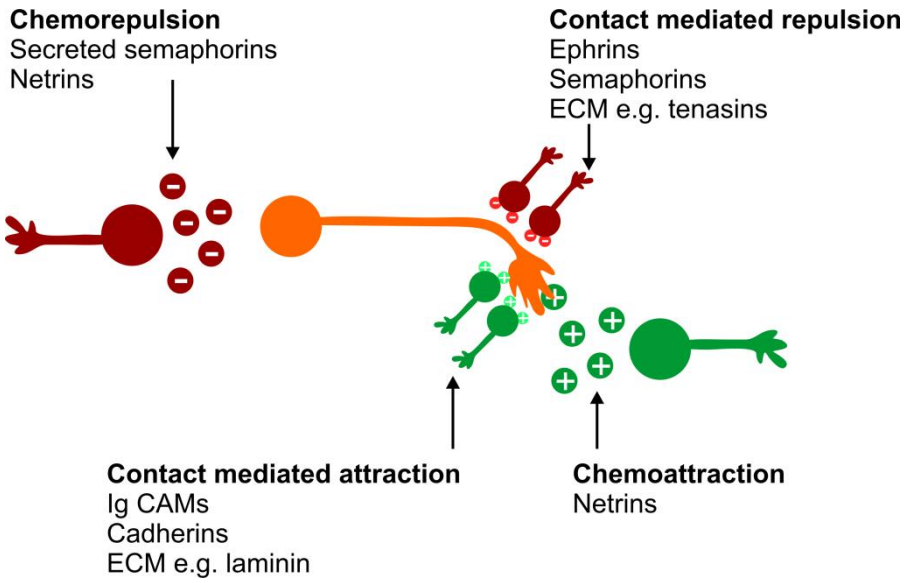

Figure 1.5.1 The principles of guidance molecule regulation of axon growth.
There are multiple signalling pathways capable of regulating axon guidance, meaning that a growing axon can be guided, probably simultaneously, by multiple guidance cues. The growth of an axon can be directed away from one area by chemorepulsion while attracted towards another by chemoattraction.

Developing neurons can respond to multiple signals to modulate the extent and direction of their growth. These broadly fall into two classes; attractive and repulsive and can be either diffusible or contact mediated.contact-mediated attractive and repulsive cues can allow the fine tuning of directionality. Many of the molecules that mediate these guidance cues and their cell surface receptors have been established have commonly been shown to be modulated by phosphorylation, specifically SFK phosphorylation. The major signalling pathways and the roles of SFK mediated phosphorylation are outlined below.

1.5.1 Eph family of ephrin receptors

The Eph family are a family of RTKs that bind to and are activated by the extracellular domain of their ligands, ephrins, which are tethered to neighbouring cells. EphA signalling results in the regulation of neurite outgrowth by linking to the

actin and microtubule cytoskeleton (Weinl et al, 2003). These signalling events are mediated through a large number of pathways including MAP kinase, PI3K, p190rhoGAP/rasGAP and SFK signalling (Kullander & Klein, 2002). EphA activation results in a repulsive response, mediated by growth cone collapse.

SFKs bind to the juxtamembrane region of the activated EphA receptor via two conserved and phosphorylated tyrosine residues (Zisch et al, 1998). This results in the activation of EphA kinase activity and allows it to phosphorylate substrate proteins. Inhibition of SFKs though chemical means or by overexpression of the regulatory kinase Csk results in the abolition of EphA mediated repulsion (Wong et al, 2004). The main protein targets of the SFK were shown by IP to be ephexin and cortactin (Knöll & Drescher, 2004). Ephexin is a RhoGEF that is activated by phosphorylation and signals to RhoA, Rac and Cdc42 in order to regulate cytoskeletal dynamics. Ephexin signalling activates RhoA, a negative regulator of neurite outgrowth.

Cortactin is an actin binding protein that plays a key role in *de novo* actin polymerisation (Weed & Parsons, 2001). It is known to localise to growth cones (Du et al, 1998) and to interact with EphA receptors (in muscle cells) (Lai et al, 2001). SFK phosphorylation is known to be Src dependent (Thomas et al, 1995) and to decrease the activity of cortactin (Huang et al, 1997), resulting in a decrease in the amount of neurite outgrowth. The SFK member responsible remains to be elucidated but it is known that while Src, Yes and Fyn all bind to Eph A, Src does so with the highest affinity (Zisch et al, 1998).

In addition to the phosphorylation of downstream signalling molecules, the SFKs are also able to directly phosphorylate EphA receptors. This was demonstrated by overexpression of Fyn and EphA in SYF cells, cells that lack essentially all tyrosine kinase activity (Klinghoffer et al, 1999). It is predicted that this phosphorylation would act to create binding sites for other EphA interacting partners.

1.5.2 Trk family of neurotrophin receptors

The Trk proteins are also a family of RTKs and act as receptors for members of the neurotrophin family. Seminal work by Rita Levi-Montalcini identified nerve growth factor (NGF) several decades prior to the discovery of Trk receptors (see Levi-

Montalcini, 1987 for review). Trk receptors are now known to be highly expressed throughout the CNS and their expression is developmentally regulated, a property that first indicated that they may play a role in the regulation of neurite outgrowth (Ringstedt et al, 1993). Trk proteins are involved in a large range of neuronal processes including the regulation of proliferation, survival, axonal and dendritic growth and remodelling, association with and remodelling of the cytoskeleton and synapse formation, function and plasticity (Huang & Reichardt, 2001). There are three main Trk receptors; TrkA, B and C that can be generally considered to be activated by the neurotrophins NGF, BDNF or NT3 or NT4 respectively, however alternative splicing adds to the complexity of their signalling (Huang & Reichardt, 2001).

Classically, Trk receptor activation results in the activation of the MAP kinase signalling pathway, resulting in gene transcription by CREB and the promotion of neurite outgrowth. There is also evidence that Trk receptors can be activated by at least two G-protein coupled receptors; the adenosineA_{2a} and PAC-1 receptors (Lee & Chao, 2001; Lee et al, 2002). Activation by this mechanism has different kinetics to classical activation and acts over hours rather than minutes. This form of activation is dependent on both intracellular calcium and SFKs but not on PKA or PKC. The SFK member required and how it acts remains to be elucidated.

Src itself is also directly implicated in mediating Trk signalling. Classical Trk signalling results in Ras activation and activated Ras can induce the sequential activation of RalGDS (guanine nucleotide disassociation stimulator), Ral and C-Src (Ouwens et al, 2002). Activated C-Src is then able to mediate effects on neuronal outgrowth through phosphorylation of proteins that play a role in cytoskeletal dynamics.

In addition to signalling downstream of Trk activation, C-Src can be directly recruited to the Trk signalling complex. Activated Trk becomes phosphorylated at Y490, resulting in the recruitment of the FGF receptor substrate-2 (Frs2). Frs2 is then itself phosphorylated, creating a binding site for a number of adaptor proteins and signalling molecules, including C-Src (Yan et al, 2002). Recruitment of C-Src to this position has been suggested to increase neurite outgrowth in a manner distinct to the MAP kinase signalling pathway because activation of C-Src is able to increase neurite outgrowth without affecting the kinetics of MAPK signalling in PC12 cells (Marshall, 1995).

1.5.3 Netrin receptors and netrin

Netrins act to promote neurite outgrowth and pathfinding through binding to netrin receptors. Netrin and netrin receptors are highly conserved in invertebrates and vertebrates (Serafini et al, 1994) and therefore a large number of the studies into their functions have been carried out in Caenorhabditis *elegans*, a genetically tractable organism. Netrin1 is the prototypical member of the netrin family in vertebrates and its homolog in *C. elegans* is UNC6. The netrin receptors are UNC40 and UNC5 in *C. elegans* and their mammalian homologues are DCC (deleted in colorectal cancer), neogenin and UNC5A-D. DCC/UNC40 are thought to mediate both attractive and repulsive forces while UNC5 solely mediates repulsive forces. Vertebrate netrin signalling is thought to act predominantly though phospholipase C (PLC), PI3K, MAP kinases and the small GTPases Cdc42 and Rac in order to mediate neurite outgrowth (Moore et al, 2007). Netrin binding to netrin receptors is known to induce phosphorylation of FAK, a cytoplasmic tyrosine kinase with documented roles in a wide range of processes including adhesion, spreading, migration, survival, cell cycle progression and proliferation (Serafini et al, 1994). The phosphorylation of FAK is required for netrin mediated neurite outgrowth (Liu et al, 2004). The activity of SFKs is required for netrin induced FAK phosphorylation and chemical inhibition of SFKs results in reduced neurite outgrowth (Li et al, 2004). Therefore, SFK activity is required to mediate the neurite outgrowth effects of netrin signalling. It is thought that SFK signalling activates a signalling cascade through RhoGTPases resulting in the regulation of actin polymerisation and cytoskeletal dynamics.

1.5.4 Semaphorins

Semaphorins are a large family of cell surface and secreted guidance proteins that are defined by a Sema domain of approximately 420 residues, at their N-termini. Semaphorins signal through large, multimeric receptor complexes and their primary receptors are thought to be plexins. Semaphorin class 3 proteins are vertebrate Semaphorins that are secreted and bind to vertebrate PlexinA proteins in a receptor complex that also contains neuropilin (Nakamura et al, 2000).

As previously described for netrin signalling, an activation and association between FAK and SFKs is also required for Semaphorin3B (Sema3B) signalling (Falk et al, 2005). Interestingly, in this case FAK/SFKs are only required for attractive signalling and not repulsive, even though both can be mediated by Sema3B binding. In the attractive condition, Sema3B binding results in the recruitment of Src to membrane associated FAK. Fyn only becomes phosphorylated and associates with FAK under attractive conditions. Notably, the application of a SFK inhibitor not only abolished the attractive response of axons to Sema3B but converted it to a repulsive response.

More recently, evidence has emerged that Src/FAK signalling may be involved in repulsive signalling pathways mediated by the semaphorin Sema3A (Bechara et al, 2008; Chacón et al, 2010).

1.5.5 Slit and Robo

Slits are secreted proteins that bind to their receptor Robo (Roundabout) and act to modulate axon guidance (Brose et al, 1999). There is currently no known requirement for tyrosine phosphorylation or SFK signalling in the modulation of Slit/Robo signalling.

1.6 Cell adhesion molecules in neuronal development

At all stages during their development, growing neurons are able to respond to extracellular cues to regulate their development. Signalling resulting from cell adhesion molecules is required at the early stages of development for neurite induction, proliferation and migration and later in development is involved in growth cone guidance to postsynaptic targets and synapse formation. Cell adhesion molecules are expressed throughout development in the mammalian nervous system and their general role is to mediate both homophilic or heterophilic interactions with neighbouring cells and with the extracellular matrix (Walsh & Doherty, 1997). These interactions initiate signalling cascades that ultimately either positively or negatively regulated neurite outgrowth. In this way the extension length and position of the growing neuron is heavily influenced by the signalling arising from the interactions of neuronal recognition molecules. With relevance to the findings presented in

Chapter 5, further discussion of cell adhesion molecules will focus on the functions of the L1 family of cell adhesion molecules belonging to the Ig superfamily.

1.6.1 L1-CAM family

L1-CAM is the founding member of the L1 family of cell adhesion molecules. The family consists of L1, CHL1 (close homolog of L1), NrCAM and neurofascin. L1 family members share a conserved domain organisation with a large extracellular portion and a short C-terminal cytoplasmic tail. The extracellular portion consists of 6 Ig domains and 4-5 fibronectin type III (FnIII) domains. It is the site of interaction for a wide range of ligands including integrins, components of the ECM and homophilic interactions with other L1 molecules. The intracellular portion links to the actin cytoskeleton and acts to relay extracellular messages across the plasma membrane and initiate intracellular signalling cascades (Walsh & Doherty, 1997). The structural similarity of the L1-CAM family members results in partial functional overlap (Sakurai et al, 2001).

L1-CAM signalling plays important roles throughout neuronal development and is implicated in migration, growth, pathfinding, synapse formation and plasticity (Crossin & Krushel, 2000). From early embryonic development (E9.5) L1-CAM is found expressed on the cell bodies of migrating neurons and later in development is strongly expressed on growing axons (Kallunki et al, 1997). This then declines to more moderate levels postnatally. L1-CAM knockout mice have errors in axon guidance (Cohen et al, 1998) and defects in LTP (Bliss et al, 2000); indicating a role for L1-CAM in both the developing and mature brain.

The importance of L1-CAM mediated signalling in neuronal function is indicated by the large number of mutations in the L1-CAM gene that have been associated with impaired cognitive ability. The L1-CAM mutations have been grouped together into the syndrome CRASH, characterised by corpus callosum hypoplasia, retardation, adducted thumbs, spasticity and hydrocephalus (Yamasaki et al, 1997). A similar phenotype is also observed in mice lacking the L1-CAM protein (Demyanenko et al, 1999).

L1-CAM is known to act as a potent regulator of axonal growth and branching in experiments where is it employed as a substrate or overexpressed. The

mechanism of this is thought to involve the linkage between L1-CAM and the cytoskeleton, mediated by ankyrins and ezrin-radixin-moesin (ERM) proteins.

1.6.1.1 L1-CAM and ankyrins

Ankyrin B (ANK2) and ankyrin G (ANK3) are both known to bind to the cytoplasmic tail of L1-CAM and to provide a link to the actin cytoskeleton. This association is thought to act to stabilise L1-CAM expression at the plasma membrane. Homophilic binding of L1-CAM is known to result in the recruitment of ankyrins and this binding is then mediated by a MAP kinase dependent pathway (Malhotra et al, 1998).

The conserved sequence FIGQY in the cytoplasmic tail is phosphorylated as a result of ERK activation (Whittard et al, 2006). The tyrosine kinase that carries out the phosphorylation remains to be elucidated but does not appear to be Src. Phosphorylation at this residue prevents the L1-CAM interaction with ankyrin and results in the promotion of neurite outgrowth (Gil et al, 2003). Transgenic mice carrying a mutation at the residue required for phosphorylation (Y1229H) have altered morphology of retinal axons and abnormal interstitial branching (branching that occurs along an established axon rather than at the growth cone) (Buhusi et al, 2008). They also have impaired elongation and branching of interneurons (Guan & Maness, 2010).

The interaction with ankyrin G is quite well established to promote stationary behaviour (Gil et al, 2003). However, the role of ankyrin B remains less clear. Neurons of mice lacking ankyrin B display hypoplasia of axonal tracts and also reduced steady state levels of L1-CAM expression (Scotland et al, 1998). This would indicate that ankyrin B mediates similar functions to ankyrin G in stabilising L1-CAM. Ankyrin B is also shown to co-localise with L1-CAM in developing axons while ankyrin B does not. Furthermore, the L1-CAM interaction with ankyrin B has been demonstrated to be involved in neurite formation but not elongation (Boiko et al, 2007). These results are somewhat contradictory to the findings of Gil et al (2003) and Cheng et al (2005) and the roles of ankyrin B interaction with L1-CAM remain controversial.

1.6.1.2 L1-CAM and ERM proteins

The ERM proteins are known to function to link the actin cytoskeleton to various transmembrane proteins, including L1-CAM (Dickson et al, 2002). There are two ezrin binding sites in the cytosplasmic tail of L1-CAM, one of which is located in the neuron specific sequence YRSLE (Cheng et al, 2005a; Sakurai et al, 2008). The interaction with ezrin is known to be involved in the modulation of neurite outgrowth and branching. Overexpression of a dominant negative form of ezrin results in an increase in the amount of branching of neurons grown on a substrate of L1-CAM (Dickson et al, 2002). This indicates that ezrin interaction normally functions to negatively regulate outgrowth. Mutation of the ezrin binding sites in the cytoplasmic tail of L1-CAM results in a decrease in the amount of branching observed (Cheng et al, 2005a). The reason for these contradictory results for the function of ezrin-L1-CAM interaction remains unclear.

The YRSLE motif also forms the binding site for the μ2 subunit of the AP2 adapter complex. Binding of both ezrin and AP2 is abolished by phosphorylation at this tyrosine residue (Sakurai et al, 2008; Schaefer et al, 2002). Therefore, in addition to modulating the interaction with ezrin, phosphorylation at this site is also able to regulate the trafficking of L1-CAM to and from the plasma membrane. It is thought that ezrin and AP2 are within different membrane domains within the cell and that competitive binding does not occur (Kamiguchi & Lemmon, 2000; Kamiguchi & Yoshihara, 2001). Phosphorylation at this residue could therefore allow for two distinct mechanisms of regulation of L1-CAM signalling.

1.6.1.3 Interplay between L1-CAM and other guidance pathways

In addition to direct linkage to the cytoskeleton, classical activation of L1-CAM through homophilic binding results in the activation of FAK in a SFK dependent manner and subsequent activation of the MAPK pathway resulting in neurite outgrowth (Schafer & Frotscher, 2012). This mechanism of signal transduction has previously been introduced in relation to netrin and semaphorin signalling and will be discussed further in section 1.7. L1 homophilic binding is also known to result in the transient activation of Src, which in turn initiates the sequential activation of phosphoinositide 3-kinase (PI3K), the Vav2 guanine nucleotide exchange factor

(GEF), Rac1 and PAK1, again resulting in MEK1/2 and ERK1/2 activation (Schafer & Frotscher, 2012). Therefore, L1-CAM signalling can proceed by at least two different signalling pathways that converge on the MAP kinase pathway to modulate outgrowth.

L1-CAM can also signal through heterophilic interactions with other guidance cue receptors, including the fibroblast growth factor receptor (FGF-R) (Saffell et al, 1997). This interaction ultimately results in neurite outgrowth in a calcium dependent manner (Doherty et al, 2000). L1-CAM and the netrin receptor DCC have been shown to co-localise in response to the application of Netrin, resulting in an increase in axon growth (Antoine-Bertrand et al, 2011) and L1-CAM expression in growth cones has been demonstrated to increase in response to neurotrophin stimulation (Marsick et al, 2012). Both of these responses are thought to be mediated through the L1-ezrin interaction. A requirement for L1-CAM is also known in Sema3A mediated growth cone collapse, a signalling pathway that mediated negative effects on neurite outgrowth (Castellani et al, 2000; Castellani et al, 2004).

L1-CAM signalling in conjunction with integrins to promote cell migration and neurite extension is also an established mechanism of heterophilic interaction. Clustering of L1-CAM molecules in the cell membrane promotes adhesion to the extracellular matrix through certain members of the integrin family and acts to potentiate mobility and migration (Felding-Habermann et al, 1997). The mechanism of this action is unclear. In some cases a conserved RGD motif in the 6^{th} Ig domain of L1-CAM is required (Thelen et al, 2002) but it can also occur through non-RGD binding integrins. In this case the interaction is possibly mediated by a dibasic motif in the 3^{rd} Fn III domain (Silletti et al, 2000). Therefore, it is unclear whether there is a direct interaction between the L1-CAM extracellular domain and the integrins or whether intermediate binding partners facilitate the interactions.

Signalling through β1 integrins can act through Src, PI3K, Rac1 and PAK1, just as L1-CAM signalling does (Ridley et al, 2003). Therefore it can be assumed either that L1-CAM is able to signal directly through its association with integrins or that the two pathways converge at an early point and mediate the same effects. It is known that L1-CAM can associate with RanBPM, an adaptor protein that couples integrins and growth factor receptors to the Ras/ERK pathway (Cheng et al, 2005b). This interaction provides a possible mechanism by which the L1-CAM and integrin signalling pathways could converge.

1.7 Src/FAK activation – a general mechanism for the modulation of neurite outgrowth

In addition to the numerous guidance cue specific SFK mediated signalling pathways, an association between SFKs and FAK has been shown to play an important role in the signalling resulting from netrins, semaphorins, ephrins (in prostatic carcinoma cells) (Parri et al, 2007), cell adhesion molecules and integrins, as described above. Therefore it seems that SFK activation and signalling represents a general mechanism used by cells to respond to guidance cues. The signalling cascades activated and how the integration of the numerous inputs is achieved remains unclear.

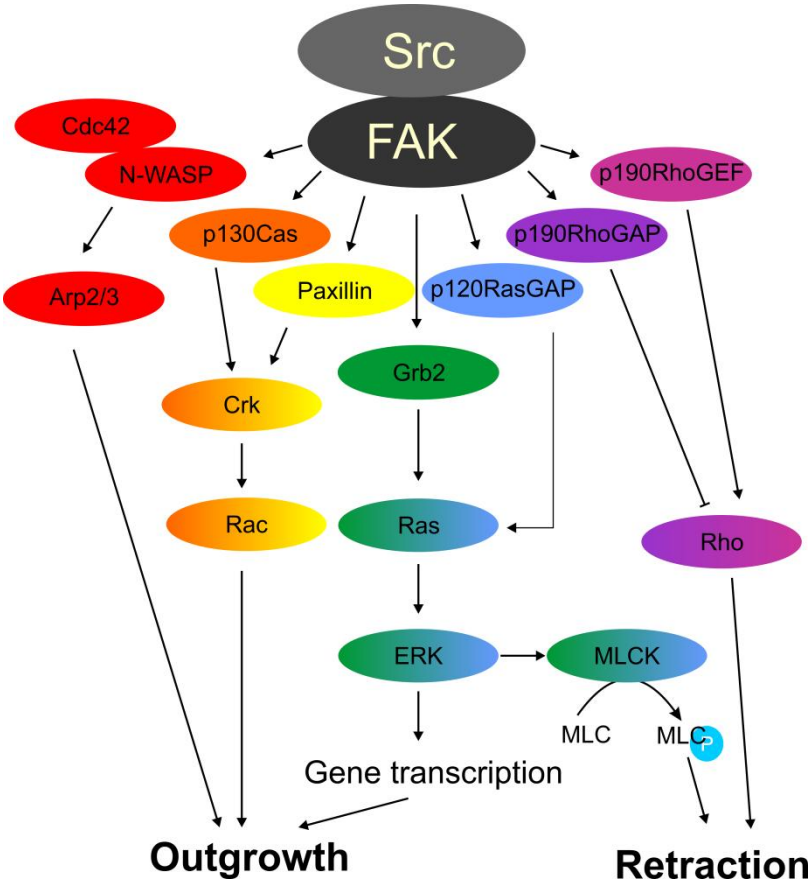

Figure 1.7.1 The Src/FAK complex acts through many distinct pathways to modulate neurite outgrowth.

The interaction of Src with FAK forms an active complex that is able to feed into many signalling pathways that act to both positively and negatively modulate neurite outgrowth. The activation of this complex is known to occur as a result of activation by many guidance cue and cell adhesion mediated interactions at the plasma membrane. The downstream signalling events of the Src/FAK complex occur predominantly through the modulation of the activities of the small GTPase Rac, Ras and Rho.

Extracellular guidance cues and adhesion molecules interact with their binding partners at the plasma membrane through homophilic and heterophilic intertactions, triggering signalling cascades in the growth cone. In order to respond appropriately to these cues a cell must be able to integrate them and to produce a co-ordinated response. This led to the hypothesis of a master regulator of guidance cue signalling. FAK is a cytoplasmic kinase that interacts with a complex network of adaptors and signalling molecules via multiple phosphorylation sites. Importantly, it is known to regulate the responses to both attractive and repulsive guidance cues in response to a wide range of guidance cues, outlined above.

FAK signalling is able to link external signals to multiple intracellular pathways and to control cell shape and motility through modulation of the cytoskeleton. This link to the cytoskeleton is crucial to elicit the cells response to guidance cues and FAK has come to be regarded as a hub for integration of guidance cue signalling (Chacon & Fazzari, 2011).

The mechanisms by which FAK signalling is able to result in cytoskeletal rearrangement are not quite well established and have been shown to be reliant on the signalling of SFKs. The autophosphorylation of FAK is known to be an early event in its signalling and this creates a binding site for the SH2 domain of Src (Schaller et al, 1994). Src binding to this residue results in Src activation and the creation of a dual activated Src-FAK signalling complex. Src phosphorylates FAK at Y576 and Y577, residues within the FAK activation loop (Calalb et al, 1995). This results in the stabilisation of the active conformation of FAK and the perpetuation of FAK signalling. Src is also able to phosphorylate FAK at multiple other residues resulting in the creation of binding sites for other proteins (Chacon & Fazzari, 2011).

Src phosphorylation of FAK at Y861 results in the SH3 domain mediated recruitment of p130Cas to FAK (Lim et al, 2004). p130Cas is subsequently phosphorylated by the Src-FAK complex which results in the recruitment of the adaptor protein Crk via its SH2 domain (Brábek et al, 2004; Cho & Klemke, 2002). This results in an increase in Rac activity and a correlated increase in motility and neurite outgrowth.

By a mechanism similar to the p130Cas mediated neurite outgrowth, the Src-FAK complex also phosphorylates paxillin, which again results in Crk binding (Petit et al, 2000; Turner, 2000) and an increase in motility (Subauste et al, 2004).

Src phosphorylation of FAK at Y925 creates a binding site for the Grb2 SH2 domain. This stimulates Ras activity and signalling through the ERK1/2 and MAP kinase pathways. It is known that one consequence of this is the ERK2 mediated phosphorylation of myosin light chain kinase that results in growth cone collapse and contraction (Chen et al, 2002). However, as previously described, ERK1/2 activation also results in gene transcription of factors that promote neurite outgrowth. How the balance between these similar pathways is achieved is unknown.

FAK signalling commonly acts through modulating the activity of small GTPases including Ras and the Rho family Rho, Rac and Cdc42. This can occur downstream as a result of recruitment of signalling proteins including p130Cas, paxillin and Grb2 as discussed above but FAK can also mediate direct effects on Ras/Rho signalling through modulation of their guanine nucleotide exchange factors (GEFs) and GTPase activating proteins (GAPs) (Tomar & Schlaepfer, 2009). GEFs and GAPs positively and negatively regulate Ras/Rho activities respectively.

FAK activation results in the binding and sequestering of p120RasGAP, reducing its association with active Ras and resulting in Ras activation (Hecker et al, 2004). The consequence of this is an increase in neurite outgrowth.

In $FAK^{-/-}$ cells RhoA activity is elevated (Ren et al, 2000), indicating that FAK normally has an inhibitory effect on RhoA signalling. In support of this, integrin signalling is known to promote neurite outgrowth by reducing RhoA activity via Src-FAK mediated phosphorylation of p190RhoGAP (Arthur et al, 2000; Sieg et al, 2000). This phosphorylation event increases the GAP activity and results in an inhibition of Rho A, resulting in a positive effect on neurite outgrowth. In contrast, FAK can also act through p190RhoGEF to activate Rho A (Lim et al, 2008; Zhai et al, 2003), which results in a stabilisation of the actin cytoskeleton and the inhibition of outgrowth.

FAK also acts through Cdc42 to modulate cell motility. FAK binds to and phosphorylates the Cdc42 effector N-WASP after it has been activated by Cdc42 (Wu et al, 2004). N-WASP acts to regulate the cytoskeleton through activation of the Arp2/3 complex. FAK phosphorylation of N-WASP results in an activation of the Arp2/3 complex and an increase in neurite outgrowth (Zhang et al, 2005).

FAK can be seen to feed into a large number of signalling pathways. Stimulation by different input mechanisms is able to fine tune the FAK response so that it can mediate the diverse responses of attraction and repulsion. It remains to be

elucidated how different inputs are able to activate FAK by different mechanisms and whether any of the pathways predominate in the cell. However, the role played by the SFKs is crucial to the actions of FAK and therefore the cellular response to guidance cues.

1.8 Hypothesis

The work presented in this thesis aimed to address the hypothesis that, due to their altered SH3 domains, the substrate preferences of the neuronal Src kinases are different to those of C-Src. It was also predicted that their altered substrate specificities would tailor the activities of the neuronal Srcs to brain specific functions.

In order to investigate the substrate preferences of the kinases an *in vitro* kinase assay was developed. This assay was able to assess phosphorylation of short GST-tagged peptides and to reveal differences in substrate preferences due to the altered SH3 domains. The technique of phage display was subsequently used to identify a novel SH3 binding motif for the N1-Src SH3 domain.

The functional roles of the neuronal Src kinases were assessed by transfection of the individual kinase isoforms into both fibroblasts and cultured neurons. The morphology of these cells was then analysed to reveal roles for the neuronal Srcs in the control of cell morphology. Finally, a role for N1-Src in the L1-CAM signalling pathway was identified by measuring the outgrowth of neurons grown on a substrate of L1-CAM.

2 Materials and Methods

2.1 Materials

Oligonucleotides were ordered from Eurogentec (Seraing, Belgium). Ligase and ligase buffer were purchased from Promega (Fitchburg, WI). The enzymes BamHI, EcoRI, SalI, NotI and BglII were purchased from NEB (Ipswich, MA). Mini prep kits were ordered from Machery-Nagal (Düren, Germany) and midi-prep kits and gel extraction kits were ordered from Qiagen (Venlo, Netherlands). Taq polymerase was a kind gift from Dr Daniel Ungar, University of York. The plasmid pGEX-6P-1 was from GE Healthcare (Waukesha, WI), pFLAG-N1 was made in house by Dr Gareth Evans by replacing GFP in pEGFP-N1 with the FLAG tag sequence and pmCer-C1 was a gift from Dr Rory Duncan (Herriot Watt University) (Rizzo et al, 2004). Glutathione-Sepharose, Ni^{2+}-Sepharose and Protein G-Sepharose beads and peptides were purchased from GenScript (Piscataway, NJ). PreScission Protease was purchased from the Technology Facility in the Department of Biology, University of York. Protein ladders were purchased from BioRad (Hercules, CA). PVDF (Immobilon-P) was purchased from Millipore (Billerica, MA). The primary antibodies used for Western Blotting, immunocytochemistry and immunoprecipitation were α-PY20 from BD Bioscience (San Diego, CA), α-GFP serum; a kind gift from Dr Paul Pryor, University of York, α-FLAG (M2) from Sigma (St. Louis, MO), α-pY416 and α-pY527 from Cell Signalling Technology (Boston, MA) and α-N1-Src; custom made by GenScript (Piscataway, NJ). Secondary antibodies for Western Blotting were purchased from Sigma (St. Louis, MO). Secondary antibodies used for immunocytochemistry were α-mouse Alexa Fluor-564 and α-rabbit Alexa Fluor-488 and purchased from Molecular Probes, Invitrogen (Paisley, UK). The ECL used was Immobilon Western, purchased from Millipore (Billerica, MA). The phage display kit used was the Ph.D.-12 kit and was purchased from NEB (Ipswich, MA). Culture media (MEM and DMEM) and EBSS were purchased from GIBCO, Invitrogen (Paisley, UK). EcoTransfect was purchased from Oz Biosciences (Marseille, France) and the calcium phosphate transfection kit purchased from Promega (Fitchburg, WI). Recombinant L1-CAM extracellular domain was purchased from R&D Systems (Minneapolis, MN). All other materials were purchased from Sigma (St. Louis, MO).

2.2 Molecular biology protocols

2.2.1 Agarose gel electrophoresis

DNA separation was carried out using agarose gel electrophosesis. Agarose concentrations between 0.7 and 2% were used depending on the size of the DNA plasmid or fragment to be analysed. The appropriate amount of agarose was added to 1x TBE buffer (89 mM Tris, 89 mM boric acid, 2 mM EDTA) and dissolved using a microwave. 3 µl SYBRSafe was added to allow visualisation of DNA. The mixture was poured into a gel tray and allowed to set. Samples loaded onto agarose gels were diluted in 5X Orange G buffer (0.5% Orange G, 25% glycerol).

2.2.2 Preparation of competent cells

Competent *Escherichia coli (E. coli)* cells were either purchased (Stratagene) or produced in the lab using the $CaCl_2$ method. For in-house production, 10 ml LB was inoculated with a small amount of competent cells and grown overnight with an appropriate antibiotic. The overnight culture was diluted into 150 ml fresh LB to an OD_{600} ~0.1 and grown at 37°C, shaking 200 rpm until the OD_{600} reached ~0.9. At this point the culture was immediately chilled in an ice bath. The culture was centrifuged at 5000 rpm, for 10 minutes at 4°C to pellet the cells. The supernatant was decanted, the pellet placed on ice and then resuspended in 100 ml ice cold 100 mM $MgCl_2$. The cells were pelleted and resuspended in 10 ml 100 mM $CaCl_2$. The solution was incubated on ice for 60 – 90 minutes with occasional agitation. The cells were spun down, drained and resuspended in 9.5 ml 85 mM $CaCl_2$, 15% glycerol. The cell suspension was distributed into 200 µl aliquots in sterile eppendorfs and snap frozen in liquid nitrogen. Competent cells were stored at -80°C.

2.2.3 Bacterial transformation

DNA plasmids were transformed into competent *E.coli* strain XL-10 for all cloning steps and strain BL-21 for protein expression. 5 µl of a ligation mix or 50 ng of a purified plasmid was added to 50 µl competent *E. coli* and incubated on ice for 15-30 minutes. Heat shock was carried out for 45 seconds at 42°C. The mixture was returned to ice for 2 minutes and, following addition of 400 µl pre-warmed LB

media (10 g tryptone, 10 g NaCl, 5 g yeast extract per litre), incubated at 37°C, shaking at 200 rpm for 1 hour. 100 µl was then plated onto an agar plate containing an appropriate antibiotic and incubated at 37°C overnight.

2.2.4 Plasmid purification

Plasmid DNA was purified from transformed *E. coli* cultures, cultures inoculated with a single colony from an agar plate or a scraping from a pre-existing glycerol stock using commercially available kits. For culture volumes of 5 - 10 ml a mini prep kit was used (Machery-Nagal) and for volumes of 100 - 200 ml a midi prep kit was used (Qiagen). Purified plasmids were eluted in 10 mM Tris, pH 8.5 and stored at -20°C. DNA quantification was carried out by analysis of absorbance at A_{260} using a spectrophotometer.

2.2.5 DNA ligation

Ligation of annealed oligonucleotides into digested plasmids was carried out using a 3:1 molar ratio of insert to vector. Standard ligations used 100 ng plasmid DNA and were carried out in a volume of 10 µl using 1 µl of DNA ligase. Ligation reactions were carried out overnight at 4°C or for 3 hours at room temperature.

2.2.6 DNA Sequencing

DNA sequencing was carried out in the Technology Facility at the University of York, Department of Biology. ~100 ng of a DNA plasmid was submitted and sequencing was carried out using 3.2 µM of an appropriate primer. Primers were either selected from the list of available primers or supplied along with the DNA. Analysis of the sequence obtained was carried out using Sequence Scanner 1.0.

2.2.7 Cloning

Plasmids were prepared for use in *in vitro* kinase assays and cell based assays by the inclusion of short (~50 bp) sequences. Appropriate oligonucleotide sequences were synthesised by Eurogentec and annealed in an annealing buffer (50 mM HEPES, pH 7.4, 100mM NaCl) by heating to 95°C followed by stepped cooling to 4°C in 1 hour

in a PCR machine. Annealed oligonucleotides were inserted into DNA plasmids as described in sections 1.2.7.1 and 1.2.7.2.

2.2.7.1 pGEX-6P-1 plasmid generation

The plasmid containing the ideal Src substrate (Y) was generated by insertion of the relevant nucleotide sequence (Table 1.2.7.1.1) using the enzymes BamHI and EcoRI. All subsequent oligonucleotides were inserted into the 'Y' plasmid using the enzymes SalI and NotI (Figure 2.2.7.1.1). The oligonucleotides used were designed to retain the enzyme sites following insertion and therefore a 5 amino acid linker was retained between the ideal Src substrate and the SH3 domain binding motifs. The linker had the sequence Glu Phe Pro Gly Arg and consisted of the region of the pGEX-6P-1 multiple cloning site (MCS) between EcoRI and SalI as shown in Figure 2.2.7.1.1. The enzymes that were used for the cloning were chosen because they allowed the disruption of the Class II PXXP motif contained within the pGEX-6P-1 MCS.

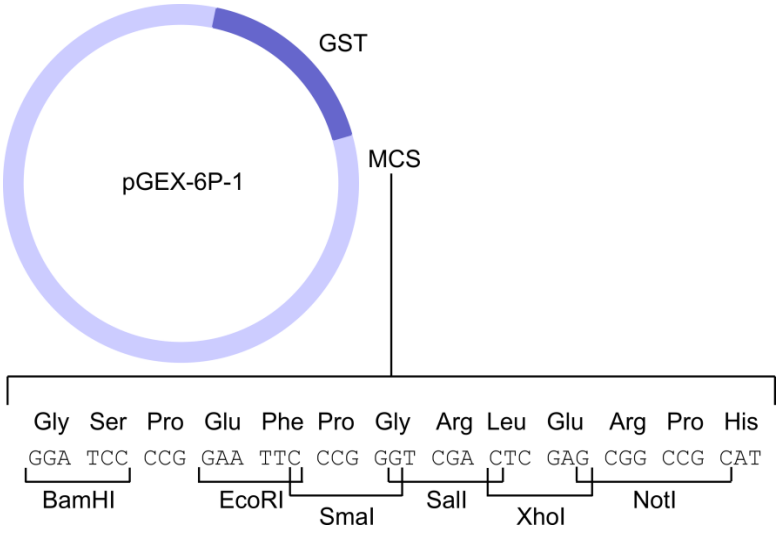

Figure 2.2.7.1.1. Cloning strategy for GST-tagged peptide generation.

To produce the GST-tagged peptides for use in *in vitro* kinase assays relevant oligonucleotides were inserted into the pGEX-GP-1 plasmid. The ideal Src substrate (Y) was inserted into the pGEX-6P-1 multiple cloning site (MCS) using the enzymes BamHI and EcoRI. The SH3 domain binding motifs were inserted using the enzymes SalI and NotI. The oligonucleotides were designed to retain the enzyme sites and therefore the resulting plasmids retained a 5 amino acid linker between the ideal Src substrate and the SH3 domain binding motif.

~1 µg pGEX-6P-1 was digested in NEB Buffer EcoRI + BSA (BamHI, EcoRI double digest) or Buffer 3 + BSA (SalI, NotI double digest) for 1 hour at 37°C. The DNA was separated using a 0.7% agarose gel and the digested plasmid extracted using a commercial gel extraction kit (Qiagen). Appropriate annealed oligonucleotides were ligated into the digested plasmids as described in section 1.2.5. The products of the ligation reactions were transformed into competent *E. coli* strain XL-10 (Section 1.2.3). Clones containing the insert were identified by PCR screen using the primers 5'GGGCTGGCAAGCCACGTTTGGTG and 5'CCGGGAGCTGCATGTGTCAGAGG. The cloning of the YL plasmid was carried out by Kathryn Hogan, under my supervision. Positive clones were isolated using a mini-prep kit (Machery-Nagal). The identity of the insert confirmed by DNA sequencing using the 5'GGGCTGGCAAGCCACGTTTGGTG.

2.2.7.2 pmCer plasmid generation

PD1 and PD1-P5A were inserted into the pmCer-C1 plasmid using the enzymes BglII and EcoRI. ~1 µg pmCer-C1 was digested in NEB buffer EcoRI + BSA for 1 hour at 37°C. All subsequent steps were carried out as for pGEX-6P-1 plasmid generation. PCR screens were carried out the primers 5'CATGGTCTTGCTGGAGTTCGTG and 5'GAAATTTGTGATGCTATTGC. DNA sequencing was carried out using the primer 5'CATGGTCTTGCTGGAGTTCGTG.

Table 2.2.7.1.1 Oligonucleotide sequences inserted into pGEX-6P-1 for use in *in vitro* kinase assays.

Oligonucleotides were annealed and then ligated into digested pGEX-6P-1. For plasmid 'Y', oligonucelotides were inserted using the enzyme sites BamHI and EcoRI. All other oligonucelotides were inserted into the 'Y' plasmid using the enzyme sites SalI and NotI.

Name	Primers	
Y	Sense	AATTCGGTGGCGGTGCAGAAGAGGAAATTTACGGTGAATTTGG
	Anti	TCGAACAAATTCACCGTAAATTTCCTCTTCTGCACCGCCACCG
YA	Sense	TCGACTCGGTGGCGGTGTGAGCCTGGCGCGTCGTGCGCTGGCAGCTCTGGCGTAAGC
	Anti	GGCCGCTTACGCCAGAGCTGCCAGCGCACGACGCGCCAGGCTCACACCGCCACCGAG
YP1	Sense	TCGACTCGTGAGCCTGGCGCGTCGTCCGCTGCCGCCGCTGCCGTAAGC
	Anti	GGCCGCTTACGGCAGCGGCAGCGGACGCGCCAGGCTCACGAG
YP2	Sense	TCGACTCGGTGGCGGTGCGCCGCCGCTGCCGCCGCGTAACCGTCCGCGTCTGTAAGC
	Anti	GGCCGCTTACTGACGCGGACGGTTACGCGGCGGCAGCGGCGGCGCACCGCCACCGAG
YL	Sense	TCGACTCGGTGGCGGTGCGTCCAAGCCTCAGACCCAGGGCCTGGCCAAGGATGCGGC
	Anti	GGCCGCCGCATCCTTGGCCAGGCCCTGGGTCTGAGGCTTGGACGCACCGCCACCGAG
PD1	Sense	TCGACTCGGTGGCGGTGCGTGGCATCGCATGCCGGCGTATACCGCGAAATATCCGGC
	Anti	GGCCGCCGGATATTTCGCGGTATACGCCGGCATGCGATGCCAGCCACCGCCACCGAG
PD2	Sense	TCGACTCGGTGGCGGTGCCGGCCATTGGCATAGCCCGCATAAACTGACCCGCAACGC
	Anti	GGCCGCGTTGCGGGTCAGTTTATGCGGGCTATGCCAATGGCCCGCACCGCCACCGAG
PD3	Sense	TCGACTCGGTGGCGGTGCCAAGAACCCGACCAGCACGCCGGCGATGTATGCGAACGC
	Anti	GGCCGCGTTCGCATACATCGCCGGCGTGCTGGTCGGGTTCTTCGCACCGCCACCGAG
PD4	Sense	TCGACTCGGTGGCGGTGCCGGCCATCGCAACCGCGCGAACACCAGCAAGAACCCGGC
	Anti	GGCCGCCGGGTTCTTGCTGGAGTTCGCGCGGTTGCGATGGCCCGCACCGCCACCGAG
PD5	Sense	TCGACTCGGTGGCGGTGCCAAACCGCCGCAGCATACCAGCGCGCCGTATCTGCCGGC
	Anti	GGCCGCCGGCAGATACGGCGCGCTGGTATGCTGCGGCGGTTTCGCACCGCCACCGAG
PD6	Sense	TCGACTCGGTGGCGGTGCCTGGCATCGCATGCCGATGCATACCGCGAAACCGCTGGC
	Anti	GGCCGCCAGCGGTTTCGCGGTATGCATCGGCATGCGATGCCACGCACCGCCACCGAG
PD1-R3A	Sense	TCGACTCGGTGGCGGTGGCTGGCATGCGATGCCGGCGTATACCGCGAAATATCCGGC
	Anti	GGCCGCCGGATATTTCGCGGTATACGCCGGCATCGCATGCCAGCCACCGCCACCGAG
PD1-P5A	Sense	TCGACTCGGTGGCGGTGGCTGGCATCGCATGGCAGCGTATACCGCGAAATATCCGGC
	Anti	GGCCGCCGGATATTTCGCGGTATACGCTGCCATGCGATGCCAGCCACCGCCACCGAG
PD1-T8A	Sense	TCGACTCGGTGGCGGTGGCTGGCATCGCATGCCGGCGTATGCTGCGAAATATCCGGC
	Anti	GGCCGCCGGATATTTCGCAGCATACGCCGGCATGCGATGCCAGCCACCGCCACCGAG
PD1-T8V	Sense	TCGACTCGGTGGCGGTGGCTGGCATCGCATGCCGGCGTATGACGCGAAATATCCGGC
	Anti	GGCCGCCGGATATTTCGCGTCATACGCCGGCATGCGATGCCAGCCACCGCCACCGAG
PD1-K10A	Sense	TCGACTCGGTGGCGGTGGCTGGCATCGCATGCCGGCGTATACCGCGGCGTATCCGGC
	Anti	GGCCGCCGGATACGCCGCGGTATACGCCGGCATGCGATGCCAGCCACCGCCACCGAG

Table 2.2.7.2.1 Oligonucleotide sequences inserted into pmCer-C1 for use in cell based assays.

Oligonucleotides were annealed and then ligated into digested pmCer using the enzyme sites BglII and EcoRI.

Name	Primers	
PD1 WT	Sense	GATCTGGCGGTGGCTGGCATCGCATGCCGGCGTATACCGCGAAATATCCGTAGTCG
	Anti	AATTCGACTACGGATATTTCGCGGTATACGCCGGCATGCGATGCCAGCCACCGCCA
PD1-P5A	Sense	GATCTGGCGGTGGCTGGCATCGCATGGCAGCGTATACCGCGAAATATCCGTAGTCG
	Anti	AATTCGACTACGGATATTTCGCGGTATACGCTGCCATGCGATGCCAGCCACCGCCA

2.3 Protein expression and purification

2.3.1 Protein expression

10 ml of LB media containing an appropriate antibiotic was inoculated with either a single colony from an agar plate or a scraping taken from a pre-existing glycerol stock containing the relevant plasmid. This culture was incubated at 37°C, shaking at 200 rpm, overnight. The overnight culture was transferred to 1 l LB media containing an appropriate antibiotic and grown at 37°C, shaking at 200 rpm, until the OD_{600} reached ~0.8. Protein expression was then induced by the addition of isopropyl-β-thiogalactopyranoside (IPTG) to a final concentration of 1 mM. The recombinant protein was expressed for 3-4 hours at 37°C or overnight at 18°C. The low temperature condition was only used for expression of active Src kinases. Cells were pelleted (4,500 rpm, 10 minutes, 4°C) and the pellets frozen overnight (-80°C). Bacterial pellets were defrosted on ice and resuspended in PBS plus PMSF (final concentration 1 mM) and lysozyme (13.3 mg/l of culture). The suspension was incubated on ice for 30 minutes. DTT (final concentration 5 mM) and Triton-X-100 (1.5 % w/v) were added and the suspension sonicated at 10kHz on ice for a total of 5 minutes 30 seconds (30 seconds on, 30 seconds off). The lysate was clarified (12,000 rpm, 30 minutes, 4°C). The clarified lysate was transferred to a clean tube and purified using affinity bead capture (section 2.3.2).

The extent of protein expression was assessed by separating ‘uninduced’ and ‘induced’ samples on an SDS-PAGE gel.

2.3.2 Purification of GST-tagged proteins

Protein expression was carried out as in section 2.3.1. Glutathione-Sepharose beads (GenScript) (1 ml per litre of culture) were washed x3 in PBS, added to the clarified lysate and the tube incubated, rotating end-over-end at 4°C, for approximately 4 hours. The beads were pelleted (5,000 rpm, 5 minutes, 4°C) and washed x5 in PBS, x1 in 1.2 M NaCl in PBS and x2 in PBS. The beads were then resuspended to a 50% slurry in PBS and stored at 4°C overnight.

GST-fusion proteins were eluted from glutathione-sepharose beads using an excess of glutathione. Glutathione elution buffer (100 mM Tris, pH 8.0,

20 mM glutathione, 100 mM NaCl) was added to an equal volume of beads and rotated end-over-end at room temperature for 20 minutes. The beads were then pelleted and the supernatant collected. Fresh glutathione elution buffer was added and the process repeated until 4 elutions had been collected. The protein content of these elutions was analysed by Bradford assay and the purity of the protein by SDS-PAGE (section 2.4.1). The protein preparation was considered to be pure if it contained a single band of the correct molecular weight on a Coomassie stained SDS-PAGE gel. If all fractions were of a high concentration and pure then they were combined and the final concentration determined using Bradford assay. For use in *in vitro* kinase assays the proteins were dialysed into 100 mM Tris, pH 7.5 using a Slide-A-Lyzer cassette (Thermo Scientific).

2.3.3 Preparation of active Src kinases

Src kinases were expressed as GST-tagged fusion proteins and purified as described in sections 2.3.1 and 2.3.2. Src proteins were expressed as a fusion to the phosphatase PTP1B. A PreScission Protease site was engineered between PTP1B and Src and therefore active Src was obtained by treatment with PreScission Protease3C. 5 µl PreScission Protease3C (7 mg/ml) (Department of Biology, Technology Facility) was added to 500 µl Src bound glutathione-sepharose beads in 500 µl PreScission Protease buffer (50 mM Tris, 100 mM NaCl, 1 mM EDTA, 1 mM DTT, pH 8.0) and incubated, rotating end-over-end at 4°C, overnight. The beads were pelleted, the supernatant recovered and immediately diluted in an equal volume of kinase storage buffer (KSB) (50 mM Tris, 10 mM NaCl, 0.05 mM EDTA, 1 mM DTT, 10% glycerol, 1 mg/ml BSA, 0.05% NP-40, pH 7.5). The solution was immediately aliquotted and stored at -80°C. The amount of kinase present and its purity was assessed by SDS-PAGE of a sample taken prior to the addition of KSB. The kinase preparation was considered to be pure if it contained a single band of the correct molecular weight on a Coomassie stained SDS-PAGE gel. A kinase assay with the control substrate (YA) was used to test the activity of the kinases and to normalise C-, N1- and N2-Src activity.

2.4 Protein based methods

2.4.1 SDS-PAGE

Protein separation was carried out by SDS-polyacrylamide gel electrophoresis (SDS-PAGE) using a Bio-Rad mini Protean Tetra gel electrophoresis kit. Resolving gel composition; 375 mM Tris pH 8.8, 0.1 % SDS, 0.05% APS, 0.01% TEMED with an appropriate acrylamide concentration depending on the size of the protein to be examined. Stacking gel composition; 125 mM Tris, pH 6.8, 0.1% SDS, 4% acrylamide, 0.05% APS, 0.01% TEMED. Protein samples were diluted in 2x Laemmli loading buffer and boiled for 5 minutes prior to loading. Gels were run at 120 V for approximately 20 minutes until the dye front passed through the staking gel and then at 160 V until the dye front reached the bottom of the gel. Running buffer composition; 25 mM Tris, 192 mM glycine, 0.1% SDS. A ladder of protein standards was used (BioRad). Gels were either stained in Coomassie (0.3% Coomassie Brilliant Blue R, 55% methanol, 9% acetic acid) followed by destaining in 14% acetic acid, 7% methanol or transferred to PVDF for immunoblotting (Section 1.4.2).

2.4.2 Transfer to PVDF and Western Blotting

SDS-PAGE gels were transferred to PVDF using the BioRad transfer system. Transfer was carried out at 66 V for 1 hour or at 20 V overnight. Following transfer membranes were blocked in either 5% Marvel or 3% BSA in PBS (1.4.2.1). Primary antibodies were used as indicated in Table 1.4.2.1 for approximately 2 hours at room temperature or overnight at 4°C. Following the application of primary antibody, membranes were washed x3 (5 minutes each) in PBS. Secondary antibodies used were conjugated to HRP and were used as indicated in Table 1.4.2.1 for approximately 1 hour at room temperature. Following the secondary antibody application, membranes were washed x3 (10 minutes each) in PBS. ECL reagents were either made in the lab (Solution A: 0.1 M Tris, 450 µg/ml luminol, pH 8.5. Solution B: 0.1 M Tris, 0.06% H_2O_2, pH 8.5) or purchased and detection was carried out using photographic film (Fisher).

Table 2.4.2.1 Antibodies used for Western Blotting.

Conditions used for blocking, primary antibody and secondary antibody application to PVDF membranes.

		Primary antibody		Secondary antibody		
Ab	**Block**	**Conc.**	**Buffer**	**Ab**	**Conc.**	**Buffer**
PY20	3 % BSA in PBS	1:1000	PBS	α-mouse HRP	1:500	PBS
pY416	3 % Marvel in PBS	1:1000	PBS, 0.1% Tween-20, 5% BSA	α-rabbit HRP	1:500	PBS + 0.1 % Tween20
pY527	3 % Marvel in PBS	1:1000	PBS, 0.1% Tween-20, 5% BSA	α-rabbit HRP	1:500	PBS + 0.1 % Tween20
FLAG (M2)	5% Marvel in PBS	1:1000	PBS + 0.1 % Tween20	α-mouse HRP	1:500	PBS + 0.1 % Tween20
GFP	5% Marvel in PBS	1:500	PBS + 0.1 % Tween20	α-rabbit HRP	1:500	PBS + 0.1 % Tween20
N1-Src	5% Marvel in PBS	As indicated	PBS + 0.1 % Tween20	α-rabbit HRP	1:500	PBS + 0.1 % Tween20

2.4.3 *In vitro* kinase assays

In vitro kinase assays were carried out in 100 mM Tris, 10 mM $MgCl_2$, pH 7.5. The reaction was carried out at 30°C and initiated by the addition of 0.5 mM ATP final concentration. Kinase assays to obtain kinetics were carried out using a kinase concentration of 5 nM and a duration of 90 minutes. Substrate concentrations were altered as indicated in the text. In kinase assays where the kinase concentration was varied, a substrate concentration of 25 µM and a duration of 90 minutes was used. The kinase concentration was varied as indicated in the text. For timecourse experiments the kinase concentration was 5 nM and the substrate concentration 25 µM. Samples were taken at timepoints as indicated in the text. Assays were halted by transfer to ice and immediate addition of 2x Laemmli buffer (Sigma). 10% of the assay mix was loaded onto a 15% SDS-PAGE gel followed by transfer to PVDF for analysis of substrate phosphotyrosine content by Western Blot. All experiments were carried out 3 times.

For peptide titration experiments a kinase concentration of 5 nM and a substrate concentration of 25 µM was used. The substrate used was YA. Free peptides of PD1-WT (CWHRMPAYTAKYP) and PD1-P5A (CWHRMAAYTAKYP) were synthesised commercially. Individual kinase assays

containing increasing peptide concentrations were set up. The peptide concentrations used were 1, 5, 10, 25, 50, 75 and 100 µM. Assays were carried out at 30°C for 90 minutes before analysis as previously described.

For analysis of kinetics identical substrate concentrations phosphorylated by all 3 kinases were loaded onto the same blot. A standard sample was included on all blots. Densitometry of the blots was analysed using ImageJ and normalisation to the standard sample used to reproduce the entire curve. Densitometry of stained Coomassie gels was used to normalise protein levels. Phosphorylation by each of the kinases was therefore directly comparable. The highest value obtained by densitometry analysis was set to 1 and all other values scaled accordingly. The kinetics of the phosphorylation reaction were then calculated using SigmaPlot according to the laws of Michaelis-Menton kinetics. The densitometry data from the 3 independent experiments was used to calculate the K_m.

2.4.4 Immunoprecipitation

75 cm^2 flasks containing a confluent layer of COS7 cells (approximately 3 x 10^6 cells) transfected with the appropriate plasmids (see section 1.5.2) were lysed in ice cold lysis buffer (20 mM Tris, pH 7, 1 mM EDTA, 1 mM EGTA, 10 mM sodium-β-glycerophosphate, 1 mM sodium-orthovanadate, 5% w/v glycerol, 270 mM sucrose, 1 mM benzaminidine, 0.1% β-mercaptoethanol, 10 µg/ml leupeptin) 48 hours following transfection. Lysates were centrifuged (13,000 rpm, 1 minute, 4°C) to pellet debris. Clarified lysates were then pre-cleared using 50 µl (settled volume) washed Protein-G-sepharose beads. 1 mg cell lysate, the appropriate antibody (2 µg α-FLAG or 4 µl α-GFP containing serum) and 30 µg washed Protein-G-sepharose beads were made up to a total volume of 1 ml and incubated at 4°C, rotating end-over-end, for at least 4 hours or overnight. Beads were washed x3 in ice cold lysis buffer. Bound proteins were eluted in 50 µl 2x Laemmli buffer and analysed by SDS-PAGE.

2.4.5 Phage display

Phage display experiments were carried out using the Ph.D.™-12 Phage Display Peptide Library Kit according to the manufacturer's instructions. 25 µl (settled

volume) glutathione-sepharose beads were washed x1 in 1ml TBS (50 mM Tris, 150 mM NaCl, pH 7.5) + 0.1% Tween20 (TBST). Beads were pelleted, the supernatant carefully removed and then resuspended in 1 ml blocking buffer (0.1 M $NaHCO_3$, 5 mg/ml BSA, 0.02% NaN_3, pH 8.6) and incubated for 60 minutes at 4°C, rotating end-over-end. During the incubation a 100-fold representation of the phage library (2 x 10^{11} plaque forming units (pfu)) was incubated with 1 µM final concentration of GST-N1-Src SH3 domain in 200 µl total volume TBST. Following blocking, the beads were washed x4 in 1 ml TBST. The GST-N1-Src-SH3 solution was then transferred into the tube with the washed beads and incubated at room temperature for 15 minutes, rotating end-over-end. The beads were pelleted, the supernatant removed and the beads washed x10 in TBST. Bound phage were eluted in 1 ml of Glycine Elution Buffer (0.2 M Glycine-HCl, pH 2.2, 1 mg/ml BSA) with a 10 minute incubation at room temperature, rotating end-over-end. The beads were pelleted and the supernatant transferred to a clean eppendorf. The eluate was neutralised with 150 µl of 1 M Tris, pH 9.1.

A small amount of the eluate was titreed as described in section 1.4.5.1. The remaining eluate was amplified by addition to 20 ml *E. coli* strain ER2738 at early log phase (OD_{600} 0.01–0.05) and incubation at 37°C, shaking at 200 rpm for 4.5 hours. Amplification was carried out either on the same day as phage binding or the next day following overnight incubation of the eluate at 4°C. Following amplification the culture was pelleted by spinning at 12,000 g for 10 minutes at 4°C. The supernatant was then transferred to a clean tube and spun again. The top 80% of the supernatant was transferred to a fresh tube and 1/6 of the volume of 20% PEG, 2.5 M NaCl added. The phage were allowed to precipitate at 4°C either for 2 hours or overnight. The PEG precipitation was spun at 12,000 g for 15 minutes at 4°C and the supernatant removed. The pellet was resuspended in 1 ml TBS, the solution transferred to a clean eppendorf and spun at 13,000 rpm for 5 minutes at 4°C to pellet residual cells. The supernatant was transferred to a clean eppendorf and reprecipitated with 1/6 volume of 20% PEG, 2.5 M NaCl for 60 minutes on ice. The solution was spun at 13,000 rpm for 10 minutes at 4°C. The supernatant was removed, the tube respun briefly and any remaining supernatant removed. The pellet was resuspended in 200 µl TBS, spun at 13,000 rpm to remove any remaining insoluble material and transferred to a clean tube. This is the amplified eluate. A small amount of the amplified eluate was titreed as described in section 1.4.5.1.

Some of the remaining amplified eluate was used for a subsequent round of panning. From round 2 onwards the Tween20 concentration in all washing steps was increased to 0.5%. A negative selection step was introduced to remove phage bound directly to the beads. 25 µl beads (settled volume) were washed and blocked as previously described. The amplified eluate containing the phage library was diluted in 200 µl TBST as previously but the GST-N1-Src-SH3 domain was excluded. The correct volume of amplified eluate was calculated from the results of the titreing so that it contained 2 x 10^{11} phage (see section 1.4.5.1). The phage solution was added to the washed beads and incubated for 15 minutes at room temperature, rotating end-over-end. The beads were pelleted, the supernatant carefully removed and added to GST-N1-Src SH3 domain to produce a final target concentration of 1 µM. Panning steps were then continued as previously described. A total of 5 rounds of panning were performed.

2.4.5.1 Phage titreing

10 ml LB was inoculated with *E. coli* strain ER2738 either from a glycerol stock scrape or a single colony from an LB-Agar plate and grown until mid-log phase (OD_{600} ~ 0.5). Unamplified phage were serially diluted 10^1 – 10^4 and amplified phage diluted 10^8 – 10^{11} in 1 ml final volumes. When the ER2738 culture reached mid-log phase, 200 µl aliquots were dispensed into sterile eppendorfs, one for each phage dilution required. 10 µl of each phage dilution was added to a tube, vortexed briefly and incubated at room temperature for up to 5 minutes. The infected cells were added, one aliquot at a time, to 3 ml aliquots of TopAgar (10 g Tryptone, 5 g yeast extract, 5 g NaCl, 7 g Agar per litre), vortexed briefly and poured immediately onto a prewarmed LB/IPTG/Xgal plate. The plates were allowed to cool at room temperature until the TopAgar had set and then inverted and incubated overnight at 37°C. The next morning, blue plaques were counted. The phage plasmid (M13) contains the β-galactosidase gene, so growth on IPTG containing plates meant phage plasmid containing plaques were coloured blue. White plaques were present due to contaminating wild type phage and were not counted.

Plates from unamplified phage titreing were used for sequencing (see section 1.9.2). Plates from amplified phage titreing were used to calculate the eluate volume needed to add to the next round of panning. The number of blue plaques on the

plates were counted. On plates with approximately 100 plaques, the number of plaques was multiplied by the dilution factor to calculate the number of pfu per 10 µl. This number was then used to calculate the volume that contained the 2 x 10^{11} phage needed for the next round of panning.

2.4.5.2 Preparation of phage clones for sequencing

Phage plasmids were sequenced from round 3 onwards. An overnight culture of *E. coli* ER2738 was diluted 1:100. 1 ml of diluted culture was dispensed into 15 ml falcon tubes, one for each clone to be sequenced. Individual blue plaques were picked from unamplified titre plates with approximately 100 plaques using sterile pipette tips and the tips dropped into the diluted culture. The tubes were incubated at 37°C, shaking 200 rpm for 4.5 hours. The cultures were transferred to eppendorfs and spun at 13,000 rpm for 30 seconds at 4°C. 500 µl of the supernatant was transferred to a fresh eppendorf tube. 200 µl of 20% PEG, 2.5 M NaCl was added, inverted to mix and incubated for 10 - 20 minutes at room temperature. The solution was spun at 13,000 rpm for 10 minutes at 4°C and the supernatant discarded. The pellet (not always visible) was resuspended Iodide Buffer (10 mM Tris, 1 mM EDTA, 4M NaI, pH 8.0), 250 µl ethanol added and incubated for 10 - 20 minutes at room temperature. The solution was spun at 13,000 rpm for 10 minutes at 4°C and the supernatant discarded. The pellet was washed with 0.5 ml 70% ice-cold ethanol, re-spun, the supernatant was removed and the pellet allowed to air dry. The pellet was then resuspended in 30 µl TE buffer (10 mM Tris, 1 mM EDTA, pH 8.0). Prior to sequencing, the presence of an insert was confirmed by PCR. Primers either side of the peptide insert site were designed (Forward: $^{5'}$ACCGATACAATTAAAGGCTC and Reverse: $^{5'}$CCCTCATAGTTAGCGTAACG). A band of 259 bp represented the presence of the 12-mer inserts and a band of 214 bp represented an empty phage plasmid. Clones shown to contain the 12-mer peptide insert were sequenced in the Technology Facility at the University of York using the primer $^{5'}$CCCTCATAGTTAGCGTAACG as suggested by NEB.

2.5 Cell culture methods

2.5.1 Culture of cell lines

COS7 cells were maintained in culture in 25 cm^2 or 75 cm^2 flasks. The culture medium was DMEM with pyruvate, high glucose and glutamine, 10 % FCS, 100 units/ml penicillin and 0.1 mg/ml streptomycin. Cells were passaged and split 1:3 as they reached confluency, approximately 3x per week. Cells were detached from the culture flask with 1 ml pre-warmed trypsin/EDTA. The action of trypsin was halted by the addition of culture medium. Cells were spun at 1000 rpm for 5 minutes. The supernatant was discarded and cells resuspended in 1 ml culture medium. If required for plating, cells would be counted using a haemocytometer and plated at a density of 3 x 10^4 cells per 13 mm coverslip in a 24 well plate. Coverslips were sterilised in an oven prior to use. Cells were maintained at 37°C in a humidified atmosphere of 5 % CO_2 and 95% air.

2.5.2 Transient transfection of cell lines

Cells were plated as described in section 1.5.1. The following day cells were transfected using EcoTransfect (Oz Biosciences) according to the manufacturer's instructions. Single transfections were carried out using 1 µg plasmid DNA and 2 µl EcoTransfect each in 50 µl DMEM. Double transfections were carried out using 1 µg of each plasmid and 4 µl EcoTransfect, both in 50 µl DMEM. The two solutions were mixed and incubated at room temperature for 15 minutes before pipetting into a well of a 24 well plate containing 500 µl media. The plate was then returned to the incubator. For transfection of more than one well volumes and amounts were scaled accordingly. For all Western Blotting and immunocytochemistry experiments COS7 cells were transfected for 48 hours. For immunoprecipitation experiments, 1 x 10^6 cells were added to a 75 cm^2 flask and co-transfected the following day with 7.5 µg of each plasmid and 30 µl EcoTransfect, each in 300 µl DMEM.

COS7 cells transfections were carried out using the following constructs. C-, N1- and N2-Src constructs were contained in the pFLAG-N1 vector and visualised using an α-FLAG antibody. The cloning of the FLAG tagged Src constructs was carried out by Kathi Mahal under the supervision of Dr Chris Dunning in the Evans lab. PD1 and PD1-P5A constructs were contained within the pmCer-C1 vector and

visualised using an α-GFP antibody. Details of the cloning carried out to produce PD1 and PD1-P5A constructs are found in section 2.2.7.2 See section 2.5.6 for details of antibody application.

2.5.3 Preparation of CGN neurons

Preparation of cerebellar granule neurons were carried out essentially as described previously (Tan et al, 2003). P7 Wistar rat pups were killed using a single lethal pentobarbital injection. Cerebellar were dissected and placed in filter sterilized solution B (100 mM PBS, 0.3 % BSA, 10 mM glucose, 0.38 % $MgSO_4.7H_2O$. The cerebellar were finely chopped using a razor blade and the diced tissue then incubated in trypsin (4 mg/ml) in solution B at 37°C for 15 - 20 minutes with agitation every 5 minutes. The action of trypsin was halted by the addition of solution W (solution B plus 0.5 mg soybean trypsin inhibitor and 500 units DNAase I). The tissue solution was spun at 1000 g for 1 minute and the supernatant discarded. The pellet was resuspended in solution C, a 6x concentrated solution W, and the cells mechanically dispersed by triturating through flamed glass pipettes of decreasing bore size. The resulting single cell suspension was centrifuged through 4 % BSA in EBSS to remove debris. The pellet was resuspended in MEM culture medium (MEM without Ca^{2+} and Mg^{2+}, 25 mM KCl, 10 % FCS, 30 mM glucose, 1 mM glutamine, 25 mM $NaHCO_3$, 100 units/ml penicillin, and 0.1 mg/ml streptomycin).

Cell yield was calculated using a haemocytometer and the cells plated onto poly-D-lysine coated 13 mm coverslips. Coverslips were prepared by first soaking in ethanol for ~2 hours, sterilising in an oven for at least 3 hours and then incubating in sterile poly-D-lysine (15 mg/l) for 2 hours at room temperature. Coverslips were allowed to air dry, placed into the wells of a 24 well plate and allowed to dry completely overnight at 37°C. Cells were plated at a density of 2.5 x 10^5 cells per coverslip and transfected 24 hours following plating (section 1.5.5), following transfection cells were grown in MEM culture medium plus 10 µM final concentration arabinofuranosyl cytidine (AraC) (+ media) for 24 hours before fixing for morphological analysis. Cells were maintained at 37°C in a humidified atmosphere of 5 % CO_2 and 95% air.

2.5.4 Preparation of hippocampal neurons

Preparation of hippocampal neurons was carried out by Dr Sangeeta Chawla (University of York). Hippocampal neurons were prepared from newborn Wistar rats as described previously (Belfield et al, 2006), and cultured in Neurobasal medium (Invitrogen) containing 2% B27 (Invitrogen), 5% foetal calf serum (PAA Lab, Pasching, Austria), 1 mM L-glutamine, 35 mM glucose, 100 units/ml penicillin, and 0.1 mg/ml streptomycin (Invitrogen).

2.5.5 Transfection of neuronal cultures

Neuronal cultures were transfected using a calcium phosphate transfection kit (Promega) according to the manufacturer's instructions. The culture medium was removed, replaced with 500 µl prewarmed MEM and incubated for 30 minutes at 37°C. Meanwhile, 0.5 µg plasmid DNA was mixed with 12.5 µl 2.5M $CaCl_2$ and made up to 100 µl with ddH_2O. 100 µl HBS (HEPES buffered saline) was added to a second tube and the DNA mix added dropwise while vortexing. The mixture was incubated for 30 minutes in the dark, then added to the cells and incubated for 45 minutes. The media was removed and the cells washed twice with prewarmed MEM before the media was replaced with + media. Unless otherwise stated, all neuronal transfections were carried out for 24 hours before the cells were fixed for morphological analysis.

2.5.6 Immunocytochemistry

Transfected cells were cultured in 24 well plates containing 13 mm coverslips as described in sections 2.5.1 and 2.5.2. The culture media was removed and cells washed x3 in PBS. Cells were fixed in 4% paraformaldehyde (PFA) or 4% PFA, 4 % sucrose for 20 minutes at room temperature and then washed x3 in PBS. Cells were permeabilised and blocked in 0.1% Triton-X-100, 1% BSA in PBS for 30 minutes at room temperature. Primary antibodies were applied in 1% BSA in PBS for approximately 2 hours at room temperature. α-FLAG (M2) (mouse) was used at 1:1000 and α-GFP serum (rabbit) (to detect CFP transfected cells) was used at 1:500. Cells were washed x3 in PBS. Secondary antibodies were applied at 1:500 in 1% BSA in PBS for approximately 1 hour in the dark. Secondary antibodies used

were α-mouse Alexa Fluor-568 and α-rabbit Alexa Fluor-488. Cells were washed x3 in PBS and x1 in dH_20. Coverslips were removed from wells, allowed to dry and mounted onto microscope slides using Mowial (0.2 M Tris, pH 8.5, 12 % w/v Mowial, 33.3 % w/v glycerol).

Images were acquired using a 40x objective on the Nikon TE 200 epifluorescence inverted microscope using a RoleraXR CCD (QImaging) camera controlled by SimplePCI Software (Hamamatsu).

2.5.7 L1-CAM neurite outgrowth assay

Coverslips were prepared as described in section 1.5.3. Prior to cell plating, a 10 µl spot containing L1-CAM extracellular domain at 25 µg/ml and fluorescein isothiocyanate (FITC) at 1 mg/ml was pipetted onto the centre of a poly-D-lysine coated coverslip. The spot was allowed to air dry for approximately 1 hour or until completely dry. CGNs were plated as described in section 1.5.3, transfected as described in section 1.5.5 and fixed for morphological analysis (section 1.5.8) 24 hours after transfection.

The constructs transfected into neuronal cultures were the same as those transfected into COS7 cells and are detailed in section 2.5.2.

2.5.8 Morphological analysis using ImageJ

Image analysis was carried out using ImageJ. To measure cell area, the outline of a cell was traced using the freehand tool and the area of the shape was calculated. A calibration image was used to allow calculation in μm^2. The NeuronJ plugin (Meijering et al, 2004) was used for the calculation of neurites in both COS7 cells and neurons. Neurites were traced using the 'add tracings' tool.

For neurons, the neurite was categorised according to whether it was an axon, a dendrite or a branch based on morphology. An axon is a process originating from the cell body and measuring over 50 µm for CGNs and over 300 µm for hippocampal neurons. The measured parameter 'axon length' refers to the length of the primary axon originating from the cell body and does not include the length of branches or dendrites. A branch is a neurite that does not originate from the cell soma and instead originates from an axon or dendrite, branches must measure more

than 10 μm. Dendrites are defined as processes longer than 10 μm and less than 40 μm originating from the cell soma, typically from the opposite pole to the axon. For hippocampal neurons the parameter 'total neurite length' refers to the total length of all axons, branches and dendrites measured. The traced neurites were measured using a calibration image to set the scale for calculation. Data for each cell were compiled in Microsoft Excel and averaged for statistical analysis.

2.6 Bioinformatics

Bioinformatic analysis was carried out using web based bioinformatic programmes. All data collected was collated using Microsoft Excel.

2.6.1 Scansite

A position site scoring matrix (PSSM) was constructed for the binding preferences of the N1-Src SH3 domain (experimental data obtained in this study) and the C-Src SH3 domain (Sparks et al, 1996) according to the directions of (Obenauer et al, 2003). A score was assigned to each amino acid representing the probability of finding it in each position of the consensus motif. Scores were in the range of 0 to 21. A score of 0 meant a residue was excluded from that position and a score of 21 meant that a residue must be found in a certain position. Scores of 1 – 20 represented an increasing likelihood of finding an amino acid in a position. Within the matrix, the residue at position 0 was fixed (given a score of 21) and residues varied 7 residues either side of it. In this study the proline residue in N1-Src SH3 domain consensus and the first P of PxxP in the C-Src SH3 domain consensus were chosen as the fixed residues. As the peptides used in the phage display experiments were 12-mers, there were 4 residues in the PSSM (positions -7 to -4) for which there were no input data. For these positions a score of 1, representing neither a positive or negative preference, was selected.

The PSSM was used to carry out a database search of proteins in the human genome containing the input motif. User defined input motifs are carried out with a medium degree of stringency by default and return protein hits in the top 5% of those examined.

Scansite output orders protein hits according to how well they fit the consensus motif and identifies them by their UNIPROT ID as well as their full name.

2.6.2 DAVID

Protein hits from Scansite analysis were entered into the DAVID database (Huang et al, 2009b) as UNIPROT IDs. DAVID analysis was carried out using GOTERM_BP_ALL as the Gene Ontology term (where BP stands for Biological Process). The Functional Annotational Clustering tool was then used to identify the biological processes that were enriched i.e. present more than would be expected based on their prevalence in the genome. An enrichment factor cut off of 1.5 was enforced (Huang et al, 2009b). Proteins within enriched clusters were exported from DAVID identified by UNIPROT IDs.

2.6.3 GPS

GPS (Xue et al, 2008) requires that input sequences are in FASTA format. UNIPROT IDs were converted to Accession numbers using the DAVID ID conversion tool (Huang et al, 2008a). The Accession numbers were entered into NCBI using the batch entry function to obtain FASTA sequences for all proteins. GPS analysis was carried out using high stringency criteria, producing a maximum false positive rate of 4% (Xue et al, 2008). GPS was used to predict phosphorylation sites for all available tyrosine kinases. The output was transferred to Microsoft Excel and individual proteins were assessed for both predicted tyrosine phosphorylation and predicted SFK phosphorylation. Subsequently, all proteins predicted to be SFK phosphorylated were entered into GPS and prediction of phosphorylation by individual SFK members carried out. These were analysed individually in Microsoft Excel.

2.6.4 PhosphoSite

UNIPROT IDs of proteins predicted to be Src phosphorylated were entered into the PhosphoSite database (Hornbeck et al, 2004). Residues with evidence of tyrosine phosphorylation were collated in Microsoft Word and compared to sites predicted to be phosphorylated by GPS. Proteins were included in the final list of putative N1-Src

substrates if there was evidence in the PhosphoSite database for phosphorylation at the same site as was predicted by GPS.

3 In vitro characterisation of N-Src activity and substrate specificity.

3.1 Introduction

3.1.1 Methods for assessing tyrosine kinase activity

The activity of a tyrosine kinase can be investigated either by assessing the activation state of the kinase itself or by monitoring the phosphorylation of a substrate. These experiments can be carried out either in cell based or *in vitro* assays and multiple methods of both forms have been developed to investigate the functions of SFKs.

Early experiments using a total Src antibody identified Src localised to endosomes and the trans-Golgi network using specific markers and was also present diffuse in the cytoplasm (Kaplan et al, 1992). In contrast, constitutively active Src was primarily localised to focal adhesions at the plasma membrane, but again had some diffuse cytoplasmic staining (Kaplan et al, 1994). These studies gave no information, however, about the activation state of the kinase enzymes in these different locations. Subsequent studies used overexpression of GFP-Src co-stained with an antibody against active, autophosphorylated Src (pY416) and this revealed that inactive Src is predominantly localised in the perinuclear area while active Src is found predominantly at the plasma membrane (Sandilands et al, 2004). Cytoplasmic Src is predominantly inactive with some active puncta (Sandilands et al, 2004). These puncta are thought to be active Src attached to the membrane of vesicles being trafficked to the plasma membrane (Sandilands et al, 2007). Cell based studies of SFK activity therefore revealed that tyrosine kinase signalling is regulated by the activity state of the kinase enzymes themselves but also by their subcellular localisation.

It is more challenging to measure substrate phosphorylation attributed to specific kinases in cell based assays. Cells express multiple kinases and proteins are often phosphorylated on more than one site. The opposing action of phosphatases also makes kinetic analysis of substrates in cells difficult. Therefore, a number of *in vitro* methods have been developed to closely monitor substrate phosphorylation by individual kinases.

The identification of Src substrates allowed monitoring of substrate phosphorylation *in vitro* and therefore assessment of the effect of Src manipulation. Enolase is phosphorylated at a single residue by SFKs both in cells and *in vitro* (Cooper et al, 1984). This made it a useful tool for the study of Src function as many Src substrates are phosphorylated at multiple sites, making the assessment of kinetics less simple. Phosphorylation of enolase was used to confirm that the kinase activity of v-Src is higher than that of C-Src (Courtneidge, 1985), as a model substrate to assess Src activity (Golden et al, 1986) and has been used multiple times since.

The mapping of the specific residues phosphorylated by tyrosine kinases in substrate proteins allowed the development of peptide assays that could specifically monitor the phosphate incorporated into a particular residue. Work by Bruce Kemp was crucial in developing these methods and assessed phosphorylation of peptides derived from chicken egg white lysozyme to determine the importance of primary sequence in phosphorylation by the serine/threonine kinase PKA (Kemp et al, 1976; Kemp et al, 1977). Subsequently, Casnellie et al (1982) used the amino acid sequence surrounding Y416, the site of Src autophosphorylation, to carry out the first assessment of peptide phosphorylation by Src. The main drawback to these methods was that the kinases used were derived from crude cell lysates as methods to recombinantly express kinases had not yet been developed.

The development of methods for the recombinant expression of kinases allowed more in-depth analysis of phosphorylation events. Expression of kinases in standard bacterial expression systems is toxic because bacterial genomes do not contain eukaryotic-like tyrosine kinases. Expression of tyrosine kinases in these systems therefore causes aberrant phosphorylation and activation of signalling pathways. A number of methods have now been developed to allow the expression and purification of active SFKs and these all involve a method to restrict the kinase activity during expression. Caspers et al (1994) overexpressed bacterial chaperones to enable the preparation of soluble Csk, Fyn and Lck from *E. coli*. Sicheri et al (1997) used *Spodoptera fruguperda* (Sf9) cells that were co-infected with baculoviruses expressing Hck and Csk to obtain pure, active Hck. Csk constitutively phosphorylates Y527 in the SFK C-terminal tail, promoting an inactive conformation. Wang et al (2006) created a vector that expresses Src as a fusion protein with maltose binding protein (MBP) and the phosphatase PTP1B. The phosphatase can dephosphorylate Src at Y416, promoting the inactive state of the

kinase, and can also dephosphorylate any aberrant bacterial protein phosphorylation that does occur. A thrombin cleavage site between PTP1B and Src allowed purification of isolated, active Src. A similar method has been employed in the Evans lab, with the cloning carried out by Dr Chris Dunning. A vector was created that expresses Src as a fusion protein with GST and PTP1B (Figure 3.5.1 A). A PreScission Protease site was engineered between PTP1B and Src and the resulting active Src protein retains a His-tag. The constructs used are Δ80 truncations and lack the first 80 residues of the Src sequence; the unique domain. This region is primarily involved in regulating the subcellular localisation of the kinases and is not required for kinase activity. Recently, Marin et al (2010) obtained active N1-Src kinase using low temperature expression alone. It is not clear how this was achieved as many other groups have reported the low temperature bacterial expression of SFKs to be toxic.

The elucidation of the consensus sequences for the domains of Src allowed detailed kinetic analysis of phosphorylation events mediated by pure preparations of kinases. Songyang et al (1995a) identified AEEEIYGEF as the consensus motif for the Src kinase domain. This sequence has now been used multiple times to assess substrate phosphorylation by Src both in cells (Graness et al, 2000) and *in vitro*. The versatility of peptide systems allowed the investigation of how the intramolecular associations of SFKs influence substrate specificity and kinase activity. Pellicena et al (1998) used peptide substrates to assess how the phosphorylation of an ideal substrate was affected by the additional ability of the substrate to bind to the SH2 domain. They found a 10-fold increase in substrate phosphorylation when SH2 domain binding could occur. Subsequent work from the same lab (Scott & Miller, 2000) showed that the presence of a SH3 domain binding motif resulted in a 3-fold decrease in the K_m of phosphorylation of the ideal substrate.

These studies all used isolated peptides and monitored the incorporation of phosphate using ^{32}P. Peptides were either separated from free ^{32}P by HPLC followed by scintillation counting or by dotting onto phosphocellulose paper followed by autoradiogram analysis. The use of GST-tagged peptides (Kim et al, 1999) allows their resolution by SDS-PAGE before ^{32}P detection by autoradiogram.

To avoid the use of ^{32}P other groups have developed spectrophotometric techniques. The advantage of this is that the phosphate incorporation can be monitored continuously. Barker et al (1995) developed a spectrophotometric assay

based on the conversion of NADH to NAD^+ and the corresponding change in absorbance. Development of a similar assay was attempted in the course of this study but was demonstrated to be prone to artefactual results and was not sensitive enough to detect the changes in substrate affinities required.

Another alternative to the use of ^{32}P is to assess phosphate incorporation using a phosphotyrosine antibody and detection using Western Blotting. The development and characterisation of an assay based on this technique will be described in this chapter.

3.2 Aims

The substrate preferences and functions of the neuronal Src kinases are currently poorly understood. We hypothesise that their substrate preferences, and therefore their functions, will differ to those of C-Src due to the inserts contained within their SH3 domains, a domain known to influence both substrate specificity and activity. To enable the investigation of these highly related kinases, a sensitive *in vitro* kinase assay has been developed. In parallel studies, the morphology and subcellular localisation of Src overexpressing cells was analysed.

3.3 Overexpression of neuronal kinases induces large scale morphological alterations

Compared to the large amount of research that has been carried out into the functions of C-Src, little is known about the functions of the neuronal Src kinases. There are technical difficulties in studying individual SFK members in cells. Most of the available inhibitors are competitive ATP analogues and the high degree of structural similarity in SFK members means that they act with low specificity (Bain et al, 2007). As the kinase domains of C-, N1- and N2-Src are identical, kinase inhibitors that target the kinase domain cannot be used to study the functions of individual isoforms in cell based assays. Primary investigations into the functions of the N-Src kinases were therefore carried out in heterologous cells to allow greater control over the isoform being investigated. The cell line chosen for the overexpression experiments was COS7 cells, a fibroblast cell line that endogenously expresses C-Src but not the neuronal Src isoforms.

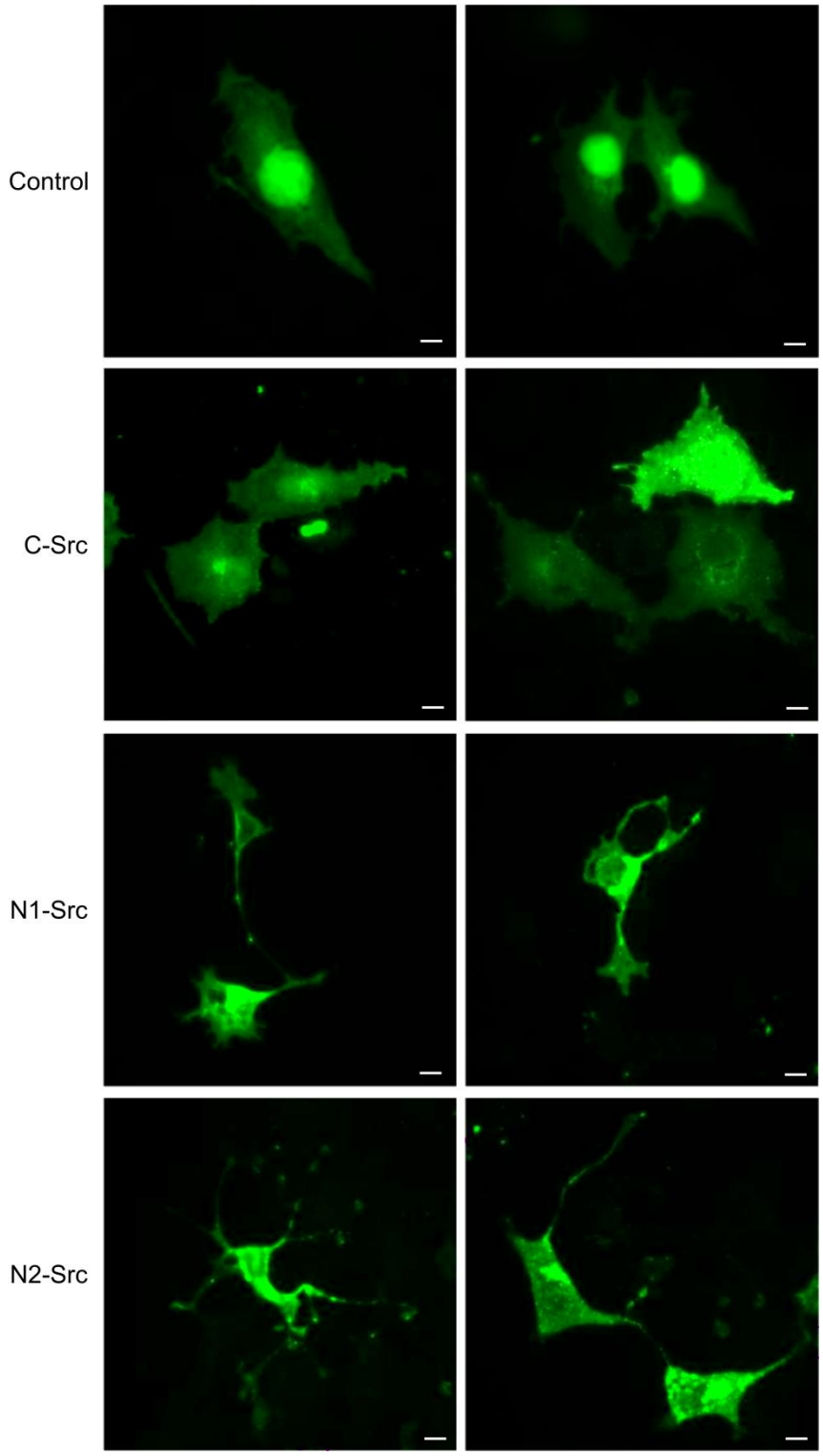

Figure 3.3.1 N-Src overexpression induces neuronal morphology in heterologous cells.

C-, N1- and N2-Src FLAG tagged constructs were overexpressed in COS7 cells for 48 hours. Control cells were transfected with CFP for visualisation. For control cells CFP signal is shown in green, for all Src constructs FLAG signal is shown in green Representative epifluorescent images. Scale bar = 10 µm. n=3 experiments, 20 fields of view, containing an average of 60 cells imaged per condition per experiment.

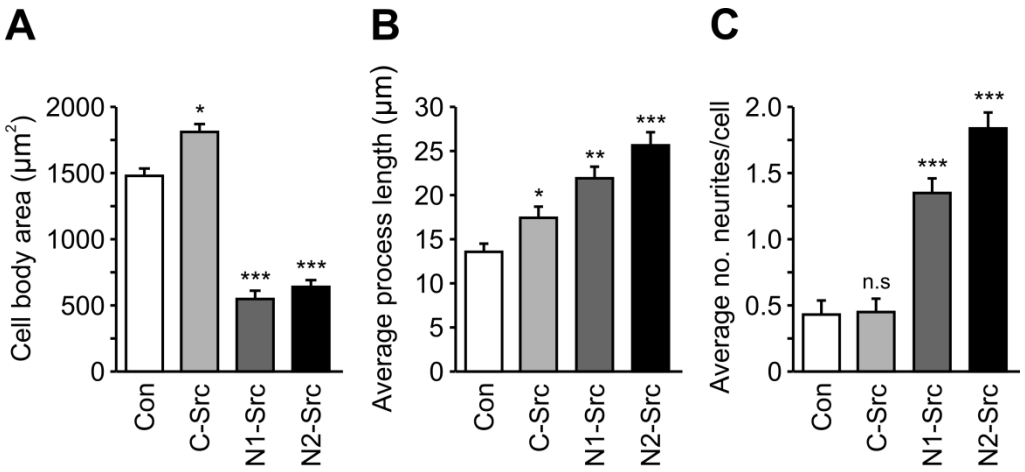

Figure 3.3.2 N-Src transfection results in reduced cell body size and production of neurites

C-, N1- and N2-Src FLAG tagged constructs were overexpressed in COS7 cells for 48 hours. Control cells were transfected with CFP for visualisation. Transfected cells were analysed for cell body area (A), process length (B) and neurite number (C) using ImageJ. n=3 experiments, 20 fields of view, containing an average of 60 cells analysed per condition per experiment. Error bars show SEM. Statistical analysis carried out using ANOVA and post hoc Tukey test. * $p<0.05$, ** $p<0.01$, *** $p<0.001$, all conditions are compared to control (CFP transfected) cells.

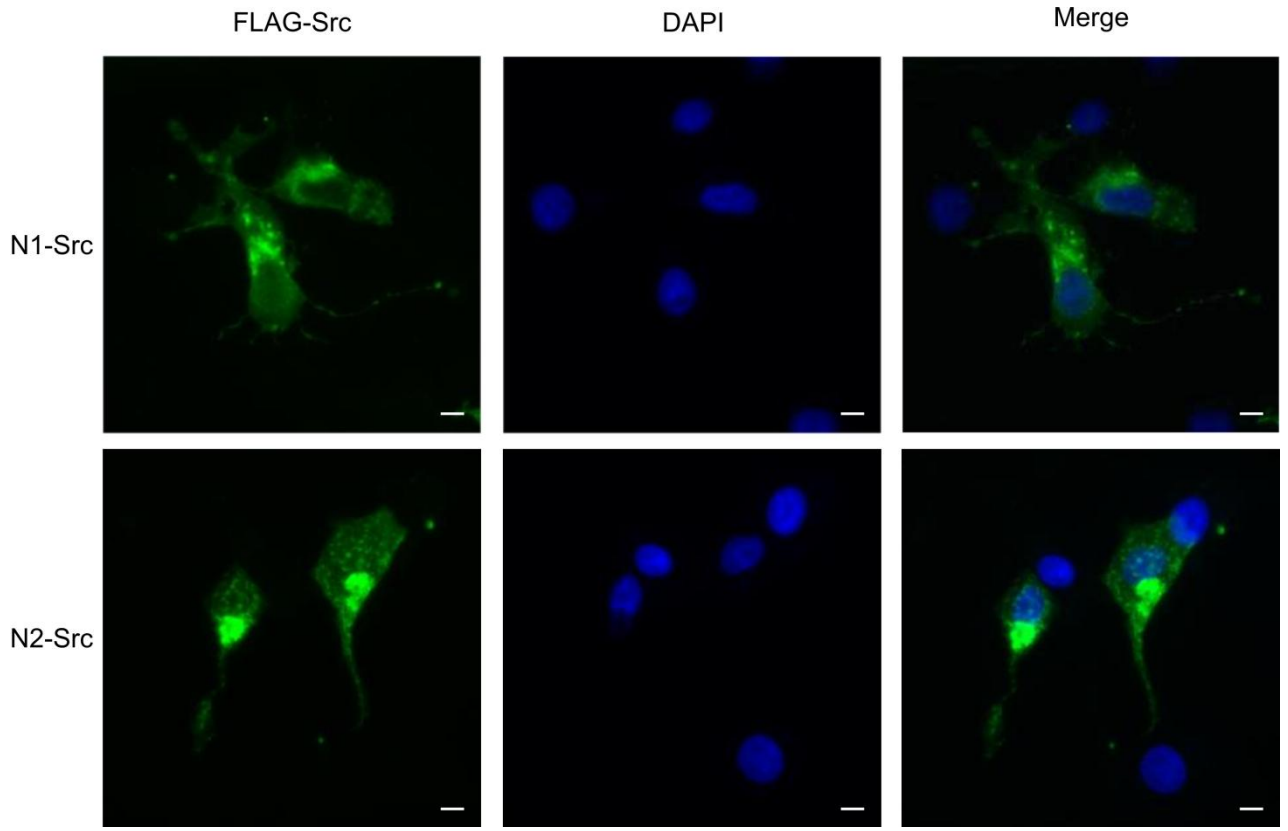

Figure 3.3.3 COS7 cells transfected with N1- or N2-Src show perinuclear localisation.

N1- and N2-Src FLAG tagged constructs were overexpressed in COS7 cells for 48 hours. Representative epifluorescent images shown. Transfected cells identified by FLAG staining (green). Nuclei identified by DAPI staining (bliue). Scale bar = 10 μm.

C-, N1- and N2-Src sequences were all inserted into a FLAG tagged vector for mammalian expression. The cloning of the Src constructs was carried out in the Evans lab by Kathi Mahal under the supervision of Dr Chris Dunning. As the extreme C-terminus of the Src sequence is involved in an intramolecular association with the SH2 domain, the FLAG tag was separated from the Src sequence by a GSGS linker. This prevents the tag from interfering with the regulation of the kinase. Tagging at the N-terminus was not possible as the extreme N-terminus is involved in membrane localisation and is required for targeting of the kinases. FLAG-tagged Src constructs have been produced previously and shown not to alter the subcellular localisation of Src (Schmitt & Stork, 2002). Other groups have added alternative tags including HA (Miller et al, 2000) and GFP (Qi et al, 2006; Sandilands et al, 2004) to the C-terminus of Src with no effect on kinase location or activity. Therefore, the addition of a FLAG tag is not predicted to alter the properties of the kinases in this study.

The Src constructs were transfected into COS7 cells and the kinases expressed for 48 hours before fixing and staining for morphological analysis. Control cells were transfected with CFP to allow visualisation of individual cells for quantification. The most striking effect of N-Src overexpression in heterologous cells was on their morphology. Overexpression of both N1- and N2-Src resulted in striking changes in cell morphology (Figure 3.3.1 A). COS7 cells are normally large, rounded cells but N-Src overexpression resulted in a dramatic contraction of the cell body, with N-Src transfected cells approximately 60% smaller than control cells (Figure 3.3.1 B) N-Src overexpression also resulted in the production of fine ‘neurite-like’ processes (3.3.1 C and D). The difference between the morphology of N-Src transfected cells and control cells was highly statistically significant (Figure 3.3.1)

In contrast, overexpression of C-Src had little effect on overall cell morphology. Quantification of the transfected cells revealed that C-Src transfected cells were approximately 15-20% larger than control cells (Figure 3.3.1 B) and had slightly longer neurites (Figure 3.3.1 C) than control cells but the overall appearance of the cells was not substantially altered. Even cells overexpressing very high levels of C-Src (Figure 3.3.1 A right hand panel) did not show any gross morphological phenotype.

For initial examination of morphology, all fine protrusions originating from the cell body were measured as processes (Figure 3.3.1 C). Control and C-Src transfected cells had an average process length of approximately 15 µm. Fibroblastic filopodia are typically approximately 10 µm long (Mallavarapu & Mitchison, 1999) and therefore the majority of these processes are probably filopodia. Therefore, for subsequent analyses, 'neurites' were defined as processes more than 15 µm in length. Figure 3.3.1 D shows that these abnormally long protrusions are much more common in N1- and N2-Src transfected cells than they are in either control or C-Src transfected cells.

N2-Src overexpressing cells were, on average approximately 100 μm^2 larger than N1-Src transfected cells (Figure 3.3.1 B) but this increase is not statistically significant. This is probably a result of the variability of the morphology of transfected cells but indicated that N2-Src overexpression does not cause as great a cell retraction as N1-Src overexpression. N2-Src overexpression also results in cells with more and longer neurites, although again this was not significant (Figure 3.3.1 C and D). Therefore, although both N1- and N2- Src overexpression induces neuronal morphology, there are some subtle differences in the morphology of N1- and N2-Src transfected cells. This implies that, while both seem to be involved in processes regulating cell morphology, they mediate slightly different functions.

In addition to morphological differences, analysis of transfected cells also revealed interesting insights into the subcellular localisation of the kinases. The subcellular localisation of C-Src is well characterised (Kaplan et al, 1994; Kaplan et al, 1992) and is in agreement with the localisation observed in this study (Figure 3.3.2). Under basal conditions C-Src adopts a generally diffuse localisation with more intense staining of the perinuclear area. This is known to relocate to intense plasma membrane staining following C-Src activation (Sandilands et al, 2004) and this relocalisation has been demonstrated within the Evans lab (K. Mahal personal communication), indicating that the Src constructs used here are physiologically active.

The subcellular localisation of the N-Srcs has not been previously reported and is hindered here by the small cell body size of N-Src transfected cells. The majority of N-Src transfected cells do seem to have staining adjacent to the nucleus but as there is so little cytoplasm surrounding the nucleus it is difficult to assess whether this is true perinuclear localisation. Assessment of the localisation of N-Srcs

is also hindered by the long exposure times needed to visualise the weakly stained processes. Examples of Src overexpressing cells more clearly showing perinuclear localisation are shown in Figure 3.3.2. In these cells, perinuclear staining can clearly be seen but correlative experiments using specific markers are required for further comparisons to C-Src to the made.

While C- and N1-Src staining is generally diffuse, closer analysis of N2-Src overexpressing cells revealed a much more punctate localisation throughout the cytoplasm (Figure 3.3.2). This is unusual for a SFK and indicates that N2-Src is localised to membrane microdomains or present in large amounts on trafficking vesicles. There is some evidence that N-Srcs are able to enter lipid rafts (Mukherjee et al, 2003) but the significance of this in relation to their signalling remains unknown.

Taken together, the results of the individual overexpression experiments provide important insights into the roles of the N-Src kinases and provide strong evidence that they differ functionally from C-Src. These data also provide evidence that the functions and possibly subcellular localisations of N1- and N2-Src are not identical. The fact that these striking alterations in cell morphology are observed in non-neuronal heterologous cells indicates that not all of the cellular substrates of N1- and N2-Src are neuronal specific.

3.4 Increased basal kinase activity levels in the neuronal kinases

Morphological analysis has revealed that the N-Src kinases are able to induce a striking alteration of COS7 cell morphology. This could be due to the substrate preferences of the neuronal Srcs being different to those of C-Src but it could also be attributed to the increased level of basal kinase activity that has been repeatedly reported for the N-Src kinases (Brugge et al, 1985; Levy & Brugge, 1989). In order to assess the activation state of the kinases and enable comparison between the isoforms, transfected COS7 cell lysates were analysed by Western blot. There are a number of phosphospecific antibodies available that are used to assess the activation state of the kinases. Phosphorylation of a residue within the kinase domain (Y416) stabilises the active state of the kinase. Therefore, phosphorylation at Y416 is associated with an active state of the kinase. Phosphorylation of the C-terminal tail

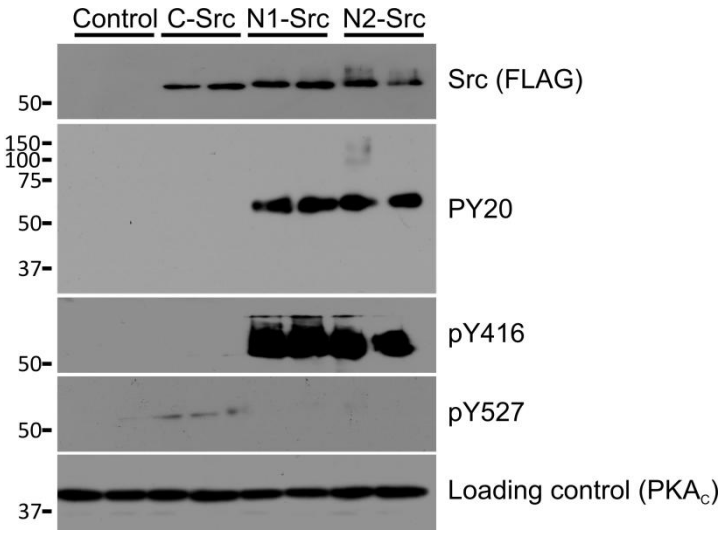

Figure 3.4.1 N-Srcs have higher levels of Y416 phosphorylation than C-Src.

C-, N1- and N2-Src FLAG tagged constructs were transfected into COS7 cells and lysed 48 hours following transfection. Transfected COS7 cell lysates were analysed for total phosphotyrosine content (PY20), active Src (pY416) and inactive Src (pY527). Equal expression levels shown by FLAG signal and equal loading shown by PKA_c loading control.

residue Y527 enables the formation of the SH2:tail intramolecular association and is associated with the inactive form of the kinase.

Blotting using antibodies specific for these residues revealed that the intrinsic kinase activities of N1- and N2-Src are much higher than that of C-Src. This experiment was carried out under basal conditions; under these conditions no pY416 signal was observed for C-Src but a pY527 signal was detected. This indicates that the majority of the kinase in the cell is in a closed, inactive conformation. Constitutive phosphorylation of C-Src at Y527 in resting fibroblasts has been reported previously (Chackalaparampil & Shalloway, 1988). In contrast, strong immunoreactivity was seen at Y416 for N1- and N2-Src, whereas no pY527 signal was observed. Taken together, these results show that the neuronal Srcs have a much higher basal level of autophosphorylation than C-Src, inferring a higher basal level of kinase activity.

It is interesting, however, that the high kinase activity of the N-Srcs does not result in high levels of substrate phosphorylation. Blotting for total phosphotyrosine content of the cells revealed that the main phosphorylated protein within the cells are the neuronal Srcs themselves (Figure 3.4.1 - PY20 blot). This is probably detection of the phosphorylated pY416 residue. If the high basal kinase activity of the N-Srcs resulted in unregulated substrate phosphorylation, it would be expected that the substrates phosphorylated would be detected by the phosphotyrosine antibody. The absence of this indicates that the signalling of the N-Srcs is regulated despite their high constitutive kinase activity and raises the question of how this is achieved.

These data from heterologous cells raise important questions about the functions of the N-Src kinases. Firstly, how do the SH3 domain inserts of N1- and N2-Src exert their impact on kinase activity and what is the result on substrate phosphorylation? Secondly, what substrates are the N-Srcs able to interact with and does this result in the regulation of cytoskeletal rearrangement? The first question will be addressed using *in vitro* biochemical techniques presented in Chapters 3 and 4. The functional aspects of N-Src signalling and their impact on cytoskeletal remodelling in neurons will be addressed in Chapter 5.

3.5 Design of an *in vitro* assay for kinase activity

Experiments in heterologous cells have provided useful insights into the potential functions of the N-Src kinases but, as there are limited tools available to manipulate specific Src isoforms in cell based assays, more detailed analysis into the substrate preferences of the kinases was carried out using *in vitro* techniques. To facilitate these investigations it was necessary to design an *in vitro* kinase assay that was capable of detecting differences in the substrate preferences of the kinases.

The *in vitro* method chosen for these investigations was the use of GST-tagged peptides. The peptides were designed to contain a tyrosine residue that could be phosphorylated by the kinase domain and also sequences designed to test the SH3 domain binding of the kinases. Appropriate oligonucelotides were commercially synthesised (Eurogentec) and cloned into a GST-expression vector. The kinase domain is identical for all three splice variants and therefore any differences in phosphorylation observed will be due to differences in the binding ability of the SH3 domain. The basis of this assay is depicted in Figure 3.5.1 B. Detection of the extent of phosphorylation of the tyrosine was carried out using an α-phosphotyrosine antibody (PY20) and detection by Western Blotting.

The peptide containing the tyrosine residue able to be phosphorylated by the kinase domain consisted of the sequence AEEEIYGEF. This was defined as the consensus sequence for recognition by the Src kinase domain by Songyang et al (1995a). This sequence is present in all of the GST-peptides produced and is referred to as 'Y' in the GST-peptide naming convention.

A linker of 5 amino acids was present between the Y peptide and the peptides inserted to assess binding to the SH3 domain due to the nature of the cloning carried out (see Materials and Methods, section 2.2.7.1 for details). This meant that there was a linker of 13 amino acids between the phosphorylatable tyrosine residue and the first amino acid known to play a structural role in the contact of the C-Src SH3 domain. This is the same as the linker separating kinase and SH3 domain interacting elements in a study of Hck phosphorylation (Scott & Miller, 2000), who calculated that it was sufficient to allow simultaneous interaction of both contacts with the kinase.

The SH3 domain binding peptides introduced into the assay were based on the known binding preferences of the SH3 domain of C-Src as the preferences of the N-Src SH3 domains were not known. Two classes of ligand are known to bind to the

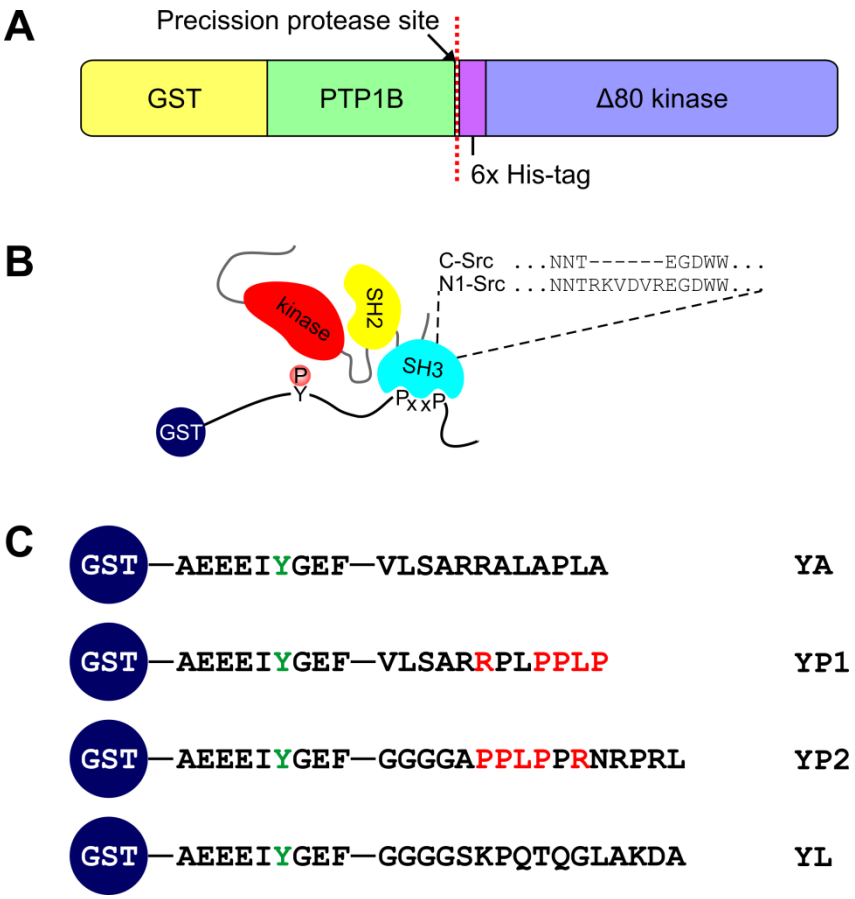

Figure 3.5.1 Schematic representation of the kinases and substrates used in the in vitro kinase assay.

A) Recombinant Src was expressed as fusion protein with GST and PTP1B. Isolated His-tagged Src is obtained by PreScission protease cleavage. B) The *in vitro* kinase assay. GST-peptide substrates contain a tyrosine residue that can be phoshorylated by the Src kinase domain. Sequences inserted at the position of PxxP assess the changes in phosphorylation induced by SH3 domain binding. C) The GST-peptide substrates. All substrates contain the phosphorylatable tyrosine residue; 'Y' in the GST-peptide naming convention, contained within a sequence known to bind well to the Src kinase domain. YP1 and YP2 represent the Class I and Class II C-Src SH3 domain binding sequences. YA is a control sequence that cannot bind to the SH3 domain. YL contains the amino acid sequence found in the linker region between the SH2 domain and the kinase domain of the Src kinases. This sequence is known to bind to the SH3 domain of C-Src, forming an intramolecular association that promotes the inactive conformation of the kinase.

C-Src SH3 domain, both with the core consensus motif PxxP. These are termed Class I and Class II based on the presence of a positively charged arginine (R) residue before or after the PxxP motif respectively. The sequence of the Class I peptide used was VSLARRPLPPLP and the Class II peptide was PPLPPRNRPRL as defined by Rickles et al (1995). An additional 4 residue glycine (G) linker was added prior to the Class II sequence to ensure that the first residue involved in binding the SH3 domain was situated an equal distance away from the phosphorylatable tyrosine residue for both the Class I and Class II peptides. The GST-peptides containing both the kinase recognition sequence (Y) and the Class I or Class II SH3 domain binding motifs were termed YP1 and YP2 respectively. To provide a control peptide, alanine substitutions of all residues involved in SH3 domain binding in the Class I peptide were made. This control was necessary as it mimicked the steric properties of a peptide not able to bind the SH3 domain. The control peptide was termed YA. The peptides are depicted schematically in Figure 3.5.1 C.

The ultimate aim for the *in vitro* kinase assay was to allow it to be used to assess the kinetics of phosphorylation of the three substrate peptides by each of the kinases. As the binding preferences of the C-Src SH3 domain were known they could be used to assess the sensitivity and accuracy of the assay. Once the validity of the assay had been confirmed it could then be used to assess the binding preferences of the N-Srcs and discover whether they differ to the preferences of C-Src. Before these experiments could be carried out the assay needed to be optimised so that the incorporation of phosphate was linear with respect to both time and kinase concentration. When the incorporation of phosphate is linear the reaction will proceed according to the laws of Michaelis-Menton kinetics. Varying the substrate concentration around the approximate K_m would then allow the elucidation of an accurate K_m and V_{max} for the phosphorylation of each substrate by each of the kinases.

The control experiments to establish concentrations where phosphate incorporation was linear were all carried out by assessing the phosphorylation of YA by C-Src. Varying the kinase concentration resulted in a concentration dependant increase in phosphorylation (Figure 3.5.2 A). Densitometry analysis showed that this increase was linear at lower concentrations and saturated at higher concentrations (Figure 3.5.2 B). Based on these data a kinase concentration of 5 nM was chosen for subsequent investigations.

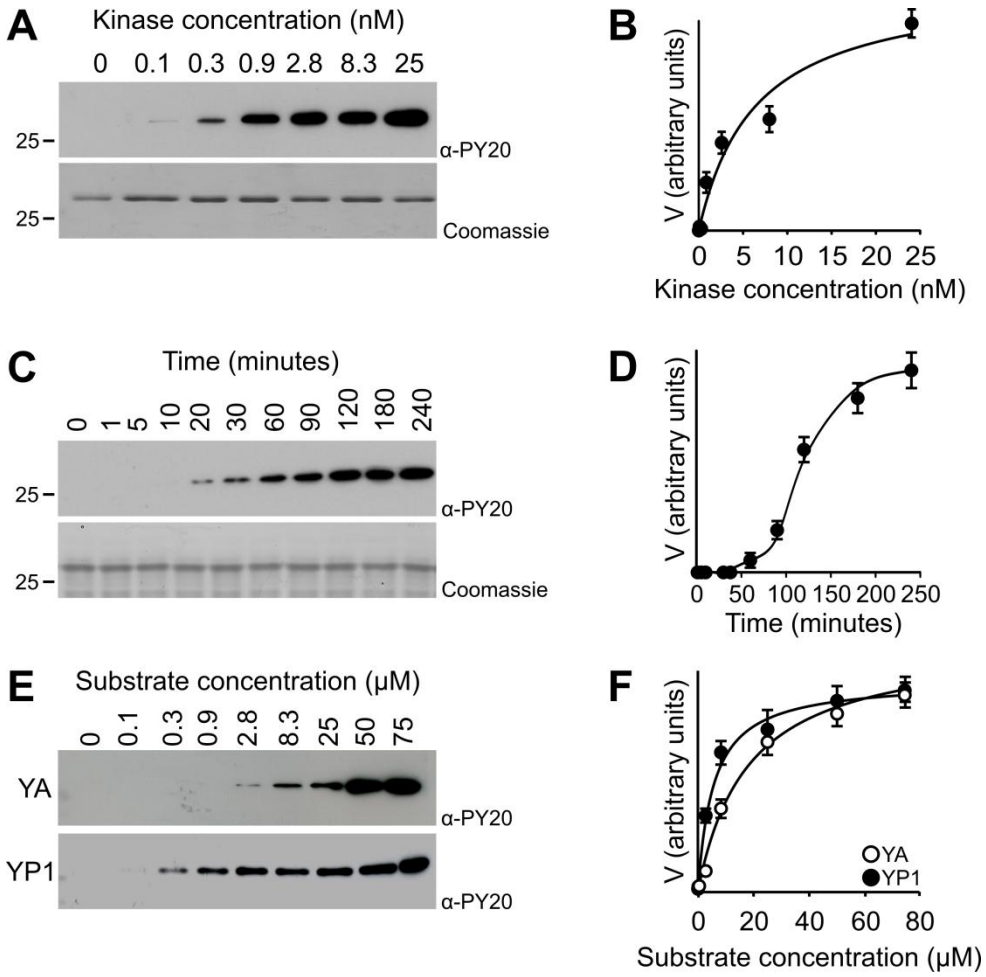

Figure 3.5.2 Characterisation of the in vitro kinase assay.

All kinase assays were carried out at 30 °C, initiated by the addition of ATP and halted by transfer to ice and immediate addition of Laemmli buffer. A) Optimisation of kinase concentration for use in the in vitro kinase assay. C-Src kinase concentration varied as indicated. YA substrate (25 μM) phosphorylation assessed after 90 minutes. B) Densitometry analysis of kinase concentration optimisation, n=3 experiments. C) Timecourse of YA phosphorylation. C-Src concentration 5 nM, YA concentration 25 μM, samples taken at the timepoints indicated. D) Densitometry analysis of timecourse experiment, n=3 experiments. E) Comparison of YA and YP1 phosphorylation by C-Src. C-Src concentration 5 nM, samples taken after 90 minutes. Substrate concentrations varied as indicated F) Densitometry analysis of substrate comparison, n = 3 experiments. Phosphotyrosine detected using the antibody PY20. All densitometry analysis carried out in Image J. All error bars show +/- SEM.

A timecourse experiment revealed that, using a kinase concentration of 5 nM, phosphorylation occurs linearly between approximately 75 and 150 minutes. A long lag phase is observed before any phosphorylation can be detected. The phosphate incorporation saturates at later timepoints (Figure 3.5.2 C and D). A timepoint for all subsequent experiments of 90 minutes was selected based on these data.

In order for the *in vitro* assay to be able to report on substrate specificity it needed to be able to distinguish between the phosphorylation of substrates that can bind the SH3 domain and those that cannot. It is known that the C-Src SH3 domain binds to the YP1 sequence but not to the control YA. Therefore, it would be predicted that phosphorylation of YP1 would be enhanced over that of YA. To assess this, the substrate concentration was varied while the kinase concentration and duration of the experiment were fixed at 5 nM and 90 minutes as previously described. Figure 3.5.2 E and F show that the assay is able to clearly distinguish between the phosphorylation of the two substrates. Phosphorylation of YP1 can be detected at approximately a 30-fold lower substrate concentration for YP1 than for YA (Figure 3.5.2 E), although both saturate at approximately the same point (Figure 3.5.2 F). Therefore the *in vitro* kinase assay was able to report on the SH3 domain binding ability of the kinases to GST-peptide substrates and was suitable for use to assess the binding preferences of the neuronal kinases.

3.6 The N-Src SH3 domain has a different ligand specificity to C-Src

It is known that the neuronal Src kinases do not bind to the majority of C-Src ligands that have been tested. It is also known that the N-Srcs have a higher level of basal kinase activity than C-Src (Figure 3.4.1). However, the substrate preferences of the neuronal kinases and how their substrate phosphorylation is affected by the increased constitutive activity were not known. The development of the sensitive *in vitro* kinase assay allowed the investigation of N-Src substrate preferences.

Increased basal kinase activity is commonly a trait of oncogenic mutation of kinases and results in unregulated and aberrant substrate phosphorylation. If this were true of the neuronal Src kinases, it would be predicted that SH3 domain docking would not be required for substrate recognition and that phosphorylation of the control peptide, YA, would be increased over C-Src. Figure 3.6.1 shows that,

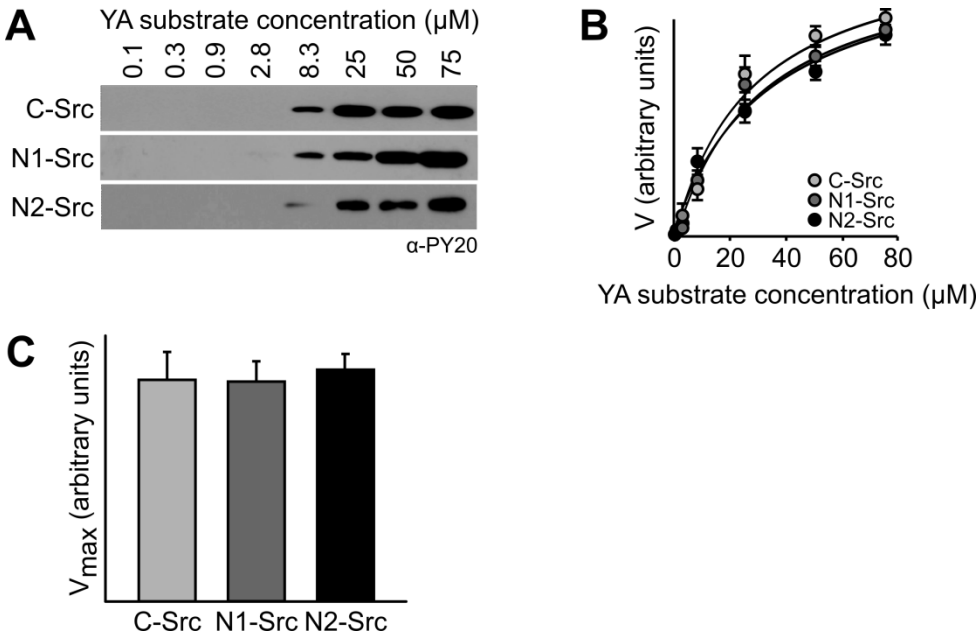

Figure 3.6.1 N-Srcs do not show increased phosphorylation of a control substrate.

Phosphorylation of the control substrate YA by C-, N1- and N2-Src was assessed. YA concentration varied as indicated, kinase concentration 5 nM, timepoint 90 minutes. A) Analysis of phosphorylation by western blot. Detection using the phosphotyrosine antibody PY20. B) Densitometry analysis of YA phosphorylation carried out using ImageJ. Equivalent substrate concentrations were loaded onto the same blot and normalised using a standard to allow direct comparison between the three kinases. See materials and methods for more details. C) Analysis of the rate of reaction, computed by SigmaPlot

surprisingly, N1-Src and N2-Src phosphorylation of YA occurs with the same kinetics as for C-Src. The densitometry data obtained from the phosphotyrosine blots was used to calculate the kinetics of the phosphorylation, according to Michaelis-Menton parameters. This analysis was carried out using SigmaPlot and the binding curve produced fitted well to the model for single site saturation. This would be predicted as the phosphorylation of a single tyrosine residue was being monitored. The calculated K_m for the phosphorylation of YA by all three kinases was approximately 30 μM (Figure 3.6.2 E). This correlates well with the known K_m of the AEEEIYGEF peptide for the kinase domain of 33 μM (Songyang et al, 1995a). The V_{max} of the phosphorylation reactions was also calculated and, although it is not possible to calculate the rate of the reaction in terms of the absolute rate of phosphate incorporation, this showed that the V_{max} of all three phosphorylation reactions was equivalent (Figure 3.6.1 C). These data indicated that an appropriate SH3 domain interaction is required for N-Src substrate recognition as it is for C-Src.

In order to assess whether the SH3 domain substrate preferences of the N-Srcs differ from those of C-Src, phosphorylation of YP1 and YP2 was investigated. This revealed that the N-Srcs phosphorylate these substrates poorly when compared to C-Src. Figure 3.6.2 A - D shows that C-Src phosphorylation of both YP1 and YP2 occurs at much lower substrate concentrations than for N1- and N2-Src. This indicates that the SH3 domains of the N-Srcs are not able to bind to the Class I and Class II sequences in YP1 and YP2 that are able to enhance phosphorylation by C-Src and implies that the substrates preferences of the N-Srcs differ from those of C-Src.

Analysis of the kinetics of the phosphorylation reactions (Figure 3.6.2 E) showed that the presence of YP1 or YP2 was able to significantly reduce the K_m of the phosphorylation by C-Src. The affinity of the C-Src SH3 domain is known to be slightly higher for Class I sequences than for Class II sequences. It is encouraging for the sensitivity of the assay that this is reflected in the calculated K_ms of the YP1 and YP2 phosphorylation. The known K_ms of the Class I and Class II sequences binding to the Src SH3 domains are 0.45 μM and 1.2 μM respectively (Feng et al, 1995). The K_ms obtained in this study are 4 μM and 6 μM for YP1 and YP2 respectively. This assay does not directly report the binding affinity of the SH3 domains to their substrate; instead, it quantifies the change in affinity of the kinase domain for the ideal kinase domain substrate induced by SH3 domain binding.

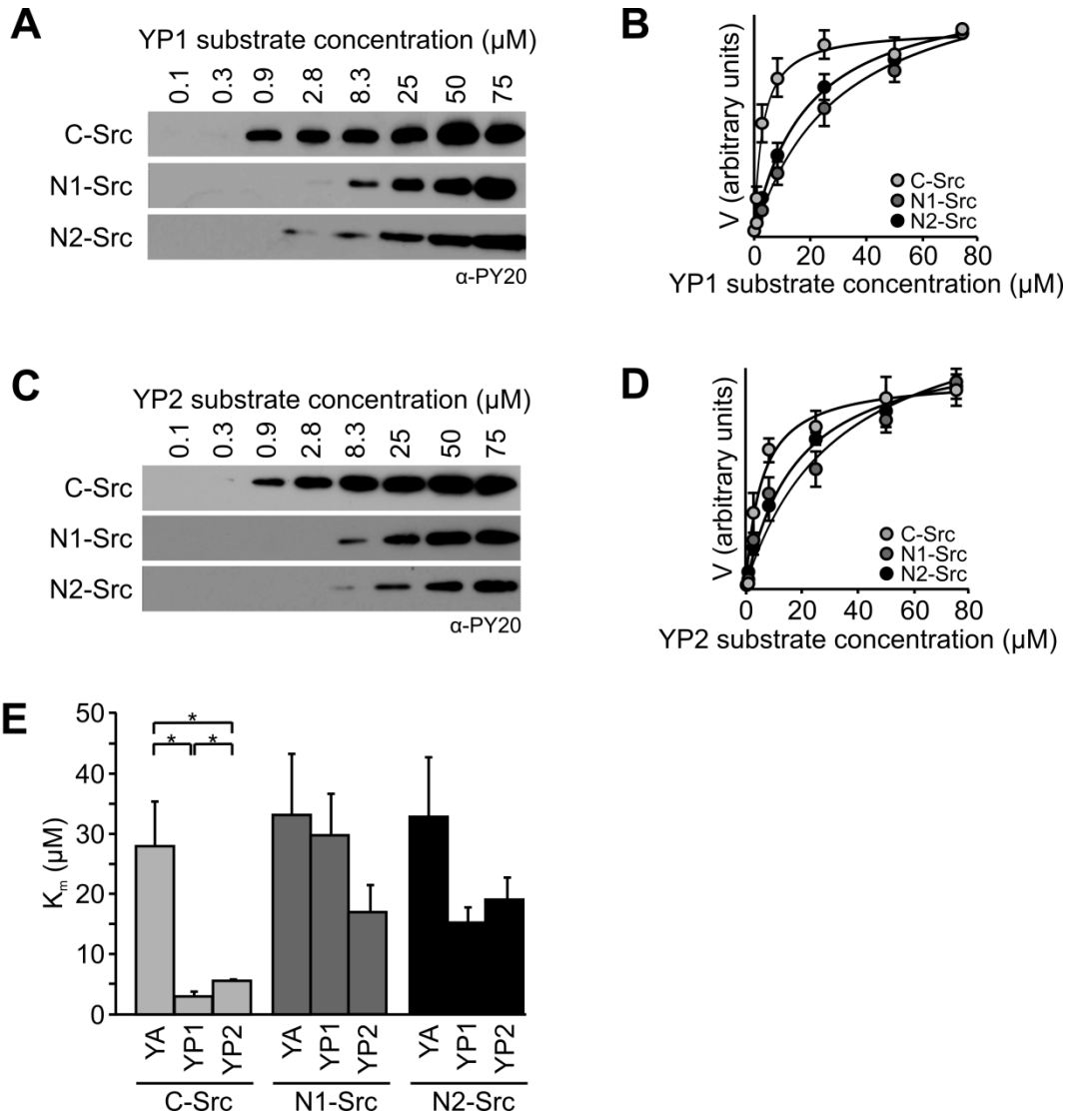

Figure 3.6.2 N-Src substrate preferences differ to those of C-Src.

Phosphorylation of substrates containing the C-Src SH3 domain binding motifs (YP1 and YP2) was analysed. A) and C) Analysis of phosphorylation by western blot. Substrate concentration varied as indicated. Kinase concentration 5 nM, timepoint 90 minutes. Detection of phosphate incorporation using the phosphotyrosine antibody PY20. B) and D) Densitometry analysis of phosphorylation carried out using ImageJ. Equivalent substrate concentrations were loaded onto the same blot and normalised using a standard to allow direct comparison between the three kinases. See materials and methods for more details. E) Comparison of the K_m of substrate phosphorlyation. Calculated using SIgmaPlot kinetics module. Data shown are n=3 experiments, error bars show SEM. Statistical analysis carried out by ANOVA and post hoc Tukey test *p<0.05, all conditions compared to YA phosphorylation.

Therefore, the trend for Class I preference over Class II implies that the assay is able to detect subtle differences in substrate affinity and report them accurately.

For N1- and N2-Src neither the presence of YP1 or YP2 had a significant effect on the K_m of phosphorylation. However, the K_m of phosphorylation was partially reduced by the presence of YP2 for N1-Src and by both YP1 and YP2 for N2-Src. This indicates that some weak binding between the substrates and the N-Src SH3 domains may have occurred. It is interesting that phosphorylation by N1-Src is only enhanced by YP2. The Class I and Class II sequences are differentiated by the presence of a positively charged arginine residue either before or after the PxxP motif. In the Class II sequence the charged residue is after the PxxP motif and the partial enhancement in N1-Src phosphorylation by a Class II motif may indicate that a charged residue in this position is important for binding to the N1-Src SH3 domain.

Phosphorylation by N2-Src was partially enhanced by both YP1 and YP2. This indicated that the substrate preferences of the N2-Src SH3 domain may not be substantially different to those of C-Src. It may be that N2-Src is able to bind to the same core consensus motif but that the preferences for the flanking residues are altered. This is surprising as the N2-Src SH3 domain has the largest insert within its n-Src loop and this would be predicted to significantly alter its substrate preferences.

Taken together, these data provide evidence that the increased basal kinase activity of the N-Srcs does not result in unregulated substrate phosphorylation and that an appropriate SH3 domain interaction is required for the N-Srcs to select their *in vivo* substrates. The SH3 domain binding preferences of N1-Src will be investigated further in Chapter 4.

3.7 Conformation of the kinases

The increased basal activity of the N-Srcs has previously been suggested to be due to a decreased ability to form the SH3:linker association that normally constrains SFK kinase activity. The existence of this linker was indicated by the fact that deletions and mutations in the SH3 domains of Src and Hck result in increased kinase activity (Murphy et al, 1993; Superti-Furga et al, 1993). The structure of full length Src revealed the residues that form the linker; it was not obvious from the primary sequence as the polypeptide contains only one proline residue (Xu et al, 1997). The linker sequence identified by Xu et al (1997) was ^{248}SKPQTQGLAKDA. This

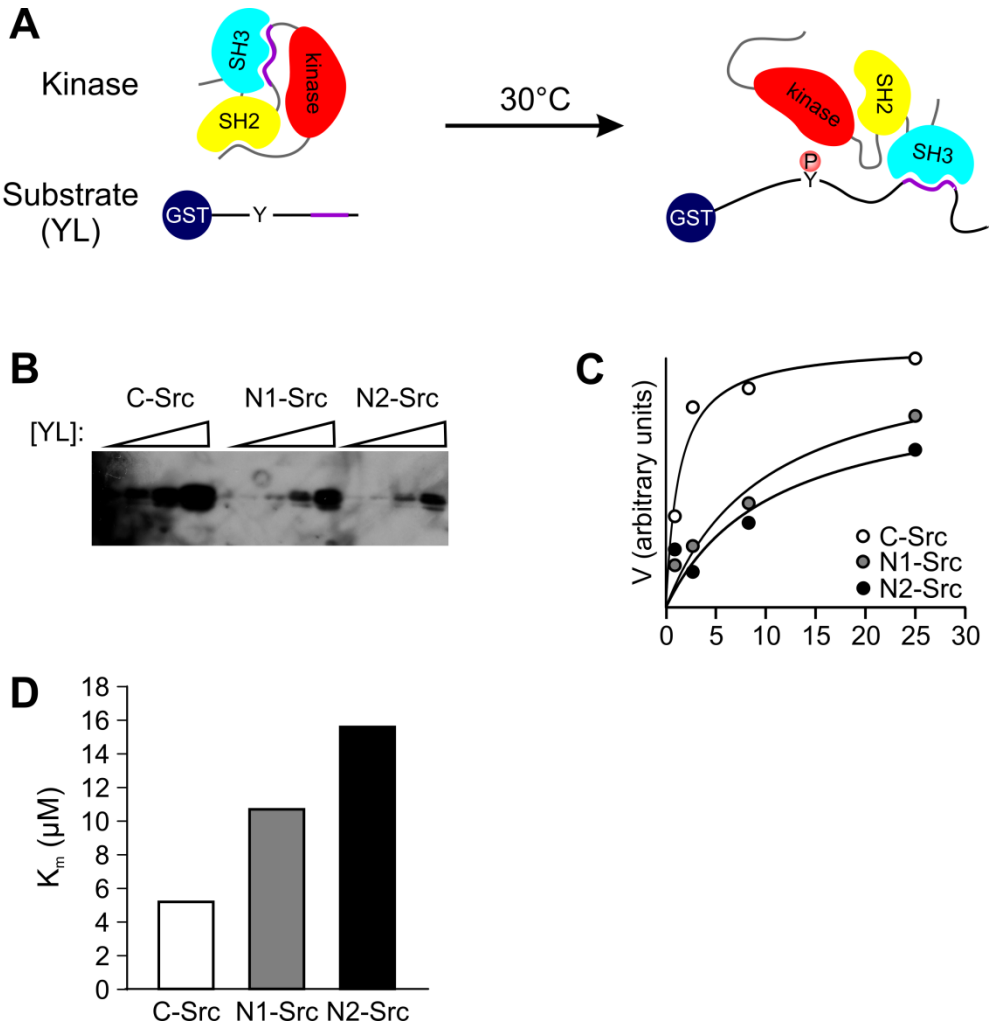

Figure 3.7.1N-Srcs interact poorly with the SH2:linker sequence.

Phosphorlyation of the YL substrate by C-, N1- and N2-Src was investigated. A) Schematic representation of the basis of the assay. The amino acid sequence of the linker region between the SH2 domain and the kinase domain (purple) was cloned into to GST-peptide system. This substrate was termed YL where L stands for linker. If the linker sequence in YL is able to bind to the SH3 domain of the kinase then substrate phosphorylation will occur as depicted in the cartoon on the right hand side. C, N1- and N2-Src kinases were incubated individually with the YL substrate at 30°C and the amount of substrate phosphorylation assessed by western blot using an α-phosphotyrosine antibody. YL concentrations of 25 μM, 8.3 μM, 2.8 μM and 0.9 μM used, kinase concentration 5 nM, timepoint 90 minutes. B) Detection of phosphotyrosine by the PY20 antibody. C) Densitometry analysis of YL phosphorylation carried out using ImageJ. D) K_m of YL phosphorylation by C-, N1- and N2-Src. Calculated using SigmaPlot kinetics module. n=1 experiment.

sequence was cloned into the GST-peptide system and termed YL (where L is an abbreviation of linker). A schematic representation of this substrate and the location of the amino acid sequence it is derived from are shown in Figure 3.7.1 A with the relevant regions highlighted in purple.

It was hypothesised that the amino acid inserts within the SH3 domains of the neuronal Src kinases would result in a reduced affinity between the SH3 domain and the linker region. If the SH3 domains of the neuronal kinases interact more weakly with the linker region then this would reduce the strength of the intramolecular associations constraining the kinase activity and result in a more open and active kinase. This could begin to explain the increased activity observed in the neuronal Src kinases.

In order to test this hypothesis phosphorylation of YL by the three kinases was investigated. If the SH3 domain of the kinase is able to bind to the YL substrate, as shown in the right hand panel of Figure 3.7.1 A, then the tyrosine residue in the substrate would be phosphorylated by the Src kinase domain and this could be detected by western blot. This experiment relies on the linker sequence in the YL substrate being able to bind to the SH3 domain in preference to the linker sequence in the endogenous kinase. Incubation of the kinases at 30°C results in autophosphorylation of Y416 and promotion of the active conformation of the kinase. This conformational rearrangement disrupts the interaction between the SH3 domain and the linker and allows binding of YL to the SH3 domain.

This experiment revealed that the neuronal kinases do indeed phosphorylate the linker substrate less efficiently than C-Src (Figure 3.7.1). The K_m of the interaction with C-Src is 5 µM. This is surprising as it is equivalent to the K_m for the phosphorylation of the ideal substrates YP1 and YP2. As the linker sequence does not contain a PxxP motif, this would not be expected. The K_m of the phosphorylation by both N1- and N2- Src are ~10 and 15 µM respectively. This implies that the N-Src SH3 domains are able to bind weakly to the linker sequence but not as well as the C-Src SH3 domain. The difference in affinity is presumably due to the inserts within their SH3 domains altering the SH3 domain binding site sufficiently to inhibit binding.

Another surprising insight into the conformation of N1-Src was gained during the characterisation of an N1-Src specific antibody. A custom antibody specific for the N1-Src SH3 domain was commercially generated (GenScript) for use

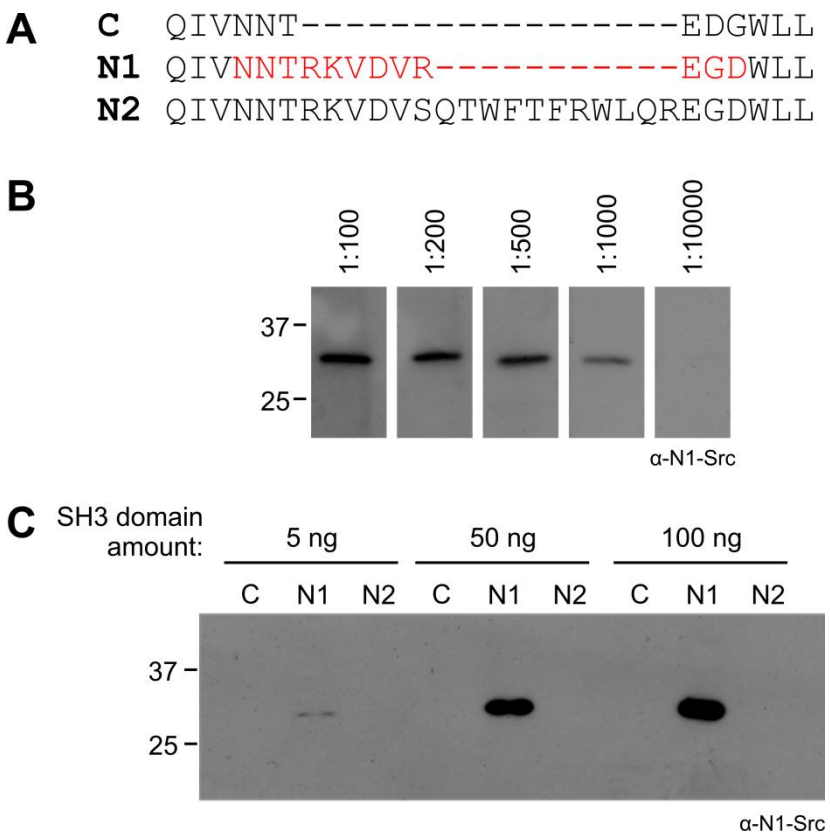

Figure 3.7.2 The N1-Src antibody detects the SH3 domain of N1-Src specifically.

A) The epitope that the antibody is raised against covers the 6 amino acid inset and is unique to N1-Src, highlighted in red. B) Detection of the recombinant GST-N1-Src SH3 domain by the N1-Src antibody. 100 ng GST-N1-Src SH3 domain loaded into each lane, antibody concentration varied as indicated. C) The sensitivity of the N1-Src antibody was tested against C- and N2-Src. Amount of GST-Src SH3 domain loaded as indicated, N1-Src antibody concentration 1:500.

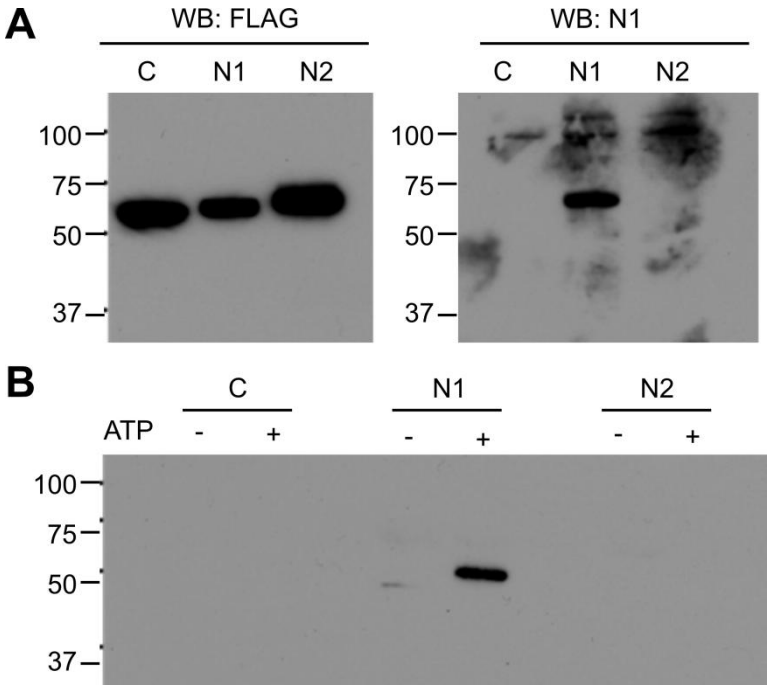

Figure 3.7.3 Kinase activation is required for detection by the N1-Src antibody.

A) Full length N1-Src kinase can be detected specifically from transfected cell lysates. COS7 cells were transfected with C-, N1- and N2-Src and lysed 48 hours following transfection. FLAG blot shows equal expression levels. N1-Src antibody blot shows specific detection of N1-Src. B) Recombinantly expressed C-, N1- and N2-Src were activated by incubation with ATP at 30°C. The N1-Src antibody specifically detects Δ80 N1-Src following this activation.

in studying the *in vivo* roles of N1-Src. The epitope that the antibody was raised against covered the six amino acid insertion in the N1-Src SH3 domain (Figure 3.7.2 A) and has previously been used to produce an N1-Src specific antibody by Sugrue et al (1990). This antibody was shown to be able to specifically recognise the isolated GST-tagged SH3 domain of N1-Src (Figure 3.7.2 B and C). However, no signal was detected using the full length recombinant kinase. In the full length kinase the antibody epitope will be on the surface of the SH3 domain adjacent to the kinase domain and would be masked if the kinase were in a closed conformation.

As an alternative to the recombinant kinase, lysates of COS7 cells expressing FLAG-tagged kinases were used. Under these conditions, the antibody was able to recognise N1-Src and do so specifically over C- and N2-Src (Figure 3.7.3 A). As previously shown (Figure 3.4.1), the neuronal kinases are in an open, active conformation within cells and it was therefore hypothesised that the antibody epitope might be masked in the recombinant kinase but accessible in the kinases contained within the lysates. To test this, recombinant kinases were activated by incubation with ATP at 30^{o}C; resulting in autophosphorylation at Y416. Surprisingly, under these conditions, the antibody was able to detect the recombinant kinase (Figure 3.7.3 B). This indicates that the antibody epitope is blocked in recombinant N1-Src prior to activation by autophosphorylation and provides evidence that the neuronal kinases are partially constrained by intramolecular associations and are not permanently in an open state. It can be concluded that, although the SH3:linker intramolecular association constraining the activity of the neuronal Src kinases are weaker than for C-Src, they are not entirely absent and regulation of the activity of the neuronal kinases is possible.

The characterisation of the N1-Src specific antibody revealed interesting insights into the conformation of the kinases. However, when it was tested for immunofluorescent applications it was found that the degree of background staining was too high to allow it to be used further. While N1-Src transfected cells could be detected using the N1-Src antibody in conjunction with FLAG staining in transfected COS7 cells, the background fluorescence made it difficult to identify N1-Src transfected cells or endogenous protein in cultured neurons based on α-N1-Src alone.

3.8 Discussion

3.8.1 Neuronal Srcs are implicated in the regulation of cytoskeletal rearrangement

Morphological analysis of neuronal Src transfected cells has revealed that their overexpression induces large scale morphological alterations, presumably due to cytoskeletal rearrangement. Cells transfected with N1- or N2-Src have much smaller cell soma than either C-Src transfected or control cells. N-Src transfection also results in the production of fine, 'neuron-like' processes and this result implies a broad role for the N-Src kinases in the regulation of cytoskeletal rearrangement, particularly in the development of neuronal morphology. This result also provides evidence that the neuronal Srcs carry out roles substantially different to those of C-Src.

The morphology of the N-Src transfected cells is similar to that observed following overexpression of a dominant positive form of Rho GTPase (Kolyada et al, 2003). The Rho family GTPases are able to link surface receptors to the organisation of the actin cytoskeleton (Hall, 1998) and signalling resulting from the Rho family has been shown to be important in neuronal cells in the processes of axonal growth and guidance (Hall & Lalli, 2010). The similarity in morphology means that it is possible that the neuronal Srcs are acting directly in the same pathway as the Rho proteins. However, it is also possible that they are acting in a parallel pathway also able to influence cell shape, such as signalling arising from adhesion molecules. Further elucidation of the substrate preferences of the neuronal Srcs will allow discrimination between these two possibilities. The potential for Src involvement in small GTPase and cell adhesion molecule signalling pathway will be discussed in detail in Chapter 6.

The striking morphological changes caused by N-Src transfection led us to question whether N-Src overexpression was able to induce a functional neuronal differentiation. However, analysis up to 14 days following transfection did not identify any expression of the neuronal tubulin (Tuj1). It has previously been shown that it is possible to directly convert fibroblasts into functional neurons through the expression of a combination of transcription factors (Abdullah et al, 2012; Vierbuchen et al, 2010). The effect of N-Src overexpression seems to be purely

morphological but it is possible that a stable form of transfection would allow sustained N-Src expression and enable reprogramming of the cells to a neuronal lineage. This type of reprogramming would rely on N-Src signalling feeding into a transcription programme in addition to the cytoskeletal rearrangement observed here.

The role in cytoskeletal rearrangement identified in this study is in agreement with the available data for neuronal Src function. Kotani et al (2007) identified a role for N1-Src in the regulation of dendritic morphogenesis and concluded, through ultrastructural analysis, that this occurred through modulation of microtubule organisation. However, this study used a constitutively active form of the kinase (Y527F) and observed only a mild phenotype following overexpression of the WT N1-Src. This supports the theory that, despite the high basal level of kinase activity in the neuronal kinases, further activation is required for substrate phosphorylation. The mechanism by which signalling downstream of N1-Src is able to influence cell morphology remains to be elucidated and will be further discussed in Chapters 5 and 6.

The induction of neuronal morphology in heterologous cells implies that neuronal Src signalling is involved in cellular differentiation. This would correlate with the fact that high levels of the neuronal kinases, in particular N2-Src, are associated with a good prognosis for the childhood cancer neuroblastoma (Matsunaga et al, 1998). Tumours expressing high levels of N2-Src kinase have an increased likelihood of spontaneously differentiating into benign neuronal tissue (Matsunaga et al, 1993). It is postulated that the N2-Src is able to drive this differentiation, although the mechanisms underlying this are not clear.

One caveat to the data presented here is that the morphological analyses were all carried out following overexpression of the Srcs. It is known that kinase overexpression can result in aberrant signalling and the activation of signalling pathways not normally controlled by the kinases. But, in the case of Src, this seems to act predominantly to exaggerate the normal signalling of the kinases. Kamps and Sefton (1988) found that the majority of the proteins phosphorylated by the oncoprotein v-Src were also phosphorylated by C-Src. Ongoing work in the Evans lab is currently aiming to establish stable cell lines expressing the N-Srcs. Stable cell lines will express lower levels of the kinases and will be more comparable to the endogenous levels. These will be useful tools for further study of N-Src function and

repeating the morphological analysis in these stable cell lines will confirm its validity.

3.8.2 An *in vitro* assay capable of detecting SH3 domain binding preferences of SFKs

The development of a novel *in vitro* kinase assay has enabled the first reported investigation of the substrate preferences of the N-Srcs. The testing of the assay has resulted in a high degree of confidence in its ability to assess the phosphorylation and, by implication, the SH3 domain binding ability of GST-peptide substrates.

The assay is carried out by detection of phosphorylation using an α-phosphotyrosine antibody followed by chemiluminescent detection on film. It has been suggested that the use of photographic film to detect chemiluminescence does not give linear results. However, this does not seem to be an issue in the context of this study. To ensure that the densitometry data collected was accurate, an initial comparison between film and computerised detection, using a BioRad Versadoc, was carried out and this gave the same calculated K_m for the phosphorylation (data not shown). The predominant factor in determining a change in K_m seems to be the detection of a band in a lane of lower substrate concentration. Therefore, even if the subsequent analysis and calculation of absolute K_m values were not accurate, the differences in the blots alone show that the phosphorylation of substrates able to interact with the SH3 domains occurs more efficiently (i.e. at lower substrate concentrations) than those that cannot.

Throughout the kinetic experiments, great care was taken to ensure that direct comparison of substrate phosphorylation by each of the kinases was possible. Equal substrate concentrations phosphorylated by the three kinases were run on the same blot, along with a control sample present on all blots. Densitometry data from these blots was analysed and normalised to the control sample to reconstruct the phosphorylation curve. Therefore, there is a high degree of confidence that the differences in phosphorylation observed are due to differential substrate preferences of the kinases rather than experimental variation.

One drawback to using α-phosphotyrosine detection of incorporated phosphate as opposed to ^{32}P is that calculation of the rate of reaction cannot be calculated as an absolute value. Analysis of the V_{max} of the reactions revealed that

they all proceed at the same rate, but comparison of this rate to other reported rates cannot be carried out.

A caveat to the use of recombinantly expressed kinases is that *E. coli* does not express the kinase that carries out the C-terminal phosphorylation of Src (Csk). Csk phosphorylation of Y527 enables the formation of the regulatory SH2 domain:tail interaction that constrains the activity of the kinases. Therefore, the kinases used for all *in vitro* applications in this study are only constrained by the SH3 domain:linker association. Yadav and Miller (2007) have confirmed that further activation of the kinase by SH3 domain displacement is possible in the absence of the SH2:tail interaction. The kinetics of the phosphorylation observed may be slightly affected by the lack of the SH2:tail interaction. It may be that the K_ms obtained are slightly lower than they would be if the SH2:tail interaction were in place but the trends should be unaffected.

The effects on substrate phosphorylation observed have been attributed solely to differences in the SH3 domain binding preferences but the kinases used also have functional SH2 domains that can influence substrate binding. The SH2 domain can dock onto phosphorylated tyrosine residues, displacing the SH2:tail interaction and resulting in an activation of the kinase. Once there are phosphorylated substrates within the reaction, SH2 domain binding may provide a mechanism for further enhancement of phosphorylation. To assess the role of the SH2 domain, production of a loss-of-function mutation (R175A) in the SH2 domain was attempted by site directed mutagenesis but was not successful. Therefore, the contribution of the SH2 domain to the kinetics in the *in vitro* assays remains unknown. However, the results are still valid and physiologically relevant as in endogenous kinases both SH2 and SH3 domains influence substrate preferences and kinase activity.

The primary difference in the phosphorylation observed in this study compared to other studies is the long lag phase before phosphorylation is observed in the timecourse experiment. There are a number of possible reasons for this. The substrate used in the timecourse experiment (YA) could not bind to the C-Src SH3 domain and its initial phosphorylation therefore required activation of the kinase by autophosphorylation. Moarefi et al (1997) carried out a comparable experiment on Hck activation and found a 30 minute lag period before phosphorylation was observed when downregulated Hck was used. The faster timepoint used in other studies are probably explained either by the use of higher substrate concentrations or

use of preactivated kinases either by prior incubation with ATP or extraction from mammalian cell lysates.

The *in vitro* kinase assay developed here has been shown to be both accurate and sensitive in reporting changes in affinity for the Src kinase domain ideal substrate by the presence of SH3 domain binding motifs, providing a valuable tool for the assessment of N-Src function. The versatility of the GST-peptide system means that it can be readily altered to assess potential substrates of the N-Srcs but also other tyrosine kinases.

3.8.3 Insights into the effect of n-Src loop inserts on kinase activity and substrate preferences

It has previously been suggested that the N-Srcs are more basally active because they are less able to form the SH3:linker intramolecular association. Both the increased basal activity of the kinases and the decreased ability to form the intramolecular association with the linker have been confirmed in this study. This is the first demonstration of the prediction that the N-Srcs show reduced binding to the linker sequence.

This result provides interesting insights into the conformation of the N-Src kinases. The N-Srcs are less constrained by the SH3:linker interaction but this does not seem to result in a complete activation of the kinase. Kotani et al (2007) observed a gain-of-function phenotype by mutating Y527F in N1-Src, indicating that the SH2:tail interaction remains intact *in vivo* and functions to prevent phosphorylation until an appropriate ligand is encountered. This is interesting because, in other SFK members, the SH3 domain intramolecular interaction is thought to be dominant. In Hck, Moarefi et al (1997) showed that further kinase activation does not occur by SH2 domain displacement following SH3 displacement. Also, in a form of Hck with a strengthened SH2:tail interaction, SH3 domain mutation overrides even this strengthened SH2:tail interaction (Porter et al, 2000).

To confirm the role of the SH2:tail interaction in N-Src activity it would be interesting to mutate the residue that forms the SH2:tail interaction (Y527) to assess whether further activation of the neuronal kinases occurs. *In vitro*, the Y527F mutation would not be expected to further activate the kinases as they are not phosphorylated at Y527 *in vitro*. In cell based assays, there is the potential for Y527

phosphorylation by Csk. The absence of the SH2:tail interaction may therefore result in a full activation of the kinase. It would be interesting to assess the morphology of Y527F N-Src transfected COS7 cells to assess whether further N-Src activation is able to exacerbate the change in morphology observed. N1-Src with a Y527F mutation has previously been generated (Marin et al, 2010) and was reported to have faster activation kinetics, assessed by autophosphorylation. However no substrate phosphorylation or cell based assays were carried out.

In vitro studies confirm that the decreased linker association does not result in a complete activation of the kinase and that substrate phosphorylation remains a highly controlled process that requires appropriate ligand binding at the SH3 domain. It has been demonstrated that the known C-Src consensus motifs are poor substrates for the neuronal Src SH3 domains and the enhancement in phosphorylation observed for C-Src when a SH3 domain ligand is present is not observed for either neuronal Src isoform. This indicates that *in vivo* the neuronal Srcs require substrate recognition via the SH3 domain in order to phosphorylate substrates. Therefore, the increased basal levels of kinase activity that are more commonly associated with disregulation of the kinase and disease states does not cause unregulated protein phosphorylation in the N-Srcs.

Analysis of the subcellular localisation of the kinases has revealed some interesting properties of the N-Srcs. Both N1- and N2-Src display some perinuclear association. In the case of C-Src, this is associated with the inactive form of the kinase (Kaplan et al, 1992) and not the active form (Kaplan et al, 1994; Sandilands et al, 2004), indicating that some N-Src in the cells may be in an inactive conformation or that active N-Src is found in different subcellular localisations than active C-Src. Further analysis is needed to identify the markers that this population is associated with. It should also be confirmed that this perinuclear Src is not the result of overexpression and subsequent accumulation in the biosynthetic pathway. The production of stable cell lines will allow this experiment to be carried out. Further analysis would also be aided by the use of confocal as opposed to epifluorescent microscopy.

The basal kinase of the N-Srcs has been shown to be greatly increased in whole cell lysates but it would be interesting to discover whether the localisation of the kinases has any effect on activation. This could be carried out by pY416 staining in cells as has been described for C-Src (Sandilands et al, 2004). Activation of C-Src

results in its relocalisation to the plasma membrane. The effect of N-Src activation is unknown. This could be investigated using vanadate treatment of the cells which results in a potent activation of kinases.

It is possible that the hyper-active state of the neuronal kinases observed in cell based assays in this study is partly a result of their overexpression. SFKs are able to carry out transphosphorylation at Y416 (Cooper & MacAuley, 1988)and an increase in local concentration caused by overexpression may be sufficient to allow extensive transphosphorylation, thus driving the active state of the kinase. The phenomenon may be more exaggerated in the neuronal kinases than for C-Src because the weaker interaction of the SH3 domain with the SH2 domain: kinase domain linker makes the transition to the active state more energetically favourable.

In addition, the N-Srcs are predominantly constrained by the SH2:linker association. The presence of a C-terminal tag may therefore be sufficient to partially disrupt this interaction. This is tolerated in C-Src as it also has the additional SH3:linker association but may result in a further activation of the N-Srcs. It has been reported that N-Src isolated from neuroblastoma cell lines do not necessarily have a higher basal kinase activity level than C-Src isolated from fibroblasts (Yang & Walter, 1988) or glioblastoma cells (O'Shaughnessy et al, 1987). However, this activation state rapidly increases following the onset of differentiation (Bjelfman et al, 1990b). In contrast, it has been consistently reported that the N-Srcs in mature neurons have a higher basal level of kinase activity. The contradiction in these results may indicate that high N-Src activity is required for the processes of differentiation and maintenance of a differentiated phenotype and therefore be lower in proliferating neuroblasts such as neuroblastoma cells. The identification of N-Src with low basal kinase activity confirms that the activity of the kinases is able to be regulated *in vivo* and confirms the *in vitro* data obtained here that show the N-Srcs do not phosphorylate the control peptide to any greater extent than C-Src. This capacity for regulation of kinase activity is necessary to enable substrate selection by the highly related kinases (Sartor & Robbins, 1993).

Taken together, the data presented here show that the N-Srcs have a high basal level of kinase activity but that this does not result in unregulated substrate phosphorylation. The SH3 domain is able to influence both substrate specificity and kinase activity. The current view is that SH3:linker binding acts to constrain the kinase activity and SH3-substrate interaction activates the kinase. In the case of the

N-Srcs, the SH3 domain still seems to be required for substrate recognition but its role in kinase activation is less clear. The activity of a Src kinase is classically assessed by the phosphorylation state at Y416 but the link between autophosphorylation and substrate phosphorylation is not entirely clear. V-Src phosphorylates substrates 10-fold more than C-Src but its autophosphoylation is only between 1 and 2 fold higher than C-Src (Coussens et al, 1985). Lyn autophosphorylation results in an increase in kinase activity but a decrease in the accessibility of the SH2 domain (Sotirellis et al, 1995). Therefore, the assessment of N-Src activity by pY416 may not give an accurate representation of the potential for substrate phosphorylation by the kinase.

4 Identification of a consensus motif for the N1-Src SH3 domain

4.1 Introduction

4.1.1 The use of phage display in establishing a consensus motif

The ligand binding specificity of the N1-Src SH3 domain has been shown to differ from that of C-Src (Chapter 3). In order to further investigate the functions of N1-Src and to identify potential *in vivo* substrates, it was necessary to establish a consensus sequence for the N1-Src SH3 domain. This consensus motif could then be used to carry out a bioinformatic screen for potential substrates. The technique chosen for these investigations was phage display. This technique is highly applicable to small, well folded, isolated domains such as the SH3 domain (recently reviewed by Vodnik et al (2011)) and was the technique initially used to identify a consensus motif for the C-Src SH3 domain (Cheadle et al, 1994; Rickles et al, 1994).

Phage display works on the principle of selective enrichment of sequences able to bind with high affinity to the protein of interest. It uses a library of random peptide sequences and can therefore be used to identify a consensus motif for a protein with no requirement for prior knowledge of interacting proteins. One possible drawback is that phage display can only identify interactions with linear peptide sequences. However, the vast majority of SH3 domains interact with linear sequences in their substrates rather than via tertiary contacts (Mayer, 2001). It is reasonable to assume that the N1-Src SH3 domain also interacts with its substrates in this manner. As there is such versatility in the sequences able to bind to SH3 domains, an unbiased peptide library was chosen to assess binding to the N1-Src SH3 domain as it cannot be assumed that an N1-Src SH3 domain interacting peptide will be proline rich.

4.1.2 Bioinformatic analysis of large datasets of gene names

In the post genomic era, bioinformatic analysis using web-based prediction tools has become a powerful technique for the identification of putative substrates. There are a number of tools available that are able to identify potential substrates based on the presence of a particular amino acid motif, prediction of PTM or assessment of

biological processes. Bioinformatic techniques are particularly applicable to assessing N1-Src function as it only differs from C-Src in the SH3 domain. The domain interactions of C-Src are well characterised and can therefore be used to aid the identification of potential N1-Src substrates. The web-based bioinformatic tools that were used in this study are outlined in Figure 4.8.1.

Scansite (Obenauer et al, 2003) is able to search genomes for short linear peptide motifs within proteins that are likely to be phosphorylated by specific protein kinases or bind to well characterised domains such as SH2 domains, 14-3-3 domains or PDZ domains. This prediction is based on experimental data obtained using peptide library experiments such as phage display. The binding peptides are isolated and sequenced and the relative abundance of each amino acid at each position used to produce a Position Specific Scoring Matrix (PSSM) that numerically indicates the probability of finding each amino acid at each position within a motif. It is also possible to search Scansite with a user defined PSSM (Yaffe et al, 2001) and this functionality enables genome searching with a novel consensus motif.

The functional roles of the potential substrates identified by Scansite can then be assessed using The Database for Annotation, Visualisation, Integrated Discovery (DAVID) (Huang et al, 2009a). DAVID assigns a function to proteins based on a series of Gene Ontology (GO) terms. It is also able to report whether any function is 'enriched' i.e. present at a frequency higher than would be expected based on occurrence within the genome. This allows unbiased assessment of the predominant functions carried out by a large dataset of proteins.

For a protein containing an appropriate SH3 domain binding motif to be considered a potential Src kinase substrate, it must also contain a tyrosine residue within a motif likely to be phosphorylated by the relevant kinase. There are a number of programmes available that are able to predict potential Src phosphorylation sites and, because the kinase domains of C- and N1-Src are identical, these can be used to predict which of the potential substrates identified as potential N1-Src SH3 domain targets are also likely to be Src phosphorylated. The programme chosen for this was the Group based Prediction System (GPS) (Xue et al, 2008). GPS is able to carry out large scale batch kinase prediction and operates with a higher degree of specificity than Scansite for Src kinase prediction (Xue et al, 2008). It is also able to differentiate between substrates likely to be phosphorylated by individual members of the Src Family Kinases (SFKs).

Substrates that are predicted to be both SH3 domain and kinase domain substrates of N1-Src can be compared against the PhosphoSite (Hornbeck et al, 2004) database of, predominantly Mass Spectrometry (MS) derived, information about post-translational modification at specific sites *in vivo*. It is therefore possible to cross reference predicted phosphorylation sites with known sites to assess whether there is any prior evidence for phosphorylation at a particular predicted tyrosine residue.

This series of bioinformatic techniques allows for both broad, unbiased assessment of large datasets in order to identify general protein functions and also more directed analysis of individual proteins where there is biological evidence for phosphorylation.

4.2 Aims

The work presented in Chapter 3 confirmed that the consensus motif for binding to the N1-Src SH3 domain differs from that of C-Src. The aim of the work presented in this chapter was therefore to establish a consensus motif for the N1-Src SH3 domain that could be shown to functionally enhance phosphorylation by N1-Src in an *in vitro* kinase assay. This consensus motif could then be used to carry out a bioinformatic search for novel potential N1-Src substrates.

4.3 A novel SH3 domain binding motif identified by phage display

The library chosen for phage display experiments was a commercially available random 12-mer library that contains $2x10^9$ unique peptides (NEB Ph.D.-12 Phage Display Peptide Library Kit). Each peptide is expressed on the surface of an M13 phage particle by fusion to one of its coat proteins. The phage are then panned over the protein of interest and those that bind are collected and amplified in order to successively enrich for high affinity peptides (Figure 4.3.1). Initial phage display experiments used the surface panning protocol in which the pool of phage was incubated with N1-Src SH3 domain bound to the plastic surface a petri dish. The peptides sequenced as a result of this were largely identified as plastic binding. Therefore, the protocol was adapted to consist of solution phase panning followed by affinity bead capture. The panning process was carried out for a total of five rounds and clones were sequenced from round three onwards.

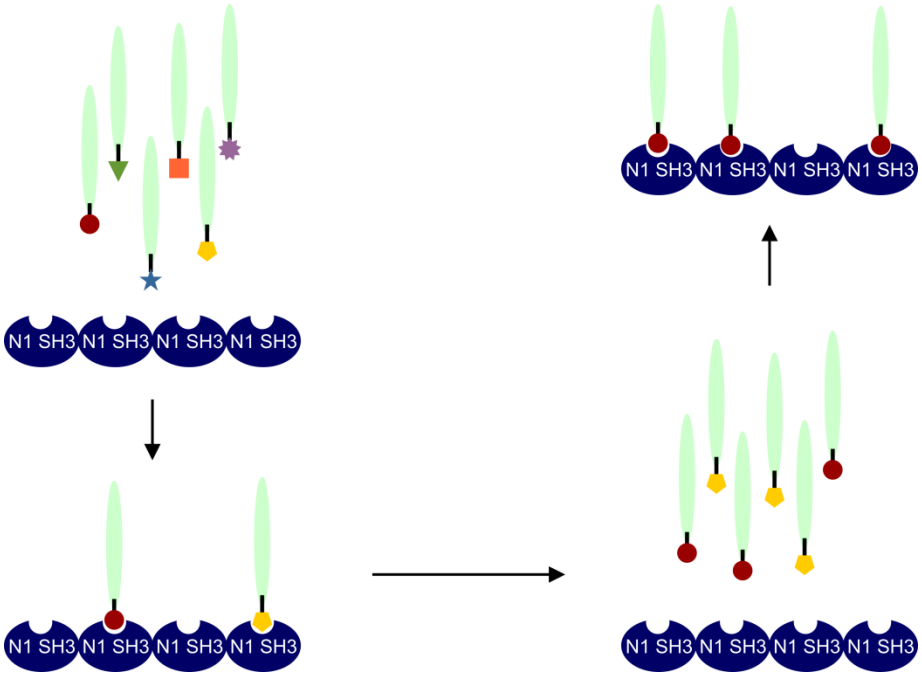

Figure 4.3.1. Schematic representation of the phage display panning process.

Phage expressing random 12-mer peptides on their surface are incubated with a protein of interest. Over successive rounds of panning, those peptides that bind with the highest affinity are selected while the remaining peptides are discarded. Phage plasmids may be sequenced following any panning round with the aim of establishing a consensus motif.

When all of the sequences obtained from rounds 3-5 were combined and analysed for amino acid content, it was revealed that certain amino acids were over-represented (Figure 4.3.2). The dotted line in Figure 4.3.2 represents the expected amino acid frequency based on codon usage. Proline (P), histidine (H), lysine (K) and to a lesser extent tryptophan (W) and tyrosine (Y) occur in the sequences more often than would be expected based on codon usage. This indicates that the phage display method is able to selectively enrich for certain amino acids, and implies that these amino acids are selected for by the binding interaction.

Looking more specifically at the sequences obtained by sequencing clones from round 3 onwards, selective enrichment of certain peptides was observed (Table 4.3.1). In rounds 3 and 4, a total of 18 clones were successfully sequenced and each contained a unique peptide sequence. In contrast, a total of 22 clones were sequenced following the fifth round of panning and 17 of these contained the same peptide sequence, WHRMPAYTAKYP. Due to this high level of enrichment it was decided that further rounds of panning were not required. Additionally, as the rounds of panning were carried out, there was an increasing degree of contamination from wild type phage.

It is interesting to note that one sequence was obtained from both rounds 4 and 5 of sequencing. This sequence was KPPQHTSAPYLP. The fact that an identical sequence was obtained from two subsequent rounds of panning indicated that the number of unique clones in the pool was being significantly reduced as the panning process selects for peptides that are able to bind. Were this not the case, then the probability of obtaining the same sequences from two subsequent rounds would be very small.

In total, there were 7 unique peptide sequences obtained following the fifth round of panning. One of these, SVWVGMKPSPRP, was immediately discarded as there is evidence that it is present due to propagation related bias (Kolb & Boiziau, 2005; Vodnik et al, 2011). The remaining peptides were named Phage Display (PD) peptides 1-6 (Figure 4.4.1), and this nomenclature will be used from this point onwards.

Table 4.3.1. Selective enrichment of peptide sequences by phage display. Individual phage clones were isolated and their plasmids sequenced following rounds 3, 4 and 5 of panning. Following the fifth round of panning, one peptide sequence was identified in 17 of 22 sequenced plasmids.

Round 3		Round 4		Round 5	
Sequence	**Freq.**	**Sequence**	**Freq.**	**Sequence**	**Freq.**
FSLPSKALPWQL	1	IELQTIYYSSTS	1	WHRMPAYTAKYP	17
GVIPPRAFNHGV	1	LPLHGMHLLRSS	1	GHWHSPHKLTRN	1
VSRHQSWHPHDL	1	FYQQPPSWPHWG	1	SVWVGMKPSPRP	1
YMPHSASLLTTP	1	APHVRDHLSSTP	1	KNPTSTPAMYAN	1
AIPNKLNVWPPH	1	LNAQPLRFNIKV	1	GHRNRANTSKNP	1
HWKHPWGAWDTL	1	ATWSHHLSSAGL	1	KPPQHTSAPYLP	1
QHANHQAWNNLR	1	ITTKYSMRYNTT	1	WHRMPMHTAKPL	1
NLGKPNYHAYYS	1	KPPQNTSAPYLP	1		
HHGHSPTSPQVR	1				
ILANDLTAPGPR	1				

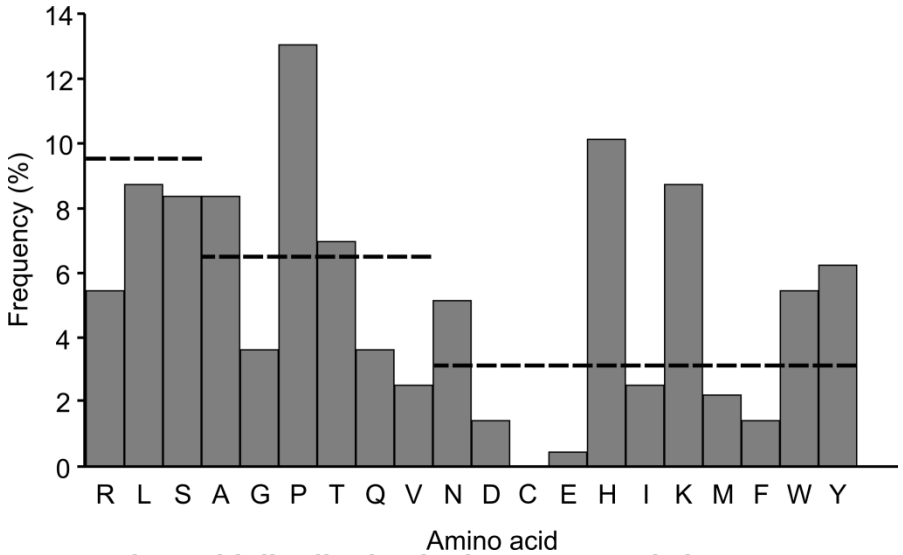

Figure 4.3.2. Amino acid distribution in the sequenced clones.

Pooled sequence information from all sequences obtained from rounds 3, 4 and 5 of panning reveal an over-representation of certain amino acids (shown using the single letter code). Dotted lines represent the expected frequency based on codon usage.

4.4 The presence of the PD GST-peptides enhances phosphorylation by N1-Src

The amino acid sequences of the PD peptides were cloned into the GST-peptide system described in Chapter 3 so that they could be tested for their ability to enhance phosphorylation by N1-Src. A schematic representation of the PD GST-peptides is shown in Figure 4.4.1 A. They contain the same ideal Src substrate as the GST-peptides described in Chapter 3 and the phosphorylation of the tyrosine residue contained in this motif can be monitored by western blot using an α-phosphotyrosine antibody. In the schematic this tyrosine residue is represented as 'Y'. The PD peptide sequences identified by phage display have been inserted in the same position as the SH3 domain binding sequences in the substrates YP1 and YP2 used in Chapter 3.

In vitro kinase assays were carried out between C- and N1-Src and the PD GST-peptides. If the amino acid sequences identified by phage display are able to bind to the SH3 domain of N1-Src then this will enhance the phosphorylation of the tyrosine residue within the PD GST-peptide substrate. In these experiments, a band in the highest substrate concentration lane represents an enhancement in phosphorylation over a construct lacking the ability to bind to the SH3 domain (YA).

The presence of the majority of the PD sequences was able to enhance phosphorylation by N1-Src (Figure 4.4.1 B), but with varying degrees of specificity and affinity. A subset of PD sequences resulted in an enhancement in phosphorylation by both N1-Src and C-Src. This result implies that the technique of phage display has been able to successfully identify peptides that are able to functionally interact with the N1-Src SH3 domain, resulting in an enhancement of phosphorylation.

Based on the results of the *in vitro* kinase experiments the PD peptides were ranked according to their specificity for N1-Src (Figure 4.4.1 C). The two GST-peptides that showed absolute specificity for N1-Src over C-Src were PD1 and PD6. This is very interesting because the sequences of these two peptides are highly similar, with only four amino acids difference between them. It is also worth noting that PD1 is the peptide that was present in 17 (77%) of the 22 clones sequenced from round 5. Once the PD GST-peptides were ordered according to their specificity for N1-Src, it was possible to align the sequences to reveal a consensus motif of +xPxxTx+ (where + represents a positively charged amino acid) (Figure 4.4.1 C).

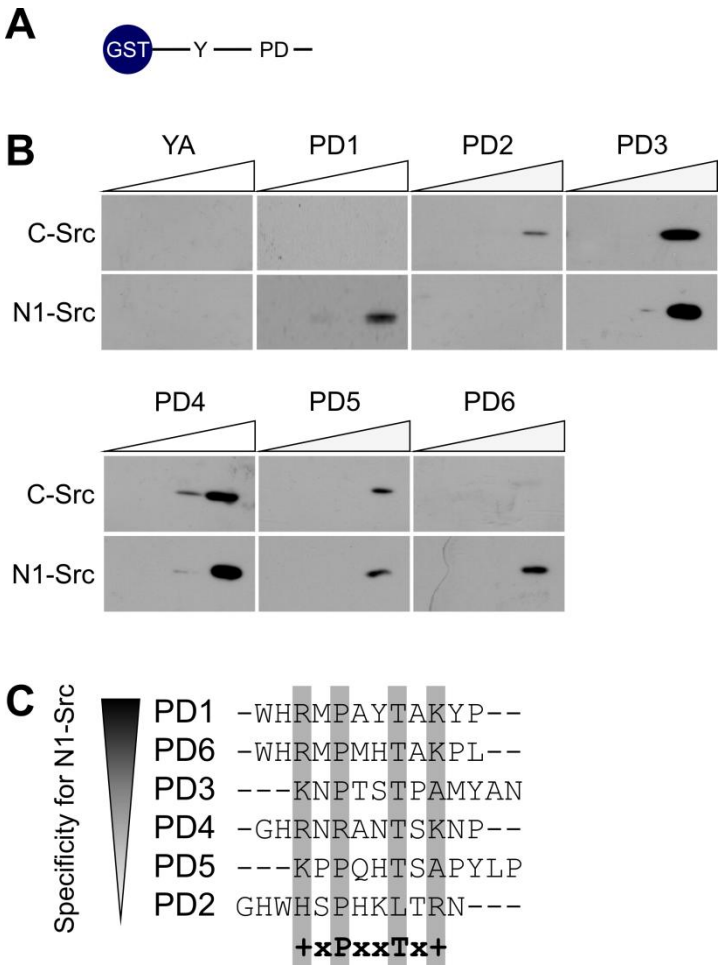

Figure 4.4.1. Enhancement in phosphorylation by the presence of the phage display (PD) GST-peptides.

A) Schematic representation of the PD GST-peptides. The amino acid sequences identified as binding to the N1-Src SH3 domain using phage display were cloned into the GST-peptide system as shown in panel A. The substrates also contained a tyrosine residue able to be phosphorylated by the Src kinase domain. Phosphorylation of this tyrosine residue was monitored by western blot. Binding of the PD sequences to the SH3 domain would result in an increase in the phosphorylation observed. B) Phosphorylation of PD GST-peptides by C- and N1-Src. GST-PD concentrations of 8.3, 2.8, 0.9 and 0.3 μM used. A band in the highest concentration lane represents an enhancement in phosphorylation over a substrate that can't bind to the SH3 domain (YA). C) A consensus motif for N1-Src. PD peptide sequences ordered based on their specificity for N1-Src over C-Src. Grey bars represent amino acids conserved between the sequences. The consensus sequence is highlighted in bold.

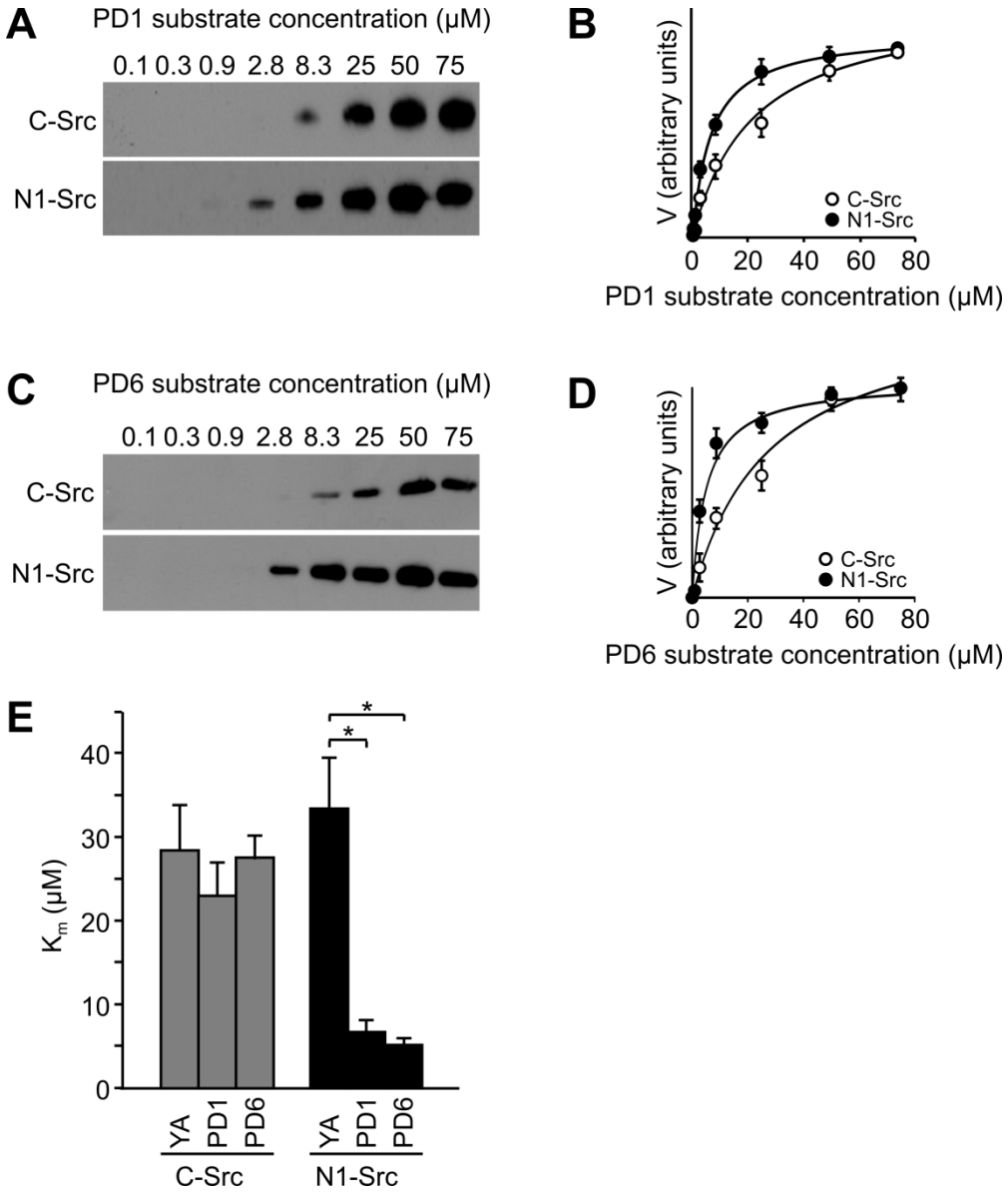

Figure 4.5.1. Kinetics of PD1 and PD6 phosphorylation by C- and N1-Src.

A) and C) Phosphorylation of A) GST-PD1 and C) GST-PD6 by C and N1-Src. Substrate concentrations varied as indicated. Analysis by α-phosphotyrosine blot and detection using the PY20 antibody. B) and D) Quantification of B) GST-PD1 and D) GST-PD6 phosphorylation by C- and N1-Src. Densitometry analysis carried out using ImageJ. n=3 experiments, error bars shoe SEM. E) K_ms of the phosphorylation of PD1, PD6 and the control YA by C- and N1-Src. K_m calculated using curve fitting in SigmaPlot, n=3 experiments. Statistical analysis carried out using ANOVA followed by post hoc Tukey test *p<0.05, all conditions compared to YA phosphorylation.

This proposed consensus motif differs from the known C-Src binding Class I and Class II PxxP motifs (+xxPxxP and PxxPx+ respectively) (Feng et al, 1994) and represents a novel SH3 domain binding sequence.

4.5 The kinetics of PD1 and PD6 phosphorylation are comparable to good C-Src ligands

Initial experiments identified both PD1 and PD6 as being highly specific for N1-Src. In order to determine the extent to which they are able to enhance phosphorylation, a more detailed analysis of the kinetics of their phosphorylation was carried out.

Full kinetic analysis over a larger substrate concentration range (Figure 4.5.1) revealed that both PD1 and PD6 enhance phosphorylation to approximately the same extent and that the K_m for the phosphorylation falls within the low micromolar range The K_m for PD1 phosphorylation is 6.5 ± 1.2 μM and the K_m for the PD6 phosphorylation is 5.0 ± 1.6 μM. Therefore, the affinity of the interaction between the N1-Src SH3 domain and PD1/6 is similar to that of known SH3 domain ligands such as the Class I and II motifs binding to the C-Src SH3 domain (Chapter 3) (Feng et al, 1995).

4.6 Mutation of the PD1 sequence reveals critical residues for binding

PD1 and PD6 have both been shown to enhance phosphorylation by N1-Src to a similar extent. However, it was decided to use the PD1 sequence as the basis of future work because it was so highly enriched during the phage display screen.

To determine the residues within the PD1 sequence that were required for the observed enhancement in phosphorylation, selected mutations were made. These mutations were based on the residues that were conserved between the PD peptides shown to enhance phosphorylation by N1-Src (Figure 4.4.1). The majority of the mutations made were substitutions to alanine (A) (Figure 4.6.1 A). An additional mutation of the threonine (T) residue at position 8 to valine (V) was made in order to determine whether the hydroxyl group in the threonine side chain was important for the interaction.

Figure 4.6.1 B shows the results of these experiments. As for Figure 4.4.1, a band present in the highest concentration lane represents an enhancement in phosphorylation over the control peptide. The majority of the mutations abolish the enhancement in phosphorylation previously observed. This implies that they are required for the binding interaction between the substrate and the N1-Src SH3 domain. The exception to this is the threonine residue at position 8. Here, mutation to either alanine or valine has little effect on the phosphorylation observed. This indicates that the presence of a threonine residue at position 8 is not absolutely required. Interestingly, there is a requirement for a positively charged amino acid at both ends of the consensus motif. The Class I and Class II SH3 binding motifs have positively charged amino acid at one end, but this dual requirement is novel for an SH3 domain binding motif.

4.7 The interaction between PD1 and the N1-Src SH3 domain is direct

In order to confirm that the enhancement in phosphorylation caused by the presence of the PD1 peptide in the *in vitro* assay is due to a direct interaction between the N1-Src SH3 domain and the PD1 peptide, a peptide titration experiment was carried out. The free peptide of the PD1 sequence was titrated into a phosphorylation reaction between the control peptide (YA) and N1-Src kinase. The presence of a high affinity SH3 domain ligand in conjunction with the ideal substrate is known to increase substrate phosphorylation (Chapter 3, (Scott & Miller, 2000) but the effect of titrating in a free peptide was not known. Surprisingly, the titration of the free PD1 peptide sequence resulted in an inhibition of phosphorylation (Figure 4.7.1). Importantly, there is no effect of titrating in the point mutant PD1-P5A, meaning that the interaction between PD1 and the N1-Src SH3 domain is sequence specific. This result implies that the PD1 sequence may also act as an N1-Src inhibitor in cell based assays.

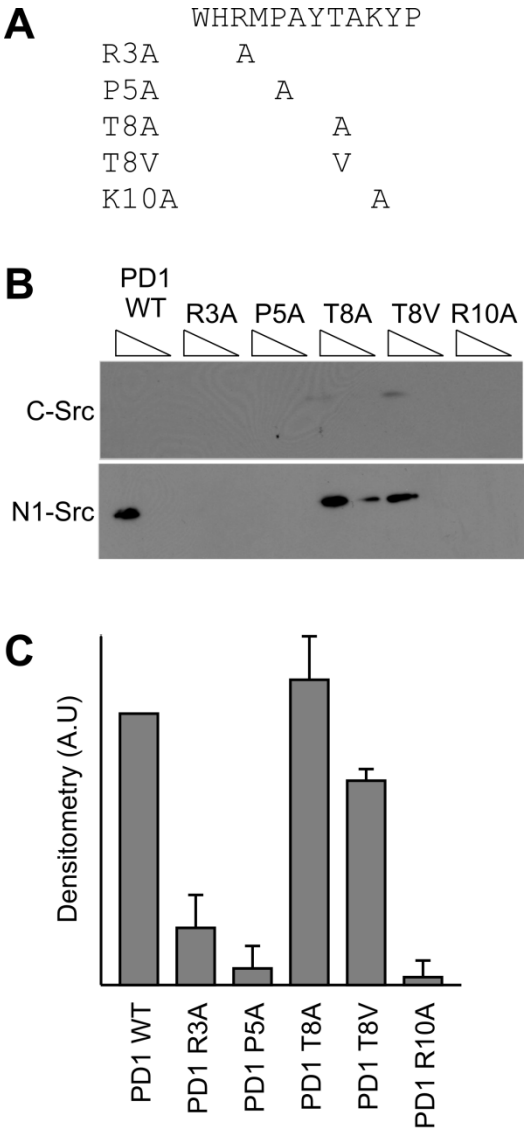

Figure 4.6.1. Mutation of PD1 sequence reveals critical residues.

A) Representation of the amino acid substitutions made within the PD1 sequence. B) Phosphorylation of the mutant GST-peptides by C- and N1-Src. Substrate concentrations of 8.3 µM and 2.8 µM used. Analysis carried out by α-phosphotyrosine blot using the PY20 antibody. C) Quantification of PD peptide mutant phosphorylation. Densitometry analysis carried out using ImageJ, n=3 experiments, normalised to the PD1 WT signal at 8.3 µM.

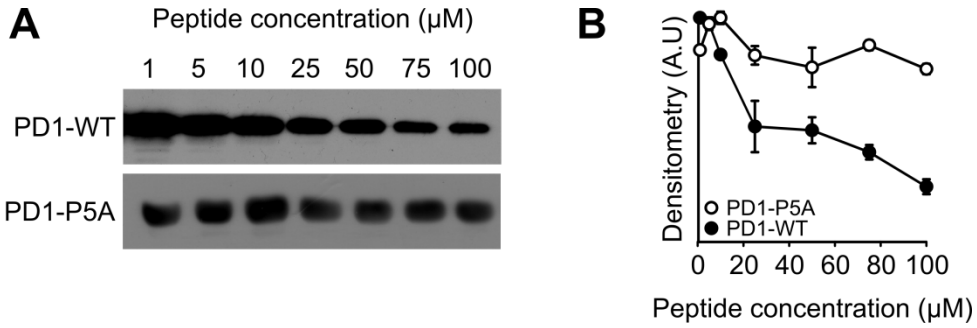

Figure 4.7.1 Titration of PD1 peptide inhibits C-Src phosphorylation of YA.

The free peptides of PD1-WT and PD1-P5A were titrated into a phosphorylation reaction between N1-Src (5 nM) and YA (25 μM). The peptide concentrations indicated were added to individual *in vitro* kinase assay reactions. A) Analysis of phosphotyrosine incorporation into YA using the PY20 antibody. B) Densitometry analysis of the phosphotyrosine incorporation, carried out using Image J. n=3 experiments, error bars show SEM.

4.8 Bioinformatics reveals a potential role for N1-Src in cytoskeletal rearrangement

The phage display consensus sequence obtained has been demonstrated to be able to specifically enhance N1-Src to an extent similar to that of known SH3 domain ligands. It therefore contains a potentially physiologically relevant sequence that can be used to predict potential N1-Src substrates using bioinformatic techniques. A series of bioinformatic techniques were utilised (depicted schematically in Figure 4.8.1) that were able to systematically identify potential N1-Src substrates based initially on the presence of the consensus motif and subsequently on the prediction of tyrosine kinase phosphorylation.

In order to identify potential SH3 domain binding partner of N1-Src, a PSSM was constructed that contained information about the probability of finding eachamino acid at each position within the motif (Table 4.8.1). A score of 21 represents an absolute requirement for that residue to be found in that position, whereas a score of 0 excludes that residue. Scores between 1 and 20 represent an increasing likelihood of a residue being present in a position with a score of 1 having neither a positive or negative effect on the selection. This matrix was then used to carry out a Scansite (Obenauer et al, 2003) search for proteins that contain sequences meeting the criteria. This produced a total of 771 unique proteins within the human genome.

To broadly identify the functions of these proteins, analysis was carried out using the online bioinformatic tool DAVID (Huang et al, 2009b). This analysis assigned functional roles to 541 (70%) of the Scansite hits using the GO Term 'Biological Process'. Proteins not assigned a functional role consisted mainly of uncharacterised or unknown proteins. DAVID was then used to assign the proteins into clusters based on their function and to assign these clusters an enrichment factor. The enrichment factor represents the prevalence of a functional group within the dataset compared to the expected prevalence based on occurrence in the genome. An enrichment factor cut off of 1.5 was enforced as suggested by Huang et al (2009b).

This analysis revealed 10 functional clusters containing 377 proteins that were present more commonly than would be expected based on their occurrence within the genome (Table 4.8.3). The enriched categories fall into six main functional groups: regulation of neuronal development, cytoskeletal rearrangement,

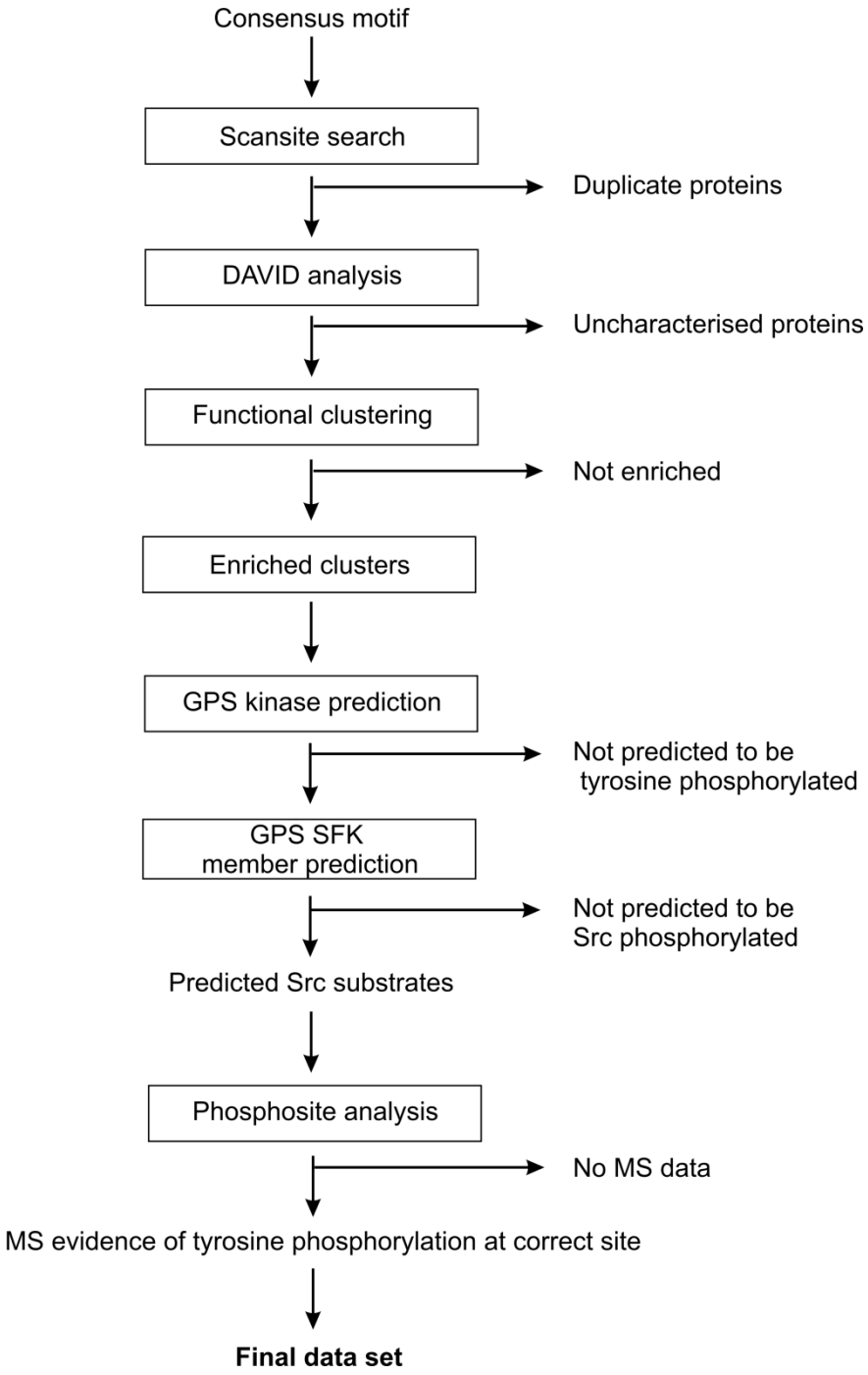

Figure 4.8.1. Schematic representation of bioinformatic analysis.

An outline of the bioinformatic toools used and the steps taken in order to identify both potential functional roles and specific protein targets of N1-Src kinase.

Table 4.8.1 PSSMs for Scansite predition of N1-Src SH3 domain substrates.

Data from the round 5 sequenced peptides and the mutational analysis was combined and the probability of finding an amino acid in a given position entered into the matrix. A score of 21 means the residue must be found in that position and a score of 0 means that it must be excluded. A score of 1 has neither a positive or negative influence and was included when there was no data about a residue. There must be one fixed residue at position 0 (P in this case).

	A	C	D	E	F	G	H	I	K	L	M	N	P	Q	R	S	T	V	W	Y
-7	1	1	1	1	1	1	1	1	1	1	1	1	1	1	1	1	1	1	1	1
-6	1	1	1	1	1	1	1	1	1	1	1	1	1	1	1	1	1	1	1	1
-5	1	1	1	1	1	1	1	1	1	1	1	1	1	1	1	1	1	1	1	1
-4	1	1	1	1	1	1	1	1	1	1	1	1	1	1	1	1	1	1	1	1
-3	1	1	1	1	1	1	1	1	1	1	1	1	1	1	1	1	1	1	1	1
-2	1	1	1	1	1	1	3	1	20	1	1	1	1	1	20	1	1	3	1	1
-1	1	1	1	1	1	3	1	1	1	1	6	6	3	1	1	3	1	1	1	1
0	0	0	0	0	0	0	0	0	0	0	0	0	21	0	0	0	0	0	0	0
1	6	1	1	1	1	1	3	1	3	1	3	1	1	3	1	3	1	1	1	1
2	1	1	1	1	1	1	9	1	3	1	1	3	3	1	1	3	1	1	1	1
3	10	1	1	1	1	1	1	1	1	1	1	1	1	1	1	1	10	10	1	1
4	6	1	1	1	1	1	1	1	1	1	1	1	6	1	1	6	6	1	1	1
5	6	1	1	1	1	1	1	1	20	1	1	1	1	1	20	1	5	1	1	1
6	1	1	1	1	1	1	1	1	1	1	3	6	9	1	1	1	1	1	1	3
7	1	1	1	1	1	1	1	1	1	4	1	1	8	1	1	1	1	1	1	4

Table 4.8.2 PSSM for Scansite prediction of C-Src SH3 domain substrates.

Constructed according to the same principles as the N1-Src PSSM but using data from a phage display experiment carried out by Sparks et al, 1996.

	A	C	D	E	F	G	H	I	K	L	M	N	P	Q	R	S	T	V	W	Y
-7	1	1	1	1	1	1	1	1	1	1	1	1	1	1	1	1	1	1	1	1
-6	1	1	1	1	1	1	1	1	1	1	1	1	1	1	1	1	1	1	1	1
-5	1	1	1	1	1	1	1	1	1	10	1	1	1	1	1	1	1	1	1	1
-4	1	1	1	1	1	1	1	1	1	1	1	1	1	1	1	1	1	1	1	1
-3	10	1	1	1	1	1	1	1	1	1	1	1	1	1	1	1	1	1	1	1
-2	10	1	1	1	1	1	1	1	1	1	1	1	10	1	20	1	1	1	1	1
-1	0	0	0	0	0	0	0	0	0	0	0	0	21	0	0	0	0	0	0	0
0	1	1	1	1	1	1	1	1	1	10	1	1	10	1	1	1	1	1	1	1
1	1	1	1	1	1	1	1	1	1	10	1	1	10	1	1	1	1		1	1
2	0	0	0	0	0	0	0	0	0	0	0	0	21	0	0	0	0	0	0	0
3	1	1	1	1	1	1	1	5	1	10	1	1	10	1	1	1	5	5	1	1
4	1	1	1	1	1	1	1	1	1	1	1	1	15	1	10	1	1	1	1	1
5	1	1	1	1	1	1	1	1	1	1	1	1	1	1	1	1	1	1	1	1
6	1	1	1	1	1	1	1	1	1	1	1	1	1	1	1	1	1	1	1	1
7	1	1	1	1	1	1	1	1	1	1	1	1	1	1	1	1	1	1	1	1

regulation of Rho/Ras signalling, adhesion molecule signalling, catabolism and chromatin rearrangement. It is particularly striking that there is such a strong association with proteins that carry out functions in neuronal development, 309 (51%) of the input proteins are reported as playing such as role. Although, N1-Src is neuronally expressed, there was no requirement for the searches carried out to produce neuronal hits.

Taken together, the functional clusters of cytoskeletal rearrangement, regulation of Rho/Ras signalling and adhesion molecule signalling are all processes that will influence cell morphology. This implies a possible role for N1-Src in the modulation of neuronal development and cell shape, which will be discussed further in Chapter 5.

To confirm that the DAVID tool is able to provide a reasonable assessment of protein function based on consensus motif, a similar analysis was carried out for C-Src, whose functional roles are already well characterised. A PSSM was produced using the known C-Src SH3 domain binding motifs (Table 4.8.2). This matrix was constructed using information about the individual peptides obtained from a phage display experiment using the C-Src SH3 domain (Sparks et al, 1996). The sequences used to construct the PSSM conform to a Class II PxxP motif. This motif was chosen because, although the C-Src SH3 domain is able to bind to both Class I and Class II PxxP motifs it has a strong bias towards Class II motifs (Wu et al, 2007).

Scansite analysis was carried out using the C-Src PSSM and this identified 1032 unique proteins containing the consensus motif. 734 of these were assigned a functional role by DAVID, with 717 being present in enriched clusters. The functional clusters identified for C-Src are shown in Table 4.8.4 and include regulation of cellular differentiation, cytoskeletal rearrangement and angiogenesis, all of which are functions that C-Src is known to carry out. Interestingly, although neuronal development appears as a cluster, there are only 11 (1%) proteins contained within this cluster, far fewer than for the N1-Src analysis.

There are a number of roles assigned to C-Src in neuronal development and it is possible that some of these are actually carried out by N1-Src. As there are no commercially available inhibitors capable of specifically inhibiting only one isoform it is difficult to assign a function to only one isoform. The overlap between C- and N1-Src kinase substrates predicted by Scansite was very small (Figure 4.8.2) and this

Table 4.8.3. Enriched functional roles for N1-Src substrates identified by Scansite analysis.

DAVID analysis of protein functions that occur more frequently than would be expected based on their occurrence in the genome (enrichment factor). Input proteins were those identified by Scansite as containing the N1-Src SH3 domain consensus motif.

Cluster name	Enrichment Factor	No. of proteins
Rho/Ras protein signal transduction	6.5	62
Chromatin rearrangement	3.3	39
Regulation of Rho/Ras GTPase activity	2.4	27
Cytoskeletal rearrangement	2.4	27
Catabolism	2.3	132
Actin rearrangement	2.3	33
Regulation of neuronal differentiation	1.9	86
Regulation of neuronal development	1.6	183
Adhesion molecule signalling	1.5	40
Regulation of cell morphology	1.5	62

Table 4.8.4 Enriched functional roles for C-Src substrates identified by Scansite analysis.

DAVID analysis of protein functions that occur more frequently than would be expected based on their occurrence in the genome (enrichment factor). Input proteins were those identified by Scansite as containing the C-Src SH3 domain consensus motif.

Cluster name	Enrichment Factor	No. of proteins
Regulation of metabolism	13.7	285
Cell differentiation	8.3	54
Actin cytoskeleton organisation	7.6	164
Regulation of transcription	6.9	148
Regulation of gene expression	6.6	135
Embryonic development	5.7	44
Cell differentiation	3.9	108
Chromatin rearrangement	3.4	42
Neuronal development	3.2	11
Angiogenesis	2.3	40

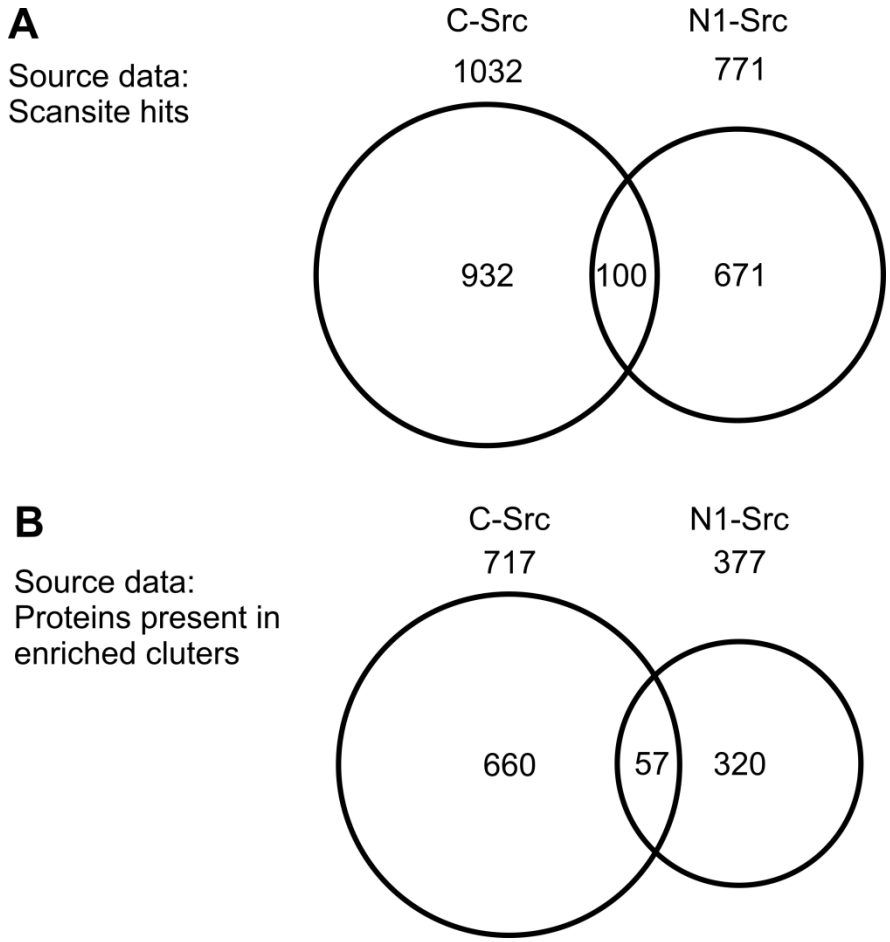

Figure 4.8.2. There is only a small degree of overlap between bioinformatic C- and N1-Src substrates.

The extent of the overlap between protein hits arising from both A) Scansite analysis and B) enriched clusters identified by DAVID analysis for C- and N1-Src. Circle sizes are proportional to the number of proteins they represent.

supports the prediction that they interact with different substrates and play different roles within the cell.

For the potential substrates to be phosphorylated by N1-Src they should contain a tyrosine residue that can be phosphorylated by the kinase domain. As the kinase domains of C- and N1-Src are identical, prediction programmes can be used to assess which of the potential N1-Src SH3 domain substrates are also likely to be phosphorylated. The GPS kinase prediction programme (Xue et al, 2008) was used to carry out this analysis.

GPS analysis was initially used to predict whether a protein can be tyrosine phosphorylated and, if it is, whether that phosphorylation is carried out by Src. This analysis was carried out for both C- and N1-Src (Figure 4.8.3) and reveals that a large proportion (~75%) of both the C- and N1-Src predicted SH3 domain substrates are also predicted to be tyrosine phosphorylated. Of these, ~70% are predicted to be Src phosphorylated. As the C-Src SH3 domain consensus motif is known to be found in *in vivo* phosphorylated substrates, it is encouraging that approximately the same proportion of C- and N1-Src predicted substrates are also predicted to be tyrosine phosphorylated.

More detailed analysis was then carried out using GPS to predict the SFK member responsible for a phosphorylation event. This revealed a preference for the Src kinase domain over that of any other SFK member for both the N1- and C-Src datasets (Figure 4.8.3 B and C). In order to confirm that this is not a general bias towards the Src kinase domain a series of controls were carried out by GPS analysis of Scansite predicted Src kinase domain, Lck SH3 domain and PKA kinase domain substrates (Figure 4.8.4).

Src was the predominant kinase predicted to phosphorylate the substrates identified by Scansite as being Src kinase domain substrates (Figure 4.8.3 A). This confirms that Scansite and GPS use similar criteria to define a Src substrate and provides confidence that this method is capable of producing meaningful results.

The Scansite defined Lck SH3 domain substrates were predicted to be predominantly phosphorylated by Lck kinase (Figure 4.8.3 B). Importantly, this demonstrates that there is a link between substrates identified by Scansite as SH3 domain interacting partners and those identified as kinase substrates by GPS. This is crucial because it shows that substrates identified as SH3 domain interacting are also highly likely to be phosphorylated by the relevant kinase. Additionally, this result

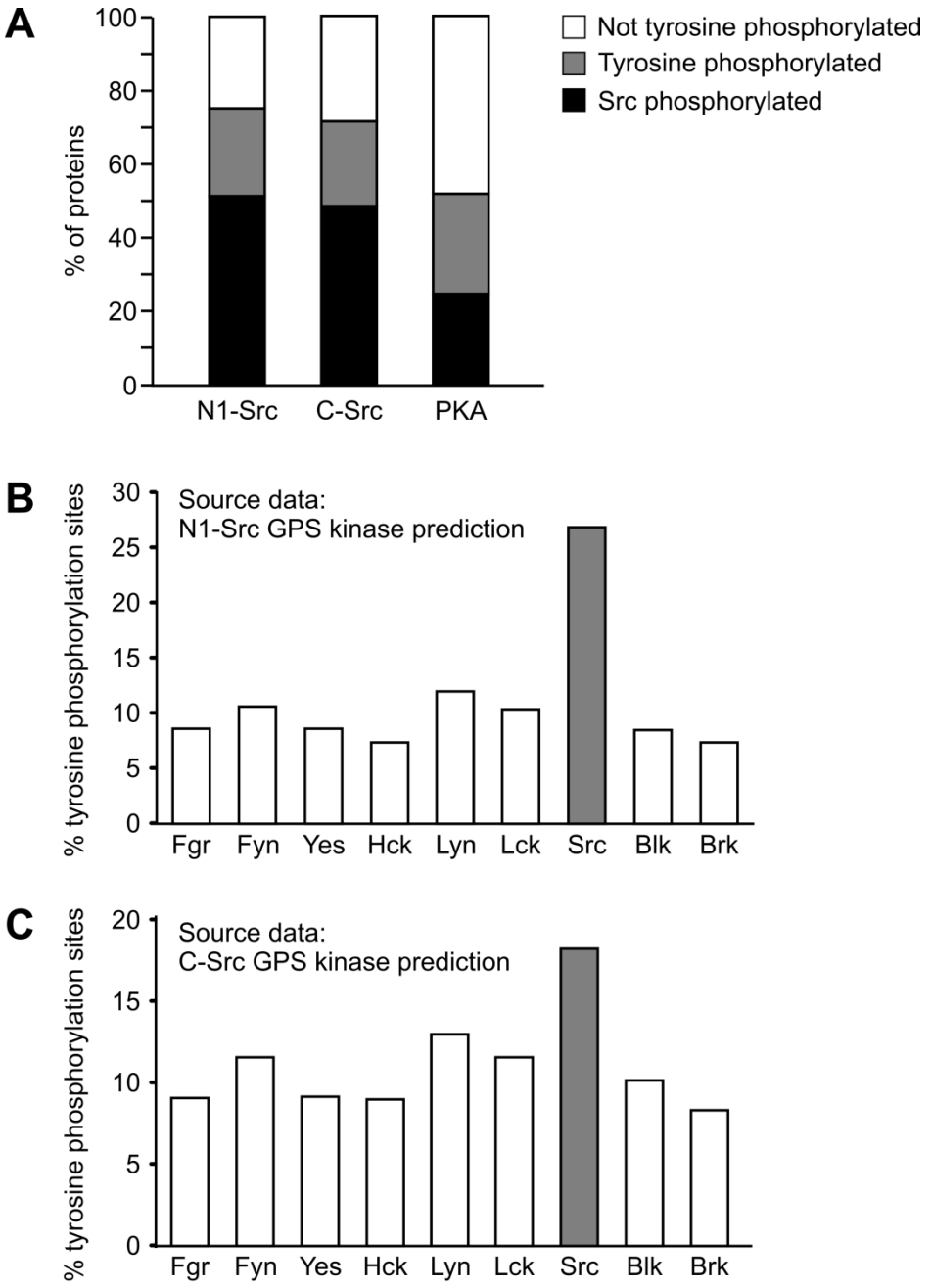

Figure 4.8.3. Scansite predicted N1-Src substrates are also predicted to be kinase substrates by GPS.

A) GPS prediction of the proportion of Scansite identified C-Src, N1-Src and PKA which are i) tyrosine phosphorylated and ii) Src phosphorylated. B) and C) GPS prediction of the SFK member which phosphorylates the substrates predicted to be Src phosphorylated for B) N1-Src and C) C-Src.

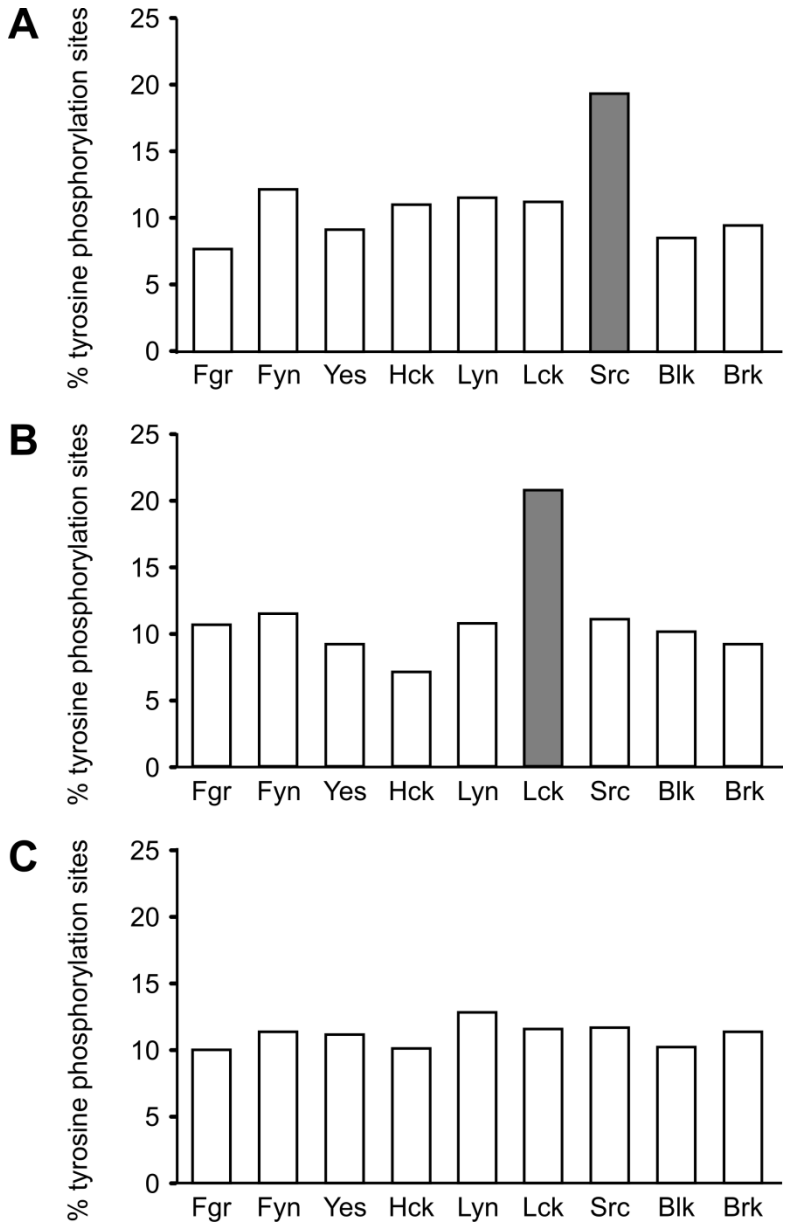

Figure 4.8.4. GPS is able to accurately predict SFK preferences from known datasets.

Scansite generated datasets for substrates of the A) Src kinase domain, B) Lck SH3 domain and C) PKA kinase domain were entered into the GPS kinase prediction programme and were predicted to be predominantly phosphorylated by A) Src, B) Lck and C) no preference.

shows that there is not an inbuilt bias into the GPS programme to predict Src kinase substrates. This was considered to be a potential problem as Src is the most extensively studied of the SFKs.

A final control experiment utilised Scansite predicted PKA substrates. PKA is not a tyrosine kinase and so there should be no reason for phosphorylation by any member of the SFKs to be enriched within its predicted substrates. The total number of substrates predicted to be tyrosine phosphorylated by PKA was approximately 20% lower than for either C- or N1-Src (Figure 4.8.2 A) and, of those predicted to be Src phosphorylated, there is no bias towards any member of the SFKs (Figure 4.8.3 C).

As a result of the GPS analysis control experiments, it can be concluded that the approach taken is able to identify potential kinase substrates from SH3 domain substrates and that there is no inbuilt bias for Src kinase. Therefore, there is a high degree of confidence in the ability of this technique to select potential N1-Src kinase domain substrates from the list of potential SH3 domain interactors.

The list of proteins identified by GPS as potentially phosphorylated by N1-Src represents a more refined set of potential N1-Src substrates as they are now predicted to both contain the consensus motif for the N1-Src SH3 domain and to be phosphorylated by the kinase domain. These substrates were re-submitted into DAVID in order to gain an updated list of enriched clusters (Table 4.8.5). This analysis revealed that the enriched clusters now no longer contain functions such as catabolism and chromatin rearrangement. It is likely that the proteins associated with these functions do not contain a potential phosphorylation site and have therefore been excluded from the analysis. The remaining enriched clusters indicate a strong relationship between N1-Src function and the regulation of cell shape during neuronal differentiation.

Following the second round of DAVID analysis, 134 proteins remained as potential N1-Src substrates. To identify whether there was any evidence of *in vivo* phosphorylation of these proteins, PhosphoSite database analysis was carried out. The PhosphoSite database is a repository of experimental data, predominantly obtained through high throughput screens, containing information about protein residues that are post translationally modified. Comparison of the potential N1-Src substrates with the PhosphoSite database produced a final list of 52 potential N1-Src substrates for which there is experimental evidence of phosphorylation at the correct

Table 4.8.5 Enriched functional roles for potential N1-Src substrates identified by GPS as being Src phosphorylated.

DAVID analysis of protein functions that occur more frequently than would be expected based on their occurrence in the genome (enrichment factor). Input proteins were those predicted by GPS as being Src phosphorylated.

Cluster name	Enrichment Factor	No. of proteins
Cell adhesion molecule signalling	4.1	23
Ras/Rho protein signalling	3.1	21
Post translational modification	2.5	46
Neuronal differentiation	2.1	56
Cytoskeletal rearrangement	1.7	73

tyrosine residue (Table 4.8.6). Of the 52 final proteins, 25 (48%) are assigned by DAVID as performing a role in neuronal development.

Processive phosphorylation is commonly carried out by SFKs as the SH2 domain docks onto a phosphorylated tyrosine residue, allowing the protein to be further phosphorylated and resulting in sustained kinase activation (Mayer et al, 1995). Scansite is also able to predict which tyrosine residues would be able to act as a scaffold for the kinase (i.e. are able to bind to the Src SH2 domain), allowing further phosphorylation to occur. When this analysis was carried out on the final set of substrates, 14 (27%) of the potential substrates were shown to also contain a tyrosine residue predicted to act as a SH2 domain scaffold (Table 4.8.6). However, only 5 (10%) of these occur at the same tyrosine residue identified as the site of potential phosphorylation.

The proteins that fit all of the criteria of an ideal potential N1-Src kinase substrate i.e. they contain the SH3 domain consensus binding motif, are predicted by GPS to be Src phosphorylated, have prior evidence of *in vivo* phosphorylation and are predicted to act as a SH2 domain scaffold are; AHNAK2, collagen alpha-1(V) chain, mitogen-activated protein kinase kinase kinase kinase 1 (MAP4K1), methionine synthase and tyrosine-protein phosphatase non-receptor type 6 (PTPN6). All of these proteins are expressed in neuronal tissue and have defined roles in the brain. They therefore represent a promising list of candidate substrates that could be further investigated as putative *in vivo* N1-Src substrates.

Table 4.8.6. Potential N1-Src substrates play a role in neuronal development.

Proteins that were shown to be phosphorylated in the Phosphosite database at the same residue predicted to be phosphorylated by GPS were included in the final list of potential N1-Src substrates. Proteins assigned by DAVID as playing a role in neuronal development are highlighted (grey). The ability of the protein to act as an SH2 domain scaffold is indicated Yes (Y) or No (N). If Y then the residue(s) predicted to act as the scaffold is stated. Proteins that fit all of the criteria for a potential N1-Src substrate are highlighted in red.

UniProt ID	Protein Name	Phosphorylated residue(s)	Phosphorylated peptide(s)	SH3 binding residue(s)	SH3 binding peptide(s)	SH2 scaffold?
ADAM9	Disintegrin and metalloproteinase domain-containing protein 9	815	PAPAPPLYSSLT***	8	MGSGARFPSGTLRVR	Y – Y42
ADNP	Activity-dependent neuroprotector homeobox protein	936	QKEDGSKYETIHLTE	779	TKYFNKQPYPTRREI	N
AFF4	AF4/FMR2 family member 4	668 712	PSSQTPKYPESNRTP LSEPDDRYPLIVKID	567	RTVGKKQPKKAEKAA	N
AHNK2	**Protein AHNAK2**	**59**	**PQGSSPVYEYTTEAA**	**1092**	**EMPSFKMPKVALKGP**	**Y – Y59**
APOL3	Apolipoprotein L3	193	LMELTQIYQRLNPCH	308	ARARARLPVTTWRIS	N
ARFGAP3	ADP-ribosylation factor GTPase-activating protein 3	279 349 408	VSSLRLAYKDLEIQM NDDSDDSYFTSSSSY TARRKPDYEPVENTD	218	SSIIKKKPNQAKKGL	N
BIG1	Brefeldin A-inhibited guanine nucleotide-exchange protein 1	662 852	HPETINRYGSLNSLE NKMTKEQYIKMNRGI	791	FLEGFRLPGEAQKID	Y-Y874
BMP2K	BMP-2-inducible protein kinase	813	YEQAKAKYSDMSSVY	1015	LKPTYRTPERARRHK	N
BSN	Bassoon	669 1126 1470 1472 3220 3388 3620 3705	EDLVGKPYSQDASRS HRSSCSEYSPSPSLD TPQPSRAYSYFASSS QPSRAYSYFASSSPP TYPSDSHYTSLEQNV VESDLASYPPPAVSS ARHSYHDYDEPPEEG GYPSSAEYSQPSRAS	2245	LTSLTRVPMIAPRVP	Y – Y1257, Y905, Y3161
BSN (cont.)		3715	PSRASSAYHHASDSK			
C1QR1	Complement component C1q receptor	628 644	PQNAADSYSWVPERA SRAMENQYSPTPGTD	506	TASPTRGPEGTPKAT	N
CBPC2	Cytosolic carboxypeptidase 2	150 764	LRSRQLLYDELDEVN RKQRNEQYQKKNLMQ	175	SILSTKRPLQAPRWP	N

UniProt ID	Protein Name	Phosphorylated residue(s)	Phosphorylated peptide(s)	SH3 binding residue(s)	SH3 binding peptide(s)	SH2 scaffold?
CKAP5	Cytoskeleton-associated protein 5	1854	KEGLAELYEYKKKYS	222	EEEWVKLPTSAPRPT	N
CO5A1	**Collagen alpha-1(V) chain**	**338** **442**	**EDVGIGDYDYVPSED** **PANQDTIYEGIGGPR**	**71** **296**	**TRRSSKGPDVAYRVT** **EPTPSKKPVEAAKET**	**Y – Y338,** **Y420, Y442**
CTRO	Citron Rho-interacting kinase	1929	NKRGPPTYNEHITKR	2007	DSSRGRLPAGAVRTP	N
CYLD	Ubiquitin carboxyl-terminal hydrolase CYLD	376	SKSKNTWYIDEVAED	151	GVVRFRGPLLAERTV	N
DNLI1	DNA ligase 1	919	GSDPEDTY*******	221	EEEQTKPPRRAPKTL	N
DSG2	Desmoglein-2	882 1013 1061 1117	MVNSENTYSSGSSFP QHLQDVPYVMVRERE ASTLQSSYQIPTENS HSTVQHSYS******	538	FSVIDKPPGMAEKWK	N
DYHC1	Cytoplasmic dynein 1 heavy chain 1	4357	EDEDDLAYAETEKKT	4239	NISPDKIPWSALKTL	Y – Y3130
GAK	Cyclin-G-associated kinase	615	VASTSQEYDKMRDFK	1167	EERGVRAPSFAQKPK	N
IQGA3	Ras GTPase-activating-like protein IQGAP3	13	AGPGWAAYERLTAEE	635	TERVLRNPAVALRGV	N
ITCH	E3 ubiquitin-protein ligase Itchy homolog	420	QFNQRFIYGNQDLFA	260	PPRPSRPPPPTPRRP	Y – Y103
L1CAM	Neural cell adhesion molecule L1	310 418	GEEDDGEYRCLAENS ELAKDQKYRIQRGAL	139	AEGAPKWPKETVKPV	N
LMTK3	Serine/threonine-protein kinase LMTK3	296 297	HSNYKEDYYLTPERL SNYKEDYYLTPERLW	1012	ENGGLRFPRNTERPP	Y – Y515
M4K1	**Mitogen-activated protein kinase kinase kinase kinase 1**	**381**	**SESSDDDYDDVDIPT**	**352**	**RGMETRPPANTARLQ**	**Y – Y381**
MAF	Transcription factor Maf	348	RDAYKEKYEKLVSSG	36	KFEVKKEPVETDRII	N
MAST2	Microtubule-associated serine/threonine-protein kinase 2	812	ESEDDTSYFDTRSER	868	LLEERRTPPPTKRSL	N
METH	**Methionine synthase**	**913**	**FEEIMEEYEDIRQDH**	**640**	**DLIWNKDPEATEKLL**	**Y – Y630,** **Y913**
MYCB2	Probable E3 ubiquitin-protein ligase MYCBP2	3902	PEGEEKVYNATSDAD	3820	IKIELKGPENTLRVR	N
NRX2A	Neurexin-2-alpha	1710	KKNKDKEYYV*****	1699	APAAPKTPSKAKKNK	N
NTHL1	Endonuclease III-like protein 1	68	AQRLRVAYEGSDSEK	58	SHSPVKRPRKAQRLR	N
NUMB	Protein numb homolog	15	FRRKKDVYVPEASRP	410	QPGHKRTPSEAERWL	N
NXF2	Nuclear RNA export factor 2	120	SQNTQDGYTRNWFKV	618	LQTEGKIPAEAFKQI	N
PGCA	Aggrecan core protein	131	RSNDSGVYRCEVMHG	212 634	ADGSLRYPIVTPRPA SDQTVRYPIQTPREA	N
PLD1	Phospholipase D1	42	FEGEEVDYDVSPSDP	140	YKAFIRIPIPTRRHT	N
PRDM9	Histone-lysine N-methyltransferase PRDM9	191	RERKGHAYKEVSEPQ	104	PRQQVKPPWMALRVE	Y – Y302
PTN6	**Tyrosine-protein phosphatase non-receptor type 6**	**276** **536** **564**	**ENKGKNRYKNILPFD** **QKGQESEYGNITYPP** **SKHKEDVYENLHTKN**	**212**	**AFVYLRQPYYATRVN**	**Y – Y412,** **Y564**

UniProt ID	Protein Name	Phosphorylated residue(s)	Phosphorylated peptide(s)	SH3 binding residue(s)	SH3 binding peptide(s)	SH2 scaffold?
PYR1	CAD protein	1890	GTPDGTCYPPPPVPR	1477	VHVHLREPGGTHKED	Y – Y1749
RBM15	Putative RNA-binding protein 15	608 684	AATSVPAYEPLDSLD LSSSRDRYNSDNDRS	52	MKGKERSPVKAKRSR	N
RELN	Reelin	2821	KGWKRITYPLPESLV	1571	LPQDAKTPATAFRWW	N
RNPS1	RNA-binding protein with serine-rich domain 1	205 207	HPHLSKGYAYVEFEN HLSKGYAYVEFENPD	26	KKSSTRAPSPTKRKD	N
RS10	40S ribosomal protein S10	12 127	KKNRIAIYELLFKEG GEADRDTYRRSAVPP	33	DVHMPKHPELADKNV	N
SCG2	Secretogranin-2	135 349	APKENKPYALNSEKN PLDSQSIYQLIEISR	467	EKVLPRLPYGAGRSR	N
SEC63	Translocation protein SEC63 homolog	106	EYQEYNPYEVLNLDP	520	WQQKSKGPKKTAKSK	Y – Y432
SHAN1	SH3 and multiple ankyrin repeat domains protein 1 (Shank1)	900	AAEDDRPYLAPPAMK	506 771	SPSRGRHPEDAKRQP EAVHKKAPQQAKRLP	N
SHRM2	Shroom2	210	HSKRDSAYGSFSTSS	363	QPRGDRRPELTDRPW	N
SI1L3	Signal-induced proliferation-associated 1-like protein 3	1265	HSKGEPQYSSHSSSN	327	EADEGRSPPEASRPW	N
SLAF5	SLAM family member 5	279 299	QPAESRIYDEILQSK EEPVNTVYSEVQFAD	270	LNTFTKNPYAASKKT	Y – Y296, Y279, Y316
SPT6H	Transcription elongation factor SPT6	321	EEEADWIYRNAFATP	812	VTDFLRLPHFTKRRT	Y – Y425
TB10A	TBC1 domain family member 10A	328	VKACQGQYETIERLR	428	SKAKPKPPKQAQKEQ	N
TDRD7	Tudor domain-containing protein 7	502	EDEMKEYYSKNPKIT	374	EMYKVKFPEDALKNL	N
UBP31	Ubiquitin carboxyl-terminal hydrolase 31	1123	KSASALTYTASSTSA	1019	PGSLAKKPESTTKRS	N
XIRP2	Xin actin-binding repeat-containing protein 2	90	KSNNTREYGRPEVLK	1847	EVNLPKAPKGTVKIV	Y – Y1156, Y3283

4.9 Discussion

4.9.1 Identification of a novel consensus motif for the N1-Src SH3 domain

The technique of phage display has been successfully used to establish a consensus motif for the N1-Src SH3 domain. This consensus motif is +xPxxTx+ (where + represents a positively charged amino acid). Phage display has been demonstrated multiple times to be an effective way of determining the consensus sequence of modular domains such as the SH3 domain (Cheadle et al, 1994; Rickles et al, 1994) and the sequences that it identified have been demonstrated to be contained in *in vivo* substrates (Songyang, 1999). Non-specific selection of peptides can occur due to plastic binding and propagation related amplification of certain peptide sequences (Vodnik et al, 2011). In this study, negative selection steps were carried out during the panning process and all peptide sequences obtained were compared to known plastic binding or propagation related sequences (Vodnik et al, 2011). Only one peptide was found to be the result of non-specific amplification and it was removed from consideration in subsequent analysis. Therefore, peptides have been included in the alignment with a high degree of confidence that they are present due to a specific interaction with the N1-Src SH3 domain.

In vitro kinase assays have been used to demonstrate that the presence of PD1 is able to enhance phosphorylation specifically by N1-Src and mutagenic analysis has confirmed that the residues identified as being part of the consensus motif are required for the observed enhancement in phosphorylation. The exception to this is the threonine residue, where mutation to both alanine and valine was shown to have little effect on the phosphorylation observed. The reason for this remains unclear, but ongoing work in the lab aims to obtain the structure of the N1-Src SH3 domain in complex with PD1. This would reveal the structural basis of the interaction and could inform any future mutations that could be made.

The consensus motif differs from the general SH3 domain consensus motif of PxxP, meaning that the N1-Src SH3 domain binds to an atypical binding motif. The motif identified is novel and has not previously been shown to bind to any other SH3 domain. As the only difference between the C- and N1-Src SH3 domains is the presence of an insert within the N1-Src n-Src loop, this structural difference must be the cause of the atypical binding. The requirement for a positively charged residue

either side of the central motif is a novel property of an SH3 binding motif and results in the consensus motif for N1-Src being longer than for many other known SH3 domains (Mayer, 2001). The structural basis for substrate binding to the C-Src SH3 domain was introduced in section 1.2.1.3 and is known to involve residues in the n-Src loop. Therefore, alteration of n-Src loop residues would be predicted to alter the substrates able to bind. It is possible that the extra residues contained within the N1-Src SH3 domain are themselves able to contribute to the substrate binding site.

Very few SH3 domains contain inserts within their n-Src loops. Two known examples are the amphiphysin1/2 (Amph1/2) and PI3K SH3 domains. Amph1/2 are brain enriched proteins implicated in the regulation of clathrin-mediated endocytosis. The Amph1/2 SH3 domains bind to the sequence PSRPNR in the proline rich domain (PRD) of dynamin (Grabs et al, 1997). This sequence corresponds to a Class II PxxP motif. However, phage display using an oriented peptide library identified the consensus motif for the Amph2 SH3 domain as PxRPxR(H)R(H) (Grabs et al, 1997), which is also longer than most SH3 domain binding sequences and contains an additional positively charged arginine residue. The crystal structure of the Amph2 domain shows that the n-Src loop projects out from the core of the SH3 domain but is positioned adjacent to the substrate binding site (Owen et al, 1998). Both the inserts in the N1-Src and the Amph1/2 n-Src loops contain predominantly basic residues (Levy & Brugge, 1989; Owen et al, 1998). In the crystal structure of the Amph2 SH3 domain this is shown to result in an extended negatively charged patch on the surface of the protein. If this is also true of the N1-Src SH3 domain then it could explain the requirement for two positively charged residues within the consensus motif. Elucidation of the structure of the N1-Src SH3 domain would determine whether this is the case.

4.9.2 Validity of the bioinformatic approach taken

The bioinformatic approach used in this study has provided insight into the possible functions of N1-Src. The validity of the subsequent bioinformatic approaches relies on the accuracy of the initial PSSM used to identify potential N1-Src SH3 domain binding substrates. The matrix constructed was based on experimental evidence, both from the initial phage display experiments and from the subsequent validation

experiments. Therefore, there is a high degree of confidence that the matrix contains accurate information about the amino acid preferences of the N1-Src SH3 domain. The only position at which the information may not be as accurate is the threonine residue at position 8. As none of the mutations made significantly affected the observed phosphorylation of the substrate it is not entirely clear what the substrate preferences are at this position. In the matrix, the amino acids that have been shown to facilitate phosphorylation (T, A and V) have been included. However, there is currently no evidence that other amino acids should be excluded from this position. The reason for imposing some constraints on the amino acids present in this position was to limit the number of potential N1-Src substrates identified to a number on which meaningful further analysis could be carried out. It is not suggested that the substrates identified may be incorrect but it is possible that some potential substrates have been excluded by constructing the matrix in this manner.

In order to ascertain whether there is any amino acid preference at position 8 it would be informative to carry out a phage display experiment using a directed peptide library. The amino acids that have been confirmed to be required for phosphorylation can be fixed to be present in all peptides in the library with other positions still randomised (R/KxPxxxxR/K). This technique has been used in order to identify the flanking residues for the Class I and Class II PxxP motifs that bind to the C-Src SH3 domain (Feng et al, 1995) and would reveal whether there is any amino acid preference at positions other than those already shown to be required.

The use of PSSMs to discover novel protein-protein interactions has been validated previously. Scansite uses a library of PSSMs derived from experimental data to predict substrates of protein domains, including a number of SH3 domains (Obenauer et al, 2003). Other groups have successfully employed user defined PSSMs to identify physiologically relevant interactions. Chan et al (2011) produced a PSSM from peptide array data and used it to carry out a Scansite search for potential 14-3-3 protein interacting proteins. This led to the identification of two residues within Cdc25C required for 14-3-3 binding and the confirmation of the interaction by immunoprecipitation.

An oriented peptide library has been used to produce a consensus phosphorylation motif for the leucine rich repeat kinase 2 (LRRK2). Construction of a PSSM and a Scansite search identified potential novel substrates and peptides derived from these novel substrates could be phosphorylated *in vitro* (Pungaliya et

al, 2010). User defined PSSMs have also been used on a larger scale to map the interactions of many individual PDZ domains (Tonikian et al, 2008) and the yeast SH3 domain interactome (Tonikian et al, 2009).

The use of a combination of bioinformatic techniques has been able to provide an informative list of potential N1-Src substrates that fit all of the criteria of a Src kinase substrate. The combination of techniques used is novel to this study and the validity of the proteins identified must be treated with caution. Applying consecutive algorithms will inevitably introduce error at each stage. All bioinformatic techniques were carried out with a high degree of stringency and therefore it can be concluded that it is more likely that potential Src substrates have been excluded rather than those that are not potential substrates included erroneously. In a recent review, Reimand et al (2012) assessed current methods for prediction of domain mediated protein-protein interaction and concluded that combined approaches are commonly able to make predictions with a higher degree of confidence than methods based on a single prediction parameter. The use of GO terms (used here to select enriched clusters by DAVID analysis) has also been shown to reduce the amount of false positive hits in bioinformatic prediction of protein-protein interactions (Mahdavi & Lin, 2007).

Other groups have also exploited the modular domain organisation of signalling molecules such as the Src kinases in order to carry out integrated bioinformatic studies. Akiva et al (2012) used Scansite prediction of SH2, SH3 and PDZ domains coupled with NetPhorest (Miller et al, 2008) prediction of phosphorylation sites in order to demonstrate the existence of interaction-regulation units whose phosphorylation prevents substrate interaction. In this case the kinase site prediction was confirmed by comparison to low throughput experimental data.

Hou et al (2011) utilised different bioinformatic tools but still employed a hierarchical approach in order to identify novel potential A-kinase anchoring proteins (AKAPs), that act as scaffolds for PKA signalling. This group carried out their initial selection of potential substrates using a PSSM, in this case obtained from virtual mutagenesis studies. Further refinement of this dataset was carried out by sequential analysis of peptide secondary structure prediction, transmembrane region prediction and sequence conservation in vertebrate genomes. Validation of the hits was carried out by confirmation of the inclusion of known AKAPs and literature

searching for evidence that proteins containing the identified peptides may act as AKAPs.

Therefore, there is a precedent for the use of a combination of bioinformatic techniques to generate potential substrates that interact with the protein of interest under physiologically relevant conditions.

4.9.3 Insights into the functions of N1-Src

The use of DAVID analysis to identify enriched clusters allows unbiased screening of the dataset. The majority of the enriched clusters identified pointed to a role for N1-Src in cytoskeletal rearrangement. This is in agreement with the morphological changes observed following overexpression of the neuronal kinases (Chapter 3). DAVID identified that N1-Src may be acting the Rho/Ras signalling and cell adhesion molecule signalling pathways, both of which have documented roles in the regulation of cell morphology and cytoskeletal rearrangement.

It is known that signalling through the Rho/Ras pathway influences cell morphology. The major role of Rho GTPases is to control the assembly, disassembly, and dynamic rearrangements of the actin and microtubule cytoskeletons (Hall, 1998). Therefore, they play crucial roles in axon growth, guidance, and branching (Hall & Lalli, 2010). Ras GTPases are activated by a large number of plasma membrane growth factor receptors and adhesion receptors to promote key signal transduction pathways, including ERK, MAP kinase, and PI3-kinase that play a variety of important roles in axonogenesis (Hall & Lalli, 2010). Overexpression of a dominant positive form of Rho causes a contractile phenotype (Kolyada et al, 2003) similar to that observed in neuronal Src transfected fibroblasts (Chapter 3).

The final list of possible protein substrates reveals some interesting potential binding partners of N1-Src. The list includes some well characterised neuronal proteins such as Reelin and L1-CAM. There are also a number of less well characterised proteins that, although they have been identified as playing a role in neuronal development, are much less well understood. The presence of L1-CAM in this final dataset is interesting as there is some evidence that Src is involved in L1-CAM signalling, but the isoform of Src responsible remains unknown (Ignelzi et al, 1994). However, both the SH3 domain interacting site and the potential phosphorylation site identified in this study are contained within the extracellular

domain of L1-CAM. The Src kinases are not known to phosphorylate extracellular residues on transmembrane proteins and it seems unlikely that N1-Src would be responsible for a physiologically relevant phosphorylation at this site. The link between L1-CAM and N1-Src will be discussed in more detail in Chapter 5.

The proteins that fulfil all of the criteria of a potential N1-Src substrate are of particular interest and the evidence for tyrosine phosphorylation involvement in the regulation of their functions is discussed further below.

4.9.3.1 AHNAK2

AHNAK2 is a member of the AHNAK family, also known as desmoyokins. They are giant proteins (~700 kDa) and the specific functions of AHNAK2, as opposed to other AHNAK family members, are poorly understood. AHNAK was first identified as a component of desmosomal plaques (Hieda & Tsukita, 1989). It was subsequently independently identified in a screen for genes that undergo transcriptional repression in non-differentiated tumours of neural crest origin; the neuroblastomas (Shtivelman & Bishop, 1993). Its expression has also been shown to increase following spinal cord injury (von Boxberg et al, 2006). The full length form of AHNAK is known to be expressed in the adult CNS but its expression is thought to be localised to the blood cells of the blood brain barrier (Gentil et al, 2005). A smaller (~300 kDa) isoform has also been identified (Carlson et al, 2010; Huang et al, 2008b) and shown to be expressed in cardiac cells and the Torpedo electric organ; a structure of the electric eel that is analogous to the mammalian neuromuscular junction (NMJ). This smaller AHNAK isoform has also been shown by PCR to be expressed in developing mouse motor neurons (Carlson et al, 2010).

In cardiac cells AHNAK is known to link voltage gated calcium channels to the cytoskeleton (Hohaus et al, 2002) and is able to bind to the Ca_vB subunit (Komuro et al, 2004). In the electric organ, AHNAK is found localised to presynaptic sites and associated with nerve terminals in a complex that also contains calcium channels, integrins and laminins (Carlson et al, 2010). AHNAK is therefore predicted to function in the modulation of cytoskeletal organisation as a result of calcium signalling in the CNS.

AHNAK2 is known to be tyrosine phosphorylated only through high throughput studies and there is currently no information available about the tyrosine

kinase that carries out the phosphorylation or the functional effect of the phosphorylation event. The sites identified as being potential N1-Src SH2, SH3 and kinase domain substrates in this study are contained within the smaller AHNAK isoform and it is therefore possible that N1-Src phosphorylation of AHNAK would occur under physiological conditions.

4.9.3.2 Collagen alpha-1(V) chain

Type V collagens are a minor component of collagen that are found in many tissues including the brain (Rhodes & Miller, 1978). The alpha-1 chain can exist as a homotrimer or as a heterotrimer in complex with alpha-2 and alpha-3 chains (Morris et al, 1990). Type V collagen fibrils are secreted and function as components of the ECM. Phosphorylation of secreted proteins is very unusual and there is currently no evidence, other than mass spectrometry data, for tyrosine phosphorylation of Type V collagen.

4.9.3.3 Mitogen activated protein kinase kinase kinase kinase 1 (MAP4K1)

MAP4K1 is more commonly known as hematopoietic progenitor kinase 1 (HPK1). It is a serine/threonine kinase that is predominantly expressed in hematopoietic cells but is also present in other tissues, including the brain (Hu et al, 1996). The majority of the work into the function of HPK1 has been carried out in T cells, where it has been shown to act in the MAP kinase pathway to link cell surface receptors to the c-Jun NH2-terminal kinase (JNK) pathway (Hu et al, 1996). To do this, HPK1 has been shown to interact with many adaptor proteins including Grb2, Nck, Crk and SLP-76 (Anafi et al, 1997; Boomer & Tan, 2005).

More recently, HPK1 has been shown to function in the brain in pathways that induce injury following cerebral ischemia. Importantly, the activation of HPK1 in this context is dependent on a tyrosine phosphorylation event (Li et al, 2008a). It is thought that Src is activated through its phosphorylation of the NMDA-R and activated Src subsequently phosphorylates HPK1 (Zhang et al, 2007). This increases the activity of HPK1 and results in the sequential activation of MLK3, MKK7 and JNK3 (Li et al, 2008b), a pathway involved in the induction of apoptosis following

ischemia. The site of phosphorylation in the HPK1 sequence has not yet been identified.

The Src isoform responsible for the HPK1 phosphorylation is currently assumed to be C-Src (Li et al, 2008b). However, these experiments were carried out using a broad spectrum SFK inhibitor and therefore the isoform responsible could be another SFK member or, as would be predicted by this study, N1-Src. As HPK1 fits all of the criteria imposed in this study for an ideal N1-Src substrate candidate it would be interesting to carry out *in vitro* experiments to determine the Src isoform responsible for the phosphorylation.

4.9.3.4 Methionine synthase

Methionine synthase is an enzyme that catalyses the remethylation of homocysteine to methionine. Mutations in methionine synthase are risk factors for sporadic Alzheimer's Disease (AD) (Beyer et al, 2003) due to the resultant accumulation of homocysteine in the cell. Homocysteine is known to sensitise hippocampal neurons to β-amyloid induced damage in cell culture experiments (Sai et al, 2002) and to increase vulnerability to DNA damage induced excitotoxicity (Kruman et al, 2000). Therefore, methionine synthase activity is required for normal neuronal function. The function of tyrosine phosphorylation of methionine synthase remains unknown and has so far only been reported in high throughput screens but could potentially regulate its activity. Further investigation is therefore required to ascertain whether tyrosine phosphorylation of methionine synthase occurs under physiological conditions and whether the phosphorylation has any effect on enzyme activity. If methionine synthase is demonstrated to be tyrosine phosphorylated then N1-Src would be a good candidate for the kinase carrying out the phosphorylation as it meets all of the criteria outlined in this study.

4.9.3.5 Tyrosine-protein phosphatase non-receptor type 6 (PTPN6)

The tyrosine protein phosphatase non-receptor type 6 (PTPN6) identified is better known as SHP-1 (SH2 domain-containing tyrosine phosphatase 1) or PTP1C (protein tyrosine phosphatase 1C). SHP-1 (along with other phosphatases) is able to catalyse the dephosphorylation of Src and catalyses the dephosphorylation of Src at

pY527 more effectively than it does at pY416 (Somani et al, 1997). SHP-1 therefore plays a role in the activation of Src by pY527 dephosphorylation and removal of the SH2:tail regulatory interaction. SHP-1 is also able to effectively catalyse the dephosphorylation of Src substrates (Frank et al, 2004).

Interestingly, Frank et al (2004) also showed that Src can phosphorylate Y538 and Y566 of SHP-1. SHP-1 phosphorylation activates its phosphatase activity and upregulates the dephosphorylation of Src substrates. This regulatory cycle means that Src signalling in the presence of SHP-1 is transient. These experiments were carried out using transfection of C-Src into HEK293 cells. Therefore C-Src is definitely able to carry out the phosphorylation event. However, it is possible that N1-Src is also able to phosphorylate SHP-1 at these or other sites. This would provide an interesting mechanism of regulation and may be a way to explain why we do not observe large numbers of N1-Src phosphorylated proteins in cells despite the high activity of N1-Src (Chapter 3). Active N1-Src would also result in active SHP-1 and therefore any substrate proteins phosphorylated by N1-Src would be rapidly dephosphorylated by SHP-1. This supports the idea that N1-Src signalling may be involved in dynamic signalling processes such as cytoskeletal rearrangement rather than more stable phosphorylation events.

The tyrosine residues identified as being potential N1-Src substrates in this study are Y276, Y536 and Y564. Y536 and Y564 in the human SHP-1 variant 1 sequence are analogous to Y538 and Y566 in the human SHP-1 variant 2 sequence used by Frank et al (2004). Phosphorylation at these residues by C-Src had an activating effect on SHP-1. It is possible that N1-Src phosphorylation here would also result in SHP-1 activation and regulation of N1-Src substrate phosphorylation. There is currently no biochemical evidence for SHP-1 at Y276 and it therefore remains unknown what effect phosphorylation at this site may have on SHP-1 activity.

The potential N1-Src substrates identified in this study provide attractive targets for further research into the functions of N1-Src. The proteins identified in this study are involved in functions in both the developing and mature brain. N1-Src is known to be highly expressed throughout development and in the adult mouse (Wiestler & Walter, 1988) and therefore it would be predicted that it is performing functions at all developmental stages.

In vitro experiments could be used to confirm firstly an interaction between N1-Src and the substrate and secondly that N1-Src is able to phosphorylate the substrate. Site directed mutagenesis could then be used to ascertain whether the interaction takes place at the residues predicted in this study. Alternatively, sites of phosphorylation could be identified by MS analysis of the recombinant phosphorylated protein. Cell based experiments using transfected or endogenous substrates and kinases would then be used to confirm that the interaction takes place under physiologically relevant conditions. The use of functional assays looking at the activity or localisation of the substrate proteins would allow elucidation of the biological relevance of the phosphorylation reaction. As there is evidence for the *in vivo* tyrosine phosphorylation of HPK1 and SHP-1 they would seem to be the best candidate substrates with which to begin further investigations into N1-Src function.

5 Functional studies of N1-Src kinase

5.1 Introduction

5.1.1 Culture based models of neuronal development

The *in vitro* and heterologous cell techniques presented in Chapter 3 pointed to a role for N1-Src in the development of neuronal morphology. This was supported by the bioinformatic analysis carried out in Chapter 4. A neuronal culture system was therefore required to allow manipulation of the endogenous protein. Cerebellar granule neurons (CGNs) are a good model culture system for studying the effects of proteins that may have a role in neuronal development. Of the main cerebellar neuronal types (granule cells, Purkinje cells and inhibitory interneurons), granule neurons are by far the most numerous and are the most abundant type of neuron in the mammalian brain. In rodents, cerebellar granule neurons are generated during the first two post-natal weeks from progenitor cells in the outermost layer of the cerebellar cortex, the external granule layer (EGL). The development of CGNs in culture closely mirrors their *in vivo* differentiation (Powell et al, 1997). To prepare CGNs in culture, the cerebellum is taken from P7 rats, at which stage the CGNs are still migrating, lack processes and therefore are able to survive the dissociation and transfer to culture. The development of CGNs is very well studied and therefore any deviation from this normal development can be clearly identified and quantified.

When CGNs are plated onto culture dishes, they begin as small, rounded cells that extend a single neurite, followed by a second from the opposite pole. One of these processes will extend further and become the axon, bifurcating to form the two arms of the parallel fibres observed *in vivo*. The second original neurite will retract and dendrites will form at this opposite pole (Tahirovic & Bradke, 2009) (Figure 5.1.1).

One drawback to the use of the CGN model culture system is that CGNs have quite a simple neuronal architecture with limited axonal branching. They are also very small. Hippocampal neurons are much larger cells with a more complex branching architecture. They can therefore be used to identify more subtle changes in neuronal architecture and have been used for this purpose in this study. Development of hippocampal neurons follows a similar programme to that of CGNs, with the

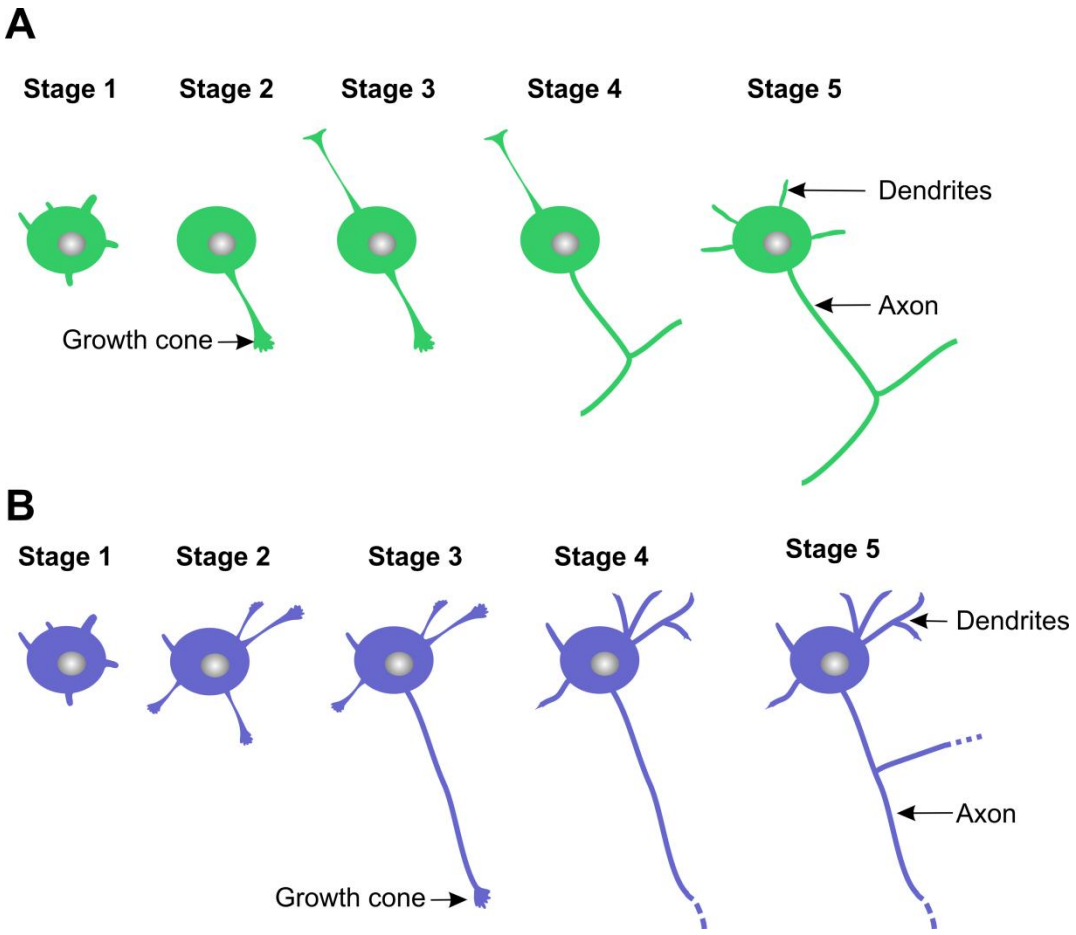

Figure 5.1.1. Development of neurons in culture.

Adapted from Tahirovic and Bradke, 2009. A) Development of rodent cerebellar granule neurons (CGNs). CGNs initially extend several short filopodia (Stage 1) and then begin to extend one longer process, led by a growth cone (Stage 2). This is followed by the growth of a second process from the opposite pole, to form a neuron with bipolar morphology (Stage 3). One of the long process will extend further, begin branching and go on to form a functional axon (Stage 4 and 5). The second long process will retract and dendrites will form at the opposite pole to the axon (Stage 5). B) Development of rodent hippocampal neurons. Hippocampal cells also begin as small cells with multiple protrusions (Stage 1) but then develop into multipolar cells (Stage 2). One neurite will rapidly extend and become the axon (Stage 3). The other neurites will become dendrites (Stage 3) while the axon continues to extend (Stage 4) and branch (Stage 5).

initial formation of multiple processes, one of which will go on to become the axon (Tahirovic & Bradke, 2009) (Figure 5.1.1). The final morphology of hippocampal neurons is much more variable than that of CGNs and this can make analysis of morphological changes caused by protein manipulation more challenging than for CGNs. In addition, cells obtained from the hippocampus are a mixed culture with CA1, CA3 and DG neurons present. This can make it difficult to assess a difference that occurs in only one or a subset of the neuronal types.

5.1.2 Mechanisms regulating neurite outgrowth and branching

The process of neuronal branching is a fundamental property of neurons, with the vast majority of neurons able to produce branched processes. The process of branching allows neurons to simultaneously connect to multiple targets, facilitating the formation of a complex neuronal network. The guidance cues that mediate axon guidance were introduced in Chapter 1 and many of the same pathways are involved in the molecular processes of axon branching.

There are two distinct mechanisms by which an axonal branch may form. Firstly, a growth cone may split with each half continuing to grow and extend, this process can only occur during axonal outgrowth and is the mechanism that CGNs use to branch. Secondly, a new outgrowth may form from the main axonal shaft; this process is known as interstitial or collateral branching and may occur in mature neurons. This process is used by hippocampal neurons. Both processes have been demonstrated to occur in culture and *in vivo* (O'Leary & Terashima, 1988; Schmidt et al, 2007). Whether the molecular mechanisms underlying these two processes are the same or distinct remains to be shown but they are known to involve broadly similar signalling pathways (Schmidt & Rathjen, 2010).

Axon guidance is a highly regulated process that needs to co-ordinate neurite size and position through growth and guidance with the addition of complexity through branching. Multiple proteins and pathways have been identified as playing a role in the regulation of the axonal branching process. These include signalling arising from; axon guidance cues, growth factors, calcium, electrical activity, extracellular ligands, morphogens, transcription factors and cell adhesion molecules (Tessier-Lavigne & Goodman, 1996). These pathways do not appear to be degenerate as perturbation of only one can be sufficient to inhibit branching and it is

likely that they respond to a variety of intracellular and extracellular cues to stimulate branching.

The formation of a branch relies on the convergence of multiple signalling pathways to result in asymmetrical remodelling of the cytoskeleton. The axonal cytoskeleton consists predominantly of filamentous actin and α/β-tubulin and is highly dynamic, being continually remodelled both during development and in mature neurons. The inhibition or destabilisation of the microtubule or F-actin networks inhibits axonal branching (Dent & Kalil, 2001), indicating the reliance of the branching process on cytoskeletal remodelling.

Some neuronal cells have highly branched and complex dendritic arbours. The signalling processes underlying dendritic branching involve the same broad classes of molecules but are considered distinct from those underlying axonal branching. As the neuronal types used within this study do not exhibit any complex dendritic branching, the molecular mechanisms controlling this process will not be discussed further (for a recent review see (Jan & Jan, 2010)).

5.1.3 N1-Src and L1-CAM

Ignelzi et al (1994) identified that the rate of growth of neurons taken from $src^{-/-}$ mice is slower than that of control neurons when grown on a substrate of the cell adhesion molecule L1-CAM. This effect is specific to signalling arising from the L1-CAM pathway as neurite outgrowth is unaffected by growth on laminin. It is also specific to Src, because the growth of neurons taken from $Fyn^{-/-}$ or $Yes^{-/-}$ mice was normal. However, the nature of the cloning carried out to create the Src knockout mouse means that it is null for all three Src isoforms, C-Src, N1-Src and N2-Src. The particular isoform responsible for the defective neurite outgrowth has not been identified.

5.2 Aims

Studies in heterologous cells (Chapter 3) and bioinformatic investigations (Chapter 4) have identified a potential role for N1-Src in the modulation of neurite outgrowth. To test this hypothesis, and to investigate the *in vivo* functions of N1-Src overexpression and inhibition, experiments were carried out in cultured neurons.

This allowed the manipulation of endogenous N1-Src activity and function. The culture systems chosen for these investigations were CGNs and hippocampal neurons, two well characterised models of neuronal differentiation. A secondary aim of this work was to investigate the possible link between N1-Src and signalling in the L1-CAM pathway. This was achieved by investigating the growth of neurons on a substrate of L1-CAM following inhibition of N1-Src.

5.3 N1-Src overexpression causes aberrant neurite outgrowth

In the experiments presented in Chapter 3, overexpression of WT N1-Src caused the induction of a neuronal phenotype in heterologous cells, characterised by the production of neuronal-like processes and a decrease in cell area. In a neuronal system, it has previously been shown that overexpression of constitutively active N1-Src (Y527F) in Purkinje neurons causes aberrant neurite outgrowth, primarily affecting dendrite morphology (Kotani et al, 2007). Kotani et al found that overexpression of the WT protein had little effect on cell morphology.

In order to further investigate the functions of N1-Src and its effects on neuronal morphology, WT N1-Src was overexpressed in cultured CGNs and the cell morphology analysed 24 hours following transfection. The morphology of N1-Src transfected cells was compared to control and C-Src transfected cells. Control neurons were visualised by transfection with CFP and stained with an α-CFP antibody. The Src constructs used were the same constructs that were used in Chapter 3 for COS7 cell transfection. The constructs were FLAG tagged and transfected cells detected using an α-FLAG antibody. Transfected neurons were identified as CGNs by morphology.

Transfection of CGNs revealed that, in contrast to the findings in Purkinje neurons, neurite outgrowth of CGNs was inhibited by overexpression of WT N1-Src (Figure 5.3.1). Morphological analysis showed that the axons are primarily affected, with approximately 40% of the cells having duplicated axons (Figure 5.3.2). During normal CGN development the cells initially extend two axonal-like processes before one retracts and dendrites form (Figure 5.1.1). The morphology observed here may be as a result of either a delayed developmental programme or a failure in the cues that distinguish axonal formation from dendrite formation. Regardless of the

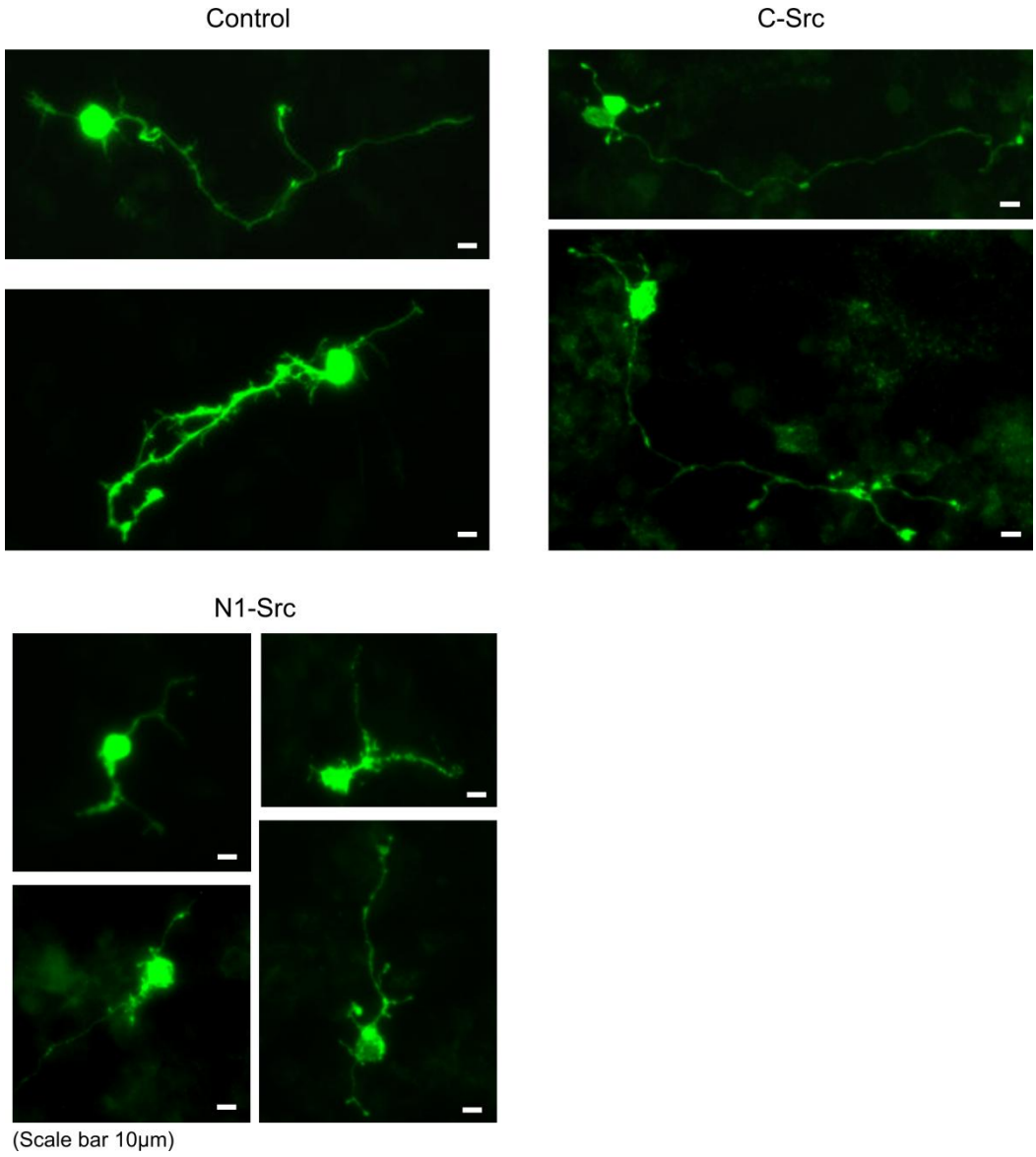

Figure 5.3.1 Overexpression of N1-Src causes aberrant neuronal morphology

CGNs were prepared from P7 rats and plated onto PDL coated coverslips. Neurons were transfected 24 hours following plating and fixed for morphological analysis 24 hours after transfection. Control cells were transfected with CFP and visualised with α-GFP. C- and N1-Src constructs were FLAG tagged and transfected cells were visualised by α-FLAG staining. Representative epifluorescent images shown.n=3 experiments.

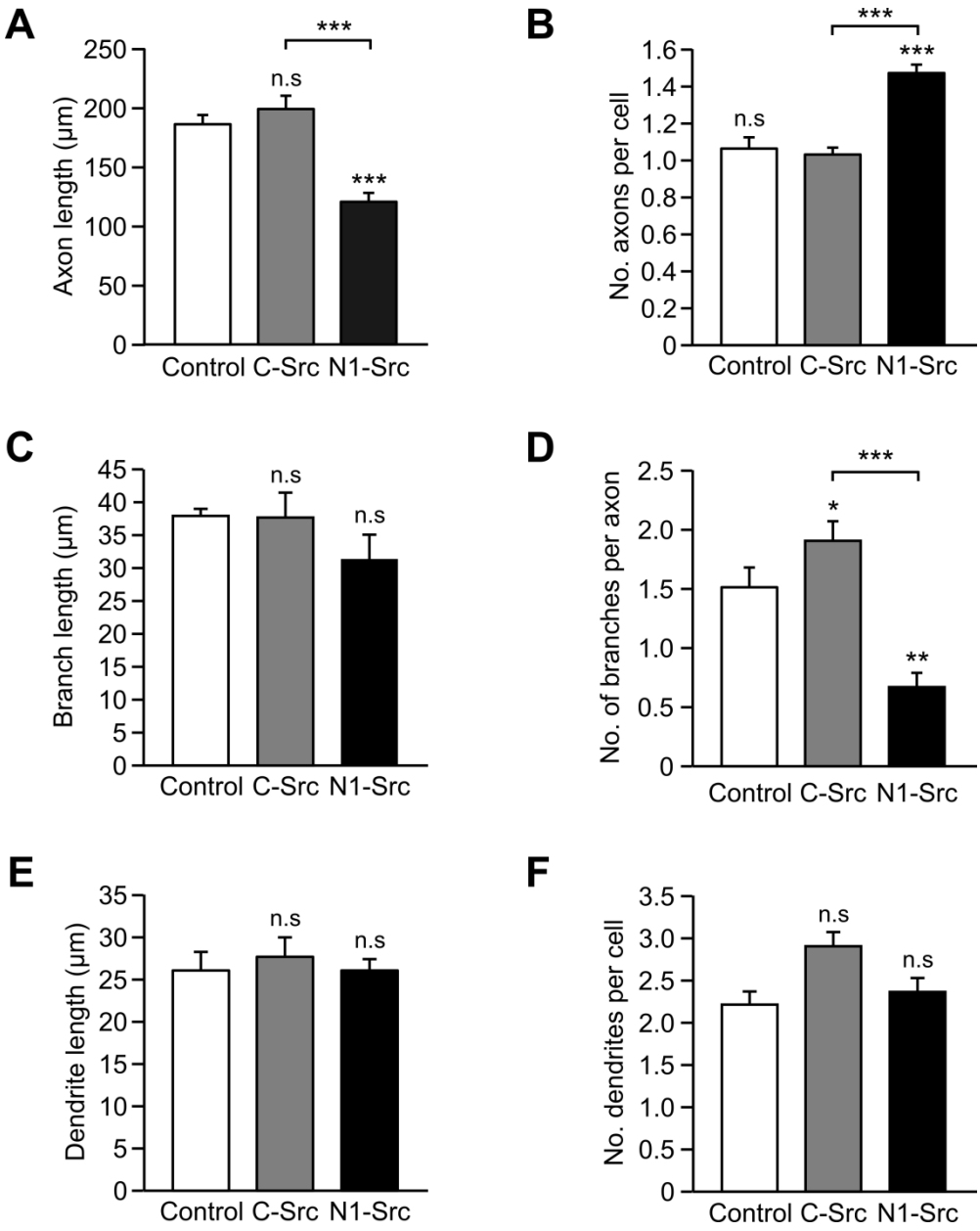

Figure 5.3.2 N1-Src overexpression induces axon duplication.

The morphology of CGNs transfected with CFP (control), C-Src and N1-Src was analysed 24 hours after transfection using the NeuronJ plugin for ImageJ. Parameters measured were A) axon length B) axon number C) branch length D) branch number E) dendrite length F) dendrite number. n=3 experiments, approximately 30 cells analysed per condition for each experiment. Error bars show SEM. Statistical analysis carried out by ANOVA and post hoc Tukey test * $p < 0.05$, ** $p < 0.01$, *** $p<0.001$.All conditions compared to control neurons.

mechanism, this result indicates that N1-Src plays a role in the initial processes of axon formation.

In addition to the axon duplication observed, the axons that form are approximately 50% shorter than either control (CFP transfected) or C-Src transfected cells. They are also much less highly branched, although the branches that do form are of approximately the same length as those found in control cells. In contrast to the study by Kotani et al (2007), the dendrite number and length remain unaffected.

While N1-Src overexpression had striking effects on CGN morphology, C-Src overexpression had little effect. The only morphological factor analysed that was significantly different to control cells following C-Src overexpression was the number of branches per axon, which increases by approximately 15%. As CGNs have so few axonal branches it is unclear whether this is a true effect of C-Src overexpression or an artefact caused by the fact that CGN axons are not highly branched and therefore a small increase in branch number produces a large percentage increase. Repeating the overexpression of C-Src in a neuronal type with more extensive axonal branching would confirm whether axonal branching is increased by C-Src overexpression.

The reasons why N1-Src overexpression has a gain-of-function phenotype while C-Src overexpression has little effect remain unclear, but may be related to the high constitutive activity of N1-Src. The high basal activity of N1-Src demonstrated in Chapter 3 may result in N1-Src overexpression having a greater effect than C-Src overexpression because, even when overexpressed, C-Src activity is tightly regulated. The differences between the effects of C-Src and N1-Src overexpression also support the view that the *in vivo* functions of C-Src and N1-Src are different and it may be that C-Src plays limited roles in the regulation of neuronal morphology

In order to determine whether the differences in cell morphology observed following N1-Src overexpression are due to a delayed developmental programme, the period of maturation in culture following the transfection was extended. Figure 5.3.3 shows that even after 72 hours in culture the N1-Src transfected cells are not able to form a normal CGN architecture. The average axon length extends slightly but does not reach that of control cells. This implies that the morphology observed is not simply the result of delayed development and that N1-Src overexpression is able to influence both the processes of axonal growth and branching. The only factor that appears to be rectified by this longer incubation is the axon number with very few

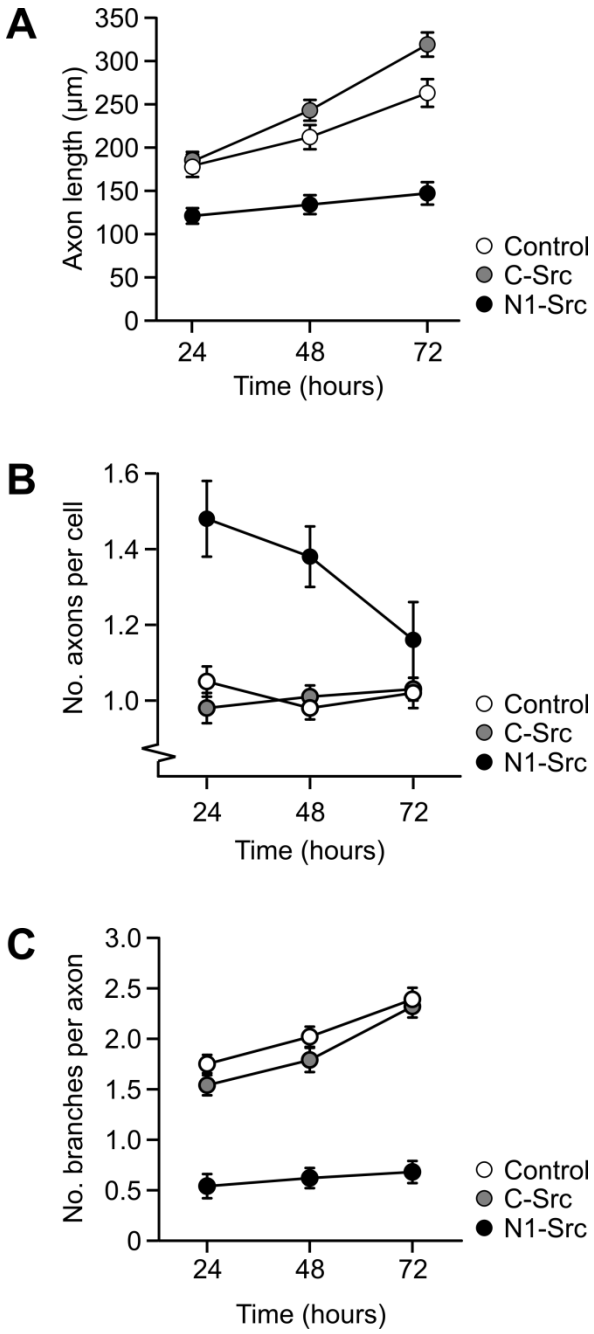

Figure 5.3.3 N1-Src transfected cell morphology is not rescued by longer expression

Control (CFP), C- and N1-Src transfected CGNs were fixed 24, 48, and 72 hours following transfection and morphology analysed using the NeuronJ plugin for ImageJ. Parameters measured were A) axon length B) axon number and C) branch number. Plotted data were obtained from 1 experiment with 15-20 neurons analysed per condition. Error bars show SEM.

cells displaying duplicated axons by the 72 hour timepoint. This may be because there are other signalling processes within the cell that are able to compensate for the perturbation of N1-Src signalling by these later timepoints or it may be that cells with duplicated axons are identified as defective and destroyed by apoptosis at later timepoints. The only cells then remaining for quantification would be those with a less severe phenotype.

At timepoints over 72 hours, both C- and N1-Src transfected cells began to die while control cells remained healthy. For C-Src transfected cells this was surprising as they appeared morphologically normal. This implies that, while C-Src was not influencing neuronal morphological development, over longer time periods, overexpression of the kinase was detrimental to the cell. C-Src plays well documented roles in signalling pathways distinct from the regulation of cell morphology including cell survival. As aberrant kinase signalling is frequently associated with disease processes, prolonged overexpression of a kinase can result in the induction of apoptosis (Zhong et al, 2002).

5.4 PD1 is a specific inhibitor of N1-Src in cells

To study the functions of N1-Src in more detail, a specific inhibitor of N1-Src was required. There are no commercially available pharmacological inhibitors of N1-Src but the PD1 peptide characterised in Chapter 4 had been shown to be able to inhibit N1-Src substrate phosphorylation *in vitro*. To confirm that PD1 is able to interact with N1-Src in cells, FLAG-tagged N1-Src and CFP-tagged PD1 constructs were co-transfected into COS7 cells. N1-Src was transfected as COS7 cells do not endogenously express neuronal Src isoforms. CFP-tagged PD1 was used because the isolated peptide is not predicted to be membrane permeable. The CFP tag also allowed for the efficient immunoprecipitation of the peptide and its resolution on an SDS-PAGE gel.

In order to confirm an association between N1-Src and PD1, an immunoprecipitation experiment was carried out. This showed that N1-Src and PD1 are present within a complex (Figure 5.4.1) and co-immunoprecipitate when the tag on either protein is used to perform the immunoprecipitation. In contrast, the point mutant PD1-P5A co-immunopreciptates poorly with N1-Src. This shows that the interaction between PD1 and N1-Src is due to the specific sequence of PD1. N1-Src

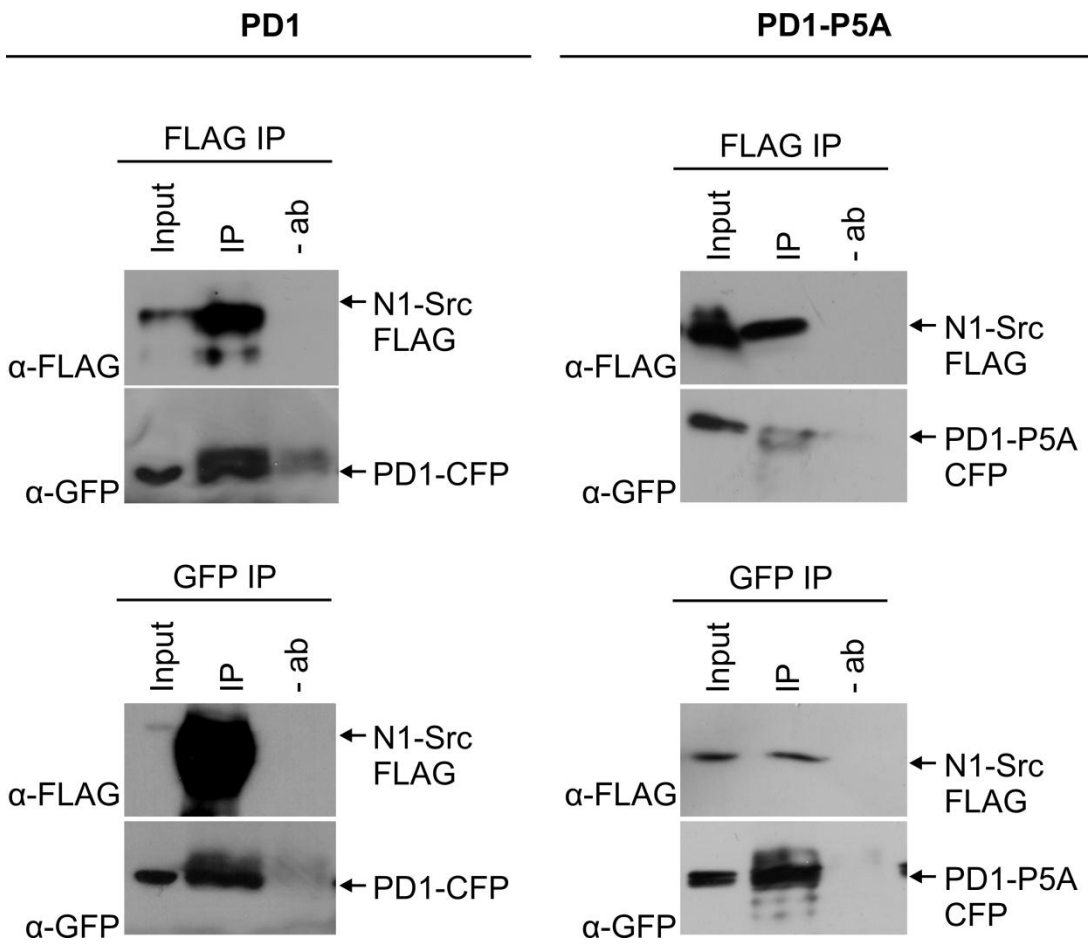

Figure 5.4.1 N1-Src and PD1 are contained within a complex

An immunoprecipitation experiment was carried out between FLAG-tagged N1-Src and CFP-tagged PD1 or the point mutant PD1-P5A. COS7 cells were co-transfected and lysed 48 hours following transfection. The immunoprecipitation experiment was set up using either α-FLAG or α-GFP (to detect CFP). The top panels show that CFP-PD1 co-immunoprecipiates with N1-Src following immunoprecipitation using the FLAG antibody whereas PD1-P5A co-immunoprecipitates much less efficiently. The lower panels show that N1-Src-FLAG co-immunoprecipitates with PD1 following immunoprecipitation with the GFP antibody but PD1-P5A does not. The input represents 1% of the cell lysate used in the immunoprecipitation.

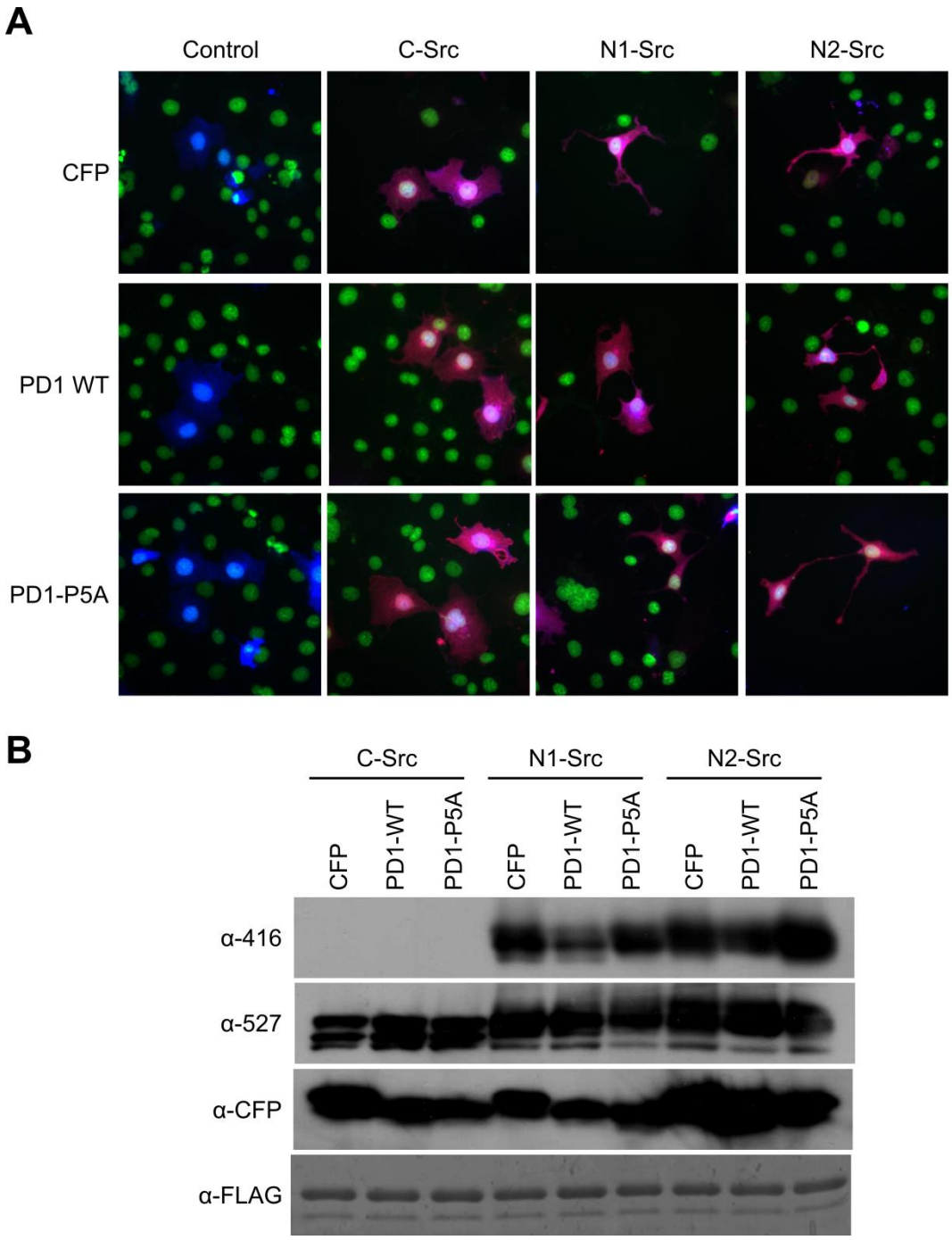

Figure 5.4.2 PD1 expression prevents induction of neuronal morphology

COS7 cells were co-transfected with C-, N1- or N2-Src and PD1-WT or PD1-P5A as indicated and either fixed or lysed 48 hours following transfection. Control cells were transfected with CFP (blue) to allow visualisation. Src constructs were FLAG tagged and visualised using an α-FLAG antibody (red). PD1 and PD1-P5A were CFP tagged and visualised using an α-GFP antibody (blue) A) Merged images are shown for co-transfected cells (purple). Nuclei are visualised using DAPI (green). Images are representative epifluorescent images from n=3 experiments. B) Analysis of Src activity was assessed using α-pY416 (active Src) and α-pY527 (inactive Src). Equal expression of shown by α-FLAG and α-GFP.

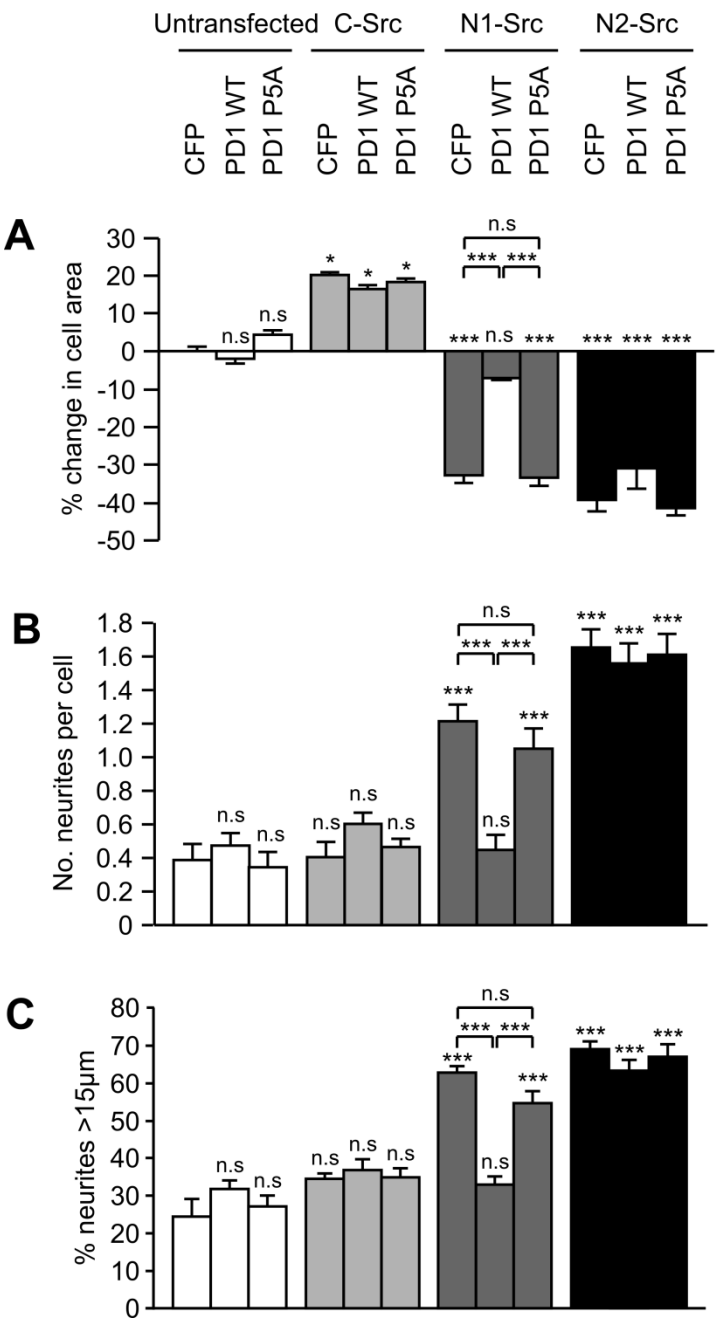

Figure 5.4.3. Morphology of N1-Src PD1 co-transfected cells is the same as control cells

COS7 cells were transfected 24 hours after plating and fixed for morphological analysis 48 hours following transfection. ImageJ analysis was used to assess A) cell body area B) neurite number and C) neurite length. n=3 experiments. 20 fields of view (approximately 50 cells) analysed for each condition per experiment. Error bars show SEM. Statistical analysis carried out using ANOVA and post hoc Tukey test. * p<0.05, ** p<0.01, ***p<0.001, all conditions compared to control cells (CFP transfected).

and PD1 are presumably linked by a direct interaction because PD1 was identified for its ability to bind to the N1-Src SH3 domain. To further confirm the suitability of PD1 as a N1-Src inhibitor, the morphology of the co-transfected COS7 cells was analysed. For this experiment COS7 cells were co-transfected with a FLAG tagged Src construct and CFP tagged PD1 or the point mutant PD1-P5A. Control cells were visualised by transfection with CFP and staining using an α-CFP antibody. The results of this experiment are shown in Figure 5.4.2 A. Control cells are transfected with CFP, shown in blue. The co-transfected cells are shown as a merged image of the FLAG-Src (red) and CFP-PD1/PD1-P5A (blue) staining and appear as purple. The nuclei are visualised using DAPI and are shown in green.

This experiment revealed that the neuronal morphology induced by N1-Src transfection into heterologous cells (described in Chapter 3) is prevented by the co-expression of CFP-PD1 (Figure 5.4.2 A). Importantly, the induction of neuronal morphology was not prevented by the point mutant PD1-P5A, indicating that the effect is specifically due to the PD1 sequence. In addition to the effect on cell morphology, biochemical analysis of the activation state of the kinases revealed that PD1 co-expression resulted in a specific decrease in N1-Src activity (characterised by a decrease in α-pY416 immunoreactivity), while C- and N2-Src activity remained unaffected (Figure 5.4.2 B).

The decrease in the α-pY416 signal is not total, indicating that some active N1-Src remains but it does not seem to be enough to induce the morphological changes previously seen. It is also possible that there is some cross-reactivity and the antibody also detects the corresponding residues of other SFK members. A third explanation for this result would be that the degree of co-transfection between N1-Src and CFP-PD1 was poor but this did not appear to be the case as when images were taken for morphological analysis, a high degree of co-transfection (>90%) was observed. The binding of PD1 to the N1-Src SH3 domain would be predicted to block the kinase-substrate interactions and so therefore be expected to perturb N1-Src function even if some pY416 immunoreactivity remained.

Quantification of the transfected cells (Figure 5.4.3) showed that, for all parameters measured, the morphology of cells co-transfected with N1-Src and PD1 is not statistically different to that of control cells. Importantly, control experiments also showed that the morphology of C-Src and N2-Src (Figure 5.4.2 and 5.4.3) transfected cells is not significantly affected by the presence of the PD1 peptide.

The PD1 peptide, identified through its ability to bind to the SH3 domain of N1-Src has been demonstrated to be a potent and specific inhibitor of N1-Src activity and function in cells. These experiments also confirm that the linkage of the PD1 peptide to CFP does not decrease its ability to interact with and inhibit N1-Src activity. CFP-PD1 transfection has no demonstrable off-target effects as the morphology of C- and N2-Src transfected cells was not affected by CFP-PD1 expression. CFP-PD1 also showed no toxic effects over the timecourse of the experiments carried out. Therefore, there is a high degree of confidence that CFP-PD1 transfection into neuronal cells will act specifically to inhibit N1-Src, allowing the investigation of endogenous N1-Src function.

5.5 N1-Src inhibition prevents axonal branching

The PD1 peptide sequence had been demonstrated to be a specific N1-Src inhibitor and to work effectively as a CFP-fusion in heterologous cells. The effects of N1-Src inhibition in CGNs were therefore investigated by CFP-PD1 transfection, followed by morphological analysis. Figure 5.5.1 shows that the morphology of PD1 transfected CGNs was perturbed, while neurons transfected with the control peptide PD1-P5A appeared morphologically normal. This means that the effects of PD1 transfection are sequence specific in CGNs as well as in heterologous cells. Unfortunately, due to the low transfection of neuronal cultures, biochemical analysis of the activation state of endogenous N1-Src in the presence of CFP-PD1 was not possible.

Quantification of the transfected CGNs (Figure 5.5.2) showed that N1-Src inhibition predominantly affected axonal growth, with dendrite number and length not being significantly different to control cells. This trend is the same as previously seen following N1-Src overexpression, but the effects of N1-Src inhibition are not identical to the effects of N1-Src overexpression. The average axonal length for PD1 transfected cells is reduced (Figure 5.5.2 A), as it was for N1-Src overexpressing cells, but the number of cells with an identifiable axon is reduced to approximately 60% (Figure 5.5.2 B). This is in contrast to N1-Src overexpression experiments that identified a tendency for axon duplication (Figure 5.3.2 B). The contrasting results of N1-Src overexpression and inhibition support the hypothesis that N1-Src plays a role in the initial processes of axon formation.

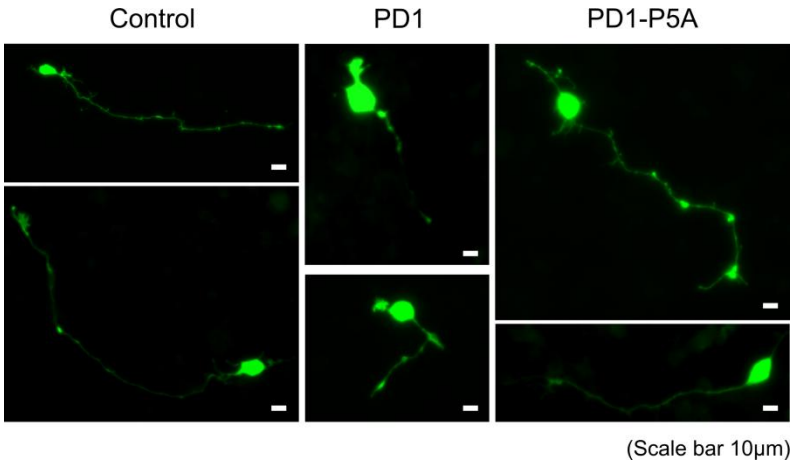

Figure 5.5.1 PD1 expression in CGNs causes aberrant neuronal morphology.

CGNs were transfected with PD1-WT or PD1-P5A 24 hours after plating and fixed for morphological analysis 24 hours after transfection. Control cells were transfected with CFP and all constructs were visualised using α-GFP. Images shown representative from n=3 experiments.

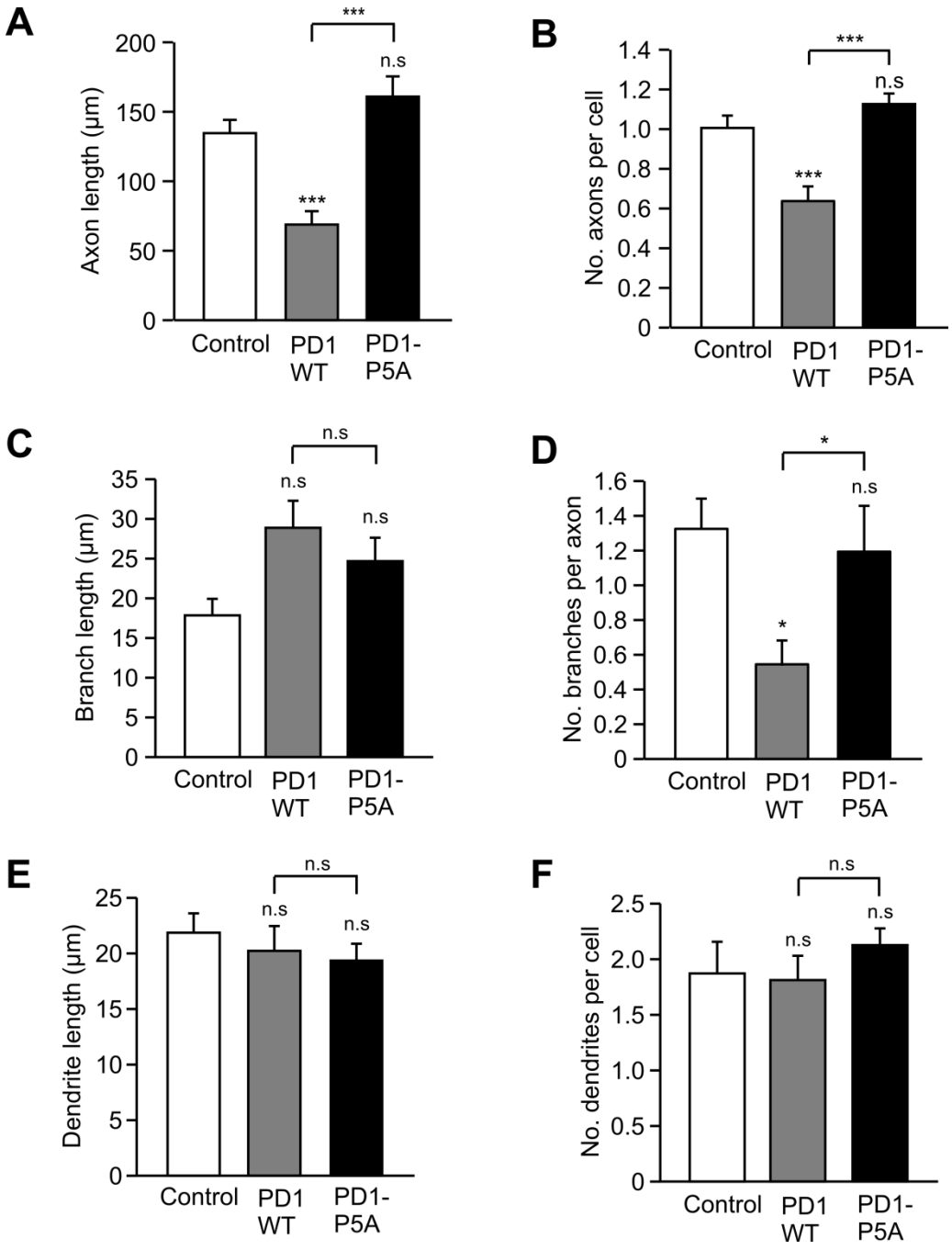

Figure 5.5.2 PD1 expression in CGNs results in inhibition of axon formation.

The morphology of CGNs transfected with CFP (control), CFP-PD1-WT and CFP-PD1-P5A was analysed 24 hours after transfection using the NeuronJ plugin for ImageJ. Parameters measured were A) axon length B) axon number C) branch length D) branch number E) dendrite length F) dendrite number. n=3 experiments, approximately 30 cells analysed per condition for each experiment. Error bars show SEM. Statistical analysis carried out by ANOVA and post hoc Tukey test * $p < 0.05$, ** $p < 0.01$, *** $p<0.001$, all conditions compared to control cells.

As previously seen in N1-Src overexpressing CGNs, axon branching is inhibited in PD1 transfected neurons (Figure 5.5.2 D), while the length of the branches that do form remain the same as control cells (Figure 5.5.2 C). This result implies that N1-Src plays a role in the formation of branches as well as axon formation. It is interesting that N1-Src overexpression and inhibition has the same effect on axonal branching in CGNs. If the normal signalling of N1-Src is required for efficient branching, perturbing N1-Src activity either by overexpression or inhibition would result in the disruption of the balance of the signalling pathways involved and the inhibition of branch formation. In contrast to this, N1-Src overexpression drove axon formation whereas N1-Src inhibition prevented axon formation. This may indicate that N1-Src acts in multiple distinct signalling pathways to regulate both axon formation and branch formation.

While CGNs are a good model system for investigating neuronal development, the cells are relatively small and their branching architecture is quite simple. As a potential role for N1-Src had been identified in the processes of axonal initiation and branching, further analysis was carried out in hippocampal neurons. The axons of hippocampal neurons are much longer and more highly branched than those of CGNs. The analysis of hippocampal neuron architecture can reveal more subtle effects such as specific effects on branch formation as opposed to elongation and effects on primary or secondary branching.

Cultured hippocampal neurons were transfected with PD1 and PD1-P5A 24 hours after plating and morphology analysed 24 hours following transfection. The traces of representative transfected cells produced using the NeuronJ plugin for ImageJ are shown in Figure 5.5.3. Quantification of these images (Figure 5.5.4) revealed that, while the total neurite length measured for PD1 transfected cells is reduced (Figure 5.5.4 A), the primary axon length remains unaffected (Figure 5.5.4 B). All transfected cells analysed had one axonal process, identified by morphology. This is in contrast to the findings in CGNs and implies that, in the hippocampal neuron system, N1-Src is not required for the initial processes of axon formation or growth.

The reduction in total neurite length indicated that PD1 transfected cells were not morphologically identical to control cells. Further analysis showed that this difference is due to a reduction in both the number (Figure 5.5.4 C) and length (Figure 5.5.4.D) of branches formed in PD1 transfected cells. This supports a role for

N1-Src in the molecular processes of axonal branching in hippocampal neurons. PD1-P5A transfected neurons did not show any morphological differences to control cells (Figure 5.5.4 A-D).

Detailed analysis of the cell morphology was carried out using Sholl analysis (Sholl, 1953). Sholl analysis measures the number of times concentric circles originating at the cell body are intersected by neurites and provides a measure of complexity of the cell. This analysis revealed that PD1 transfected neurons were indeed less complex than control cells (Figure 5.5.4 E). However, as in the CGNs, the differences were specific to axonal branching. The intersections that occur closest to the cell body (within ~50 μm) will primarily represent the dendrites and this peak was identical for PD1 and control transfected cells. There was a second peak approximately 180 μm from the cell body and this was also identical for PD1 and control transfected cells. This indicates that branching that occurs close to the cell body is able to occur in PD1 transfected cells as in control cells. The difference between PD1 and control cells becomes evident in the region over 200 μm from the cell body and represents distal axonal branches. Inhibition of N1-Src can therefore be said to specifically inhibit distal axonal branching in hippocampal neurons.

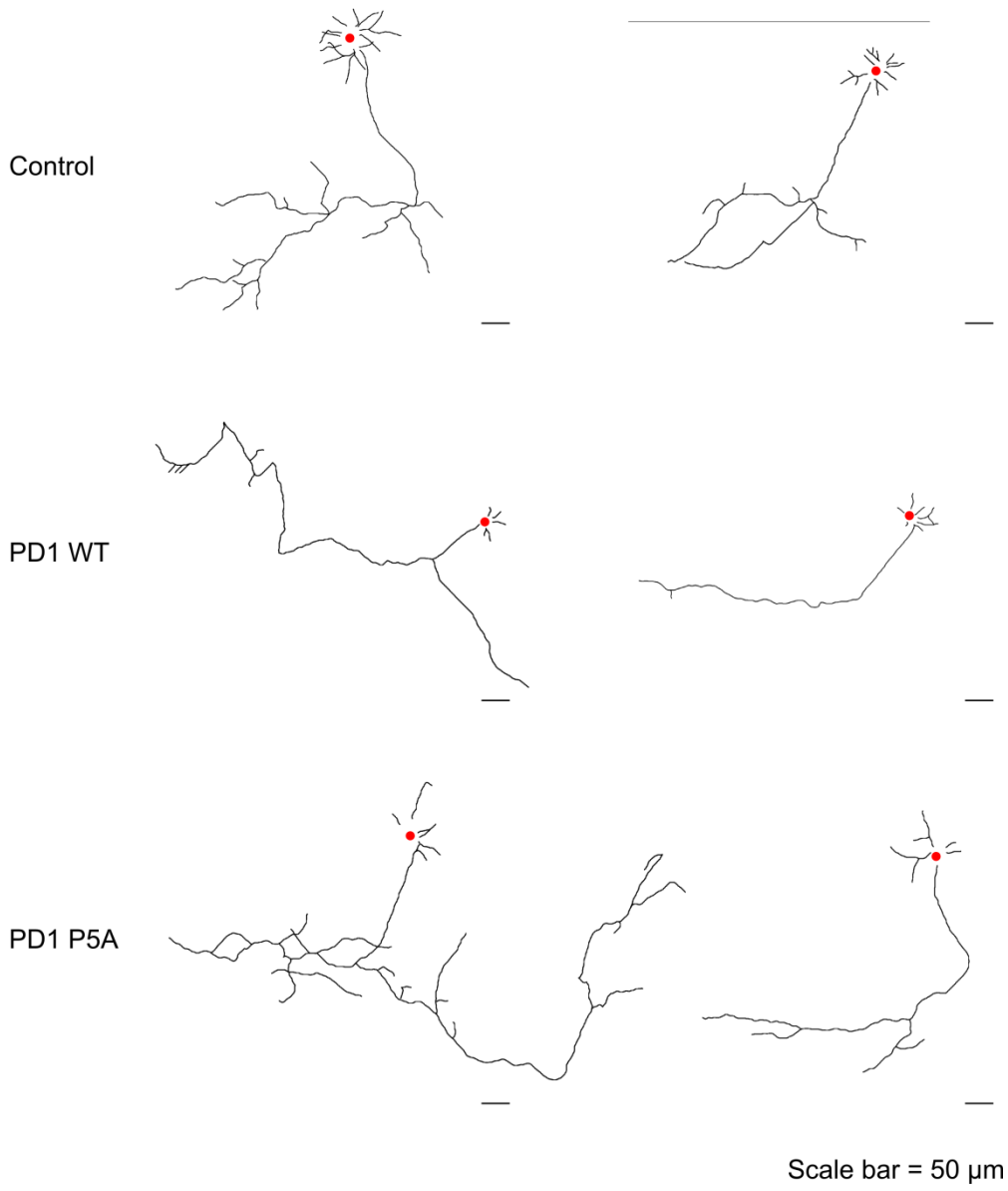

Figure 5.5.3. Expression of PD1 in hippocampal neurons causes aberrant neuronal morphology.

Hippocampal neurons were transfected with the indicated constructs 24 hours after plating and fixed for morphological analysis 24 hours after transfection. Control cells were transfected with CFP for visualisation. PD1 WT and PD1 P5A constructs were CFP tagged. All transfected cells were detected using an α-CFP antibody. Traces were created using the NeuronJ plugin for ImageJ are shown. Red dot represents the centre of the cell body used for Sholl analysis. Representative images shown from n=3 experiments with approximately 20 neurons analysed per condition.

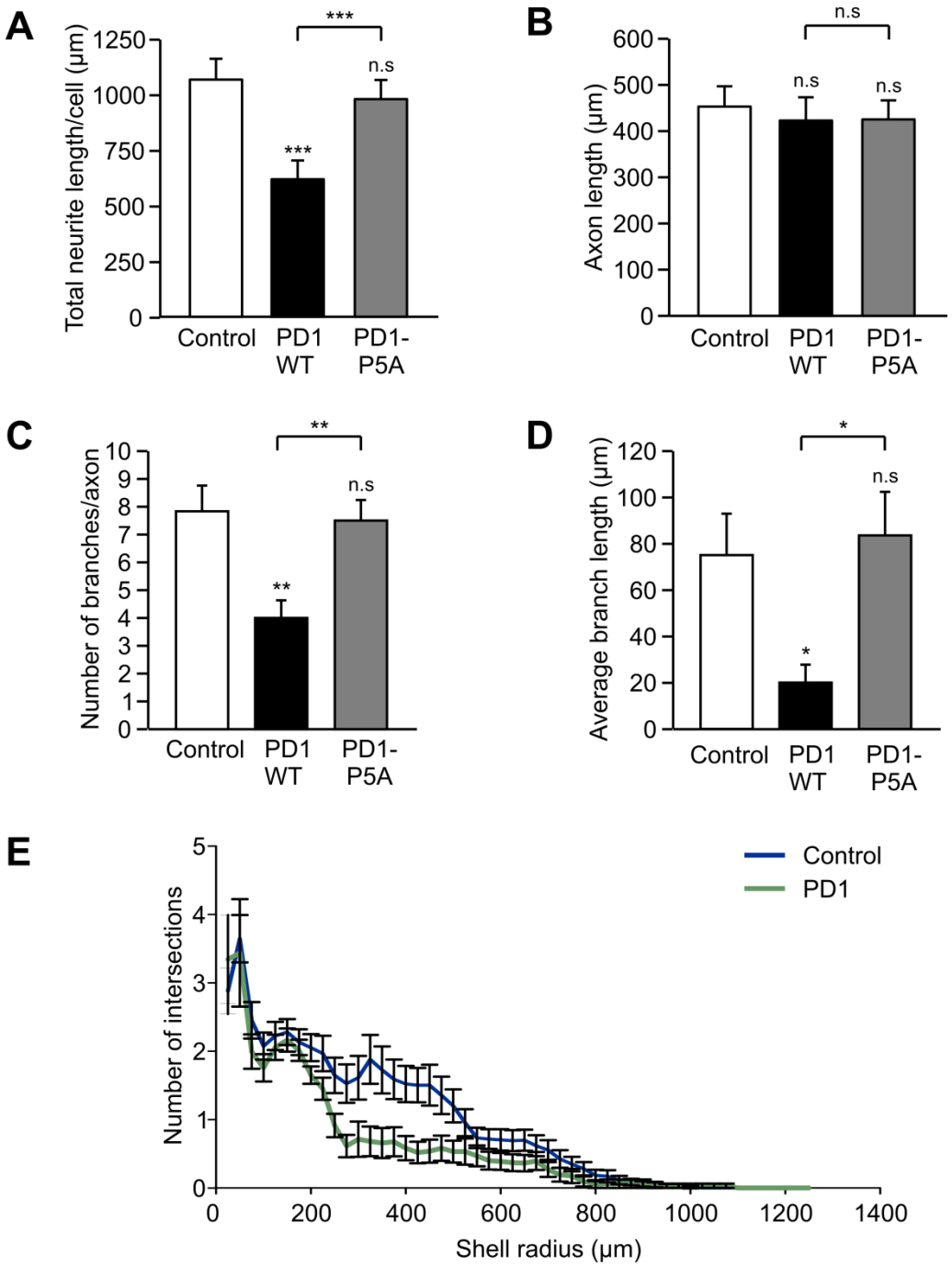

Figure 5.5.4 Expression of PD1 in hippocampal neurons inhibits axonal branching.

Hippocampal neuron morphology was analysed 24 hours after transfection using the Neuron J plugin for ImageJ. Transfected cells were visualised using α-CFP. Parameters measured were A) total neurite length, B) axon length, C) branch number and D) branch length. Sholl analysis (E) was carried out using an ImageJ plugin. Data shown calculated from n=3 with approximately 20 neurons analysed per condition per experiment. Error bars show SEM. Statistical analysis carried out by ANOVA followed by post hoc Tukey test * $p<0.05$, ** $p<0.01$, *** $p<0.001$.

5.6 N1-Src inhibition impairs L1-CAM dependent neurite outgrowth

The SFKs have previously been identified as playing a role in the processes of neuronal outgrowth. In particular, it is known that cerebellar neurons taken from $src^{-/-}$ mice are unable to extend neurites when the adhesion molecule L1-CAM is provided as a substrate (Ignelzi et al, 1994). $Src^{-/-}$ mice lack the Src gene and therefore C-, N1- and N2-Src protein. The isoform responsible for the impaired neurite outgrowth on L1-CAM has not been identified. Due to the link between N1-Src and neuronal outgrowth identified in this study, an experiment was designed to test whether N1-Src is the isoform responsible.

The assay used is depicted in Figure 5.6.1 A and involved plating a spot of recombinant L1-CAM (extracellular domain) mixed with the fluorescent dye FITC onto the centre of a 13 mm coverslip. The L1-CAM dried onto the coverslip and its location could subsequently be identified using the fluorescence of FITC (Figure 12 A). CGNs were then plated over the whole surface of the coverslip. The neurons were transfected 24 hours after plating and their morphology analysed 24 hours after transfection. The advantage of this technique was that the growth of transfected neurons on and off the L1-CAM substrate could be compared on the same coverslip.

Growth of CGNs on L1-CAM is known to result in an increase in axon length of WT neurons. An appropriate L1-CAM concentration was determined by assessing the extent of axon elongation of neurons grown on L1-CAM as compared to control cells. An L1-CAM concentration that induces a quantifiable increase in control neuron length was required in order to assess whether inhibition of N1-Src could prevent this and recapitulate the effect of $src^{-/-}$ neurons seen by Ignelzi et al (1994). A concentration of 25 µg/ml was chosen because this induces approximately a 50% increase in the axon length of control (CFP transfected) CGNs (Figure 5.6.1 B).

Transfection of PD1 resulted in the generation of axons shorter than those in the control neurons, as previously seen when grown on PDL (Figure 5.6.2). However, when PD1 transfected neurons were grown on the L1-CAM substrate they failed to extend any further (Figure 5.6.2). This implies that N1-Src is acting within the signalling pathway that would normally result in neurite elongation following interaction with extracellular L1-CAM. This result positively identifies N1-Src as the

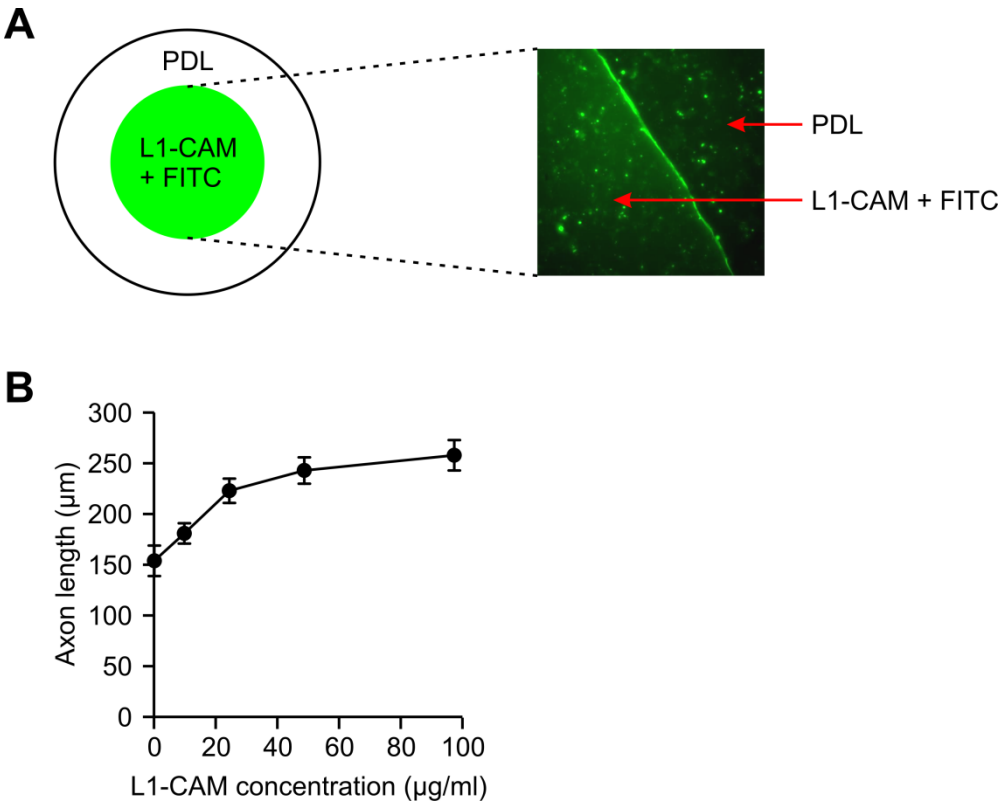

Figure 5.6.1 Basis of the L1-CAM neurite outgrowth assay.

A) Schematic representation of the L1-CAM neurite outgrowth assay. Coverslips were coated with PDL followed by a spot of recombinant L1-CAM mixed with FITC. FITC fluorescence used to identify the location of L1-CAM as shown in the image on the right. B) Determination of the L1-CAM substrate concentration for use in the assay. Individual neurons visualised by transfection with CFP and detection using α-GFP. Data shown n=1 experiment, 12-15 neurons measured per condition. Error bars show SEM.

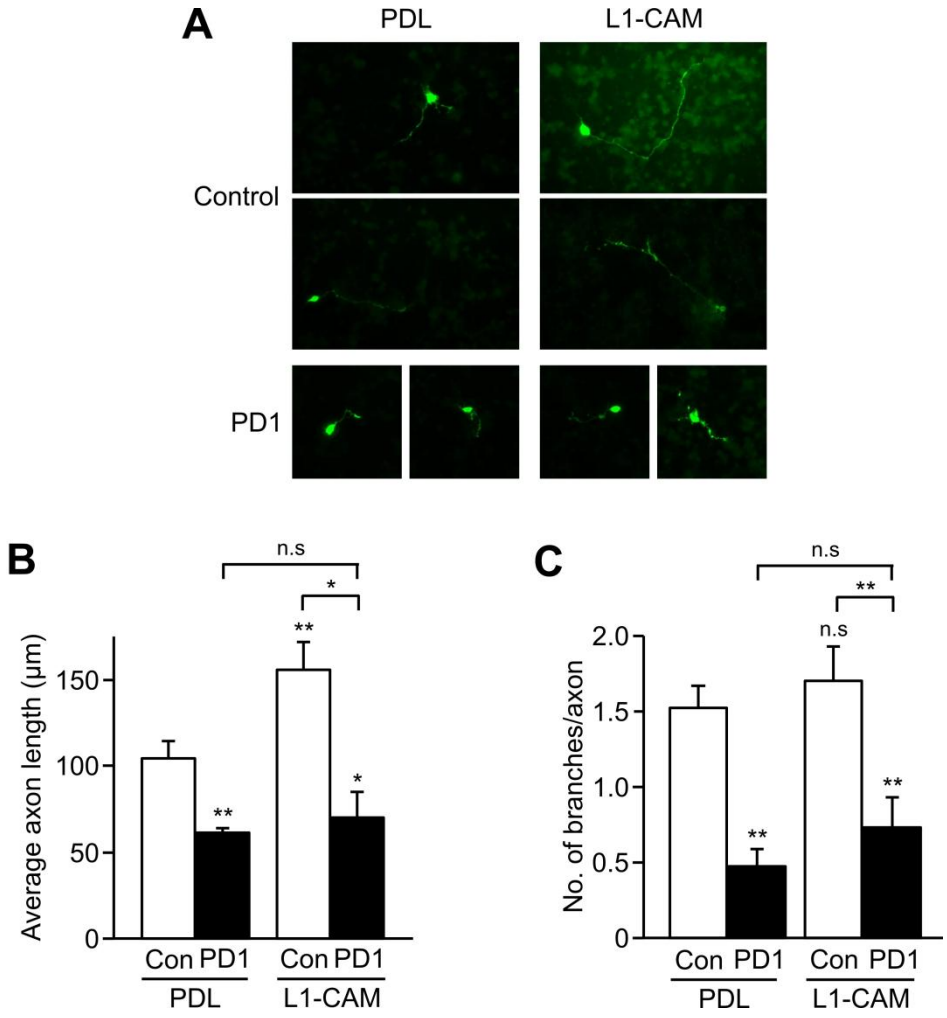

Figure 5.6.2 CGN axons cannot extend when grown on L1-CAM following N1-Src inhibition.

CGNs were transfected 24 hours following plating and fixed for morphological analysis 24 hours after transfection. Control cells were transfected with CFP and all transfected neurons visualised using α-CFP. FITC fluorescence was used to assess whether a transfected neuron was on the L1-CAM substrate A) Representative images of transfected neurons on and off the L1-CAM substrate. B) and C) Transfected neurons were quantified using the NeuronJ plugin for ImageJ. Data plotted from n=3 with 15-20 neurons analysed per condition per experiment. Error bars show SEM. Statistical analysis carried out by ANOVA and post hoc Tukey test.*p<0.05, **p<0.01

isoform responsible because the neurons in this study still have active C- and N2-Src.

5.7 Discussion

The work presented in this chapter comprises studies carried out in two distinct neuronal cell types that have demonstrated a role for N1-Src in axonal growth and branching through both overexpression and inhibition techniques. This role in neurite outgrowth has been demonstrated to be, at least partially, mediated through the L1-CAM signalling pathway. In order to study the functions of N1-Src in cells, a potent and specific inhibitor of N1-Src activity and function has been characterised.

5.7.1 Characterisation of a specific N1-Src inhibitor

The characterisation of the PD1 peptide sequence as a specific inhibitor of N1-Src provides a valuable tool for the study of the kinase both in the context of this study and for further study of N1-Src function. The PD1 peptide, expressed as a CFP fusion, has been demonstrated to be a potent and specific inhibitor of N1-Src in cell based assays and is able to functionally inhibit N1-Src while not affecting the activities of either C- or N2-Src.

The techniques chosen to confirm N1-Src inhibition by CFP-PD1 give a high degree of confidence in its effectiveness. In heterologous cells, co-transfection of CFP-PD1 along with N1-Src was demonstrated to prevent the induction of neuronal morphology caused by N1-Src alone. The expression level of N1-Src following overexpression in COS7 cells is likely to be higher than the endogenous levels found in CGNs or hippocampal neurons because expression in COS7 cells was driven by the strong promoter CMV. As CFP-PD1 is able to inhibit the actions of overexpressed N1-Src, it is thought that transfection of CFP-PD1 into neurons will also effectively inhibit endogenous N1-Src. The specific targeting and effective inhibition of N1-Src by CFP-PD1 is supported by the fact that the results of N1-Src overexpression and inhibition experiments are well correlated, with both indicating a role for N1-Src in axon formation and elongation.

No off-target effects of CFP-PD1 expression were observed in COS7 cells. The most likely off-target effects would be the simultaneous inhibition of C- or

N2-Src because of their high degree of structural similarity. This did not occur when C- and N2-Src were overexpressed in COS7 cells so it would be predicted that cross reactivity would also not occur in CGNs or hippocampal neurons where the expression levels of the kinases are lower. The low transfection efficiency of neurons meant that confirmation of N1-Src inhibition in neurons by biochemical analysis was not possible.

In order to confirm that PD1 transfection does not have off-target effects and that the changes in morphology observed were due to N1-Src inhibition it would be informative to also knockdown N1-Src expression using shRNA. shRNA constructs specific to each isoform of the kinase have been generated in the Evans lab and their effectiveness at inhibiting the expression of the specific Src isoforms in COS7 cells confirmed. However, the transfection of the shRNA plasmids into CGN cultures was toxic to the transfected neurons. This was true even of the control, empty shRNA plasmid. Further optimisation of the transfection protocol should allow for the comparative experiment between PD1 expression and N1-Src knockdown to be carried out.

It is likely that there will be a small amount of N1-Src remaining active within the PD1 transfected cells but as this is not sufficient to induce morphological change in COS7 cells then it is not considered to be a significant amount. Biochemical analysis of transfected COS7 cells showed that, while CFP-PD1 expression reduced the amount of α-pY416 (active Src) immunoreactivity, it did not eliminate it. In neurons, where N1-Src expression is lower, it may be that less active Src remains but this cannot currently be tested. As PD1 binding to the N1-Src SH3 domain will prevent correct substrate targeting then the function of N1-Src will be perturbed even if some pY416 immunoreactivity remains.

Further investigation into the interaction between PD1 and the N1-Src SH3 domain by biochemical techniques such as ITC will be able to accurately ascertain the affinity of the interaction. However, it is estimated to be in the low micromolar range as this is typical of SH3 domain interactions with their ligands. Preliminary results show that the phosphorylation of the YA-PD1 peptide occurs with a K_m of 6.5 μM (Chapter 4) and that the titration of the free PD1 peptide has an IC_{50} of approximately 20 μM (Chapter 4).

Peptide inhibitors of kinases have been the focus of a large amount of recent research due to the prevalence of unregulated kinase signalling in disease processes

including cancer. Inhibitory peptides may target a number of locations within the structure of a tyrosine kinase. Pseudosubstrates for the kinase domain have been developed but would not have been applicable in this study because the kinase domains are identical for the three isoforms of C-, N1- and N2-Src. As an alternative to the pseudosubstrate, there is also interest in the development of SH2 and SH3 domain inhibitors due to their ability to regulate signalling pathways in cancer and their potential as anti-tumour agents. However, therapeutic research into the development of SH2/SH3 domain inhibitors has stalled because SH3 domain binding peptides commonly interact with too low affinity for therapeutic use and SH2 domain binding peptides have limited cell permeability. The binding preferences of a large number of tyrosine kinase SH3 domains are known these have not commonly been shown to be able to inhibit kinase activity in cell based assays. Currently, the majority of high affinity SH3 domain peptide based inhibitors contain non-natural amino acids. These have been developed for C-Src, Lck, PI3K and Zap70 (Vidal et al, 2001; Yeh et al, 2001).

Within the context of this study, it is not necessary that the SH3 domain inhibition occurs with an affinity as low as that required for therapeutic applications. There are examples of SH3 domain inhibitory peptides that have been used to successfully inhibit kinase function in cell based assays. For instance, Kardinal et al (2000) developed a SH3 domain peptide inhibitor for the tyrosine kinase Abl that is capable of inhibiting proliferation. The data presented here show that PD1 is capable of functionally inhibiting N1-Src in cells but further research would be required before the isolated peptide could be used because, in its current state, it is not predicted to be membrane permeable.

5.7.2 A role for N1-Src in the regulation of axon and branch initiation

The PD1 peptide provided a useful tool to allow the comparison of overexpression and inhibition of N1-Src in cultured neurons. CGNs overexpressing N1-Src tended to have a duplicated axon whereas those expressing PD1 were more likely not to have an identifiable axon. Together, these results suggest that N1-Src may be playing a role in the processes driving the initial formation of axons.

Evidence for a role of N1-Src in the determination of neuronal morphology is strengthened by the use of the complementary techniques of N1-Src overexpression

and inhibition. Without the correlative result from N1-Src inhibition, the effect of N1-Src overexpression would need to be treated with caution because kinase overexpression can result in aberrant signalling and effects not mediated by the kinase under endogenous conditions. In this case both N1-Src overexpression and inhibition indicate a role for N1-Src in axon formation in CGNs. These opposing results strengthen the evidence that the manipulations are having physiologically relevant effects.

The axons that do form in N1-Src overexpressing or inhibited CGNs are shorter than control axons. As there seems to be a fundamental defect in the process of axon initiation caused by N1-Src manipulation it is difficult to assess whether the shorter axons occur as a consequence of the defect in axon initiation or are due to a secondary defect in axon elongation. The branching of CGN axons is reduced following N1-Src manipulation but this may also be a secondary effect of the reduced axon length. CGN axons bifurcate at the growth cone and the primary axon therefore needs to reach a certain length before branching occurs. It is likely that CGN axons do not reach this minimum length following N1-Src manipulation, making the assessment of the role of N1-Src in CGN axon branching difficult. Therefore, although the data presented here suggest a role for N1-Src in axon initiation, further investigation is required to ensure that this is not due to a branching defect as it is currently difficult to distinguish the effects of axon initiation and branching.

It is interesting that both N1-Src overexpression and inhibition resulted in a decrease in axon outgrowth in CGNs. In heterologous cells, N1-Src overexpression resulted in the induction of a neuronal morphology (Chapter 3). The opposing effects of N1-Src overexpression in these cell types may be due to the fact that N1-Src is not endogenously expressed in COS7 cells, they do not normally grow long processes and probably lack neuronal regulation mechanisms. N1-Src therefore provides the only mechanism for process growth and proceeds unhindered. In cultured neuronal cells there are multiple pathways that are involved in the initiation and elongation of neurites. Overexpression of N1-Src therefore perturbs the normal balance of signalling processes and results in aberrant neurite outgrowth.

In a previous study of N1-Src function, Kotani et al (2007) reported that overexpression of WT N1-Src had little effect on neuronal morphology. This contradicts the finding in this study that WT N1-Src induces large scale alterations in

neuronal morphology. Kotani et al (2007) expressed N1-Src under the control of the Purkinje cell specific L7 promoter. This promoter does not drive expression of transgenes as strongly as the CMV promoter used for overexpression in all mammalian cell types in this study. Therefore, the greater expression levels and high constitutive activity of N1-Src may explain the morphological effects of WT N1-Src overexpression observed in this study.

In this study N1-Src overexpression predominantly affected the axons, with dendrite morphology not significantly altered from control cells. This is again in contrast to the findings of Kotani et al (2007) and is probably explained by the fact that the Purkinje neurons studied by Kotani et al (2007) have complex dendritic and simple axonal architectures. N1-Src may function in the process of branching in both axons and dendrites but the dendritic arbours of the neurons used in this study were not complex enough to reveal any effect on dendrite branching. This could be confirmed by overexpressing and inhibiting N1-Src in cultured Purkinje neurons.

In contrast to the studies in CGNs, there was no observed decrease in axon initiation or elongation when N1-Src was inhibited in hippocampal neurons. One explanation for this is the fact that the hippocampal neurons taken from neonatal rodents are predominantly post-mitotic, polarised cells that are already committed to axon formation (Polleux & Snider, 2010). As CGN development continues postnatally, CGNs taken from P7 mice are still migrating and, at least a subpopulation, are not committed to a neuronal lineage (Okano-Uchida et al, 2004). It may be that N1-Src is involved in the molecular processes of axon generation in hippocampal neurons but that this is masked because they are already polarised prior to N1-Src inhibition. *In utero* or *ex utero* electroporation of CFP-PD1 into developing hippocampal neurons before their exit from the cell cycle would be required in order to elucidate whether N1-Src is required for axon generation in hippocampal neurons. These techniques have been developed and used successfully by Saito and Nakatsuji (2001) and Tabata and Nakajima (2001).

In hippocampal neurons, the primary axonal projections of PD1 transfected cells reached the same length as control cell axons. However, they were significantly less highly branched, implying that N1-Src activity is required for axonal branches to form. Sholl analysis revealed that the effect of N1-Src inhibition was specific to the distal axonal branches. The reason for this is unclear as there is no evidence that the mechanism of axonal branching is different in different parts of the axon. This result

may have been caused by the mixed population of neurons in the hippocampal culture. During the analysis it was noted that there was a large amount of variation in the size of the transfected cells. It may be that the branching phenotype is specific to the largest neurons, with the branches of shorter neurons appearing as proximal branches in the Sholl analysis. To test this, markers for specific neuronal types could be used and analysis of the morphology carried out. This would reveal whether the branching defect is specific to a certain neuronal cell type.

The differences in the results between CGNs and hippocampal neurons may be due to differences in the mechanisms by which axons form and branch in these two cell types. *In vivo,* CGNs put out an initial axon that then bifurcates at the growth cone, with the two portions growing in opposite directions to form parallel fibres. In culture the same process occurs, although the lack of guidance cues means that the parallel fibres do not necessarily grow in opposite directions (Tahirovic & Bradke, 2009). In contrast, hippocampal neurons undergo interstitial branching, with branches forming from the existing axonal shaft. These two methods of branching are considered mechanistically distinct and may involve different signalling pathways and molecules (Dent & Kalil, 2001). There are a limited number of studies that assess the role of a protein in both bifurcation and interstitial branching, but it is known that inhibition of the receptor guanylyl cyclase, Npr2, selectively prevents bifurcation in sensory axons while not affecting interstitial branching (Schmidt et al, 2007).

Taken together, the studies in CGNs and hippocampal neurons provide informative insights into the endogenous roles of N1-Src. In CGNs N1-Src played a role in the initial processes of axon formation, while in hippocampal neurons it was required for the initiation of interstitial branches. There are a number of parallels between the molecular basis of these processes, notably that both require the formation of a novel protrusion that extends away from the existing cell body or axonal shaft. Therefore, it would be predicted that N1-Src plays a role in the regulation of the cytoskeletal rearrangements that are required in order for these processes to occur.

All morphological analyses carried out in this study were based on neurite appearance rather than identification through the use of specific markers. Identification of axons and dendrites in this manner means that there is the potential for mis-identification. As the neuronal types used in this study are highly polarised

and their morphology is well characterised, we are confident that axon and dendrite assignments were made correctly. In CGNs, the stunted axons caused by N1-Src overexpression or inhibition were still longer than the dendrites and could therefore be identified. The dendrite morphology remained unchanged following N1-Src manipulation, which aided their identification. In hippocampal neurons each neuron had a single long process that was easily identified by morphology as an axon.

In order to further investigate the role of N1-Src in axon formation it would be beneficial to repeat the experiments presented here using axonal markers, such as neurofilament. Processes that morphologically appear to be axons and those that are expressing the relevant axonal markers could then be distinguished. Analysis of how far through the developmental programme the stunted axons are able to progress could then be carried out. This result would help to identify whether N1-Src is required for the initial steps of axonal formation or is more involved in the subsequent growth and elongation processes.

There is a growing body of work investigating the molecules that are able to promote the formation of an axon but there is considerable debate about factors that are true determinants of axon formation and those that only promote growth once axon formation has been initiated. It is agreed that axon formation is commonly, although not exclusively, promoted by exposure to extracellular factors including laminin, BDNF and TGFβ (Polleux & Snider, 2010) but the downstream signalling processes that respond to these extracellular factors are less clear.

Cheng and Poo (2012) defined several determinants of axon formation that adhere to the following criteria: i) a change in concentration or activity in the neurite immediately prior to the development of axonal characteristics; ii) removal or inhibition prevents axon formation and iii) upregulation of expression or activity triggers axonal differentiation. Under these criteria they identified Ras, cAMP/PKA, PI3K/PIP3 and pLKB1 as being determinants of axon formation. It is likely that multiple independent axon determinants exist in order to allow integration of diverse extracellular signals. If N1-Src is able to modulate axon generation, it would be predicted to be acting within one or more of these pathways.

There is limited evidence for the role of kinases signalling the formation of axons. The serine/threonine kinase PI3K is involved in the cytoskeletal rearrangement required to form branches in sensory neurons (Ketschek & Gallo, 2010). The actions of tyrosine kinases in the processes of axon guidance are quite

well known and are outlined in Chapter 1, but their specific roles in the processes governing axon initiation are less well understood. The lack of evidence for tyrosine kinase signalling in neurite initiation is probably because there is so much debate about the molecular basis of initiation as opposed to elongation. The data presented here provide strong evidence that N1-Src is required for axon initiation in CGNs and branch initiation in hippocampal neurons. This implies a role for N1-Src in the modulation of the cytoskeletal rearrangements that need to occur to generate a new neurite. Further elucidation of the substrates of N1-Src will allow determination of the signalling processes through which N1-Src mediates its effects. It is interesting that small GTPase signalling was identified as a determinant of axon initiation (Cheng & Poo, 2012) as targets in this signalling pathway were identified in Chapter 4 as possible substrates of N1-Src. This will be discussed further in Chapter 6.

5.7.3 A role for N1-Src in the L1-CAM signalling pathway

A significant finding of this study is the link between L1-CAM mediated signalling and N1-Src function. N1-Src function is required for neurite outgrowth on L1-CAM as CFP-PD1 expressing neurons still have functional C- and N2-Src. The additional involvement of C- and N2-Src in the L1-CAM signalling pathway cannot be ruled out, however, as individual inhibition of these isoforms has not been carried out in this study.

The neuronal adhesion molecule L1-CAM is strongly expressed on the surface of migrating neurons and developing axons from E9.5 onwards (Kallunki et al, 1997). There is also a large body of research that has identified L1-CAM as a potent regulator of axon growth when overexpressed, mutated or offered as a substrate for developing neurons (Cheng & Lemmon, 2004; Hoffman et al, 2008; Moon & Gomez, 2010; Schäfer et al, 2010). Notably, in relation to this study, the development and branching of dendrites appears to be unaffected by L1-CAM manipulation (Schäfer et al, 2010). Additionally, L1-CAM signalling does not seem to be required for initial axon formation (Cohen et al, 1998) and results predominantly in axon branching rather than growth (Cheng & Lemmon, 2004). These findings correlate well with the findings presented here that N1-Src function does not affect dendrite formation and is required for axonal branching. As L1-CAM signalling has not been demonstrated to be required for axon formation N1-Src may

also act in other signalling pathways that are able to regulate axon formation. This would be typical of tyrosine kinases as they commonly play diverse roles in multiple signalling pathways.

Previous studies have shown that branching of wild type CGNs is increased when grown on a substrate of L1-CAM (Cheng and Lemmon, 2004) but this study found no effect on axonal branching. Cheng and Lemmon (2004) used L1-CAM covalently linked to the coverslip; this eliminated the need for the use of FITC. It is possible that the FITC is having a slightly toxic effect on neuronal development and that this is preventing the axons from branching. The control neurons in this experiment are shorter than those in experiments where no FITC is used. Optimisation of the FITC concentration, or covalent L1-CAM linkage, may rectify this problem. It would also be interesting to repeat the L1-CAM outgrowth assay using cultured hippocampal neurons. The more highly branched architecture of hippocampal neurons may reveal an effect of N1-Src inhibition on axonal branching.

The mechanisms by which L1-CAM signalling affects axonal branching are not fully understood. Ankyrin and ERM proteins can both bind to the cytoplasmic tail of L1-CAM and provide links to the actin cytoskeleton. L1-CAM binding to ankyrin is controlled by MAPK pathway-dependent phosphorylation of the cytoplasmic tail (Whittard et al, 2006). Phosphorylation by an unknown kinase abolishes the L1-CAM-ankyrin interaction, releasing the ties between the actin cytoskeleton and L1-CAM and promoting axon growth. Transgenic mice that cannot be phosphorylated at the MAPK dependent residue (Y1229) have abnormal interstitial branching of their retinal axons (Buhusi et al, 2008) and impaired elongation and branching of interneurons (Guan & Maness, 2010). However, truncation of L1-CAM at residue 1180, prior to the ankyrin interaction site, has no effect on axon branching (Cheng et al, 2005). Therefore the role of the L1-CAM ankyrin interaction in axonal branching is not clear.

In contrast to the association with ankyrin, a direct role for the ERM protein ezrin has been identified in L1-CAM mediated axonal branching. Two binding sites for ezrin have been identified in the L1-CAM cytoplasmic tail and ezrin interaction via these sites has been demonstrated to be required for L1-CAM mediated axon branching (Cheng et al, 2005a; Sakurai et al, 2008).

The direct links between L1-CAM and the actin cytoskeleton are quite well understood. Further research into the regulatory mechanisms controlling these

interactions and the downstream effects of L1-CAM signalling is required to understand how L1-CAM is able to exert its influence on axonal branching. This study has shown that N1-Src is likely to be involved in one or more of these regulatory pathways but further work is required to ascertain how this regulation is achieved.

The Src kinases are known to regulate L1-CAM signalling, with C-Src directly phosphorylating the L1-CAM tail at Y1176, the site of interaction of L1-CAM with the adaptor AP2. This affects the trafficking of L1-CAM (Schaefer et al, 2002) and also presumably influences axon growth. Stimulation of L1-CAM also results in a transient upregulation of Src expression in embryonic carcinoma cells (Takayama et al, 1997), indicating that Src kinases are also acting downstream of L1-CAM mediated signalling.

Taken together, the data presented here provide strong evidence for a role of N1-Src in the regulation of axonal growth and branching. This signalling has been demonstrated to act through the L1-CAM pathway, a pathway that is known to influence axonal growth and branching. The immediate effectors of L1-CAM signalling are well characterised but much of the downstream signalling pathways remain to be elucidated. N1-Src has been identified as acting downstream of L1-CAM although the mechanism of this action remains unknown. It is also possible that the kinase is acting in other pathways, such as the small GTPase signalling pathways, to influence axon initiation. These concepts will be discussed further in Chapter 6.

6 Discussion

The work presented in this thesis represents the first comprehensive assessment of N-Src activity and function, with a focus on how these properties are affected by the presence of inserts within the n-Src loop. It was previously known that the N-Srcs do not bind to many of the binding partners identified for C-Src (Cicchetti et al, 1992; Foster-Barber & Bishop, 1998; Messina et al, 2003; Reynolds et al, 2008). The work presented here has shown that this difference is due to the altered substrate preferences of the N-Src SH3 domains (Chapter 3). Further investigation into the binding preferences of the N1-Src SH3 domain has shown that it binds to the consensus motif R/KxPxxTxR/K (Chapter 4). This requirement for a positively charged residue at both ends of a SH3 domain binding motif is novel and the possible structural basis of this binding is discussed in Chapter 4. Functional studies into the roles of N1-Src kinase have identified a role in cytoskeletal rearrangement both in heterologous cells (Chapter 3) and cultured neurons (Chapter 5) and a role for N1-Src in the L1-CAM signalling pathway. Finally, a number of putative N1-Src substrates capable of mediating the observed cytoskeletal rearrangements have been identified though bioinformatic techniques (Chapter 4) and these will form the basis of further study into N1-Src function. The development of a specific inhibitor of N1-Src will aid further investigations.

6.1 Insights into the effect of n-Src loop insertion on Src kinase activity and function

The most important point made by the combinatorial approaches used here to study N-Src function is that the SH3 domain mediates two separate functions. Firstly, it acts as a scaffold to anchor substrates to the kinase. This allows both substrate selection and phosphorylation. Secondly, the SH3 domain is able to control the activity of the kinase; constraining it by forming intramolecular associations and activating it by SH3 domain displacement. In the majority of kinases there is a direct link between these two processes with SH3 domain displacement directly resulting in a functional activation of the kinase. In the case of the N-Srcs there appears to be a distinction between the two processes. The SH3 domains of the N-Srcs are less able to form the SH3:linker intramolecular association that normally constrains kinase

activity and this results in a higher basal level of activity as measured by Y416 autophosphorylation. However, the SH3 domains of the N-Srcs are still required for the substrate selection of the kinases. It may be that, despite the high pY416 levels, the kinase domain is not able to associate with its substrates with a high enough affinity unless the SH3 domain is also able to bind.

Kinase activity is generally assessed by the measurement of pY416 but, for the N-Srcs, there does not seem to be a linear relationship between the level of Y416 phosphorylation and the level of substrate phosphorylation. It would be interesting to monitor the pY416 signal *in vitro* while the N1-Srcs are phosphorylating substrates but the low kinase concentrations (5 nM) used in the *in vitro* assay currently means that assessment of Y416 phosphorylation *in vitro* is not possible under the ideal conditions required for kinetic analysis.

The identification of N1-Src SH3 domain ligands capable of reducing the K_m of ideal substrate phosphorylation indicated that, despite their increased basal level of kinase activity, the signalling of the N-Srcs in cells is regulated and substrate selection is dependent on appropriate SH3 domain interactions. In support of this, in the absence of an SH3 binding interaction, phosphorylation by the three Src splice variants occurs with the same kinetics. In addition, overexpression of the N-Srcs in heterologous cells does not reveal a large number of phosphoproteins in cell lysates. The identification of SHP-1 as a potential N1-Src substrate (Chapter 4) could explain the lack of N1-Src substrates. Activation of SHP-1 by N1-Src phosphorylation would result in the rapid dephosphorylation of N1-Src substrates. If SHP-1 could be confirmed as a N1-Src substrate then it would provide evidence that N1-Src signals transiently in highly dynamic signalling processes, such as the modulation of cytoskeletal rearrangement.

To test whether SHP-1 is an N1-Src substrate, SHP-1 could be expressed as a recombinant fusion protein for use in an *in vitro* kinase assay. If this confirms SHP-1 as a N1-Src substrate then the sequence identified as being the SH3 domain binding region could be cloned into the GST-peptide kinase assay system to assess its ability to enhance phosphorylation of the ideal substrate. The site of phosphorylation in SHP-1 could be confirmed by MS. To assess whether SHP-1 acts to dephosphorylate N1-Src substrates *in vivo*, SHP-1 expression could be knocked down using shRNA either in COS7 cells overexpressing N1-Src or in cultured neurons. Analysis of the cell lysates by Western blotting with an α-phosphotyrosine would reveal whether this

results in more observable N1-Src substrates. More detailed analysis using phosphoproteomic MS analysis may then be able to reveal novel N1-Src substrates. SHP-1 acts to dephosphorylate substrates phosphorylated by other kinases, including C-Src (Frank et al, 2004). Therefore, potential substrates identified by SHP-1 inhibition must be verified by further *in vitro* kinase assays.

6.2 A suggested role for N1-Src in cytoskeletal modelling required for neurite outgrowth

A role for N1-Src in the modulation of the cytoskeleton was first implied through investigations in heterologous cells. More specifically, studies in cultured neurons sugguested a role in the regulation of the molecular processes underlying axon initiation (in CGNs) and axon branching (in hippocampal neurons). The role in axon elongation is less clear but as the molecular processes involved in initiation and elongation use broadly the same pathways then it is conceivable that N1-Src acts in both. In contrast to the work of Kotani et al (2007), no role for N1-Src was identified in dendritic growth.

The dynamic regulation of the actin and microtubule cytoskeleton is critical in the polarisation of neurons required for axon formation. Localised actin-depolymerisation in the neurite of a morphologically unpolarised hippocampal neuron is sufficient to induce that neurite to become an axon (Bradke & Dotti, 1999). In contrast, the stabilisation of the microtubule cytoskeleton promotes axon growth (Witte et al, 2008). There are many signalling pathways that are able to regulate the neuronal cytoskeleton; see Polleux and Snider (2010) for a comprehensive review. Modulation of the cytoskeleton for neurite outgrowth is activated downstream of the interaction of guidance cues with their plasma membrane receptors and as such can occur through multiple pathways. The signalling cascades downstream of guidance cue signalling are now quite well established but how they interact with each other to create a co-ordinated response is still unclear.

The suggested role of N1-Src in cytoskeletal rearrangement could occur at any point during the pathway. It is not practical to assess the potential of substrates of N1-Src at all points in these pathways as the number of candidates is vast. A recent review by Dent et al (2011) produced a comprehensive list of actin and microtubule associated proteins that have been identified as playing a role in

neuronal development. Cross referencing this list with that of N1-Src SH3 domain interacting proteins (Appendix 1) revealed N1-Src SH3 domain binding sites in 7 proteins known to both interact with cytoskeletal elements and play a role in axon growth. The proteins identified in this way were Ankyrin B, dynein, MAP1B, Neuron Navigator, Profilin, Tau and β-Spectrin. These putative N1-Src substrates are all known to play roles in neuronal development and therefore represent attractive targets to explain the role of N1-Src in cytoskeletal rearrangement. The potential functional implications of Ankyrin B phosphorylation by N1-Src are discussed in section 6.2.2.

In addition to direct phosphorylation of cytoskeletal interacting proteins, N1-Src signalling could also act further upstream. Two signalling pathways were highlighted in the course of this study; small GTPase signalling and the L1-CAM pathway.

6.2.1 Small GTPase signalling

The morphology of N-Src transfected cells (Chapter 3) resembled that of RhoA overexpressing cells (Kolyada et al, 2003), indicating that N1-Src may act to regulate small GTPase signalling. In addition, the small GTPases were identified as potential N1-Src targets in the bioinformatic analysis carried out in Chapter 4.

The small GTPase families play well defined roles in the regulation of neurite initiation, elongation, guidance and branching. The major role of Rho GTPases is to control the dynamic rearrangement of the actin and microtubule cytoskeleton. Ras GTPases are activated by signalling from many guidance cues and feed into many signalling transduction pathways including PI3K, ERK and MAPK all known to play roles in the regulation of axonogenesis (Huber et al, 2003).

A recent review by Hall and Lalli (2010) outlined the roles of Rho and Ras GTPases in axon initiation and growth. Cross referencing the proteins in the major signalling pathways identified in axon initiation and elongation with putative N1-Src SH3 domain ligands (Appendix 1) showed that N1-Src regulation of small GTPases is largely restricted to regulation of the factors that activate and inhibit the GTPases, GEFs and GAPs respectively (Table 6.2.1.1). GAPs and GEFs for Rho, Rac and Arf, but not Ras or Cdc42, were identified. Domain analysis using UniProt data showed that the majority of these sites are not contained within any defined domain. This

implies that N1-Src phosphorylation may regulate the formation of protein-protein interactions rather than GAP and GEF activity.

Table 6.2.1.1 GAP and GEF proteins that contain the N1-Src SH3 domain consensus motif.

ID	Protein name	Res.	Sequence
GTPase activating proteins (GAPs)			
ARFG2	ADP-ribosylation factor GTPase activating protein 2	218	SIIGKKKPAAAKKGL
ARFG3	ADP-ribosylation factor GTPase activating protein 3	218	SSIIKKKPNQAKKGL
ASAP3	ArfGAP with SH3 domain, ankyrin repeat and PH domain 3	825	SEEGLREPPGTSRPS
IQGA3	IQ motif containing GTPase activating protein 3	635	TERVLRNPAVALRGV
RGAP1	Rac GTPase activating protein 1	432	FLRNLKEPLLTFRLN
RHG01	Rho GTPase activating protein 1	224	LKSTQKSPATAPKPM
RHG05	Rho GTPase activating protein 5	1361	LLEAAKIPDKTERLH
RHG18	Rho GTPase activating protein 18	367	TEGLLRIPGAAIRIK
RICH2	Rho-type GTPase-activating protein RICH2	485	DPADRRQPEQARRPL
SRGP2	SLIT-ROBO Rho GTPase activating protein 3	2870	PPKKNRSPADAGRGV
GTPase exchange factors (GEFs)			
ARHG1	Rho guanine nucleotide exchange factor (GEF) 1	765	TAGSLKVPAPASRPK
ARHGH	Rho guanine nucleotide exchange factor (GEF) 17	439	ARTRAKGPGGTSRAL
BIG1	ADP-ribosylation factor guanine nucleotide-exchange factor 1(brefeldin A-inhibited)	791	FLEGFRLPGEAQKID
BIG2	ADP-ribosylation factor guanine nucleotide-exchange factor 2 (brefeldin A-inhibited)	736	FLEGFRLPGEAQKID
KALRN	Kalirin, RhoGEF kinase	2948	NGSYSKIPLDTSRLA
OBSCN	Obscurin, cytoskeletal calmodulin and titin-interacting RhoGEF	709	GLTANKPPAAAAREV
PREX2	Phosphatidylinositol-3,4,5-trisphosphate-dependent Rac exchange factor 2	1587	LGVRDRTPQSAPRLY

If these interactions could be confirmed then N1-Src signalling may represent a general mechanism of regulation of the activity of small GTPases. Cloning of the individual GAPs and GEFs for bacterial expression followed by *in vitro* kinase assays would confirm whether they are able to be phosphorylated by N1-Src. If N1-Src is able to act at multiple points in the pathway and regulate both GEFs and

GAPs, then perturbing its signalling either by overexpression or inhibition would result in aberrant neurite outgrowth, as has been observed in this study. It is interesting that GAPs and GEFs for both Rho and Rac were identified. Classically, Rac signalling is associated with increased neurite outgrowth, while Rho signalling is associated with inhibition of neurite outgrowth (Hall & Lalli, 2010).

There is a precedent for the regulation of both GAPs and GEFs by tyrosine phosphorylation. The best characterised of these is probably the phosphorylation of the Ras GAP p120. p120RasGAP was found to be phosphorylated *in vivo* following activation of receptor and non-receptor tyrosine kinases, including SFK family members (Ellis et al, 1990; Molloy et al, 1989). It was subsequently shown that both Src and Lck phosphorylate p120RasGAP but that the phosphorylation events have different effects on GAP activity (Giglione et al, 2001). Phosphorylation by Src results in an increase in GAP activity, whereas phosphorylation by Lck does not affect GAP activity but may play a role in mediating interactions with SH2 domain containing proteins (Amrein et al, 1992; Pleiman et al, 1993). p190RhoGAP has also been identified as a major Src substrate in the brain (Brouns et al, 2001) and Src phosphorylation of p190RhoGAP is required for EGF-induced actin disassembly (Haskell et al, 2001). Therefore, phosphorylation of GAPs and GEFs can modulate both activity and interacting proteins and have functional effects on cytoskeletal rearrangement.

6.2.2 L1-CAM signalling

Signalling in the L1-CAM pathway has also been identified as a role of N1-Src during this study. A literature search was carried out to identify the downstream effectors of homophilic or heterophilic L1-CAM interaction at the plasma membrane. The proteins identified as containing the N1-Src SH3 domain motif (Appendix 1) are shown in Table 6.2.2.1. A direct phosphorylation of L1-CAM by N1-Src was also identified in the bioinformatic study but this seems unlikely as both the SH3 domain binding site and predicted phosphorylation site are extracellular.

The proteins identified as potential N1-Src substrates in the L1-CAM pathway act at multiple points. Neurocan and EphB2 are plasma membrane receptors that L1-CAM is able to heterodimerise with to induce intracellular signalling

Table 6.2.2.1 Proteins in the L1-CAM signalling pathway that contain the N1-Src SH3 domain consensus motif.

ID	Protein Name	Res.	Sequence
ANK2	Ankyrin 2 (Ankyrin B), neuronal	2002	RVEKEKGPILTQREA
NUMB	Numb	437	QAGHRRTPSEADRWL
EPHB2	EPH receptor B2	993	GQPLARRPRATGRTK
NCAN	Neurocan	317	ADGSVRYPIQTPRRR
RAF1	Raf1	311	GWSQPKTPVPAQRER
SOS1	Sos1	1306	SQHIPKLPPKTYKRE

(Buhusi et al, 2008; Oleszewski et al, 2000). Ankyrin B provides a direct link between the C-terminal tail of L1-CAM and the actin cytoskeleton (Whittard et al, 2006). Sos and Raf act in the MAPK signalling pathway known to be activated by the interaction of many guidance cues with their receptors (Hall & Lalli, 2010). Numb interacts with L1-CAM in axonal growth cones and is implicated in the regulation of L1-CAM endocytosis (Nishimura et al, 2003b).

Of the potential N1-Src substrates identified in this study, further characterisation of the potential N1-Src interaction with ankyrin B would be particularly interesting. N1-Src signalling has been shown experimentally to be involved in the L1-CAM signalling pathway (Chapter 5). Ankyrin B interacts directly with both L1-CAM and the actin cytoskeleton and is able to modulate cytoskeletal rearrangement. Ankyrin B binds a well-defined motif on L1-CAM (FIGQY) and phosphorylation of the tyrosine residue in this sequence prevents the L1-CAM-ankyrin B interaction (Whittard et al, 2006). The interaction with ankyrin B is of interest as mutations in L1-CAM that prevent its interaction with ankyrin are implicated in the rare X-linked neurological disorder CRASH (Needham et al, 2001).

The association of ankyrin with the cytoskeleton is known to be regulated by the serine/threonine kinase CKII (casein kinase II). Phosphorylation of ankyrin by CKII reduces its ability to bind spectrin (Ghosh & Cox, 2001; Ghosh et al, 2002). Tyrosine phosphorylation of ankyrin has never been investigated in detail. Interestingly, a study in MDCK cells found that ankyrin G was tyrosine phosphorylated following ATP depletion (Woroniecki et al, 2003). The site of this phosphorylation and its functional effect was not further investigated. Therefore, there is some preliminary evidence for stimulus dependent ankyrin tyrosine phosphorylation.

To pursue Ankyrin B as a potential N1-Src substrate it would be informative to carry out an *in vitro* kinase assay. As ankyrin B is such a large protein, bacterial expression of the entire protein may not be applicable. The region of Ankyrin B predicted to be Src phosphorylation could be expressed in isolation or alternatively, ankyrin B could be immunoprecipitated from CGN lysates using ankyrin specific antibodies (Ghosh et al, 2002). The immunoprecipitate could then be heat treated to eliminate the activity of co-precipitating kinases and an *in vitro* kinase assay using N1-Src carried out. If ankyrin B was shown to be an N1-Src substrate, mutation of the predicted SH3 domain binding site would reveal whether this site is required for the phosphorylation. The functional effects of the N1-Src – ankyrin B interaction can be assessed using the L1-CAM outgrowth assay that has been developed (Chapter 5).

6.3 Development of a specific inhibitor of N1-Src

Due to the highly related nature of the SFKs, and in particular C-Src and its splice variants, there were no commercially available tools capable of functionally inhibiting only one splice variant specifically. During the course of this study it has been discovered that the PD1 sequence, identified for its ability to bind to the N1-Src SH3 domain, also acts as a potent inhibitor of N1-Src function both in heterologous cells and in neurons. It therefore represents a valuable tool for the further study of N1-Src function. The PD1 sequence could either be transfected into developing neuronal cultures using lentiviral transfection or by fusion to an arginine/lysine rich sequence such as Penetratin, which has been shown to induce membrane permeability in cultured neurons (Ahmed et al, 2006). These approaches would vastly increase the efficiency of transfection and allow assessment of N1-Src function through biochemical techniques such as Western blotting and high throughput techniques such as MS.

Currently, the affinity of PD1 for the N1-Src SH3 domain is unknown but is likely to be in the region of 1 – 10 μM as this is typical for SH3 domain peptide ligands (Pawson, 2004). Also, its presence enhances phosphorylation of the ideal substrate to approximately the same extent as the C-Src SH3 domain binding Class I and Class II sequences known to interact with low micromolar affinity. Planned ITC experiments will elucidate the precise affinity of the interaction.

The establishment of the structure of the N1-Src SH3 domain in complex with PD1 will reveal the nature of the binding interaction and could potentially inform further mutations that could be made to improve the affinity of the interaction in a rational design approach. Another approach to produce an inhibitor of a higher affinity would be to carry out a screen for small molecule inhibitors that are able to disrupt the interaction of PD1 with the N1-Src SH3 domain. A similar approach has been used by Atatreh et al (2008) to design small molecule inhibitors that prevent the interaction of C-Src with its SH3 domain ligands.

Further functional characterisation of N-Src function would be benefitted by the creation of knockout mice. The genetics of creating a N1-Src knockout mouse is complex but its production could potentially be very informative. The C-Src knockout mouse that exists is also null for N1- and N2-Src due to the nature of the cloning carried out but surprisingly shows no gross morphological or developmental abnormalities. There are examples of strain background having a large effect on Src knockout phenotype (Grant et al, 1992; Yagi et al, 1993) and this could possibly explain the lack of phenotype observed. It would therefore be informative to create individual splice variant knockouts of C-, N1- and N2-Src in the same strain background so that they could be directly compared. As the N2-Src n-Src loop insert is created from both the N1- and N2- exons spliced together then preventing the expression of the N1- exon would also prevent the expression of N2-Src. Therefore, the simplest way to create a N1-Src null mouse would be to constitutively express an N1-Src siRNA. This technique was developed by Tiscornia et al (2003) and has been used successfully to assess neuronal morphology following specific protein knockdown (Grasselli et al, 2011).

The development of a high affinity, membrane permeable inhibitor of the N1-Src SH3 domain, either a modified peptide or a small molecule, would open up the potential for N1-Src inhibition to be used as a therapeutic. Evidence from hippocampal neurons presented in this study shows that N1-Src inhibition acts to prevent the formation of axonal branches. There are a number of disease states that are associated with an overgrowth of axonal branching but therapeutic use of N1-Src inhibition would probably only be applicable if excess branching occurs following normal initial neuronal development.

Temporal lobe epilepsy (TLE) is one of the most common types of epilepsy in adult humans and is characterised clinically by the progressive development of

spontaneous and recurrent epileptic seizures. Abnormal morphology of hippocampal neurons is commonly observed in TLE patients (Masukawa et al, 1995) and animal models (Wenzel et al, 2000), characterised by the addition of axonal branches in a process known as sprouting. Importantly, the neurons are morphologically normal before the onset of seizures. Therefore, N1-Src inhibition may be able to prevent the production of these abnormal branches without affecting the morphology of already established neurons. For the study of TLE in mouse models, normal initial neuronal development is required. This could be achieved either by chemical inhibition of N1-Src in adult mice or use of an inducible siRNA (Seibler et al, 2007) that would prevent N1-Src protein expression only when desired.

6.4 Future directions

The N-Srcs have been demonstrated in this study to have a striking effect on cell morphology. The insights into N1-Src SH3 domain binding specificity and the identification of some potential binding partners should allow further elucidation into the molecular basis of N-Src mediated cytoskeletal rearrangement.

The majority of the potential N1-Src substrates identified in this study are involved in the processes of initial neurite outgrowth and elongation. N-Src expression is known to remain high throughout development and in the adult mouse (Wiestler & Walter, 1988) and would therefore be predicted to also play roles in the adult brain. Recent work by Groveman et al (2011) has investigated a potential role for N1-Src in the modulation of the NMDA-R. Phosphorylation of the NMDA-R subunits by C-Src and Fyn is already known (Groveman et al, 2012; Salter & Kalia, 2004). Groveman et al (2011) identified an *in vitro* interaction between the N1-Src and the NMDA-R NR2A subunit. However, mutation of the kinase, SH2 and SH3 domains of N1-Src had little effect on the interaction. They therefore conclude that the binding is not mediated by a classical interaction with any of these domains. However, the SH3 domain mutation they made is a point mutation known to prevent C-Src interaction with classical PxxP motif containing proteins. The N1-Src SH3 domain is now known to bind an atypical motif and such motifs do not necessarily form the same contacts with the SH3 domain as classical ligands, further mutational analysis of the SH3 domain should be carried out before its role in the interaction is ruled out.

I would predict that as a result of further work into the N-Src kinases they will come to be considered functionally distinct from C-Src. Currently, there are many neuronal roles assigned to C-Src that may in the future be reassigned to the N-Srcs. In particular, the role of C-Src in cytoskeletal rearrangement and neurite outgrowth is not supported by the overexpression experiments both in heterologous cells (Chapter 3) and in cultured neurons (Chapter 5) presented in this study. Furthermore, bioinformatic prediction of N1-Src and C-Src SH3 domain substrates showed very little overlap (Chapter 4). There is a high degree of functional redundancy between SFK family members and it may be that roles assigned to C-Src through cell based Src inhibition studies are those that cannot be compensated for by Fyn or Yes and are actually carried out by the N-Srcs, that will also be inhibited by C-Src kinase domain inhibitors. This issue will only be resolved when C-Src kinase domain inhibitors are replaced by splice-variant specific inhibitors targeted to the SH3 domain, such as PD1.

Appendix 1

ID	Protein	Res.	Sequence
ABCAC	ATP-binding cassette, sub-family A (ABC1), member 12	1448	LYGSIKVPHWTKKQL
ABCAD	ATP-binding cassette, sub-family A (ABC1), member 13	3945	LFASIKAPQWTKKEL
ABCC8	ATP-binding cassette, sub-family C (CFTR/MRP), member 8	1413	GIDIAKLPLHTLRSR
ABCC9	ATP-binding cassette, sub-family C (CFTR/MRP), member 9	1381	GIDISKLPLHTLRSR
ACACB	acetyl-Coenzyme A carboxylase beta	82	EPASHKGPKDAGRRR
ACOT1	acyl-CoA thioesterase 1	138	PPGVRREPVRAGRVR
ACOX3	acyl-Coenzyme A oxidase 3, pristanoyl	20	LPEFPRGPLDAYRAR
ACPH	N-acylaminoacyl-peptide hydrolase	197	EIARLKKPDQAIKGD
ADA19	ADAM metallopeptidase domain 19 (meltrin beta)	28	RPRAAREPGWTSKGS
ADA1D	adrenergic, alpha-1D-, receptor	490	PVASRRKPPSAFREW
ADAM9	ADAM metallopeptidase domain 9 (meltrin gamma)	8	MGSGARFPSGTLRVR
ADNP	activity-dependent neuroprotector homeobox	779	TKYFNKQPYPTRREI
ADO	aldehyde oxidase 1	1118	EPIISKNPKGTWKDW
AEBP1	AE binding protein 1	125	KKGKEKPPKATKKPK
AFF3	AF4/FMR2 family, member 3	200	LQTQERPPAMAAKHS
AFF4	AF4/FMR2 family, member 4	567	RTVGKKQPKKAEKAA
AHNK	AHNAK nucleoprotein	532	VQGDVKGPQVALKGS
AHNK2	AHNAK nucleoprotein 2	1092	EMPSFKMPKVALKGP
AIFM3	apoptosis-inducing factor, mitochondrion-associated, 3	320	NVFTIRTPEDANRVV
AKAP2	A kinase (PRKA) anchor protein 2; paralemmin 2; PALM2-AKAP2 readthrough transcript	235	SQAVKKNPGIAAKWW
ALEX	GNAS complex locus	12	PVDPQRSPDPTFRSS
AMD	peptidylglycine alpha-amidating monooxygenase	64	FALDIRMPGVTPKQS
AMPH	Amphiphysin	294	APARPRSPSQTRKGP
AMZ1	archaelysin family metallopeptidase 1	89	ASLQHRKPRLARKHI
ANDR	androgen receptor	15	GRVYPRPPSKTYRGA
ANK2	ankyrin 2, neuronal	2002	RVEKEKGPILTQREA
ANR11	ankyrin repeat domain 11; hypothetical protein LOC100128265	1239	KKNKQKLPEKAEKKH
ANT3	serpin peptidase inhibitor, clade C (antithrombin), member 1	73	EGSEQKIPEATNRRV
AP2C	transcription factor AP-2 gamma (activating enhancer binding protein 2 gamma)	372	LLSQDRTPHGTSRLA
APOL3	apolipoprotein L, 3	308	ARARARLPVTTWRIS
ARFG2	ADP-ribosylation factor GTPase activating protein 2	218	SIIGKKKPAAAKKGL
ARFG3	ADP-ribosylation factor GTPase activating protein 3	218	SSIIKKKPNQAKKGL
ARHG1	Rho guanine nucleotide exchange factor (GEF) 1	765	TAGSLKVPAPASRPK
ARHG8	neuroepithelial cell transforming 1	132	LRGDHRSPASAQKFS
ARHGH	Rho guanine nucleotide exchange factor (GEF) 17	439	ARTRAKGPGGTSRAL
ARP5	ARP5 actin-related protein 5 homolog (yeast)	580	IYVPIRLPKQASRSS
ASAP3	ArfGAP with SH3 domain, ankyrin repeat and PH domain 3	825	SEEGLREPPGTSRPS
ASH1L	ash1 (absent, small, or homeotic)-like (Drosophila)	119	IKTTIKHPRKALKSG
ASNS	asparagine synthetase	506	ANAAQKFPFNTPKTK
ATP4B	ATPase, H+/K+ exchanging, beta polypeptide	80	YQDQLRSPGVTLRPD
ATP9A	ATPase, class II, type 9A	442	DPPAQKGPTLTTKVR
ATR	ataxia telangiectasia and Rad3 related; similar to ataxia telangiectasia and Rad3 related protein	1899	NSYRAKEPILALRRA
ATS16	ADAM metallopeptidase with thrombospondin type 1 motif, 16	46	SPSVPRPPPPAERPG
ATS17	ADAM metallopeptidase with thrombospondin type 1 motif, 17	68	RRRRPRTPPAAPRAR
ATS18	ADAM metallopeptidase with thrombospondin type 1 motif, 18	852	ILMQGKNPGIAWKYA
B2L10	BCL2-like 10 (apoptosis facilitator)	102	GTLLERGPLVTARWK
B3A2	solute carrier family 4, anion exchanger, member 2 (erythrocyte membrane protein band 3-like 1)	306	SGREGREPGPTPRAR
BAI3	brain-specific angiogenesis inhibitor 3	1469	NPAPNKNPWDTFKNP
BAIP3	BAI1-associated protein 3	193	RVRKAKAPTYALKVS
BANK1	B-cell scaffold protein with ankyrin repeats 1	612	SFIINRPPAPTPRPT

BAZ1B	bromodomain adjacent to zinc finger domain, 1B	902	KLVMRRTPIGTDRNH
BIG1	ADP-ribosylation factor guanine nucleotide-exchange factor 1(brefeldin A-inhibited)	791	FLEGFRLPGEAQKID
BIG2	ADP-ribosylation factor guanine nucleotide-exchange factor 2 (brefeldin A-inhibited)	736	FLEGFRLPGEAQKID
BIRC6	baculoviral IAP repeat-containing 6	2520	GIPVAKPPANTEKNG
BIRC8	baculoviral IAP repeat-containing 8	99	VQTTKKTPSLTKRIS
BMP2K	BMP2 inducible kinase	265	LKPTYRTPERARRHK
BMP8A	bone morphogenetic protein 8a	63	GRPRPRAPPAASRLP
BMP8B	bone morphogenetic protein 8b	63	GRPRPRAPPAASRLP
BMS1	BMS1 homolog, ribosome assembly protein (yeast) pseudogene; BMS1 homolog, ribosome assembly protein (yeast)	1078	IKKALRAPEGAFRAS
BPTF	bromodomain PHD finger transcription factor	573	DIDNVKSPEETEKDK
BRD2	bromodomain containing 2	102	FAWPFRQPVDAVKLG
BSN	bassoon (presynaptic cytomatrix protein)	2245	LTSLTRVPMIAPRVP
C1QR1	CD93 molecule	506	TASPTRGPEGTPKAT
CA2D4	calcium channel, voltage-dependent, alpha 2/delta subunit 4	73	AWGQAKIPLETVKLW
CABL2	Cdk5 and Abl enzyme substrate 2	32	PTSAARAPPQALRRR
CAD22	cadherin-like 22	421	GVVTARDPDAANRPV
CAF1B	chromatin assembly factor 1, subunit B (p60)	395	PVLNMRTPDTAKKTK
CAN12	calpain 12	482	LLRADRSPLSARRDV
CBPC2	ATP/GTP binding protein-like 2	175	SILSTKRPLQAPRWP
CBX7	chromobox homolog 7	142	LPFPLRKPRKAHKYL
CC14A	CDC14 cell division cycle 14 homolog A (S. cerevisiae)	111	VIYLKKTPEEAYRAL
CC14B	CDC14 cell division cycle 14 homolog B (S. cerevisiae)	148	VIYLGRTPEEAYRIL
CD28	CD28 molecule	199	MNMTPRRPGPTRKHY
CDA7L	cell division cycle associated 7-like	247	DFFPVRTPTSASRKK
CE290	centrosomal protein 290kDa	1719	KEANSRAPTTTMRNL
CELF3	trinucleotide repeat containing 4	458	LKVQLKRPKDANRPY
CELF4	bruno-like 4, RNA binding protein (Drosophila)	479	LKVQLKRPKDANRPY
CELF6	bruno-like 6, RNA binding protein (Drosophila)	474	LKVQLKRPKDANRPY
CENPE	centromere protein E, 312kDa	2369	TTQDNKNPHVTSRAT
CHD3	chromodomain helicase DNA binding protein 3	1890	PATLSRIPPIAARLQ
CHD4	chromodomain helicase DNA binding protein 4	1879	PATIARIPPVAVRLQ
CHD5	chromodomain helicase DNA binding protein 5	1886	PSMLSRIPPVAARLQ
CHD6	chromodomain helicase DNA binding protein 6	342	MEELEKDPRIAQKIK
CKAP5	cytoskeleton associated protein 5	222	EEEWVKLPTSAPRPT
CKLF6	CKLF-like MARVEL transmembrane domain containing 6	168	QESQLRKPENTTRAE
CLC1A	C-type lectin domain family 1, member A	43	RRTEHRAPSSTWRPV
CLIC5	chloride intracellular channel 5	261	TLTPEKYPKLAAKHR
CLK3	CDC-like kinase 3	248	RRSRERGPYRTRKHA
CLSPN	claspin homolog (Xenopus laevis)	1238	SKSLLRNPFEAIRPG
CO5A1	collagen, type V, alpha 1	71	TRRSSKGPDVAYRVT
CO5A3	collagen, type V, alpha 3	296	EPTPSKKPVEAAKET
COPE	coatomer protein complex, subunit epsilon	267	SQHLGKPPEVTNRYL
CORA1	collagen, type XXVII, alpha 1	385	SIVPIKSPHPTQKTA
CP250	centrosomal protein 250kDa	1716	RAEEGKGPSKAQRGS
CP2B6	cytochrome P450, family 2, subfamily B, polypeptide 6	318	FLLMLKYPHVAERVY
CP2C8	cytochrome P450, family 2, subfamily C, polypeptide 8	317	LLLLLKHPEVTAKVQ
CP2C9	cytochrome P450, family 2, subfamily C, polypeptide 9	317	LLLLLKHPEVTAKVQ
CP2CI	cytochrome P450, family 2, subfamily C, polypeptide 18	317	LLLLLKYPEVTAKVQ
CP2CJ	cytochrome P450, family 2, subfamily C, polypeptide 19	317	LLLLLKHPEVTAKVQ
CP2U1	cytochrome P450, family 2, subfamily U, polypeptide 1	392	VIGANRAPSLTDKAQ
CPEB2	cytoplasmic polyadenylation element binding protein 2	481	TDPELKYPKGAGRVA
CPLX1	complexin 1	28	GGDEEKDPDAAKKEE
CPT1A	carnitine palmitoyltransferase 1A (liver)	175	QTSLPRLPVPAVKDT
CPXM2	carboxypeptidase X (M14 family), member 2	79	RPQEPRPPKRATKPK
CROCC	ciliary rootlet coiled-coil, rootletin	1450	GLGLGRAPSPAPRPV

CRX	cone-rod homeobox	272	DSLEFKDPTGTWKFT
CSKI1	CASK interacting protein 1	923	RSHSVRAPAGADKNV
CSPG2	Versican	209	ADQTVRYPIRAPRVG
CTBL1	catenin, beta like 1	254	KRLKAKMPFDANKLY
CTR9	Ctr9, Paf1/RNA polymerase II complex component, homolog (S. cerevisiae)	986	PKPKKRRPPKAEKKK
CTRO	citron (rho-interacting, serine/threonine kinase 21)	2007	DSSRGRLPAGAVRTP
CY24A	cytochrome b-245, alpha polypeptide	160	SNPPPRPPAEARKKP
CYH1	cytohesin 1	155	FLWSFRLPGEAQKID
CYH2	cytohesin 2	154	FLWSFRLPGEAQKID
CYH3	cytohesin 3	159	FLWSFRLPGEAQKID
CYH4	cytohesin 4	154	FLWSFRLPGEAQKID
CYLD	cylindromatosis (turban tumor syndrome)	151	GVVRFRGPLLAERTV
DGC14	DiGeorge syndrome critical region gene 14	340	TPYVDRTPGPAFKIL
DGKZ	diacylglycerol kinase, zeta 104kDa	440	WILRARRPQNTLKAS
DHB1	hydroxysteroid (17-beta) dehydrogenase 1	248	FLTALRAPKPTLRYF
DHCR7	7-dehydrocholesterol reductase	90	SDIWAKTPPITRKAA
DIAP1	diaphanous homolog 1 (Drosophila)	1218	AFRRKRGPRQANRKA
DIDO1	death inducer-obliterator 1	68	LRRSGRQPKRTERVE
DJC30	DnaJ (Hsp40) homolog, subfamily C, member 30	141	DPGSPRTPPPTSRTH
DLG5	discs, large homolog 5 (Drosophila)	1195	VSSILRNPIYTVRSH
DNLI1	ligase I, DNA, ATP-dependent	221	EEEQTKPPRRAPKTL
DNM1L	dynamin 1-like	274	AFLQKKYPSLANRNG
DNMBP	dynamin binding protein	1459	VARDVKQPTATPRSY
DNS2B	deoxyribonuclease II beta	329	IGDLNRSPHQAFRSG
DOK5	docking protein 5	72	VKNVARLPKSTKKHA
DPOD3	polymerase (DNA-directed), delta 3, accessory subunit	428	TSSVHRPPAMTVKKE
DPOG1	polymerase (DNA directed), gamma	507	AKKVKKEPATASKLP
DPOLZ	REV3-like, catalytic subunit of DNA polymerase zeta (yeast)	2494	HVLHQRFPLFTFRVL
DPP9	dipeptidyl-peptidase 9	313	PRTGSKNPKIALKLA
DSG2	desmoglein 2	538	FSVIDKPPGMAEKWK
DTX4	deltex homolog 4 (Drosophila)	425	APSGYKGPQPTVKPD
DUS2	dual specificity phosphatase 2	21	LGTLLRDPREAERTL
DUX1	double homeobox, 1	119	AFEKDRFPGIAAREE
DUX4	double homeobox, 4-like; similar to double homeobox 4c; similar to double homeobox, 4; double homeobox, 4	119	AFEKDRFPGIAAREE
DUX5	double homeobox, 5	146	AFEKDRFPGIAAREE
DVL2	dishevelled, dsh homolog 2 (Drosophila)	32	TPYLVKIPVPAERIT
DVL3	dishevelled, dsh homolog 3 (Drosophila)	22	TPYLVKLPLPAERVT
DYH2	dynein, axonemal, heavy chain 2	1804	RGGSPKGPAGTGKTE
DYHC1	dynein, cytoplasmic 1, heavy chain 1	4239	NISPDKIPWSALKTL
E2AK1	eukaryotic translation initiation factor 2-alpha kinase 1	485	NRNGKRTPTHTSRVG
EA3L1	transcription elongation factor B polypeptide 3C-like; transcription elongation factor B polypeptide 3C-like 2; transcription elongation factor B polypeptide 3C (elongin A3)	459	FNSVAKTPYDASRRQ
ECT2	epithelial cell transforming sequence 2 oncogene	816	AFSFSKTPKRALRRA
ELOA2	transcription elongation factor B polypeptide 3B (elongin A2)	651	FKSVAKTPYDTSRRQ
EMAL4	echinoderm microtubule associated protein like 4	175	PTKSIKRPSPAEKSH
EME1	essential meiotic endonuclease 1 homolog 1 (S. pombe)	30	FAFLKKEPSSTKRRQ
ENL	myeloid/lymphoid or mixed-lineage leukemia (trithorax homolog, Drosophila); translocated to, 1	254	PKAAFKEPKMALKET
ENPP1	ectonucleotide pyrophosphatase/phosphodiesterase 1	598	LNHLLKNPVYTPKHP
ENPP7	ectonucleotide pyrophosphatase/phosphodiesterase 7	266	LVEFHKFPNFTFRDI
EPHB2	EPH receptor B2	993	GQPLARRPRATGRTK
ERCC1	excision repair cross-complementing rodent repair deficiency, complementation group 1 (includes overlapping antisense sequence)	178	VQVDVKDPQQALKEL
ERI1	exoribonuclease 1	251	QLSRLKYPPFAKKWI

F10A1	similar to heat shock 70kD protein binding protein; suppression of tumorigenicity 13 (colon carcinoma) (Hsp70 interacting protein)	43	ESMGGKVPPATQKAK
FAKD1	FAST kinase domains 1	771	EIVGSRLPPGAERIA
FBX21	F-box protein 21	240	RGINSRHPSLAFKAG
FBX46	F-box protein 46	28	SQNQPRPPSAALKPS
FBXL6	F-box and leucine-rich repeat protein 6	75	PRQPPRGPSAAAKPK
FBXW8	F-box and WD repeat domain containing 8	29	APKKRRRPEAAERRA
FGD2	FYVE, RhoGEF and PH domain containing 2	25	VFENSRTPEAAPRGQ
FGD5	FYVE, RhoGEF and PH domain containing 5	881	EDSASRDPSVTHKVE
FGD6	FYVE, RhoGEF and PH domain containing 6	10	SAAEIKKPPVAPKPK
FGF5	fibroblast growth factor 5	248	SPIKPKIPLSAPRKN
FHOD3	formin homology 2 domain containing 3	29	FPEPSRPPLFTFRED
FIG4	FIG4 homolog (S. cerevisiae)	718	SPFTVRKPDETGKSV
FMNL	formin-like 1	1032	EPPAPKSPPKARRPQ
FND3B	fibronectin type III domain containing 3B	1011	FISIYRGPSHTYKVQ
FOXS1	forkhead box S1	126	GAEGTRGPAKARRGP
FREM3	FRAS1 related extracellular matrix 3	8	MAGASRHPTGTPRQL
GAK	cyclin G associated kinase	1167	EERGVRAPSFAQKPK
GCN1L	GCN1 general control of amino-acid synthesis 1-like 1 (yeast)	891	FLPLLKSPLAAPRIK
GCYB1	guanylate cyclase 1, soluble, beta 3	411	NELRHKRPVPAKRYD
GDF5	growth differentiation factor 5	246	LRILRKKPSDTAKPA
GMDS	GDP-mannose 4,6-dehydratase	178	TPFYPRSPYGAAKLY
GP157	G protein-coupled receptor 157	307	SQPPTKSPAGTPKAP
GP179	G protein-coupled receptor 179	1728	AEAIRKSPNDTGKVS
GPI8	phosphatidylinositol glycan anchor biosynthesis, class K	140	RVLTGRIPPSTPRSK
GPNMB	glycoprotein (transmembrane) nmb	18	LLLAARLPLDAAKRF
GPR56	G protein-coupled receptor 56	193	LSQFLKHPQKASRRP
H11	histone cluster 1, H1a	159	TPKKAKKPAATRKSS
H12	histone cluster 1, H1c	131	GGTKPKKPVGAAKKP
H13	histone cluster 1, H1d	132	GAAKPRKPAGAAKKP
H14	histone cluster 1, H1e	131	GAAKAKKPAGAAKKP
H15	histone cluster 1, H1b	156	KKAVKKTPKKAKKPA
H1BP3	HCLS1 binding protein 3	216	SKKPKKHPKVAVKAK
HAUS5	HAUS augmin-like complex, subunit 5	27	VPVAARAPESTLRRL
HELC1	activating signal cointegrator 1 complex subunit 3	1103	IALRKRWPTMTYRLL
HERC1	hect (homologous to the E6-AP (UBE3A) carboxyl terminus) domain and RCC1 (CHC1)-like domain (RLD) 1	4508	NASDLRLPSRAWKVK
HIP1R	huntingtin interacting protein 1 related	1038	RSVTTKKPPLAQKPS
HPLN2	hyaluronan and proteoglycan link protein 2	207	LEGSVRYPVLTARAP
HPS1	Hermansky-Pudlak syndrome 1	137	IRKELRPPDLAQRVQ
HRH1	histamine receptor H1	276	GGSVLKSPSQTPKEM
HSPB8	heat shock 22kDa protein 8	73	SGMVPRGPTATARFG
HUWE1	HECT, UBA and WWE domain containing 1	3128	LSAILRSPAFTSRLS
HXA1	homeobox A1	214	WMKVKRNPPKTGKVG
HXB1	homeobox B1	189	WMKVKRNPPKTAKVS
HXK2	hexokinase 2 pseudogene; hexokinase 2	421	GSVYKKHPHFAKRLH
HYOU1	hypoxia up-regulated 1	93	ASMAIKNPKATLRYF
IDHC	isocitrate dehydrogenase 1 (NADP+), soluble	95	LKQMWKSPNGTIRNI
IDHP	isocitrate dehydrogenase 2 (NADP+), mitochondrial	135	LKKMWKSPNGTIRNI
IF140	intraflagellar transport 140 homolog (Chlamydomonas)	734	YYYFTRKPEEADRED
IFT88	intraflagellar transport 88 homolog (Chlamydomonas)	59	RTSHGRRPPITAKIS
IKBE	nuclear factor of kappa light polypeptide gene enhancer in B-cells inhibitor, epsilon	101	PHSPGRRPPRAGRPL
IL16	interleukin 16 (lymphocyte chemoattractant factor)	783	SSTVKKGPPVAPKPA
IL31R	interleukin 31 receptor A	312	YNSLGKSPVATLRIP
ILDR2	immunoglobulin-like domain containing receptor 2	518	PRLVSRTPGTAPKYD
ILK	integrin-linked kinase	365	PEALQKKPEDTNRRS

IMB1	karyopherin (importin) beta 1	307	AAEQGRPPEHTSKFY
INP5E	inositol polyphosphate-5-phosphatase, 72 kDa	552	STSKQRTPSYTDRVL
INP5K	inositol polyphosphate-5-phosphatase K	265	TSEKKRKPAWTDRIL
INT1	integrator complex subunit 1	12	KPTTVRRPSAAAKPS
INVS	Inversin	688	QGTNSRRPNETAREH
IPO9	importin 9	99	QSEKFRPPETTERAK
IQGA3	IQ motif containing GTPase activating protein 3	635	TERVLRNPAVALRGV
IRX3	iroquois homeobox 3	406	SAPLGKFPAWTNRPF
ISL1	ISL LIM homeobox 1	178	RPHVHKQPEKTTRVR
ITAD	integrin, alpha D	696	IFNETKNPTLTRRKT
ITCH	itchy E3 ubiquitin protein ligase homolog (mouse)	260	PPRPSRPPPPTPRRP
JAG1	jagged 1 (Alagille syndrome)	1194	NGTPTKHPNWTNKQD
JHD2C	jumonji domain containing 1C	1646	EQRTKRQPKPTYKKK
K1C12	keratin 12	464	STDSSKDPTKTRKIK
KALRN	kalirin, RhoGEF kinase	2948	NGSYSKIPLDTSRLA
KCD19	potassium channel tetramerisation domain containing 19	712	AGAKDKGPEPTFKPY
KCNQ2	potassium voltage-gated channel, KQT-like subfamily, member 2	597	DQIVGRGPAITDKDR
KCNT1	potassium channel, subfamily T, member 1	944	LAFMFRLPFAAGRVF
KCNT2	potassium channel, subfamily T, member 2	881	LAFMFRLPFAAGRVF
KDM3B	lysine (K)-specific demethylase 3B	790	FSQENKAPFEAVKRF
KDM6A	lysine (K)-specific demethylase 6A	1078	SGRRRKGPFKTIKFG
KI18B	kinesin family member 18B	815	RSRIARLPSSTLKRP
KI67	antigen identified by monoclonal antibody Ki-67	845	NGNVAKTPRNTYKMT
KIF1A	kinesin family member 1A	43	TIVNPKQPKETPKSF
KIF1B	kinesin family member 1B	43	SIINPKNPKEAPKSF
KLF10	Kruppel-like factor 10	141	FKEEEKSPVSAPKLP
KLH12	kelch-like 12 (Drosophila)	225	LLQYVRMPLLTPRYI
KLH13	kelch-like 13 (Drosophila)	520	DKWIQKAPMTTVRGL
KLH36	kelch-like 36 (Drosophila)	478	DVWEERRPMTTARGW
KLHL9	kelch-like 9 (Drosophila)	478	DKWMQKAPMTTVRGL
KPRA	phosphoribosyl pyrophosphate synthetase-associated protein 1	178	AVIVAKSPDAAKRAQ
KPRB	phosphoribosyl pyrophosphate synthetase-associated protein 2	190	AVIVAKSPASAKRAQ
KRIT1	KRIT1, ankyrin repeat containing	595	TKLKSKAPHWTNRIL
KS6B2	ribosomal protein S6 kinase, 70kDa, polypeptide 2	467	APLPIRPPSGTKKSK
L1CAM	L1 cell adhesion molecule	139	AEGAPKWPKETVKPV
LAMA1	laminin, alpha 1	2227	MSSNQKSPTKTSKSP
LAMA3	laminin, alpha 3	280	ISKAQRDPTVTRRYY
LAMA4	laminin, alpha 4	435	EEIRSRQPFFTQREL
LAMA5	laminin, alpha 5	281	MGKALRDPTVTRRYY
LASS1	growth differentiation factor 1; LAG1 homolog, ceramide synthase 1	100	PRDAAKMPESAWKFL
LEG12	lectin, galactoside-binding, soluble, 12	124	WQREARWPHLALRRG
LHX1	LIM homeobox 1	183	LGAKRRGPRTTIKAK
LHX5	LIM homeobox 5	183	SGTKRRGPRTTIKAK
LIN54	lin-54 homolog (C. elegans)	315	AISPLKSPNKAVKST
LINCR	neuralized homolog 3 (Drosophila) pseudogene	14	FEANAKAPREALRFH
LMTK3	lemur tyrosine kinase 3	1012	ENGGLRFPRNTERPP
LOX5	arachidonate 5-lipoxygenase	575	APPTMRAPPPTAKGV
LT4R2	leukotriene B4 receptor 2	166	LAPRLRSPALARRLL
LTBP2	latent transforming growth factor beta binding protein 2	10	PRTKARSPGRALRNP
M3K11	mitogen-activated protein kinase kinase kinase 11	626	EPEEPKRPVPAERGS
M4K1	mitogen-activated protein kinase kinase kinase kinase 1	352	RGMETRPPANTARLQ
MADD	MAP-kinase activating death domain	1096	PQLGPRAPSATGKGP
MAF	v-maf musculoaponeurotic fibrosarcoma oncogene homolog (avian)	36	KFEVKKEPVETDRII
MAGT1	magnesium transporter 1	242	MWNHIRGPPYAHKNP
MAP1A	microtubule-associated protein 1A	292	HLDFLRYPVATQKDL

MAP1B	microtubule-associated protein 1B	514	HLDFLKQPLATQKDL
MAP9	microtubule-associated protein 9	16	TLAYTKSPKVTKRTT
MAST2	microtubule associated serine/threonine kinase 2	868	LLEERRTPPPTKRSL
MAST4	microtubule associated serine/threonine kinase family member 4	1906	FKRDRKGPHPTARSP
MAZ	MYC-associated zinc finger protein (purine-binding transcription factor)	221	GAKAGRVPSGAMKMP
MBD1	methyl-CpG binding domain protein 1	409	PYRRRKRPSSARRHH
MED1	mediator complex subunit 1	1043	STGGSKSPGSAGRSQ
MED26	mediator complex subunit 26	222	DKHSGKIPVNAVRPH
METH	5-methyltetrahydrofolate-homocysteine methyltransferase	640	DLIWNKDPEATEKLL
MGRN1	mahogunin, ring finger 1	451	GRPQSKAPDSTLRSP
MILK2	MICAL-like 2	135	EPSGKKAPVQAAKLP
MINT	spen homolog, transcriptional regulator (Drosophila)	1971	EENEAKEPAETLKPP
MIS	anti-Mullerian hormone	446	RGRDPRGPGRAQRSA
MOSC1	MOCO sulphurase C-terminal domain containing 1	290	GVMSRKEPLETLKSY
MOSC2	MOCO sulphurase C-terminal domain containing 2	289	GVIDRKQPLDTLKSY
MRE11	MRE11 meiotic recombination 11 homolog A (S. cerevisiae)	300	KMNMHKIPLHTVRQF
MRF	chromosome 11 open reading frame 9	744	VPHKKRPPKVASKSS
MTBP	Mdm2, transformed 3T3 cell double minute 2, p53 binding protein (mouse) binding protein, 104kDa	16	IWGEGKFPSAASREA
MTCH1	mitochondrial carrier homolog 1 (C. elegans)	43	VEARARDPPPAHRAH
MUC20	mucin 20, cell surface associated	599	MDIATKGPFPTSRDP
MVP	major vault protein	555	EVNDRKDPQETAKLF
MYCB2	MYC binding protein 2	3820	IKIELKGPENTLRVR
MYT1	myelin transcription factor 1	432	KSYYSKDPSRAEKRE
MYT1L	myelin transcription factor 1-like	496	KPYYGKDPSRTEKKE
NAL12	NLR family, pyrin domain containing 12	125	LVTPRKDPQETYRDY
NANG2	Nanog homeobox pseudogene 1	20	TSPKGKQPTTAEKSA
NANOG	Nanog homeobox pseudogene 8; Nanog homeobox	77	TSPKGKQPTSAEKSV
NAT8L	N-acetyltransferase 8-like (GCN5-related, putative)	104	DGIMERIPNTAFRGL
NAV2	neuron navigator 2	1114	ASQVKRSPSDAGRSS
NCAN	Neurocan	317	ADGSVRYPIQTPRRR
NEIL1	nei endonuclease VIII-like 1 (E. coli)	321	ALPPSKAPSRTRRAK
NEK5	NIMA (never in mitosis gene a)-related kinase 5	334	HRNEWRPPAGAQKAR
NFE2	nuclear factor (erythroid-derived 2), 45kDa	236	RALAMKIPFPTDKIV
NLGN2	neuroligin 2	623	FTTTTRLPPYATRWP
NOG1	GTP binding protein 4	509	NTQGPRMPRTAKKVQ
NOP2	NOP2 nucleolar protein homolog (yeast)	692	KAEGIREPKVTGKLK
NPHP1	nephronophthisis 1 (juvenile)	9	LARRQRDPLQALRRR
NRCAM	neuronal cell adhesion molecule	93	HFDIDKDPLVTMKPG
NRX2A	neurexin 2	1699	APAAPKTPSKAKKNK
NRX2B		653	APAAPKTPSKAKKNK
NTHL1	nth endonuclease III-like 1 (E. coli)	58	SHSPVKRPRKAQRLR
NTRK3	neurotrophic tyrosine kinase, receptor, type 3	577	AVKALKDPTLAARKD
NUMB	numb homolog (Drosophila)	437	QAGHRRTPSEADRWL
NUMBL	numb homolog (Drosophila)-like	410	QPGHKRTPSEAERWL
NUP54	nucleoporin 54kDa	249	IYVVERSPNGTSRRV
NXF2	nuclear RNA export factor 2; nuclear RNA export factor 2B	618	LQTEGKIPAEAFKQI
O10A3	olfactory receptor, family 10, subfamily A, member 3	229	LFAILKMPSTTGRQK
O10A6	olfactory receptor, family 10, subfamily A, member 6	229	LFAILKMPSTTGRQK
O10C1	olfactory receptor, family 10, subfamily C, member 1	228	LVTIFRIPSVAGRRK
O11A1	olfactory receptor, family 11, subfamily A, member 1	230	VVAVLRVPAGASRRR
O11G2	olfactory receptor, family 11, subfamily G, member 2	267	VRAVLRVPSAAGRRK
OBSCN	obscurin, cytoskeletal calmodulin and titin-interacting RhoGEF	709	GLTANKPPAAAAREV
ODB2	dihydrolipoamide branched chain transacylase E2	245	PILVSKPPVFTGKDK
OLA1	Obg-like ATPase 1	328	IRKGTKAPQAAGKIH
OR1B1	olfactory receptor, family 1, subfamily B, member 1	235	GAAILRLPSAAGRRR
OR1L1	olfactory receptor, family 1, subfamily L, member 1	279	LITVLKIPSAAGKRK

OR1L3	olfactory receptor, family 1, subfamily L, member 3	229	LIAVLKIPSAAGKHK
OR1L4	olfactory receptor, family 1, subfamily L, member 4	230	IVTVLRIPSAAGKWK
OR1L6	olfactory receptor, family 1, subfamily L, member 6	266	MVTVLRIPSAAGKWK
OR6T1	olfactory receptor, family 6, subfamily T, member 1	229	LATVLRAPTAAERRK
OSB10	oxysterol binding protein-like 10	224	TITHHKSPAAARRAK
OSR1	odd-skipped related 1 (Drosophila)	168	KPTRGRLPSKTKKEF
OSR2	odd-skipped related 2 (Drosophila)	165	KPSRGRLPSKTKKEF
P20D2	peptidase M20 domain containing 2	99	EPPEARAPSATPRPL
P53	tumor protein p53	67	PDEAPRMPEAAPRVA
P66B	GATA zinc finger domain containing 2B	566	GIGGHKGPSLADRQR
PABP1	poly(A) binding protein, cytoplasmic pseudogene 5; poly(A) binding protein, cytoplasmic 1	462	RPAAPRPPFSTMRPA
PABP3	poly(A) binding protein, cytoplasmic 3	456	RPGAPRVPFSTMRPA
PALLD	palladin, cytoskeletal associated protein	678	QEAGARQPPPAPRSA
PARF	chromosome 9 open reading frame 86	615	PPPPPKLPLPAFRLK
PCD10	protocadherin 10	1032	TRAPYKPPYLTRKRI
PCD21	protocadherin 21	744	RRVLRKRPSPAPRTI
PCDH8	protocadherin 8	290	FAFGARTPPEARRLF
PD1L2	programmed cell death 1 ligand 2	261	SKDTTKRPVTTTKRE
PDE2A	phosphodiesterase 2A, cGMP-stimulated	199	QVLQQRGPREAPRAV
PDZD2	PDZ domain containing 2	851	LGTPLKSPSLAKKDS
PECI	peroxisomal D3,D2-enoyl-CoA isomerase	341	LKAFAKLPPNALRIS
PERE	eosinophil peroxidise	79	LLSYFKQPVAATRTV
PERM	Myeloperoxidase	105	LLSYFKQPVAATRTA
PEX19	peroxisomal biogenesis factor 19	55	SGPQKRSPGDTAKDA
PGCA	Aggrecan	212	ADQTVRYPIHTPREG
PGCB	Brevican	216	SDQTVRYPIQTPREA
PHX2A	paired-like homeobox 2a	275	LSSFHRKPGPALKTN
PIAS4	protein inhibitor of activated STAT, 4	123	LNGLGRLPAKTLKPE
PISD	phosphatidylserine decarboxylase	42	LQPLRKLPFRAFRTD
PITM1	phosphatidylinositol transfer protein, membrane-associated 1	1213	QLLRSRGPSQAEREG
PJA1	praja ring finger 1	71	TTKRSRSPFSTTRRS
PK1L3	polycystic kidney disease 1-like 3	1269	INSPTKHPERTLKKK
PKHG3	pleckstrin homology domain containing, family G (with RhoGef domain) member 3	489	RRPSGRSPTSTEKRM
PLD1	phospholipase D1, phosphatidylcholine-specific	140	YKAFIRIPIPTRRHT
PM2L3	postmeiotic segregation increased 2-like 3; zinc finger protein 12	35	RLDLPRSPARAPREQ
PPIB	peptidylprolyl isomerase B (cyclophilin B)	40	ADEKKKGPKVTVKVY
PPIC	peptidylprolyl isomerase C (cyclophilin C)	34	EGFRKRGPSVTAKVF
PPM1D	protein phosphatase 1D magnesium-dependent, delta isoform	68	GEVSGKGPAVAAREA
PPR3A	protein phosphatase 1, regulatory (inhibitor) subunit 3A	756	KAIIAKLPQETARSD
PPRC1	peroxisome proliferator-activated receptor gamma, coactivator-related 1	1114	TRPREKPPLPATKAV
PRD16	PR domain containing 16	758	VKAEPKSPRDALKVG
PRDM7	PR domain containing 7	104	PRQQVKPPWMAFRGE
PRDM9	PR domain containing 9	104	PRQQVKPPWMALRVE
PREX2	phosphatidylinositol-3,4,5-trisphosphate-dependent Rac exchange factor 2	1587	LGVRDRTPQSAPRLY
PRG4	proteoglycan 4	467	TPTTPKEPAPTTKEP
PRLD1	PRELI domain containing 1; similar to Px19-like protein (25 kDa protein of relevant evolutionary and lymphoid interest) (PRELI)	63	LTKTNRMPRWAERLF
PROF4	profilin family, member 4	56	VNGFAKNPLQARREG
PRS4	proteasome (prosome, macropain) 26S subunit, ATPase, 1; similar to protease (prosome, macropain) 26S subunit, ATPase 1	43	KKKKTKGPDAASKLP
PTN11	protein tyrosine phosphatase, non-receptor type 11; similar to protein tyrosine phosphatase, non-receptor type 11	215	TVLQLKQPLNTTRIN
PTN6	protein tyrosine phosphatase, non-receptor type 6	212	AFVYLRQPYYATRVN

PTPM1	protein tyrosine phosphatase, mitochondrial 1	30	TLFRGKVPGRAHRDW
PUR6	phosphoribosylaminoimidazole carboxylase, phosphoribosylaminoimidazole succinocarboxamide synthetase	306	VTSAHKGPDETLRIK
PUS7	pseudouridylate synthase 7 homolog (S. cerevisiae)	431	EWAKTKDPTAALRKL
PYR1	carbamoyl-phosphate synthetase 2, aspartate transcarbamylase, and dihydroorotase	1477	VHVHLREPGGTHKED
RAF1	v-raf-1 murine leukemia viral oncogene homolog 1	311	GWSQPKTPVPAQRER
RAG1	recombination activating gene 1	42	VRSFEKTPEEAQKEK
RBM15	RNA binding motif protein 15	52	MKGKERSPVKAKRSR
RECQ5	RecQ protein-like 5	543	EASSRRIPRLTVKAR
RELN	Reelin	1571	LPQDAKTPATAFRWW
RFA1	replication protein A1, 70kDa	374	KFDGSRQPVLAIKGA
RFNG	RFNG O-fucosylpeptide 3-beta-N-acetylglucosaminyltransferase	39	APAPARTPAPAPRAP
RFX6	regulatory factor X, 6	175	KTIRQKFPLLTTRRL
RGAP1	Rac GTPase activating protein 1 pseudogene; Rac GTPase activating protein 1	432	FLRNLKEPLLTFRLN
RGL3	ral guanine nucleotide dissociation stimulator-like 3	369	WGAVSREPLSTFRKL
RGPD7	RANBP2-like and GRIP domain containing 5; RANBP2-like and GRIP domain containing 4; RANBP2-like and GRIP domain containing 3; RANBP2-like and GRIP domain containing 8; RANBP2-like and GRIP domain containing 7; RANBP2-like and GRIP domain containing 6	466	KQLFHRLPHETSRLE
RGRF1	Ras protein-specific guanine nucleotide-releasing factor 1	731	YGEPPKSPRATRKFS
RGS20	regulator of G-protein signaling 20	94	SHLLRRPPPEAPRRR
RGS22	regulator of G-protein signaling 22	258	HPRTKKDPSKTNKLI
RGS7	regulator of G-protein signaling 7	223	KSSRMRNPHKTRKSV
RHG01	Rho GTPase activating protein 1	224	LKSTQKSPATAPKPM
RHG05	Rho GTPase activating protein 5	1361	LLEAAKIPDKTERLH
RHG18	Rho GTPase activating protein 18	367	TEGLLRIPGAAIRIK
RICH2	Rho-type GTPase-activating protein RICH2	485	DPADRRQPEQARRPL
RIF1	RAP1 interacting factor homolog (yeast)	697	IFSEQRFPVATMKTL
RL3	ribosomal protein L3; similar to 60S ribosomal protein L3 (L4)	241	RWHTKKLPRKTHRGL
RL3L	ribosomal protein L3-like	241	RWHTKKLPRKTHKGL
RL9	ribosomal protein L9; ribosomal protein L9 pseudogene 25	30	RTVIVKGPRGTLRRD
RNF17	ring finger protein 17	1540	PSHLMRYPARAIKVL
RNPS1	similar to ribonucleic acid binding protein S1; RNA binding protein S1, serine-rich domain	26	KKSSTRAPSPTKRKD
RPC4	polymerase (RNA) III (DNA directed) polypeptide D, 44kDa	235	EEAKMKAPPKAARKT
RRP5	programmed cell death 11	51	RKKSQKGPAKTKKLK
RRS1	RRS1 ribosome biogenesis regulator homolog (S. cerevisiae)	93	EAIVARLPEPTTRLP
RS10	ribosomal protein S10; ribosomal protein S10 pseudogene 4; ribosomal protein S10 pseudogene 11; ribosomal protein S10 pseudogene 22; ribosomal protein S10 pseudogene 7; ribosomal protein S10 pseudogene 13	33	DVHMPKHPELADKNV
RS20	ribosomal protein S20	57	VKGPVRMPTKTLRIT
RTN3	reticulon 3	1024	EKIQAKLPGIAKKKA
RTN4	reticulon 4	982	KEAEKKLPSDTEKED
S12A5	solute carrier family 12 (potassium-chloride transporter), member 5	114	NEGGKKKPVQAPRMG
S15A4	solute carrier family 15, member 4	188	DQVKDRGPEATRRFF
S1PR4	sphingosine-1-phosphate receptor 4	238	QASGQKAPRPAARRK
S38AA	solute carrier family 38, member 10	653	SDHGGKPPLPAEKPA
S40A1	solute carrier family 40 (iron-regulated transporter), member 1	231	WKVYQKTPALAVKAG
SAHH2	adenosylhomocysteinase-like 1	55	MQEFTKFPTKTGRRS
SC16A	SEC16 homolog A (S. cerevisiae)	1913	PAPETKRPGQAAKKE
SC31B	SEC31 homolog B (S. cerevisiae)	112	ILSSGKEPVIAQKQK
SCG2	secretogranin II (chromogranin C)	467	EKVLPRLPYGAGRSR
SCN1A	sodium channel, voltage-gated, type I, alpha subunit	473	ASEHSREPSAAGRLS

SCNNB	sodium channel, nonvoltage-gated 1, beta	18	LHRLQKGPGYTYKEL
SEC63	SEC63 homolog (S. cerevisiae)	520	WQQKSKGPKKTAKSK
SEM7A	semaphorin 7A, GPI membrane anchor (John Milton Hagen blood group)	385	FQVADRHPEVAQRVE
SEPT9	septin 9	143	EVLGHKTPEPAPRRT
SET1A	SET domain containing 1A	1192	TPPQAKFPGPASRKA
SF3B1	splicing factor 3b, subunit 1, 155kDa	110	PFAEHRPPKIADRED
SG269	NKF3 kinase family member	69	RPPVAKKPTIAVKPT
SGOL1	shugoshin-like 1 (S. pombe)	487	ASVNYKEPTLASKLR
SH319	SH3 domain containing 19	35	TSGLPKKPEITPRSL
SHAN1	SH3 and multiple ankyrin repeat domains 1	506	SPSRGRHPEDAKRQP
SHAN3	SH3 and multiple ankyrin repeat domains 3	986	GGSFAREPSPTHRGP
SHRM2	shroom family member 2	363	QPRGDRRPELTDRPW
SHRM3	shroom family member 3	545	LSPVEKKPEATAKYV
SI1L3	signal-induced proliferation-associated 1 like 3	327	EADEGRSPPEASRPW
SIA7A	ST6 (alpha-N-acetyl-neuraminyl-2,3-beta-galactosyl-1,3)-N-acetylgalactosaminide alpha-2,6-sialyltransferase 1	116	PEEQDKVPHTAQRAA
SIRT2	sirtuin (silent mating type information regulation 2 homolog) 2 (S. cerevisiae)	277	ASLISKAPLSTPRLL
SIX4	SIX homeobox 4	248	LYKQNRYPSPAEKRH
SLAF5	CD84 molecule	270	LNTFTKNPYAASKKT
SMTN	Smoothelin	282	AQSPTRGPSDTKRAD
SN	sialic acid binding Ig-like lectin 1, sialoadhesin	601	VLYPPRQPTFTTRLD
SNCAP	synuclein, alpha interacting protein	860	SGDQLKRPFGAFRSI
SNRK	SNF related kinase	471	QVVLRRKPSVTNRLT
SOBP	sine oculis binding protein homolog (Drosophila)	682	HVKAEREPSAAERRT
SORC1	sortilin-related VPS10 domain containing receptor 1	147	PGTRERDPDKATRFR
SORC2	sortilin-related VPS10 domain containing receptor 2	13	PSRASKGPGPTARAP
SORC3	sortilin-related VPS10 domain containing receptor 3	922	EHVHLRVPFVAIRNK
SOS1	son of sevenless homolog 1 (Drosophila)	1306	SQHIPKLPPKTYKRE
SOS2	son of sevenless homolog 2 (Drosophila)	1306	SPHLPKLPPKTYKRE
SPT18	spermatogenesis associated 18 homolog (rat)	260	RSSRSRSPSPAPRSR
SPT6H	suppressor of Ty 6 homolog (S. cerevisiae)	812	VTDFLRLPHFTKRRT
SPTA1	spectrin, alpha, erythrocytic 1 (elliptocytosis 2)	781	RFEALKEPLATRKKK
SPTA2	spectrin, alpha, non-erythrocytic 1 (alpha-fodrin)	772	RYEALKEPMVARKQK
SPTB2	spectrin, beta, non-erythrocytic 1	354	YRTVEKPPKFTEKGN
SPTN2	spectrin, beta, non-erythrocytic 2	357	YRTVEKPPKFTEKGN
SPTN4	spectrin, beta, non-erythrocytic 4	1053	ALLAERFPAQAARLH
SPTN5	spectrin, beta, non-erythrocytic 5	2502	TSPAPRSPVEARRML
SRCAP	Snf2-related CREBBP activator protein	2437	SPARERVPRPAPRPR
SRGP2	SLIT-ROBO Rho GTPase activating protein 3	2870	PPKKNRSPADAGRGV
SRRM2	serine/arginine repetitive matrix 2; hypothetical LOC100132779	1928	RRSRSRTPPVTRRRS
SSF1	PPAN-P2RY11 readthrough transcript	452	GAQARRGPRGASRDG
SSH1	slingshot homolog 1 (Drosophila)	1025	PQGTPRDPAATSKPS
SSH3	slingshot homolog 3 (Drosophila)	593	GQQVDRGPQPALKSR
STAR8	StAR-related lipid transfer (START) domain containing 8	209	PVASFRHPQWTHRGD
STEA3	STEAP family member 3	61	VVVGSRNPKRTARLF
STIM1	stromal interaction molecule 1	645	ASRNTRIPHLAGKKA
STIP1	stress-induced-phosphoprotein 1	525	LSEHLKNPVIAQKIQ
STK39	serine threonine kinase 39 (STE20/SPS1 homolog, yeast)	357	EKLLTRTPDIAQRAK
STK6	aurora kinase A; aurora kinase A pseudogene 1	58	SNSSQRVPLQAQKLV
STRBP	spermatid perinuclear RNA binding protein	156	IIRNTKEPTLTLKVI
SYCP2	synaptonemal complex protein 2	184	NAMLDKMPQDARKIL
SYDE1	synapse defective 1, Rho GTPase, homolog 1 (C. elegans)	160	KASRTKSPGPARRLS
SYDE2	synapse defective 1, Rho GTPase, homolog 2 (C. elegans)	106	GPSFLRPPAVTVKKL
SYEM	glutamyl-tRNA synthetase 2, mitochondrial (putative)	183	AQKLAKDPKPAIRFR
SYG	glycyl-tRNA synthetase	479	HARATKVPLVAEKPL
SYNJ1	synaptojanin 1	1135	PPSGARSPAPTRKEF

SYNJ2	synaptojanin 2	1057	LAPPSKSPALTKKKQ
T2FA	general transcription factor IIF, polypeptide 1, 74kDa	19	TEYVVRVPKNTTKKY
TAF2	TAF2 RNA polymerase II, TATA box binding protein (TBP)-associated factor, 150kDa	673	ILALEKFPTPASRLA
TAU	microtubule-associated protein tau	246	PAQDGRPPQTAAREA
TB10A	TBC1 domain family, member 10A	428	SKAKPKPPKQAQKEQ
TBL1R	transducin (beta)-like 1 X-linked receptor 1	268	TLGQHKGPIFALKWN
TBL1X	transducin (beta)-like 1X-linked	331	TLGQHKGPIFALKWN
TBL1Y	transducin (beta)-like 1Y-linked	278	TLGQHKGPIFALKWN
TBX2	T-box 2	236	ANDILKLPYSTFRTY
TBX3	T-box 3	264	ANDILKLPYSTFRTY
TCF25	transcription factor 25 (basic helix-loop-helix)	48	RELGVRRPGGAGKEG
TDRD7	tudor domain containing 7	407	AILYAKLPLPTDKIQ
TITIN	Titin	16173	KMHTWRQPIETERSK
TMPS4	transmembrane protease, serine 4	25	PLRKPRIPMETFRKV
TNR11	tumor necrosis factor receptor superfamily, member 11a, NFKB activator	601	GPEGLREPEKASRPV
TNR4	tumor necrosis factor receptor superfamily, member 4	247	LRRDQRLPPDAHKPP
TNR8	tumor necrosis factor receptor superfamily, member 8	140	AGMIVKFPGTAQKNT
TP53B	tumor protein p53 binding protein 1	1444	SRVVPRVPDSTRRTD
TPST2	tyrosylprotein sulfotransferase 2	41	VLAGLRSPRGAMRPE
TPX2	TPX2, microtubule-associated, homolog (Xenopus laevis)	487	PITVPKSPAFALKNR
TREM1	triggering receptor expressed on myeloid cells 1	155	TQNVYKIPPTTTKAL
TRIO	triple functional domain (PTPRF interacting)	1769	SSPGPKRPGNTLRKW
TRM44	chromosome 4 open reading frame 23	748	GPAELRPPRTTPRKK
TRPM1	transient receptor potential cation channel, subfamily M, member 1	420	TEKEKKPPMATTKGG
TSG10	testis specific, 10	12	RSKSPRRPSPTARGA
TUSC3	tumor suppressor candidate 3	254	MWNHIRGPPYAHKNP
TXD16	thioredoxin domain containing 16	791	KSAVRKEPIETLRIK
TXND6	thioredoxin domain containing 6	254	TVMGPRDPNVARREQ
UB2E1	ubiquitin-conjugating enzyme E2E 1 (UBC4/5 homolog, yeast)	111	PEYPFKPPKVTFRTR
UB2E2	ubiquitin-conjugating enzyme E2E 2 (UBC4/5 homolog, yeast)	119	PDYPFKPPKVTFRTR
UB2E3	ubiquitin-conjugating enzyme E2E 3 (UBC4/5 homolog, yeast)	125	SDYPFKPPKVTFRTR
UB2L3	ubiquitin-conjugating enzyme E2L 3	66	AEYPFKPPKITFKTK
UBP26	ubiquitin specific peptidase 26	159	TGVLQRMPLLTSKLT
UBP31	ubiquitin specific peptidase 31	1019	PGSLAKKPESTTKRS
UBP38	ubiquitin specific peptidase 38	515	FFEASRPPWFTPRSQ
UBP43	ubiquitin specific peptidase 43	1074	APSSLRLPRKASRAP
UBP49	ubiquitin specific peptidase 49	236	LPTSRRVPAATLKLR
UBP54	ubiquitin specific peptidase 54	978	RQGLPKAPGWTEKNS
UBR1	ubiquitin protein ligase E3 component n-recognin 1	1088	ALGPKRGPSVTEKEV
UBR2	ubiquitin protein ligase E3 component n-recognin 2	823	AVAHFKKPGLTGRGM
UBR4	ubiquitin protein ligase E3 component n-recognin 4	4027	LQKLIKPPAPTSKKN
UHRF2	ubiquitin-like with PHD and ring finger domains 2	658	KGQSKKQPSGTTKRP
UTY	ubiquitously transcribed tetratricopeptide repeat gene, Y-linked	1025	SGRRRKGPFKTIKFG
V1AR	arginine vasopressin receptor 1A	80	LLALHRTPRKTSRMH
VTDB	group-specific component (vitamin D binding protein)	431	ERLKAKLPDATPKEL
WBS14	MLX interacting protein-like	836	LTDPGRIPEQATRAV
WDR67	WD repeat domain 67	19	GKIWHRKPSPATRDG
XIAP	X-linked inhibitor of apoptosis	360	VRTTEKTPSLTRRID
XIRP2	xin actin-binding repeat containing 2	1847	EVNLPKAPKGTVKIV
XRRA1	X-ray radiation resistance associated 1	592	KEKDQKKPPTAPREV
YETS2	YEATS domain containing 2	1162	TAVVKKIPLITAKSE
YSK4	YSK4 Sps1/Ste20-related kinase homolog (S. cerevisiae)	595	PRFQKKMPQIAKKQS
YYAP1	YY1 associated protein 1; gon-4-like (C. elegans)	446	KPVADRFPKKAWRQK
Z3H7B	zinc finger CCCH-type containing 7B	406	NSQDHRPPSGAQKPA

Z512B	zinc finger protein 512B	334	TRSENKAPRATGRNS
ZBT12	zinc finger and BTB domain containing 12	160	LLPPARTPKPAPKPP
ZC3H3	zinc finger CCCH-type containing 3	321	VAASSKSPRVARRAL
ZF161	zinc finger protein 161 homolog (mouse)	191	SQEDGKSPTTTLRVQ
ZN213	zinc finger protein 213	127	VEDLQKQPVKAWRQD
ZN335	zinc finger protein 335	553	SRDRKKRPDPTPKLS
ZN566	zinc finger protein 566	64	YLEQGKEPWLADREL
ZN592	zinc finger protein 592	335	SPKSPRSPLEATRKS
ZN624	zinc finger protein 624	112	HLENGKGPWVTVREI
ZN727	zinc finger protein 727	62	YLEQRKEPWNARRQK
ZN837	zinc finger protein 837	330	AERHRRGPVLARRAF
ZN862	zinc finger protein 862	211	NALAARDPIWAARFR
ZO1	tight junction protein 1 (zona occludens 1)	1294	DTGSFKPPEVASKPS
ZRAN1	zinc finger, RAN-binding domain containing 1	217	GNSQRRSPPATKRDS

List of abbreviations

AKAP	A Kinase Anchoring Protein
AMPA	2-amino-3-(3-hydroxy-5-methyl-isoxazol-4-yl)propanoic acid
Amph	Amphiphysin
ATP	Adenosine triphosphate
BDNF	Brain-derived neurotrophic factor
CAM	Cell adhesion molecule
cAMP	Cyclic adenosine monophosphate
CFP	Cyan fluorescent protien
CGN	Cerebellar Granule Neuron
Chk	Csk-homologous kinas
CML	Chronic myeloid leukaemia
CMV	*Cytomegalovirus*
CNS	Central nervous system
CRASH	Corpus callosum hypoplasia, Retardation, Adducted thumbs, Spasticity and Hydrocephalus
CSF-1	Colony Stimulating Factor 1
Csk	C-terminal Src kinase
DAVID	Database for Annotation, Visualization and IntegratedDiscovery
DCC	Deleted in Colorectal Cancer
ECM	Extracellular Martix
ERK	Extracellular-Signal-Regulated kinase
ERM	Ezrin-Radixin-Moesin
FAK	Focal Adhesion Kinase
FGF	Fibroblast Growth Factor
FITC	Fluorescein isothiocyanate
Frs2	Fibroblast growth factor receptor substrate 2
GABA	γ-Aminobutyric acid
GAP	GTPase activating protein
GEF	Guanine nucleotide exchange factor
GFP	Green fluorescent protein
GO term	Gene Ontology term
GPS	Group-based prediction System
GST	Gluathione-S-transferase
HCN	Hyperpolarization-activated cyclic nucleotide-gated
HPK1	Hematopoietic Progenitor Kinase 1
HPLC	High-performance liquid chromatography
Ig	Immunoglobulin
JNK	c-Jun N-terminal kinase
LRRK2	Leucine-rich repeat kinase 2
LTP	Long term potentiation

MAPK	Mitogen activated protein kinase
MCS	Multiple Cloning Site
MBP	Maltose binding protein
MS	Mass spectrometry
NGF	Nerve growth factor
NMDA	N-Methyl-D-aspartic acid
NT	Neutotrophin
PD	Phage Display
PDGF	Platelet-derived growth factor
PI3K	Phosphoinositide-3 kinase
PKA	Protein kinase A
PKC	Protein kinase C
PLC	Phospholipase C
PPII	Polyproline type II
PRD	Proline rich domain
PSSM	Position Site Scoring Matrix
PTM	Post-translational modification
PTP	Protein tyrosine phosphatase
RTK	Receptor tyrosine kinase
Sema	Semaphorin
SFK	Src Family Kinase
SH2	Src homology 2
SH3	Src homolgy 3
SHP-1	Src homology region 2 domain-containing phosphatase-1
shRNA	short hairpin RNA
siRNA	short interfering RNA

References

Abdullah A, Pollock A, Sun T (2012) The Path from Skin to Brain: Generation of Functional Neurons from Fibroblasts. *Molecular Neurobiology* **45:** 586-595

Ahmed I, Calle Y, Iwashita S, Nur EKA (2006) Role of Cdc42 in neurite outgrowth of PC12 cells and cerebellar granule neurons. *Mol Cell Biochem* **281:** 17-25

Akiva E, Friedlander G, Itzhaki Z, Margalit H (2012) A dynamic view of domain-motif interactions. *PLoS Comput Biol* **8:** e1002341

Ali DW, Salter MW (2001) NMDA receptor regulation by Src kinase signalling in excitatory synaptic transmission and plasticity. *Curr Opin Neurobiol* **11:** 336-342

Alonso A, Sasin J, Bottini N, Friedberg I, Osterman A, Godzik A, Hunter T, Dixon J, Mustelin T (2004) Protein tyrosine phosphatases in the human genome. *Cell* **117:** 699-711

Alonso G, Koegl M, Mazurenko N, Courtneidge SA (1995) Sequence requirements for binding of Src family tyrosine kinases to activated growth factor receptors. *J Biol Chem* **270:** 9840-9848

Amrein KE, Flint N, Panholzer B, Burn P (1992) Ras GTPase-activating protein: a substrate and a potential binding protein of the protein-tyrosine kinase p56lck. *Proc Natl Acad Sci U S A* **89:** 3343-3346

Anafi M, Kiefer F, Gish GD, Mbamalu G, Iscove NN, Pawson T (1997) SH2/SH3 adaptor proteins can link tyrosine kinases to a Ste20-related protein kinase, HPK1. *J Biol Chem* **272:** 27804-27811

Antoine-Bertrand J, Ghogha A, Luangrath V, Bedford FK, Lamarche-Vane N (2011) The activation of ezrin-radixin-moesin proteins is regulated by netrin-1 through Src kinase and RhoA/Rho kinase activities and mediates netrin-1-induced axon outgrowth. *Mol Biol Cell* **22:** 3734-3746

Arinsburg SS, Cohen IS, Yu HG (2006) Constitutively active Src tyrosine kinase changes gating of HCN4 channels through direct binding to the channel proteins. *J Cardiovasc Pharmacol* **47:** 578-586

Arthur WT, Petch LA, Burridge K (2000) Integrin engagement suppresses RhoA activity via a c-Src-dependent mechanism. *Curr Biol* **10:** 719-722

Atashi JR, Klinz SG, Ingraham CA, Matten WT, Schachner M, Maness PF (1992) Neural cell adhesion molecules modulate tyrosine phosphorylation of tubulin in nerve growth cone membranes. *Neuron* **8:** 831-842

Atatreh N, Stojkoski C, Smith P, Booker GW, Dive C, Frenkel AD, Freeman S, Bryce RA (2008) In silico screening and biological evaluation of inhibitors of Src-SH3 domain interaction with a proline-rich ligand. *Bioorg Med Chem Lett* **18:** 1217-1222

Bain J, Plater L, Elliott M, Shpiro N, Hastie CJ, McLauchlan H, Klevernic I, Arthur JSC, Alessi DR, Cohen P (2007) The selectivity of protein kinase inhibitors: a further update. *Biochemical Journal* **408:** 297-315

Barford D, Johnson LN (1989) The allosteric transition of glycogen phosphorylase. *Nature* **340:** 609-616

Barker SC, Kassel DB, Weigl D, Huang X, Luther MA, Knight WB (1995) Characterization of pp60c-src tyrosine kinase activities using a continuous assay: autoactivation of the enzyme is an intermolecular autophosphorylation process. *Biochemistry* **34:** 14843-14851

Barnekow A, Schartl M (1984) Cellular src gene product detected in the freshwater sponge Spongilla lacustris. *Mol Cell Biol* **4:** 1179-1181

Bechara A, Nawabi H, Moret F, Yaron A, Weaver E, Bozon M, Abouzid K, Guan JL, Tessier-Lavigne M, Lemmon V, Castellani V (2008) FAK-MAPK-dependent adhesion disassembly downstream of L1 contributes to semaphorin3A-induced collapse. *EMBO J* **27:** 1549-1562

Beggs HE, Soriano P, Maness PF (1994) NCAM-dependent neurite outgrowth is inhibited in neurons from Fyn-minus mice. *J Cell Biol* **127:** 825-833

Belfield JL, Whittaker C, Cader MZ, Chawla S (2006) Differential effects of Ca2+ and cAMP on transcription mediated by MEF2D and cAMP-response element-binding protein in hippocampal neurons. *J Biol Chem* **281:** 27724-27732

Bennett V, Chen L (2001) Ankyrins and cellular targeting of diverse membrane proteins to physiological sites. *Curr Opin Cell Biol* **13:** 61-67

Beyer K, Lao JI, Latorre P, Riutort N, Matute B, Fernández-Figueras MT, Mate JL, Ariza A (2003) Methionine synthase polymorphism is a risk factor for Alzheimer disease. *Neuroreport* **14:** 1391-1394

Bixby JL, Jhabvala P (1993) Tyrosine phosphorylation in early embryonic growth cones. *J Neurosci* **13:** 3421-3432

Bjelfman C, Hedborg F, Johansson I, Nordenskjold M, Pahlman S (1990a) Expression of the neuronal form of pp60c-src in neuroblastoma in relation to clinical stage and prognosis. *Cancer Res* **50:** 6908-6914

Bjelfman C, Meyerson G, Cartwright CA, Mellstrom K, Hammerling U, Pahlman S (1990b) Early activation of endogenous pp60src kinase activity during neuronal differentiation of cultured human neuroblastoma cells. *Mol Cell Biol* **10:** 361-370

Black DL (1992) Activation of c-src neuron-specific splicing by an unusual RNA element in vivo and in vitro. *Cell* **69:** 795-807

Bliss T, Errington M, Fransen E, Godfraind JM, Kauer JA, Kooy RF, Maness PF, Furley AJ (2000) Long-term potentiation in mice lacking the neural cell adhesion molecule L1. *Curr Biol* **10:** 1607-1610

Bliss TV, Collingridge GL (1993) A synaptic model of memory: long-term potentiation in the hippocampus. *Nature* **361:** 31-39

Boiko T, Vakulenko M, Ewers H, Yap CC, Norden C, Winckler B (2007) Ankyrin-dependent and -independent mechanisms orchestrate axonal compartmentalization of L1 family members neurofascin and L1/neuron-glia cell adhesion molecule. *J Neurosci* **27:** 590-603

Boomer JS, Tan TH (2005) Functional interactions of HPK1 with adaptor proteins. *J Cell Biochem* **95:** 34-44

Boonyaratanakornkit V, Scott MP, Ribon V, Sherman L, Anderson SM, Maller JL, Miller WT, Edwards DP (2001) Progesterone receptor contains a proline-rich motif that directly interacts with SH3 domains and activates c-Src family tyrosine kinases. *Mol Cell* **8:** 269-280

Bradke F, Dotti CG (1999) The role of local actin instability in axon formation. *Science* **283:** 1931-1934

Briggs SD, Smithgall TE (1999) SH2-kinase linker mutations release Hck tyrosine kinase and transforming activities in Rat-2 fibroblasts. *J Biol Chem* **274:** 26579-26583

Brodeur GM, Seeger RC, Barrett A, Castleberry RP, D'Angio G, De Bernardi B, Evans AE, Favrot M, Freeman AI, Haase G, et al. (1988) International criteria for diagnosis, staging and response to treatment in patients with neuroblastoma. *Prog Clin Biol Res* **271:** 509-524

Brose K, Bland KS, Wang KH, Arnott D, Henzel W, Goodman CS, Tessier-Lavigne M, Kidd T (1999) Slit proteins bind Robo receptors and have an evolutionarily conserved role in repulsive axon guidance. *Cell* **96:** 795-806

Brouns MR, Matheson SF, Settleman J (2001) p190 RhoGAP is the principal Src substrate in brain and regulates axon outgrowth, guidance and fasciculation. *Nat Cell Biol* **3:** 361-367

Brown MT, Cooper JA (1996) Regulation, substrates and functions of src. *Biochim Biophys Acta* **1287:** 121-149

Brugge JS, Cotton PC, Queral AE, Barrett JN, Nonner D, Keane RW (1985) Neurones express high levels of a structurally modified, activated form of pp60c-src. *Nature* **316:** 554-557

Brábek J, Constancio SS, Shin NY, Pozzi A, Weaver AM, Hanks SK (2004) CAS promotes invasiveness of Src-transformed cells. *Oncogene* **23:** 7406-7415

Brábek J, Mojzita D, Novotný M, Půta F, Folk P (2002) The SH3 domain of Src can downregulate its kinase activity in the absence of the SH2 domain-pY527 interaction. *Biochem Biophys Res Commun* **296:** 664-670

Buhusi M, Schlatter MC, Demyanenko GP, Thresher R, Maness PF (2008) L1 interaction with ankyrin regulates mediolateral topography in the retinocollicular projection. *J Neurosci* **28:** 177-188

Burnham MR, Bruce-Staskal PJ, Harte MT, Weidow CL, Ma A, Weed SA, Bouton AH (2000) Regulation of c-SRC activity and function by the adapter protein CAS. *Mol Cell Biol* **20:** 5865-5878

Buss JE, Kamps MP, Sefton BM (1984) Myristic acid is attached to the transforming protein of Rous sarcoma virus during or immediately after synthesis and is present in both soluble and membrane-bound forms of the protein. *Mol Cell Biol* **4:** 2697-2704

Calalb MB, Polte TR, Hanks SK (1995) Tyrosine phosphorylation of focal adhesion kinase at sites in the catalytic domain regulates kinase activity: a role for Src family kinases. *Mol Cell Biol* **15:** 954-963

Carlson SS, Valdez G, Sanes JR (2010) Presynaptic calcium channels and α3-integrins are complexed with synaptic cleft laminins, cytoskeletal elements and active zone components. *J Neurochem* **115:** 654-666

Carrera AC, Paradis H, Borlado LR, Roberts TM, Martinez C (1995) Lck unique domain influences Lck specificity and biological function. *J Biol Chem* **270:** 3385-3391

Casnellie JE, Harrison ML, Hellstrom KE, Krebs EG (1982) A lymphoma protein with an in vitro site of tyrosine phosphorylation homologous to that in pp60src. *J Biol Chem* **257:** 13877-13879

Caspers P, Stieger M, Burn P (1994) Overproduction of bacterial chaperones improves the solubility of recombinant protein tyrosine kinases in Escherichia coli. *Cell Mol Biol (Noisy-le-grand)* **40:** 635-644

Castellani V, Chédotal A, Schachner M, Faivre-Sarrailh C, Rougon G (2000) Analysis of the L1-deficient mouse phenotype reveals cross-talk between Sema3A and L1 signaling pathways in axonal guidance. *Neuron* **27:** 237-249

Castellani V, Falk J, Rougon G (2004) Semaphorin3A-induced receptor endocytosis during axon guidance responses is mediated by L1 CAM. *Mol Cell Neurosci* **26:** 89-100

Cataldi M, Taglialatela M, Guerriero S, Amoroso S, Lombardi G, di Renzo G, Annunziato L (1996) Protein-tyrosine kinases activate while protein-tyrosine phosphatases inhibit L-type calcium channel activity in pituitary GH3 cells. *J Biol Chem* **271:** 9441-9446

Chackalaparampil I, Shalloway D (1988) Altered phosphorylation and activation of pp60c-src during fibroblast mitosis. *Cell* **52:** 801-810

Chacon MR, Fazzari P (2011) FAK: dynamic integration of guidance signals at the growth cone. *Cell Adh Migr* **5:** 52-55

Chacón MR, Fernández G, Rico B (2010) Focal adhesion kinase functions downstream of Sema3A signaling during axonal remodeling. *Mol Cell Neurosci* **44:** 30-42

Chan PM, Ng YW, Manser E (2011) A robust protocol to map binding sites of the 14-3-3 interactome: Cdc25C requires phosphorylation of both S216 and S263 to bind 14-3-3. *Mol Cell Proteomics* **10:** M110.005157

Chan RC, Black DL (1997) The polypyrimidine tract binding protein binds upstream of neural cell-specific c-src exon N1 to repress the splicing of the intron downstream. *Mol Cell Biol* **17:** 4667-4676

Chang CM, Shu HK, Kung HJ (1995) Disease specificity of kinase domains: the src-encoded catalytic domain converts erbB into a sarcoma oncogene. *Proc Natl Acad Sci U S A* **92:** 3928-3932

Cheadle C, Ivashchenko Y, South V, Searfoss GH, French S, Howk R, Ricca GA, Jaye M (1994) Identification of a Src SH3 domain binding motif by screening a random phage display library. *J Biol Chem* **269:** 24034-24039

Chen BH, Tzen JT, Bresnick AR, Chen HC (2002) Roles of Rho-associated kinase and myosin light chain kinase in morphological and migratory defects of focal adhesion kinase-null cells. *J Biol Chem* **277:** 33857-33863

Chen C, Leonard JP (1996) Protein tyrosine kinase-mediated potentiation of currents from cloned NMDA receptors. *J Neurochem* **67:** 194-200

Chen S, Bing R, Rosenblum N, Hillman DE (1996) Immunohistochemical localization of Lyn (p56) protein in the adult rat brain. *Neuroscience* **71:** 89-100

Cheng L, Itoh K, Lemmon V (2005a) L1-mediated branching is regulated by two ezrin-radixin-moesin (ERM)-binding sites, the RSLE region and a novel juxtamembrane ERM-binding region. *J Neurosci* **25:** 395-403

Cheng L, Lemmon S, Lemmon V (2005b) RanBPM is an L1-interacting protein that regulates L1-mediated mitogen-activated protein kinase activation. *J Neurochem* **94:** 1102-1110

Cheng L, Lemmon V (2004) Pathological missense mutations of neural cell adhesion molecule L1 affect neurite outgrowth and branching on an L1 substrate. *Mol Cell Neurosci* **27:** 522-530

Cheng PL, Poo MM (2012) Early events in axon/dendrite polarization. *Annu Rev Neurosci* **35:** 181-201

Cheung HH, Gurd JW (2001) Tyrosine phosphorylation of the N-methyl-D-aspartate receptor by exogenous and postsynaptic density-associated Src-family kinases. *J Neurochem* **78:** 524-534

Cho SY, Klemke RL (2002) Purification of pseudopodia from polarized cells reveals redistribution and activation of Rac through assembly of a CAS/Crk scaffold. *J Cell Biol* **156:** 725-736

Choi HJ, Smithgall TE (2004) Conserved residues in the HIV-1 Nef hydrophobic pocket are essential for recruitment and activation of the Hck tyrosine kinase. *J Mol Biol* **343:** 1255-1268

Chou MY, Underwood JG, Nikolic J, Luu MH, Black DL (2000) Multisite RNA binding and release of polypyrimidine tract binding protein during the regulation of c-src neural-specific splicing. *Mol Cell* **5:** 949-957

Cicchetti P, Mayer BJ, Thiel G, Baltimore D (1992) Identification of a protein that binds to the SH3 region of Abl and is similar to Bcr and GAP-rho. *Science* **257:** 803-806

Cline H (2005) Synaptogenesis: a balancing act between excitation and inhibition. *Curr Biol* **15:** R203-205

Cohen NR, Taylor JS, Scott LB, Guillery RW, Soriano P, Furley AJ (1998) Errors in corticospinal axon guidance in mice lacking the neural cell adhesion molecule L1. *Curr Biol* **8:** 26-33

Cohen P (2002a) Protein kinases--the major drug targets of the twenty-first century? *Nat Rev Drug Discov* **1:** 309-315

Cohen P (2002b) The origins of protein phosphorylation. *Nat Cell Biol* **4:** E127-130

Collett JW, Steele RE (1992) Identification and developmental expression of Src+ mRNAs in Xenopus laevis. *Dev Biol* **152:** 194-198

Collett JW, Steele RE (1993) Alternative splicing of a neural-specific Src mRNA (Src+) is a rapid and protein synthesis-independent response to neural induction in Xenopus laevis. *Dev Biol* **158:** 487-495

Collett MS, Erikson E, Erikson RL (1979) Structural analysis of the avian sarcoma virus transforming protein: sites of phosphorylation. *J Virol* **29:** 770-781

Cooke MP, Perlmutter RM (1989) Expression of a novel form of the fyn proto-oncogene in hematopoietic cells. *New Biol* **1:** 66-74

Cooper JA, Esch FS, Taylor SS, Hunter T (1984) Phosphorylation sites in enolase and lactate-dehydrogenase utilized by tyrosine protein-kinases in vivo and in vitro. *Journal of Biological Chemistry* **259:** 7835-7841

Cooper JA, Gould KL, Cartwright CA, Hunter T (1986) Tyr527 is phosphorylated in pp60c-src: implications for regulation. *Science* **231:** 1431-1434

Cooper JA, MacAuley A (1988) Potential positive and negative autoregulation of p60c-src by intermolecular autophosphorylation. *Proc Natl Acad Sci U S A* **85:** 4232-4236

Cotton PC, Brugge JS (1983) Neural tissues express high levels of the cellular src gene product pp60c-src. *Mol Cell Biol* **3:** 1157-1162

Courtneidge SA (1985) Activation of the pp60c-src kinase by middle T antigen binding or by dephosphorylation. *EMBO J* **4:** 1471-1477

Courtneidge SA, Levinson AD, Bishop JM (1980) The protein encoded by the transforming gene of avian sarcoma virus (pp60src) and a homologous protein in normal cells (pp60proto-src) are associated with the plasma membrane. *Proc Natl Acad Sci U S A* **77:** 3783-3787

Coussens PM, Cooper JA, Hunter T, Shalloway D (1985) Restriction of the in vitro and in vivo tyrosine protein kinase activities of pp60c-src relative to pp60v-src. *Mol Cell Biol* **5:** 2753-2763

Cowan-Jacob SW, Fendrich G, Manley PW, Jahnke W, Fabbro D, Liebetanz J, Meyer T (2005) The crystal structure of a c-Src complex in an active conformation suggests possible steps in c-Src activation. *Structure* **13:** 861-871

Cross FR, Garber EA, Pellman D, Hanafusa H (1984) A short sequence in the p60src N terminus is required for p60src myristylation and membrane association and for cell transformation. *Mol Cell Biol* **4:** 1834-1842

Cross FR, Hanafusa H (1983) Local mutagenesis of Rous sarcoma virus: the major sites of tyrosine and serine phosphorylation of pp60src are dispensable for transformation. *Cell* **34:** 597-607

Crossin KL, Krushel LA (2000) Cellular signaling by neural cell adhesion molecules of the immunoglobulin superfamily. *Dev Dyn* **218:** 260-279

David-Pfeuty T, Bagrodia S, Shalloway D (1993) Differential localization patterns of myristoylated and nonmyristoylated c-Src proteins in interphase and mitotic c-Src overexpresser cells. *J Cell Sci* **105 (Pt 3):** 613-628

Davis JQ, Bennett V (1993) Ankyrin-binding activity of nervous system cell adhesion molecules expressed in adult brain. *J Cell Sci Suppl* **17:** 109-117

Davis LH, Bennett V (1994) Identification of two regions of beta G spectrin that bind to distinct sites in brain membranes. *J Biol Chem* **269:** 4409-4416

Demyanenko GP, Tsai AY, Maness PF (1999) Abnormalities in neuronal process extension, hippocampal development, and the ventricular system of L1 knockout mice. *J Neurosci* **19:** 4907-4920

Dengl S, Mayer A, Sun M, Cramer P (2009) Structure and in vivo requirement of the yeast Spt6 SH2 domain. *J Mol Biol* **389:** 211-225

Dent E, Kalil K (2001) Axon branching requires interactions between dynamic microtubules and actin filaments. *Journal of Neuroscience* **21:** 9757-9769

Dent EW, Gupton SL, Gertler FB (2011) The growth cone cytoskeleton in axon outgrowth and guidance. *Cold Spring Harb Perspect Biol* **3**

Dickson TC, Mintz CD, Benson DL, Salton SR (2002) Functional binding interaction identified between the axonal CAM L1 and members of the ERM family. *J Cell Biol* **157:** 1105-1112

Dingledine R, Borges K, Bowie D, Traynelis SF (1999) The glutamate receptor ion channels. *Pharmacol Rev* **51:** 7-61

Doherty P, Williams G, Williams EJ (2000) CAMs and axonal growth: a critical evaluation of the role of calcium and the MAPK cascade. *Mol Cell Neurosci* **16:** 283-295

Du Y, Weed SA, Xiong WC, Marshall TD, Parsons JT (1998) Identification of a novel cortactin SH3 domain-binding protein and its localization to growth cones of cultured neurons. *Mol Cell Biol* **18:** 5838-5851

Eck MJ, Shoelson SE, Harrison SC (1993) Recognition of a high-affinity phosphotyrosyl peptide by the Src homology-2 domain of p56lck. *Nature* **362:** 87-91

Eckhart W, Hutchinson MA, Hunter T (1979) An activity phosphorylating tyrosine in polyoma T antigen immunoprecipitates. *Cell* **18:** 925-933

Eichinger L, Pachebat J, Glöckner G, Rajandream MA, Sucgang R, Berriman M, Song J, Olsen R, Szafranski K, Xu Q, Tunggal B, Kummerfeld S, Madera M, Konfortov BA, Rivero F, Bankier AT, Lehmann R, Hamlin N, Davies R, Gaudet P, Fey P, Pilcher K, Chen G, Saunders D, Sodergren E, Davis P, Kerhornou A, Nie X, Hall N, Anjard C, Hemphill L, Bason N, Farbrother P, Desany B, Just E, Morio T, Rost R, Churcher C, Cooper J, Haydock S, van Driessche N, Cronin A, Goodhead I, Muzny D, Mourier T, Pain A, Lu M, Harper D, Lindsay R, Hauser H, James K, Quiles M, Babu MM, Saito T, Buchrieser C, Wardroper A, Felder M, Thangavelu M, Johnson D, Knights A, Loulseged H, Mungall K, Oliver K, Price C, Quail M, Urushihara H, Hernandez J, Rabbinowitsch E, Steffen D, Sanders M, Ma J, Kohara Y, Sharp S, Simmonds M, Spiegler S, Tivey A, Sugano S, White B, Walker D, Woodward J, Winckler T, Tanaka Y, Shaulsky G, Schleicher M, Weinstock G, Rosenthal A, Cox E, Chisholm RL, Gibbs R, Loomis WF, Platzer M, Kay RR, Williams J, Dear PH, Noegel AA, Barrell B, Kuspa A (2005) The genome of the social amoeba Dictyostelium discoideum. *Nature* **435:** 43-57

Ellis C, Moran M, McCormick F, Pawson T (1990) Phosphorylation of GAP and GAP-associated proteins by transforming and mitogenic tyrosine kinases. *Nature* **343:** 377-381

Engen JR, Wales TE, Hochrein JM, Meyn MA, Banu Ozkan S, Bahar I, Smithgall TE (2008) Structure and dynamic regulation of Src-family kinases. *Cell Mol Life Sci* **65:** 3058-3073

Evans AE, Chatten J, D'Angio GJ, Gerson JM, Robinson J, Schnaufer L (1980) A review of 17 IV-S neuroblastoma patients at the children's hospital of philadelphia. *Cancer* **45:** 833-839

Evans GJ, Cousin MA (2005) Tyrosine phosphorylation of synaptophysin in synaptic vesicle recycling. *Biochem Soc Trans* **33:** 1350-1353

Fadool DA, Holmes TC, Berman K, Dagan D, Levitan IB (1997) Tyrosine phosphorylation modulates current amplitude and kinetics of a neuronal voltage-gated potassium channel. *J Neurophysiol* **78:** 1563-1573

Falk J, Julien F, Bechara A, Fiore R, Nawabi H, Zhou H, Hoyo-Becerra C, Bozon M, Rougon G, Grumet M, Püschel AW, Sanes JR, Castellani V (2005) Dual functional activity of semaphorin 3B is required for positioning the anterior commissure. *Neuron* **48:** 63-75

Feder D, Bishop JM (1990) Purification and enzymatic characterization of pp60c-src from human platelets. *J Biol Chem* **265:** 8205-8211

Fehon RG, McClatchey AI, Bretscher A (2010) Organizing the cell cortex: the role of ERM proteins. *Nat Rev Mol Cell Biol* **11:** 276-287

Felding-Habermann B, Silletti S, Mei F, Siu CH, Yip PM, Brooks PC, Cheresh DA, O'Toole TE, Ginsberg MH, Montgomery AM (1997) A single immunoglobulin-like domain of the human neural cell adhesion molecule L1 supports adhesion by multiple vascular and platelet integrins. *J Cell Biol* **139:** 1567-1581

Feng S, Chen JK, Yu H, Simon JA, Schreiber SL (1994) Two binding orientations for peptides to the Src SH3 domain: development of a general model for SH3-ligand interactions. *Science* **266:** 1241-1247

Feng S, Kasahara C, Rickles RJ, Schreiber SL (1995) Specific interactions outside the proline-rich core of two classes of Src homology 3 ligands. *Proc Natl Acad Sci U S A* **92:** 12408-12415

Foster-Barber A, Bishop JM (1998) Src interacts with dynamin and synapsin in neuronal cells. *Proc Natl Acad Sci U S A* **95:** 4673-4677

Frank C, Burkhardt C, Imhof D, Ringel J, Zschörnig O, Wieligmann K, Zacharias M, Böhmer FD (2004) Effective dephosphorylation of Src substrates by SHP-1. *J Biol Chem* **279:** 11375-11383

Garber EA, Krueger JG, Hanafusa H, Goldberg AR (1983) Only membrane-associated RSV src proteins have amino-terminally bound lipid. *Nature* **302:** 161-163

Gentil BJ, Benaud C, Delphin C, Remy C, Berezowski V, Cecchelli R, Feraud O, Vittet D, Baudier J (2005) Specific AHNAK expression in brain endothelial cells with barrier properties. *J Cell Physiol* **203:** 362-371

Ghose R, Shekhtman A, Goger MJ, Ji H, Cowburn D (2001) A novel, specific interaction involving the Csk SH3 domain and its natural ligand. *Nat Struct Biol* **8:** 998-1004

Ghosh S, Cox JV (2001) Dynamics of ankyrin-containing complexes in chicken embryonic erythroid cells: role of phosphorylation. *Mol Biol Cell* **12:** 3864-3874

Ghosh S, Dorsey FC, Cox JV (2002) CK2 constitutively associates with and phosphorylates chicken erythroid ankyrin and regulates its ability to bind to spectrin. *J Cell Sci* **115:** 4107-4115

Giglione C, Gonfloni S, Parmeggiani A (2001) Differential actions of p60c-Src and Lck kinases on the Ras regulators p120-GAP and GDP/GTP exchange factor CDC25Mm. *Eur J Biochem* **268:** 3275-3283

Gil OD, Sakurai T, Bradley AE, Fink MY, Cassella MR, Kuo JA, Felsenfeld DP (2003) Ankyrin binding mediates L1CAM interactions with static components of the cytoskeleton and inhibits retrograde movement of L1CAM on the cell surface. *J Cell Biol* **162:** 719-730

Golden A, Nemeth SP, Brugge JS (1986) Blood platelets express high levels of the pp60C-Src-specific tyrosine kinase activity. *Proceedings of the National Academy of Sciences of the United States of America* **83:** 852-856

Grabs D, Slepnev V, Zhou S, David C, Lynch M, Cantley L, DeCamilli P (1997) The SH3 domain of amphiphysin binds the proline-rich domain of dynamin at a single site that defines a new SH3 binding consensus sequence. *Journal of Biological Chemistry* **272:** 13419-13425

Graness A, Hanke S, Boehmer FD, Presek P, Liebmann C (2000) Protein-tyrosine-phosphatase-mediated epidermal growth factor (EGF) receptor transinactivation and EGF receptor-independent stimulation of mitogen-activated protein kinase by bradykinin in A431 cells. *Biochem J* **347:** 441-447

Grant SG, Karl KA, Kiebler MA, Kandel ER (1995) Focal adhesion kinase in the brain: novel subcellular localization and specific regulation by Fyn tyrosine kinase in mutant mice. *Genes Dev* **9:** 1909-1921

Grant SG, O'Dell TJ, Karl KA, Stein PL, Soriano P, Kandel ER (1992) Impaired long-term potentiation, spatial learning, and hippocampal development in fyn mutant mice. *Science* **258:** 1903-1910

Grantcharova VP, Riddle DS, Baker D (2000) Long-range order in the src SH3 folding transition state. *Proc Natl Acad Sci U S A* **97:** 7084-7089

Grasselli G, Mandolesi G, Strata P, Cesare P (2011) Impaired sprouting and axonal atrophy in cerebellar climbing fibres following in vivo silencing of the growth-associated protein GAP-43. *PLoS One* **6:** e20791

Groveman BR, Feng S, Fang XQ, Pflueger M, Lin SX, Bienkiewicz EA, Yu X (2012) The regulation of N-methyl-D-aspartate receptors by Src kinase. *FEBS J* **279:** 20-28

Groveman BR, Xue S, Marin V, Xu J, Ali MK, Bienkiewicz EA, Yu XM (2011) Roles of the SH2 and SH3 domains in the regulation of neuronal Src kinase functions. *FEBS J* **278:** 643-653

Grzesiek S, Bax A, Clore GM, Gronenborn AM, Hu JS, Kaufman J, Palmer I, Stahl SJ, Wingfield PT (1996) The solution structure of HIV-1 Nef reveals an unexpected fold and permits delineation of the binding surface for the SH3 domain of Hck tyrosine protein kinase. *Nat Struct Biol* **3:** 340-345

Guan H, Maness PF (2010) Perisomatic GABAergic innervation in prefrontal cortex is regulated by ankyrin interaction with the L1 cell adhesion molecule. *Cereb Cortex* **20:** 2684-2693

Hall A (1998) Rho GTPases and the actin cytoskeleton. *Science* **279:** 509-514

Hall A, Lalli G (2010) Rho and Ras GTPases in axon growth, guidance, and branching. *Cold Spring Harbor perspectives in biology* **2:** a001818

Haskell MD, Nickles AL, Agati JM, Su L, Dukes BD, Parsons SJ (2001) Phosphorylation of p190 on Tyr1105 by c-Src is necessary but not sufficient for EGF-induced actin disassembly in C3H10T1/2 fibroblasts. *J Cell Sci* **114:** 1699-1708

Hecker TP, Ding Q, Rege TA, Hanks SK, Gladson CL (2004) Overexpression of FAK promotes Ras activity through the formation of a FAK/p120RasGAP complex in malignant astrocytoma cells. *Oncogene* **23:** 3962-3971

Hieda Y, Tsukita S (1989) A new high molecular mass protein showing unique localization in desmosomal plaque. *J Cell Biol* **109:** 1511-1518

Hoffman EJ, Mintz CD, Wang S, McNickle DG, Salton SR, Benson DL (2008) Effects of ethanol on axon outgrowth and branching in developing rat cortical neurons. *Neuroscience* **157:** 556-565

Hoffman-Kim D, Kerner JA, Chen A, Xu A, Wang TF, Jay DG (2002) pp60(c-src) is a negative regulator of laminin-1-mediated neurite outgrowth in chick sensory neurons. *Mol Cell Neurosci* **21:** 81-93

Hohaus A, Person V, Behlke J, Schaper J, Morano I, Haase H (2002) The carboxyl-terminal region of ahnak provides a link between cardiac L-type Ca2+ channels and the actin-based cytoskeleton. *FASEB J* **16:** 1205-1216

Hornbeck P, Chabra I, Kornhauser J, Skrzypek E, Zhang B (2004) Phosphosite: A bioinformatics resource dedicated to physiological protein phosphorylation. *Proteomics* **4:** 1551-1561

Hou T, Li Y, Wang W (2011) Prediction of peptides binding to the PKA RIIalpha subunit using a hierarchical strategy. *Bioinformatics* **27:** 1814-1821

Hu MC, Qiu WR, Wang X, Meyer CF, Tan TH (1996) Human HPK1, a novel human hematopoietic progenitor kinase that activates the JNK/SAPK kinase cascade. *Genes Dev* **10:** 2251-2264

Huang C, Ni Y, Wang T, Gao Y, Haudenschild CC, Zhan X (1997) Down-regulation of the filamentous actin cross-linking activity of cortactin by Src-mediated tyrosine phosphorylation. *J Biol Chem* **272:** 13911-13915

Huang D, Sherman B, Lempicki R (2009a) Bioinformatics enrichment tools: paths toward the comprehensive functional analysis of large gene lists. *Nucleic Acids Research* **37:** 1-13

Huang D, Sherman B, Lempicki R (2009b) Systematic and integrative analysis of large gene lists using DAVID bioinformatics resources. *Nature Protocols* **4:** 44-57

Huang DW, Sherman BT, Stephens R, Baseler MW, Lane HC, Lempicki RA (2008a) DAVID gene ID conversion tool. *Bioinformation* **2:** 428-430

Huang EJ, Reichardt LF (2001) Neurotrophins: roles in neuronal development and function. *Annu Rev Neurosci* **24:** 677-736

Huang Y, de Morrée A, van Remoortere A, Bushby K, Frants RR, Dunnen JT, van der Maarel SM (2008b) Calpain 3 is a modulator of the dysferlin protein complex in skeletal muscle. *Hum Mol Genet* **17:** 1855-1866

Huang Y, Lu W, Ali DW, Pelkey KA, Pitcher GM, Lu YM, Aoto H, Roder JC, Sasaki T, Salter MW, MacDonald JF (2001) CAKbeta/Pyk2 kinase is a signaling link for induction of long-term potentiation in CA1 hippocampus. *Neuron* **29:** 485-496

Hubbard SR, Till JH (2000) Protein tyrosine kinase structure and function. *Annu Rev Biochem* **69:** 373-398

Hubbard SR, Wei L, Ellis L, Hendrickson WA (1994) Crystal structure of the tyrosine kinase domain of the human insulin receptor. *Nature* **372:** 746-754

Huber AB, Kolodkin AL, Ginty DD, Cloutier JF (2003) Signaling at the growth cone: ligand-receptor complexes and the control of axon growth and guidance. *Annu Rev Neurosci* **26:** 509-563

Hunter T (2009) Tyrosine phosphorylation: thirty years and counting. *Curr Opin Cell Biol* **21:** 140-146

Husi H, Ward MA, Choudhary JS, Blackstock WP, Grant SG (2000) Proteomic analysis of NMDA receptor-adhesion protein signaling complexes. *Nat Neurosci* **3:** 661-669

Ignelzi MA, Miller DR, Soriano P, Maness PF (1994) Impaired neurite outgrowth of src-minus cerebellar neurons on the cell adhesion molecule L1. *Neuron* **12:** 873-884

Imamoto A, Soriano P (1993) Disruption of the csk gene, encoding a negative regulator of Src family tyrosine kinases, leads to neural tube defects and embryonic lethality in mice. *Cell* **73:** 1117-1124

Inomata M, Takayama Y, Kiyama H, Nada S, Okada M, Nakagawa H (1994) Regulation of Src family kinases in the developing rat brain: correlation with their regulator kinase, Csk. *J Biochem* **116:** 386-392

Jan Y, Jan L (2010) Branching out: mechanisms of dendritic arborization. *Nature Reviews Neuroscience* **11:** 316-328

Jin J, Xie X, Chen C, Park JG, Stark C, James DA, Olhovsky M, Linding R, Mao Y, Pawson T (2009) Eukaryotic protein domains as functional units of cellular evolution. *Sci Signal* **2:** ra76

Kalia LV, Salter MW (2003) Interactions between Src family protein tyrosine kinases and PSD-95. *Neuropharmacology* **45:** 720-728

Kallunki P, Edelman GM, Jones FS (1997) Tissue-specific expression of the L1 cell adhesion molecule is modulated by the neural restrictive silencer element. *J Cell Biol* **138:** 1343-1354

Kami K, Takeya R, Sumimoto H, Kohda D (2002) Diverse recognition of non-PxxP peptide ligands by the SH3 domains from p67(phox), Grb2 and Pex13p. *EMBO J* **21:** 4268-4276

Kamiguchi H, Lemmon V (2000) Recycling of the cell adhesion molecule L1 in axonal growth cones. *J Neurosci* **20:** 3676-3686

Kamiguchi H, Yoshihara F (2001) The role of endocytic l1 trafficking in polarized adhesion and migration of nerve growth cones. *J Neurosci* **21:** 9194-9203

Kamps MP, Sefton BM (1988) Most of the substrates of oncogenic viral tyrosine protein kinases can be phosphorylated by cellular tyrosine protein kinases in normal cells. *Oncogene Res* **3:** 105-115

Kang H, Freund C, Duke-Cohan JS, Musacchio A, Wagner G, Rudd CE (2000) SH3 domain recognition of a proline-independent tyrosine-based RKxxYxxY motif in immune cell adaptor SKAP55. *EMBO J* **19:** 2889-2899

Kaplan KB, Bibbins KB, Swedlow JR, Arnaud M, Morgan DO, Varmus HE (1994) Association of the amino-terminal half of c-Src with focal adhesions alters their properties and is regulated by phosphorylation of tyrosine 527. *EMBO J* **13:** 4745-4756

Kaplan KB, Swedlow JR, Varmus HE, Morgan DO (1992) Association of p60c-src with endosomal membranes in mammalian fibroblasts. *J Cell Biol* **118:** 321-333

Kardinal C, Konkol B, Schulz A, Posern G, Lin H, Adermann K, Eulitz M, Estrov Z, Talpaz M, Arlinghaus R, Feller S (2000) Cell-penetrating SH3 domain blocker peptides inhibit proliferation of primary blast cells from CML patients. *Faseb Journal* **14:** 1529-1538

Kemp BE, Benjamini E, Krebs EG (1976) Synthetic hexapeptide substrates and inhibitors of 3':5'-cyclic AMP-dependent protein kinase. *Proc Natl Acad Sci U S A* **73:** 1038-1042

Kemp BE, Graves DJ, Benjamini E, Krebs EG (1977) Role of multiple basic residues in determining the substrate specificity of cyclic AMP-dependent protein kinase. *J Biol Chem* **252:** 4888-4894

Kennelly PJ (2001) Protein phosphatases--a phylogenetic perspective. *Chem Rev* **101:** 2291-2312

Ketschek A, Gallo G (2010) Nerve Growth Factor Induces Axonal Filopodia through Localized Microdomains of Phosphoinositide 3-Kinase Activity That Drive the Formation of Cytoskeletal Precursors to Filopodia. *Journal of Neuroscience* **30:** 12185-12197

Kim ST, Lim DS, Canman CE, Kastan MB (1999) Substrate specificities and identification of putative substrates of ATM kinase family members. *J Biol Chem* **274:** 37538-37543

King N, Hittinger CT, Carroll SB (2003) Evolution of key cell signaling and adhesion protein families predates animal origins. *Science* **301:** 361-363

King N, Westbrook MJ, Young SL, Kuo A, Abedin M, Chapman J, Fairclough S, Hellsten U, Isogai Y, Letunic I, Marr M, Pincus D, Putnam N, Rokas A, Wright KJ, Zuzow R, Dirks W, Good M, Goodstein D, Lemons D, Li W, Lyons JB, Morris A, Nichols S, Richter DJ, Salamov A, Sequencing JG, Bork P, Lim WA, Manning G, Miller WT, McGinnis W, Shapiro H, Tjian R, Grigoriev IV, Rokhsar D (2008) The genome of the choanoflagellate Monosiga brevicollis and the origin of metazoans. *Nature* **451:** 783-788

Klinghoffer RA, Sachsenmaier C, Cooper JA, Soriano P (1999) Src family kinases are required for integrin but not PDGFR signal transduction. *EMBO J* **18:** 2459-2471

Kmiecik TE, Shalloway D (1987) Activation and suppression of pp60c-src transforming ability by mutation of its primary sites of tyrosine phosphorylation. *Cell* **49:** 65-73

Knöll B, Drescher U (2004) Src family kinases are involved in EphA receptor-mediated retinal axon guidance. *J Neurosci* **24:** 6248-6257

Koegl M, Zlatkine P, Ley SC, Courtneidge SA, Magee AI (1994) Palmitoylation of multiple Src-family kinases at a homologous N-terminal motif. *Biochem J* **303 (Pt 3):** 749-753

Kolb G, Boiziau C (2005) Selection by phage display of peptides targeting the HIV-1 TAR element. *RNA Biol* **2:** 28-33

Kolyada A, Riley K, Herman I (2003) Rho GTPase signaling modulates cell shape and contractile phenotype in an isoactin-specific manner. *American Journal of Physiology-Cell Physiology* **285:** C1116-C1121

Komuro A, Masuda Y, Kobayashi K, Babbitt R, Gunel M, Flavell RA, Marchesi VT (2004) The AHNAKs are a class of giant propeller-like proteins that associate with calcium channel proteins of cardiomyocytes and other cells. *Proc Natl Acad Sci U S A* **101:** 4053-4058

Konopka JB, Watanabe SM, Witte ON (1984) An alteration of the human c-abl protein in K562 leukemia cells unmasks associated tyrosine kinase activity. *Cell* **37:** 1035-1042

Kotani T, Morone N, Yuasa S, Nada S, Okada M (2007) Constitutive activation of neuronal Src causes aberrant dendritic morphogenesis in mouse cerebellar Purkinje cells. *Neuroscience Research* **57:** 210-219

Kruman II, Culmsee C, Chan SL, Kruman Y, Guo Z, Penix L, Mattson MP (2000) Homocysteine elicits a DNA damage response in neurons that promotes apoptosis and hypersensitivity to excitotoxicity. *J Neurosci* **20:** 6920-6926

Kullander K, Klein R (2002) Mechanisms and functions of Eph and ephrin signalling. *Nat Rev Mol Cell Biol* **3:** 475-486

Kussick SJ, Basler K, Cooper JA (1993) Ras1-dependent signaling by ectopically-expressed Drosophila src gene product in the embryo and developing eye. *Oncogene* **8:** 2791-2803

Kussick SJ, Cooper JA (1992) Phosphorylation and regulatory effects of the carboxy terminus of a Drosophila src homolog. *Oncogene* **7:** 1577-1586

Köhr G, Seeburg PH (1996) Subtype-specific regulation of recombinant NMDA receptor-channels by protein tyrosine kinases of the src family. *J Physiol* **492 (Pt 2):** 445-452

Köles L, Wirkner K, Illes P (2001) Modulation of ionotropic glutamate receptor channels. *Neurochem Res* **26:** 925-932

Lai KO, Ip FC, Cheung J, Fu AK, Ip NY (2001) Expression of Eph receptors in skeletal muscle and their localization at the neuromuscular junction. *Mol Cell Neurosci* **17:** 1034-1047

Lambrechts A, Kwiatkowski AV, Lanier LM, Bear JE, Vandekerckhove J, Ampe C, Gertler FB (2000) cAMP-dependent protein kinase phosphorylation of EVL, a Mena/VASP relative, regulates its interaction with actin and SH3 domains. *J Biol Chem* **275:** 36143-36151

Lee CH, Leung B, Lemmon MA, Zheng J, Cowburn D, Kuriyan J, Saksela K (1995) A single amino acid in the SH3 domain of Hck determines its high affinity and specificity in binding to HIV-1 Nef protein. *EMBO J* **14:** 5006-5015

Lee DC, Jia Z (2009) Emerging structural insights into bacterial tyrosine kinases. *Trends Biochem Sci* **34:** 351-357

Lee FS, Chao MV (2001) Activation of Trk neurotrophin receptors in the absence of neurotrophins. *Proc Natl Acad Sci U S A* **98:** 3555-3560

Lee FS, Rajagopal R, Chao MV (2002) Distinctive features of Trk neurotrophin receptor transactivation by G protein-coupled receptors. *Cytokine Growth Factor Rev* **13:** 11-17

Lerner EC, Smithgall TE (2002) SH3-dependent stimulation of Src-family kinase autophosphorylation without tail release from the SH2 domain in vivo. *Nat Struct Biol* **9:** 365-369

Levi-Montalcini R (1987) The nerve growth factor: thirty-five years later. *EMBO J* **6:** 1145-1154

Levy JB, Brugge JS (1989) Biological and biochemical properties of the c-src+ gene product overexpressed in chicken embryo fibroblasts. *Mol Cell Biol* **9:** 3332-3341

Li T, Han D, Chen J, Yu XJ, Zhang GY (2008a) Neuroprotection against ischemic brain injury by knockdown of hematopietic progenitor kinase 1 expression. *Neuroreport* **19:** 647-651

Li T, Yu XJ, Zhang GY (2008b) Tyrosine phosphorylation of HPK1 by activated Src promotes ischemic brain injury in rat hippocampal CA1 region. *FEBS Lett* **582:** 1894-1900

Li W, Lee J, Vikis HG, Lee SH, Liu G, Aurandt J, Shen TL, Fearon ER, Guan JL, Han M, Rao Y, Hong K, Guan KL (2004) Activation of FAK and Src are receptor-proximal events required for netrin signaling. *Nat Neurosci* **7:** 1213-1221

Lim Y, Han I, Jeon J, Park H, Bahk YY, Oh ES (2004) Phosphorylation of focal adhesion kinase at tyrosine 861 is crucial for Ras transformation of fibroblasts. *J Biol Chem* **279:** 29060-29065

Lim Y, Lim ST, Tomar A, Gardel M, Bernard-Trifilo JA, Chen XL, Uryu SA, Canete-Soler R, Zhai J, Lin H, Schlaepfer WW, Nalbant P, Bokoch G, Ilic D, Waterman-Storer C, Schlaepfer DD (2008) PyK2 and FAK connections to p190Rho guanine nucleotide exchange factor regulate RhoA activity, focal adhesion formation, and cell motility. *J Cell Biol* **180:** 187-203

Linstedt AD, Vetter ML, Bishop JM, Kelly RB (1992) Specific association of the proto-oncogene product pp60c-src with an intracellular organelle, the PC12 synaptic vesicle. *J Cell Biol* **117:** 1077-1084

Liu G, Beggs H, Jurgensen C, Park HT, Tang H, Gorski J, Jones KR, Reichardt LF, Wu J, Rao Y (2004) Netrin requires focal adhesion kinase and Src family kinases for axon outgrowth and attraction. *Nat Neurosci* **7:** 1222-1232

Lock P, Ralph S, Stanley E, Boulet I, Ramsay R, Dunn AR (1991) Two isoforms of murine hck, generated by utilization of alternative translational initiation codons, exhibit different patterns of subcellular localization. *Mol Cell Biol* **11:** 4363-4370

Lowell CA, Soriano P (1996) Knockouts of Src-family kinases: stiff bones, wimpy T cells, and bad memories. *Genes Dev* **10:** 1845-1857

Lu YM, Roder JC, Davidow J, Salter MW (1998) Src activation in the induction of long-term potentiation in CA1 hippocampal neurons. *Science* **279:** 1363-1367

Mahdavi MA, Lin YH (2007) Prediction of protein-protein interactions using protein signature profiling. *Genomics Proteomics Bioinformatics* **5:** 177-186

Malhotra JD, Tsiotra P, Karagogeos D, Hortsch M (1998) Cis-activation of L1-mediated ankyrin recruitment by TAG-1 homophilic cell adhesion. *J Biol Chem* **273:** 33354-33359

Mallavarapu A, Mitchison T (1999) Regulated actin cytoskeleton assembly at filopodium tips controls their extension and retraction. *J Cell Biol* **146:** 1097-1106

Maness PF (1992) Nonreceptor protein tyrosine kinases associated with neuronal development. *Dev Neurosci* **14:** 257-270

Maness PF, Shores CG, Ignelzi M (1990) Localization of the normal cellular src protein to the growth cone of differentiating neurons in brain and retina. *Adv Exp Med Biol* **265:** 117-125

Maness PF, Sorge LK, Fults DW (1986) An early developmental phase of pp60c-src expression in the neural ectoderm. *Dev Biol* **117:** 83-89

Manning G, Plowman GD, Hunter T, Sudarsanam S (2002a) Evolution of protein kinase signaling from yeast to man. *Trends Biochem Sci* **27:** 514-520

Manning G, Whyte DB, Martinez R, Hunter T, Sudarsanam S (2002b) The protein kinase complement of the human genome. *Science* **298:** 1912-1934

Manning G, Young SL, Miller WT, Zhai Y (2008) The protist, Monosiga brevicollis, has a tyrosine kinase signaling network more elaborate and diverse than found in any known metazoan. *Proc Natl Acad Sci U S A* **105:** 9674-9679

Marin V, Groveman BR, Qiao H, Xu J, Ali MK, Fang XQ, Lin SX, Rizkallah R, Hurt MH, Bienkiewicz EA, Yu XM (2010) Characterization of neuronal Src kinase purified from a bacterial expression system. *Protein Expr Purif* **74:** 289-297

Marshall CJ (1995) Specificity of receptor tyrosine kinase signaling: transient versus sustained extracellular signal-regulated kinase activation. *Cell* **80:** 179-185

Marsick BM, San Miguel-Ruiz JE, Letourneau PC (2012) Activation of ezrin/radixin/moesin mediates attractive growth cone guidance through regulation of growth cone actin and adhesion receptors. *J Neurosci* **32:** 282-296

Marth JD, Cooper JA, King CS, Ziegler SF, Tinker DA, Overell RW, Krebs EG, Perlmutter RM (1988) Neoplastic transformation induced by an activated lymphocyte-specific protein tyrosine kinase (pp56lck). *Mol Cell Biol* **8:** 540-550

Martinez R, Mathey-Prevot B, Bernards A, Baltimore D (1987) Neuronal pp60c-src contains a six-amino acid insertion relative to its non-neuronal counterpart. *Science* **237:** 411-415

Masukawa LM, O'Connor WM, Lynott J, Burdette LJ, Uruno K, McGonigle P, O'Connor MJ (1995) Longitudinal variation in cell density and mossy fiber reorganization in the dentate gyrus from temporal lobe epileptic patients. *Brain Res* **678:** 65-75

Matsunaga T, Shirasawa H, Enomoto H, Yoshida H, Iwai J, Tanabe M, Kawamura K, Etoh T, Ohnuma N (1998) Neuronal src and trk a protooncogene expression in neuroblastomas and patient prognosis. *International Journal of Cancer* **79:** 226-231

Matsunaga T, Shirasawa H, Tanabe M, Ohnuma N, Takahashi H, Simizu B (1993) Expression of alternatively spliced src messenger RNAs related to neuronal differentiation in human neuroblastomas. *Cancer Res* **53:** 3179-3185

Mayer BJ (2001) SH3 domains: complexity in moderation. *J Cell Sci* **114:** 1253-1263

Mayer BJ, Hirai H, Sakai R (1995) Evidence that SH2 domains promote processive phosphorylation by protein-tyrosine kinases. In *Curr Biol* Vol. 5, pp 296-305. England

Meijering E, Jacob M, Sarria JC, Steiner P, Hirling H, Unser M (2004) Design and validation of a tool for neurite tracing and analysis in fluorescence microscopy images. *Cytometry A* **58:** 167-176

Messa M, Congia S, Defranchi E, Valtorta F, Fassio A, Onofri F, Benfenati F (2010) Tyrosine phosphorylation of synapsin I by Src regulates synaptic-vesicle trafficking. *J Cell Sci* **123:** 2256-2265

Messina S, Onofri F, Bongiorno-Borbone L, Giovedì S, Valtorta F, Girault JA, Benfenati F (2003) Specific interactions of neuronal focal adhesion kinase isoforms with Src kinases and amphiphysin. *J Neurochem* **84:** 253-265

Miller ML, Jensen LJ, Diella F, Jørgensen C, Tinti M, Li L, Hsiung M, Parker SA, Bordeaux J, Sicheritz-Ponten T, Olhovsky M, Pasculescu A, Alexander J, Knapp S, Blom N, Bork P, Li S, Cesareni G, Pawson T, Turk BE, Yaffe MB, Brunak S, Linding R (2008) Linear motif atlas for phosphorylation-dependent signaling. *Sci Signal* **1:** ra2

Miller WE, Maudsley S, Ahn S, Khan KD, Luttrell LM, Lefkowitz RJ (2000) beta-arrestin1 interacts with the catalytic domain of the tyrosine kinase c-SRC. Role of beta-arrestin1-dependent targeting of c-SRC in receptor endocytosis. *J Biol Chem* **275:** 11312-11319

Miyagi Y, Yamashita T, Fukaya M, Sonoda T, Okuno T, Yamada K, Watanabe M, Nagashima Y, Aoki I, Okuda K, Mishina M, Kawamoto S (2002) Delphilin: a novel PDZ and formin homology domain-containing protein that synaptically colocalizes and interacts with glutamate receptor delta 2 subunit. *J Neurosci* **22:** 803-814

Moarefi I, LaFevre-Bernt M, Sicheri F, Huse M, Lee CH, Kuriyan J, Miller WT (1997) Activation of the Src-family tyrosine kinase Hck by SH3 domain displacement. *Nature* **385:** 650-653

Modafferi EF, Black DL (1997) A complex intronic splicing enhancer from the c-src pre-mRNA activates inclusion of a heterologous exon. *Mol Cell Biol* **17:** 6537-6545

Molloy CJ, Bottaro DP, Fleming TP, Marshall MS, Gibbs JB, Aaronson SA (1989) PDGF induction of tyrosine phosphorylation of GTPase activating protein. *Nature* **342:** 711-714

Mongioví AM, Romano PR, Panni S, Mendoza M, Wong WT, Musacchio A, Cesareni G, Di Fiore PP (1999) A novel peptide-SH3 interaction. *EMBO J* **18:** 5300-5309

Moniakis J, Funamoto S, Fukuzawa M, Meisenhelder J, Araki T, Abe T, Meili R, Hunter T, Williams J, Firtel RA (2001) An SH2-domain-containing kinase negatively regulates the phosphatidylinositol-3 kinase pathway. *Genes Dev* **15:** 687-698

Moon MS, Gomez TM (2010) Balanced Vav2 GEF activity regulates neurite outgrowth and branching in vitro and in vivo. *Mol Cell Neurosci* **44:** 118-128

Moore SW, Tessier-Lavigne M, Kennedy TE (2007) Netrins and their receptors. *Adv Exp Med Biol* **621:** 17-31

Moran MF, Koch CA, Anderson D, Ellis C, England L, Martin GS, Pawson T (1990) Src homology region 2 domains direct protein-protein interactions in signal transduction. *Proc Natl Acad Sci U S A* **87:** 8622-8626

Morgan DO, Kaplan JM, Bishop JM, Varmus HE (1989) Mitosis-specific phosphorylation of p60c-src by p34cdc2-associated protein kinase. *Cell* **57:** 775-786

Morris NP, Watt SL, Davis JM, Bächinger HP (1990) Unfolding intermediates in the triple helix to coil transition of bovine type XI collagen and human type V collagens alpha 1(2) alpha 2 and alpha 1 alpha 2 alpha 3. *J Biol Chem* **265:** 10081-10087

Moss SJ, Gorrie GH, Amato A, Smart TG (1995) Modulation of GABAA receptors by tyrosine phosphorylation. *Nature* **377:** 344-348

Mukherjee A, Arnaud L, Cooper JA (2003) Lipid-dependent recruitment of neuronal Src to lipid rafts in the brain. *J Biol Chem* **278:** 40806-40814

Murphy SM, Bergman M, Morgan DO (1993) Suppression of c-Src activity by C-terminal Src kinase involves the c-Src SH2 and SH3 domains: analysis with Saccharomyces cerevisiae. *Mol Cell Biol* **13:** 5290-5300

Musacchio A, Saraste M, Wilmanns M (1994) High-resolution crystal structures of tyrosine kinase SH3 domains complexed with proline-rich peptides. *Nat Struct Biol* **1:** 546-551

Nada S, Okada M, MacAuley A, Cooper JA, Nakagawa H (1991) Cloning of a complementary DNA for a protein-tyrosine kinase that specifically phosphorylates a negative regulatory site of p60c-src. *Nature* **351:** 69-72

Nada S, Yagi T, Takeda H, Tokunaga T, Nakagawa H, Ikawa Y, Okada M, Aizawa S (1993) Constitutive activation of Src family kinases in mouse embryos that lack Csk. *Cell* **73:** 1125-1135

Nakamura F, Kalb RG, Strittmatter SM (2000) Molecular basis of semaphorin-mediated axon guidance. *J Neurobiol* **44:** 219-229

Nakazawa T, Komai S, Tezuka T, Hisatsune C, Umemori H, Semba K, Mishina M, Manabe T, Yamamoto T (2001) Characterization of Fyn-mediated tyrosine phosphorylation sites on GluR epsilon 2 (NR2B) subunit of the N-methyl-D-aspartate receptor. *J Biol Chem* **276:** 693-699

Nakazawa T, Komai S, Watabe AM, Kiyama Y, Fukaya M, Arima-Yoshida F, Horai R, Sudo K, Ebine K, Delawary M, Goto J, Umemori H, Tezuka T, Iwakura Y, Watanabe M, Yamamoto T, Manabe T (2006) NR2B tyrosine phosphorylation modulates fear learning as well as amygdaloid synaptic plasticity. *EMBO J* **25:** 2867-2877

Needham LK, Thelen K, Maness PF (2001) Cytoplasmic domain mutations of the L1 cell adhesion molecule reduce L1-ankyrin interactions. *J Neurosci* **21:** 1490-1500

Nishimura K, Yoshihara F, Tojima T, Ooashi N, Yoon W, Mikoshiba K, Bennett V, Kamiguchi H (2003a) L1-dependent neuritogenesis involves ankyrinB that mediates L1-CAM coupling with retrograde actin flow. *J Cell Biol* **163:** 1077-1088

Nishimura T, Fukata Y, Kato K, Yamaguchi T, Matsuura Y, Kamiguchi H, Kaibuchi K (2003b) CRMP-2 regulates polarized Numb-mediated endocytosis for axon growth. *Nat Cell Biol* **5:** 819-826

O'Leary DD, Terashima T (1988) Cortical axons branch to multiple subcortical targets by interstitial axon budding: implications for target recognition and "waiting periods". *Neuron* **1:** 901-910

O'Shaughnessy J, Deseau V, Amini S, Rosen N, Bolen JB (1987) Analysis of the c-src gene product structure, abundance, and protein kinase activity in human neuroblastoma and glioblastoma cells. *Oncogene Res* **2:** 1-18

Obenauer J, Cantley L, Yaffe M (2003) Scansite 2.0: proteome-wide prediction of cell signaling interactions using short sequence motifs. *Nucleic Acids Research* **31:** 3635-3641

Okada M, Nada S, Yamanashi Y, Yamamoto T, Nakagawa H (1991) CSK: a protein-tyrosine kinase involved in regulation of src family kinases. *J Biol Chem* **266:** 24249-24252

Okano-Uchida T, Himi T, Komiya Y, Ishizaki Y (2004) Cerebellar granule cell precursors can differentiate into astroglial cells. *Proc Natl Acad Sci U S A* **101:** 1211-1216

Oleszewski M, Gutwein P, von der Lieth W, Rauch U, Altevogt P (2000) Characterization of the L1-neurocan-binding site. Implications for L1-L1 homophilic binding. *J Biol Chem* **275:** 34478-34485

Ottilie S, Raulf F, Barnekow A, Hannig G, Schartl M (1992) Multiple src-related kinase genes, srk1-4, in the fresh water sponge Spongilla lacustris. *Oncogene* **7:** 1625-1630

Ouwens DM, de Ruiter ND, van der Zon GC, Carter AP, Schouten J, van der Burgt C, Kooistra K, Bos JL, Maassen JA, van Dam H (2002) Growth factors can activate ATF2 via a two-step mechanism: phosphorylation of Thr71 through the Ras-MEK-ERK pathway and of Thr69 through RalGDS-Src-p38. *EMBO J* **21:** 3782-3793

Owen D, Wigge P, Vallis Y, Moore J, Evans P, McMahon H (1998) Crystal structure of the amphiphysin-2 SH3 domain and its role in the prevention of dynamin ring formation. *Embo Journal* **17:** 5273-5285

Paige LA, Nadler MJ, Harrison ML, Cassady JM, Geahlen RL (1993) Reversible palmitoylation of the protein-tyrosine kinase p56lck. *J Biol Chem* **268:** 8669-8674

Parri M, Buricchi F, Giannoni E, Grimaldi G, Mello T, Raugei G, Ramponi G, Chiarugi P (2007) EphrinA1 activates a Src/focal adhesion kinase-mediated motility response leading to rho-dependent actino/myosin contractility. *J Biol Chem* **282:** 19619-19628

Parsons JT, Parsons SJ (1997) Src family protein tyrosine kinases: cooperating with growth factor and adhesion signaling pathways. *Curr Opin Cell Biol* **9:** 187-192

Pawson T (2004) Specificity in signal transduction: from phosphotyrosine-SH2 domain interactions to complex cellular systems. *Cell* **116:** 191-203

Pawson T, Scott JD (2005) Protein phosphorylation in signaling--50 years and counting. *Trends Biochem Sci* **30:** 286-290

Pellicena P, Miller WT (2001) Processive phosphorylation of p130Cas by Src depends on SH3-polyproline interactions. *J Biol Chem* **276:** 28190-28196

Pellicena P, Stowell KR, Miller WT (1998) Enhanced phosphorylation of Src family kinase substrates containing SH2 domain binding sites. *J Biol Chem* **273:** 15325-15328

Petit V, Boyer B, Lentz D, Turner CE, Thiery JP, Vallés AM (2000) Phosphorylation of tyrosine residues 31 and 118 on paxillin regulates cell migration through an association with CRK in NBT-II cells. *J Cell Biol* **148:** 957-970

Pincus D, Letunic I, Bork P, Lim WA (2008) Evolution of the phospho-tyrosine signaling machinery in premetazoan lineages. *Proc Natl Acad Sci U S A* **105:** 9680-9684

Pleiman CM, Clark MR, Gauen LK, Winitz S, Coggeshall KM, Johnson GL, Shaw AS, Cambier JC (1993) Mapping of sites on the Src family protein tyrosine kinases p55blk, p59fyn, and p56lyn which interact with the effector molecules phospholipase C-gamma 2, microtubule-associated protein kinase, GTPase-activating protein, and phosphatidylinositol 3-kinase. *Mol Cell Biol* **13:** 5877-5887

Polleux F, Snider W (2010) Initiating and growing an axon. *Cold Spring Harb Perspect Biol* **2:** a001925

Porter M, Schindler T, Kuriyan J, Miller WT (2000) Reciprocal regulation of Hck activity by phosphorylation of Tyr(527) and Tyr(416). Effect of introducing a high affinity intramolecular SH2 ligand. *J Biol Chem* **275:** 2721-2726

Powell SK, Rivas RJ, Rodriguez-Boulan E, Hatten ME (1997) Development of polarity in cerebellar granule neurons. *J Neurobiol* **32:** 223-236

Pungaliya PP, Bai Y, Lipinski K, Anand VS, Sen S, Brown EL, Bates B, Reinhart PH, West AB, Hirst WD, Braithwaite SP (2010) Identification and characterization of a leucine-rich repeat kinase 2 (LRRK2) consensus phosphorylation motif. *PLoS One* **5:** e13672

Pyper JM, Bolen JB (1989) Neuron-specific splicing of C-SRC RNA in human brain. *J Neurosci Res* **24:** 89-96

Pyper JM, Bolen JB (1990) Identification of a novel neuronal C-SRC exon expressed in human brain. *Mol Cell Biol* **10:** 2035-2040

Qi JF, Wang JF, Romanyuk E, Siu CH (2006) Involvement of Src family kinases in N-cadherin phosphorylation and beta-catenin dissociation during transendothelial migration of melanoma cells. *Molecular Biology of the Cell* **17:** 1261-1272

Raulf F, Robertson SM, Schartl M (1989) Evolution of the neuron-specific alternative splicing product of the c-src proto-oncogene. *J Neurosci Res* **24:** 81-88

Reimand J, Hui S, Jain S, Law B, Bader GD (2012) Domain-mediated protein interaction prediction: From genome to network. *FEBS Lett* **586:** 2751-2763

Ren XD, Kiosses WB, Sieg DJ, Otey CA, Schlaepfer DD, Schwartz MA (2000) Focal adhesion kinase suppresses Rho activity to promote focal adhesion turnover. *J Cell Sci* **113 (Pt 20):** 3673-3678

Resh MD (1994) Myristylation and palmitylation of Src family members: the fats of the matter. *Cell* **76:** 411-413

Reynolds CH, Garwood CJ, Wray S, Price C, Kellie S, Perera T, Zvelebil M, Yang A, Sheppard PW, Varndell IM, Hanger DP, Anderton BH (2008) Phosphorylation regulates tau interactions with Src homology 3 domains of phosphatidylinositol 3-kinase, phospholipase Cgamma1, Grb2, and Src family kinases. *J Biol Chem* **283:** 18177-18186

Rhodes RK, Miller EJ (1978) Physicochemical characterization and molecular organization of the collagen A and B chains. *Biochemistry* **17:** 3442-3448

Rickles RJ, Botfield MC, Weng Z, Taylor JA, Green OM, Brugge JS, Zoller MJ (1994) Identification of Src, Fyn, Lyn, PI3K and Abl SH3 domain ligands using phage display libraries. *EMBO J* **13:** 5598-5604

Rickles RJ, Botfield MC, Zhou XM, Henry PA, Brugge JS, Zoller MJ (1995) Phage display selection of ligand residues important for Src homology 3 domain binding specificity. *Proc Natl Acad Sci U S A* **92:** 10909-10913

Ridley AJ, Schwartz MA, Burridge K, Firtel RA, Ginsberg MH, Borisy G, Parsons JT, Horwitz AR (2003) Cell migration: integrating signals from front to back. *Science* **302:** 1704-1709

Ringstedt T, Lagercrantz H, Persson H (1993) Expression of members of the trk family in the developing postnatal rat brain. *Brain Res Dev Brain Res* **72:** 119-131

Rizzo MA, Springer GH, Granada B, Piston DW (2004) An improved cyan fluorescent protein variant useful for FRET. In *Nat Biotechnol* Vol. 22, pp 445-449. United States

Robbins SM, Quintrell NA, Bishop JM (1995) Myristoylation and differential palmitoylation of the HCK protein-tyrosine kinases govern their attachment to membranes and association with caveolae. *Mol Cell Biol* **15:** 3507-3515

Roche S, Fumagalli S, Courtneidge SA (1995) Requirement for Src family protein tyrosine kinases in G2 for fibroblast cell division. *Science* **269:** 1567-1569

Rodrigues GA, Park M (1994) Oncogenic activation of tyrosine kinases. *Curr Opin Genet Dev* **4:** 15-24

Rudolph P, Lappe T, Hero B, Berthold F, Parwaresch R, Harms D, Schmidt D (1997) Prognostic significance of the proliferative activity in neuroblastoma. *Am J Pathol* **150:** 133-145

Saffell JL, Williams EJ, Mason IJ, Walsh FS, Doherty P (1997) Expression of a dominant negative FGF receptor inhibits axonal growth and FGF receptor phosphorylation stimulated by CAMs. *Neuron* **18:** 231-242

Sai X, Kawamura Y, Kokame K, Yamaguchi H, Shiraishi H, Suzuki R, Suzuki T, Kawaichi M, Miyata T, Kitamura T, De Strooper B, Yanagisawa K, Komano H (2002) Endoplasmic reticulum stress-inducible protein, Herp, enhances presenilin-mediated generation of amyloid beta-protein. *J Biol Chem* **277:** 12915-12920

Saito T, Nakatsuji N (2001) Efficient gene transfer into the embryonic mouse brain using in vivo electroporation. *Dev Biol* **240:** 237-246

Saksela K, Cheng G, Baltimore D (1995) Proline-rich (PxxP) motifs in HIV-1 Nef bind to SH3 domains of a subset of Src kinases and are required for the enhanced growth of Nef+ viruses but not for down-regulation of CD4. *EMBO J* **14:** 484-491

Saksela K, Permi P (2012) SH3 domain ligand binding: What's the consensus and where's the specificity? *FEBS Lett* **586:** 2609-2614

Sakurai T, Gil OD, Whittard JD, Gazdoiu M, Joseph T, Wu J, Waksman A, Benson DL, Salton SR, Felsenfeld DP (2008) Interactions between the L1 cell adhesion molecule and ezrin support traction-force generation and can be regulated by tyrosine phosphorylation. *J Neurosci Res* **86:** 2602-2614

Sakurai T, Lustig M, Babiarz J, Furley AJ, Tait S, Brophy PJ, Brown SA, Brown LY, Mason CA, Grumet M (2001) Overlapping functions of the cell adhesion molecules Nr-CAM and L1 in cerebellar granule cell development. *J Cell Biol* **154:** 1259-1273

Salter MW, Kalia LV (2004) Src kinases: a hub for NMDA receptor regulation. *Nat Rev Neurosci* **5:** 317-328

Sandilands E, Brunton VG, Frame MC (2007) The membrane targeting and spatial activation of Src, Yes and Fyn is influenced by palmitoylation and distinct RhoB/RhoD endosome requirements. *J Cell Sci* **120:** 2555-2564

Sandilands E, Cans C, Fincham VJ, Brunton VG, Mellor H, Prendergast GC, Norman JC, Superti-Furga G, Frame MC (2004) RhoB and actin polymerization coordinate Src activation with endosome-mediated delivery to the membrane. In *Dev Cell* Vol. 7, pp 855-869. United States

Santoro B, Grant SG, Bartsch D, Kandel ER (1997) Interactive cloning with the SH3 domain of N-src identifies a new brain specific ion channel protein, with homology to eag and cyclic nucleotide-gated channels. *Proc Natl Acad Sci U S A* **94:** 14815-14820

Sartor O, Robbins KC (1993) Substrate specificity for normal but not mutationally activated variants of src family kinases. *J Biol Chem* **268:** 21014-21020

Schaefer AW, Kamei Y, Kamiguchi H, Wong EV, Rapoport I, Kirchhausen T, Beach CM, Landreth G, Lemmon SK, Lemmon V (2002) L1 endocytosis is controlled by a phosphorylation-dephosphorylation cycle stimulated by outside-in signaling by L1. *J Cell Biol* **157:** 1223-1232

Schafer MK, Frotscher M (2012) Role of L1CAM for axon sprouting and branching. *Cell Tissue Res* **349:** 39-48

Schaller MD, Hildebrand JD, Shannon JD, Fox JW, Vines RR, Parsons JT (1994) Autophosphorylation of the focal adhesion kinase, pp125FAK, directs SH2-dependent binding of pp60src. *Mol Cell Biol* **14:** 1680-1688

Schieven G, Thorner J, Martin GS (1986) Protein-tyrosine kinase activity in Saccharomyces cerevisiae. *Science* **231:** 390-393

Schmidt H, Rathjen FG (2010) Signalling mechanisms regulating axonal branching in vivo. *Bioessays* **32:** 977-985

Schmidt H, Stonkute A, Jüttner R, Schäffer S, Buttgereit J, Feil R, Hofmann F, Rathjen FG (2007) The receptor guanylyl cyclase Npr2 is essential for sensory axon bifurcation within the spinal cord. *J Cell Biol* **179:** 331-340

Schmidt JW, Brugge JS, Nelson WJ (1992) pp60src tyrosine kinase modulates P19 embryonal carcinoma cell fate by inhibiting neuronal but not epithelial differentiation. *J Cell Biol* **116:** 1019-1033

Schmitt JM, Stork PJ (2002) PKA phosphorylation of Src mediates cAMP's inhibition of cell growth via Rap1. *Mol Cell* **9:** 85-94

Schreiner SJ, Schiavone AP, Smithgall TE (2002) Activation of STAT3 by the Src family kinase Hck requires a functional SH3 domain. *J Biol Chem* **277:** 45680-45687

Schäfer MK, Nam YC, Moumen A, Keglowich L, Bouché E, Küffner M, Bock HH, Rathjen FG, Raoul C, Frotscher M (2010) L1 syndrome mutations impair neuronal L1 function at different levels by divergent mechanisms. *Neurobiol Dis* **40:** 222-237

Scotland P, Zhou D, Benveniste H, Bennett V (1998) Nervous system defects of AnkyrinB (-/-) mice suggest functional overlap between the cell adhesion molecule L1 and 440-kD AnkyrinB in premyelinated axons. *J Cell Biol* **143:** 1305-1315

Scott MP, Miller WT (2000) A peptide model system for processive phosphorylation by Src family kinases. *Biochemistry* **39:** 14531-14537

Seibler J, Kleinridders A, Küter-Luks B, Niehaves S, Brüning JC, Schwenk F (2007) Reversible gene knockdown in mice using a tight, inducible shRNA expression system. *Nucleic Acids Res* **35:** e54

Serafini T, Kennedy TE, Galko MJ, Mirzayan C, Jessell TM, Tessier-Lavigne M (1994) The netrins define a family of axon outgrowth-promoting proteins homologous to C. elegans UNC-6. *Cell* **78:** 409-424

Shenoy S, Choi JK, Bagrodia S, Copeland TD, Maller JL, Shalloway D (1989) Purified maturation promoting factor phosphorylates pp60c-src at the sites phosphorylated during fibroblast mitosis. *Cell* **57:** 763-774

Shenoy-Scaria AM, Gauen LK, Kwong J, Shaw AS, Lublin DM (1993) Palmitylation of an amino-terminal cysteine motif of protein tyrosine kinases p56lck and p59fyn mediates interaction with glycosyl-phosphatidylinositol-anchored proteins. *Mol Cell Biol* **13:** 6385-6392

Sholl DA (1953) Dendritic organization in the neurons of the visual and motor cortices of the cat. *J Anat* **87:** 387-406

Shtivelman E, Bishop JM (1993) The human gene AHNAK encodes a large phosphoprotein located primarily in the nucleus. *J Cell Biol* **120:** 625-630

Sicheri F, Moarefi I, Kuriyan J (1997) Crystal structure of the Src family tyrosine kinase Hck. *Nature* **385:** 602-609

Sieg DJ, Hauck CR, Ilic D, Klingbeil CK, Schaefer E, Damsky CH, Schlaepfer DD (2000) FAK integrates growth-factor and integrin signals to promote cell migration. *Nat Cell Biol* **2:** 249-256

Silletti S, Mei F, Sheppard D, Montgomery AM (2000) Plasmin-sensitive dibasic sequences in the third fibronectin-like domain of L1-cell adhesion molecule (CAM) facilitate homomultimerization and concomitant integrin recruitment. *J Cell Biol* **149:** 1485-1502

Smart JE, Oppermann H, Czernilofsky AP, Purchio AF, Erikson RL, Bishop JM (1981) Characterization of sites for tyrosine phosphorylation in the transforming protein of Rous sarcoma virus (pp60v-src) and its normal cellular homologue (pp60c-src). *Proc Natl Acad Sci U S A* **78:** 6013-6017

Soderling TR, Derkach VA (2000) Postsynaptic protein phosphorylation and LTP. *Trends Neurosci* **23:** 75-80

Somani AK, Bignon JS, Mills GB, Siminovitch KA, Branch DR (1997) Src kinase activity is regulated by the SHP-1 protein-tyrosine phosphatase. *J Biol Chem* **272:** 21113-21119

Songyang Z (1999) Recognition and regulation of primary-sequence motifs by signaling modular domains. *Prog Biophys Mol Biol* **71:** 359-372

Songyang Z, Cantley LC (2004) ZIP codes for delivering SH2 domains. *Cell* **116:** S41-43, 42 p following S48

Songyang Z, Carraway KL, 3rd, Eck MJ, Harrison SC, Feldman RA, Mohammadi M, Schlessinger J, Hubbard SR, Smith DP, Eng C, et al. (1995a) Catalytic specificity of protein-tyrosine kinases is critical for selective signalling. *Nature* **373:** 536-539

Songyang Z, Carraway KL, Eck MJ, Harrison SC, Feldman RA, Mohammadi M, Schlessinger J, Hubbard SR, Smith DP, Eng C (1995b) Catalytic specificity of protein-tyrosine kinases is critical for selective signalling. *Nature* **373:** 536-539

Songyang Z, Shoelson SE, Chaudhuri M, Gish G, Pawson T, Haser WG, King F, Roberts T, Ratnofsky S, Lechleider RJ (1993a) SH2 domains recognize specific phosphopeptide sequences. *Cell* **72:** 767-778

Songyang Z, Shoelson SE, Chaudhuri M, Gish G, Pawson T, Haser WG, King F, Roberts T, Ratnofsky S, Lechleider RJ, et al. (1993b) SH2 domains recognize specific phosphopeptide sequences. *Cell* **72:** 767-778

Sotirellis N, Johnson TM, Hibbs ML, Stanley IJ, Stanley E, Dunn AR, Cheng HC (1995) Autophosphorylation induces autoactivation and a decrease in the Src homology 2 domain accessibility of the Lyn protein kinase. *J Biol Chem* **270:** 29773-29780

Sparks AB, Rider JE, Hoffman NG, Fowlkes DM, Quillam LA, Kay BK (1996) Distinct ligand preferences of Src homology 3 domains from Src, Yes, Abl, Cortactin, p53bp2, PLCgamma, Crk, and Grb2. *Proc Natl Acad Sci U S A* **93:** 1540-1544

Spencer DM, Graef I, Austin DJ, Schreiber SL, Crabtree GR (1995) A general strategy for producing conditional alleles of Src-like tyrosine kinases. *Proc Natl Acad Sci U S A* **92:** 9805-9809

Sperber BR, Boyle-Walsh EA, Engleka MJ, Gadue P, Peterson AC, Stein PL, Scherer SS, McMorris FA (2001) A unique role for Fyn in CNS myelination. *J Neurosci* **21:** 2039-2047

Sperry RW (1963) Chemoaffinity in the orderly growth of nerve fiber patterns and connections. *Proc Natl Acad Sci U S A* **50:** 703-710

Stein PL, Vogel H, Soriano P (1994) Combined deficiencies of Src, Fyn, and Yes tyrosine kinases in mutant mice. *Genes Dev* **8:** 1999-2007

Subauste MC, Pertz O, Adamson ED, Turner CE, Junger S, Hahn KM (2004) Vinculin modulation of paxillin-FAK interactions regulates ERK to control survival and motility. *J Cell Biol* **165:** 371-381

Sudol M, Hanafusa H (1986) Cellular proteins homologous to the viral yes gene product. *Mol Cell Biol* **6:** 2839-2846

Sugimoto Y, Erikson E, Graziani Y, Erikson RL (1985) Inter- and intramolecular interactions of highly purified Rous sarcoma virus-transforming protein, pp60v-src. *J Biol Chem* **260:** 13838-13843

Sugrue MM, Brugge JS, Marshak DR, Greengard P, Gustafson EL (1990) Immunocytochemical localization of the neuron-specific form of the c-src gene product, pp60c-src(+), in rat brain. *J Neurosci* **10:** 2513-2527

Superti-Furga G, Fumagalli S, Koegl M, Courtneidge SA, Draetta G (1993) Csk inhibition of c-Src activity requires both the SH2 and SH3 domains of Src. *EMBO J* **12:** 2625-2634

Suzuki T, Okumura-Noji K (1995) NMDA receptor subunits epsilon 1 (NR2A) and epsilon 2 (NR2B) are substrates for Fyn in the postsynaptic density fraction isolated from the rat brain. *Biochem Biophys Res Commun* **216:** 582-588

Swope SL, Moss SJ, Raymond LA, Huganir RL (1999) Regulation of ligand-gated ion channels by protein phosphorylation. *Adv Second Messenger Phosphoprotein Res* **33:** 49-78

Tabata H, Nakajima K (2001) Efficient in utero gene transfer system to the developing mouse brain using electroporation: visualization of neuronal migration in the developing cortex. *Neuroscience* **103:** 865-872

Tahirovic S, Bradke F (2009) Neuronal polarity. *Cold Spring Harb Perspect Biol* **1:** a001644

Takahashi F, Endo S, Kojima T, Saigo K (1996) Regulation of cell-cell contacts in developing Drosophila eyes by Dsrc41, a new, close relative of vertebrate c-src. *Genes Dev* **10:** 1645-1656

Takayama Y, Nada S, Nagai K, Okada M (1997) Role of Csk in neural differentiation of the embryonic carcinoma cell line P19. *FEBS Lett* **406:** 11-16

Tan TC, Valova VA, Malladi CS, Graham ME, Berven LA, Jupp OJ, Hansra G, McClure SJ, Sarcevic B, Boadle RA, Larsen MR, Cousin MA, Robinson PJ (2003) Cdk5 is essential for synaptic vesicle endocytosis. *Nat Cell Biol* **5:** 701-710

Taylor SS, Buechler JA, Yonemoto W (1990) cAMP-dependent protein kinase: framework for a diverse family of regulatory enzymes. *Annu Rev Biochem* **59:** 971-1005

Tessier-Lavigne M, Goodman CS (1996) The molecular biology of axon guidance. *Science* **274:** 1123-1133

Thelen K, Kedar V, Panicker AK, Schmid RS, Midkiff BR, Maness PF (2002) The neural cell adhesion molecule L1 potentiates integrin-dependent cell migration to extracellular matrix proteins. *J Neurosci* **22:** 4918-4931

Thomas SM, Brugge JS (1997) Cellular functions regulated by Src family kinases. *Annu Rev Cell Dev Biol* **13:** 513-609

Thomas SM, Soriano P, Imamoto A (1995) Specific and redundant roles of Src and Fyn in organizing the cytoskeleton. *Nature* **376:** 267-271

Tiscornia G, Singer O, Ikawa M, Verma IM (2003) A general method for gene knockdown in mice by using lentiviral vectors expressing small interfering RNA. *Proc Natl Acad Sci U S A* **100:** 1844-1848

Tomar A, Schlaepfer DD (2009) Focal adhesion kinase: switching between GAPs and GEFs in the regulation of cell motility. *Curr Opin Cell Biol* **21:** 676-683

Tonikian R, Xin X, Toret CP, Gfeller D, Landgraf C, Panni S, Paoluzi S, Castagnoli L, Currell B, Seshagiri S, Yu H, Winsor B, Vidal M, Gerstein MB, Bader GD, Volkmer R, Cesareni G, Drubin DG, Kim PM, Sidhu SS, Boone C (2009) Bayesian modeling of the yeast SH3 domain interactome predicts spatiotemporal dynamics of endocytosis proteins. *PLoS Biol* **7:** e1000218

Tonikian R, Zhang Y, Sazinsky SL, Currell B, Yeh JH, Reva B, Held HA, Appleton BA, Evangelista M, Wu Y, Xin X, Chan AC, Seshagiri S, Lasky LA, Sander C, Boone C, Bader GD, Sidhu SS (2008) A specificity map for the PDZ domain family. *PLoS Biol* **6:** e239

Trible RP, Emert-Sedlak L, Smithgall TE (2006) HIV-1 Nef selectively activates Src family kinases Hck, Lyn, and c-Src through direct SH3 domain interaction. *J Biol Chem* **281:** 27029-27038

Turner CE (2000) Paxillin and focal adhesion signalling. *Nat Cell Biol* **2:** E231-236

Umemori H, Ogura H, Tozawa N, Mikoshiba K, Nishizumi H, Yamamoto T (2003) Impairment of N-methyl-D-aspartate receptor-controlled motor activity in LYN-deficient mice. *Neuroscience* **118:** 709-713

Vidal M, Gigoux V, Garbay C (2001) SH2 and SH3 domains as targets for anti-proliferative agents. *Critical Reviews in Oncology Hematology* **40:** 175-186

Vierbuchen T, Ostermeier A, Pang Z, Kokubu Y, Sudhof T, Wernig M (2010) Direct conversion of fibroblasts to functional neurons by defined factors. *Nature* **463:** 1035-U1050

Vodnik M, Zager U, Strukelj B, Lunder M (2011) Phage Display: Selecting Straws Instead of a Needle from a Haystack. *Molecules* **16:** 790-817

von Boxberg Y, Salim C, Soares S, Baloui H, Alterio J, Ravaille-Veron M, Nothias F (2006) Spinal cord injury-induced up-regulation of AHNAK, expressed in cells delineating cystic cavities, and associated with neoangiogenesis. *Eur J Neurosci* **24:** 1031-1041

Wahl-Schott C, Biel M (2009) HCN channels: structure, cellular regulation and physiological function. *Cell Mol Life Sci* **66:** 470-494

Waksman G, Kominos D, Robertson SC, Pant N, Baltimore D, Birge RB, Cowburn D, Hanafusa H, Mayer BJ, Overduin M, Resh MD, Rios CB, Silverman L, Kuriyan J (1992) Crystal structure of the phosphotyrosine recognition domain SH2 of v-src complexed with tyrosine-phosphorylated peptides. *Nature* **358:** 646-653

Walsh FS, Doherty P (1997) Neural cell adhesion molecules of the immunoglobulin superfamily: role in axon growth and guidance. *Annu Rev Cell Dev Biol* **13:** 425-456

Wang K, Hackett JT, Cox ME, Van Hoek M, Lindstrom JM, Parsons SJ (2004) Regulation of the neuronal nicotinic acetylcholine receptor by SRC family tyrosine kinases. *J Biol Chem* **279:** 8779-8786

Wang YH, Ayrapetov MK, Lin X, Sun G (2006) A new strategy to produce active human Src from bacteria for biochemical study of its regulation. In *Biochem Biophys Res Commun* Vol. 346, pp 606-611. United States

Wang YT, Salter MW (1994) Regulation of NMDA receptors by tyrosine kinases and phosphatases. *Nature* **369:** 233-235

Wang YT, Yu XM, Salter MW (1996) Ca(2+)-independent reduction of N-methyl-D-aspartate channel activity by protein tyrosine phosphatase. *Proc Natl Acad Sci U S A* **93:** 1721-1725

Weed SA, Parsons JT (2001) Cortactin: coupling membrane dynamics to cortical actin assembly. *Oncogene* **20:** 6418-6434

Weinl C, Drescher U, Lang S, Bonhoeffer F, Löschinger J (2003) On the turning of Xenopus retinal axons induced by ephrin-A5. *Development* **130:** 1635-1643

Weng Z, Taylor JA, Turner CE, Brugge JS, Seidel-Dugan C (1993) Detection of Src homology 3-binding proteins, including paxillin, in normal and v-Src-transformed Balb/c 3T3 cells. *J Biol Chem* **268:** 14956-14963

Wenzel HJ, Woolley CS, Robbins CA, Schwartzkroin PA (2000) Kainic acid-induced mossy fiber sprouting and synapse formation in the dentate gyrus of rats. *Hippocampus* **10:** 244-260

Whittard JD, Sakurai T, Cassella MR, Gazdoiu M, Felsenfeld DP (2006) MAP kinase pathway-dependent phosphorylation of the L1-CAM ankyrin binding site regulates neuronal growth. *Mol Biol Cell* **17:** 2696-2706

Wiestler OD, Walter G (1988) Developmental expression of two forms of pp60c-src in mouse brain. *Mol Cell Biol* **8:** 502-504

Winkler DG, Park I, Kim T, Payne NS, Walsh CT, Strominger JL, Shin J (1993) Phosphorylation of Ser-42 and Ser-59 in the N-terminal region of the tyrosine kinase p56lck. *Proc Natl Acad Sci U S A* **90:** 5176-5180

Witte H, Neukirchen D, Bradke F (2008) Microtubule stabilization specifies initial neuronal polarization. *J Cell Biol* **180:** 619-632

Wong EV, Kerner JA, Jay DG (2004) Convergent and divergent signaling mechanisms of growth cone collapse by ephrinA5 and slit2. *J Neurobiol* **59:** 66-81

Worley TL, Cornel E, Holt CE (1997) Overexpression of c-src and n-src in the developing Xenopus retina differentially impairs axonogenesis. *Mol Cell Neurosci* **9:** 276-292

Woroniecki R, Ferdinand JR, Morrow JS, Devarajan P (2003) Dissociation of spectrin-ankyrin complex as a basis for loss of Na-K-ATPase polarity after ischemia. *Am J Physiol Renal Physiol* **284:** F358-364

Wu C, Ma MH, Brown KR, Geisler M, Li L, Tzeng E, Jia CY, Jurisica I, Li SS (2007) Systematic identification of SH3 domain-mediated human protein-protein interactions by peptide array target screening. *Proteomics* **7:** 1775-1785

Wu X, Suetsugu S, Cooper LA, Takenawa T, Guan JL (2004) Focal adhesion kinase regulation of N-WASP subcellular localization and function. *J Biol Chem* **279:** 9565-9576

Xing Z, Chen HC, Nowlen JK, Taylor SJ, Shalloway D, Guan JL (1994) Direct interaction of v-Src with the focal adhesion kinase mediated by the Src SH2 domain. *Mol Biol Cell* **5:** 413-421

Xu W, Harrison SC, Eck MJ (1997) Three-dimensional structure of the tyrosine kinase c-Src. *Nature* **385:** 595-602

Xue Y, Ren J, Gao X, Jin C, Wen L, Yao X (2008) GPS 2.0, a tool to predict kinase-specific phosphorylation sites in hierarchy. *Molecular & Cellular Proteomics* **7:** 1598-1608

Yadav S, Miller W (2007) Cooperative activation of Src family kinases by SH3 and SH2 ligands. *Cancer Letters* **257:** 116-123

Yaffe MB, Leparc GG, Lai J, Obata T, Volinia S, Cantley LC (2001) A motif-based profile scanning approach for genome-wide prediction of signaling pathways. *Nat Biotechnol* **19:** 348-353

Yagi T, Aizawa S, Tokunaga T, Shigetani Y, Takeda N, Ikawa Y (1993) A role for Fyn tyrosine kinase in the suckling behaviour of neonatal mice. *Nature* **366:** 742-745

Yaka R, Thornton C, Vagts AJ, Phamluong K, Bonci A, Ron D (2002) NMDA receptor function is regulated by the inhibitory scaffolding protein, RACK1. *Proc Natl Acad Sci U S A* **99:** 5710-5715

Yamasaki M, Thompson P, Lemmon V (1997) CRASH syndrome: mutations in L1CAM correlate with severity of the disease. *Neuropediatrics* **28:** 175-178

Yan KS, Kuti M, Yan S, Mujtaba S, Farooq A, Goldfarb MP, Zhou MM (2002) FRS2 PTB domain conformation regulates interactions with divergent neurotrophic receptors. *J Biol Chem* **277:** 17088-17094

Yang M, Leonard JP (2001) Identification of mouse NMDA receptor subunit NR2A C-terminal tyrosine sites phosphorylated by coexpression with v-Src. *J Neurochem* **77:** 580-588

Yang XM, Martinez R, Le Beau J, Wiestler O, Walter G (1989) Evolutionary expression of the neuronal form of the src protein in the brain. *Proc Natl Acad Sci U S A* **86:** 4751-4755

Yang XM, Walter G (1988) Specific kinase activity and phosphorylation state of pp60c-src from neuroblastomas and fibroblasts. *Oncogene* **3:** 237-244

Yeh R, Lee T, Lawrence D (2001) From consensus sequence peptide to high affinity ligand, a "library scan" strategy. *Journal of Biological Chemistry* **276:** 12235-12240

Young MA, Gonfloni S, Superti-Furga G, Roux B, Kuriyan J (2001) Dynamic coupling between the SH2 and SH3 domains of c-Src and Hck underlies their inactivation by C-terminal tyrosine phosphorylation. *Cell* **105:** 115-126

Yu H, Chen JK, Feng S, Dalgarno DC, Brauer AW, Schreiber SL (1994) Structural basis for the binding of proline-rich peptides to SH3 domains. *Cell* **76:** 933-945

Yu H, Rosen MK, Shin TB, Seidel-Dugan C, Brugge JS, Schreiber SL (1992) Solution structure of the SH3 domain of Src and identification of its ligand-binding site. *Science* **258:** 1665-1668

Yu XM, Askalan R, Keil GJ, Salter MW (1997) NMDA channel regulation by channel-associated protein tyrosine kinase Src. *Science* **275:** 674-678

Zhai J, Lin H, Nie Z, Wu J, Cañete-Soler R, Schlaepfer WW, Schlaepfer DD (2003) Direct interaction of focal adhesion kinase with p190RhoGEF. *J Biol Chem* **278:** 24865-24873

Zhang F, Li C, Wang R, Han D, Zhang QG, Zhou C, Yu HM, Zhang GY (2007) Activation of GABA receptors attenuates neuronal apoptosis through inhibiting the tyrosine phosphorylation of NR2A by Src after cerebral ischemia and reperfusion. *Neuroscience* **150:** 938-949

Zhang W, Wu Y, Du L, Tang DD, Gunst SJ (2005) Activation of the Arp2/3 complex by N-WASp is required for actin polymerization and contraction in smooth muscle. *Am J Physiol Cell Physiol* **288:** C1145-1160

Zhao YH, Krueger JG, Sudol M (1990) Expression of cellular-yes protein in mammalian tissues. *Oncogene* **5:** 1629-1635

Zhao YL, Takagawa K, Oya T, Yang HF, Gao ZY, Kawaguchi M, Ishii Y, Sasaoka T, Owada K, Furuta I, Sasahara M (2003) Active Src expression is induced after rat peripheral nerve injury. *Glia* **42:** 184-193

Zhao Z, Shen SH, Fischer EH (1993) Stimulation by phospholipids of a protein-tyrosine-phosphatase containing two src homology 2 domains. *Proc Natl Acad Sci U S A* **90:** 4251-4255

Zhong M, Lu Z, Foster DA (2002) Downregulating PKC delta provides a PI3K/Akt-independent survival signal that overcomes apoptotic signals generated by c-Src overexpression. *Oncogene* **21:** 1071-1078

Zisch AH, Kalo MS, Chong LD, Pasquale EB (1998) Complex formation between EphB2 and Src requires phosphorylation of tyrosine 611 in the EphB2 juxtamembrane region. *Oncogene* **16:** 2657-2670

Zong X, Eckert C, Yuan H, Wahl-Schott C, Abicht H, Fang L, Li R, Mistrik P, Gerstner A, Much B, Baumann L, Michalakis S, Zeng R, Chen Z, Biel M (2005) A novel mechanism of modulation of hyperpolarization-activated cyclic nucleotide-gated channels by Src kinase. *J Biol Chem* **280:** 34224-34232